

A STUDY OF THE KIMBERLITES, DIAMONDS AND ASSOCIATED  
ROCKS AND MINERALS FROM THE MONASTERY MINE,  
SOUTH AFRICA

by

RORY O. MOORE

VOLUME 1

TEXT

UNIVERSITY OF CAPE TOWN

THESIS SUBMITTED IN FULFILMENT OF THE REQUIREMENTS  
FOR THE DEGREE OF  
DOCTOR OF PHILOSOPHY

DEPARTMENT OF GEOCHEMISTRY  
UNIVERSITY OF CAPE TOWN

DECEMBER, 1986

The copyright of this thesis vests in the author. No quotation from it or information derived from it is to be published without full acknowledgement of the source. The thesis is to be used for private study or non-commercial research purposes only.

Published by the University of Cape Town (UCT) in terms of the non-exclusive license granted to UCT by the author.

DECLARATION

I hereby declare that all the work presented in this thesis is my own, except where otherwise stated in the text.

Signed by candidate

R.O. Moore  
December, 1986

## TABLE OF CONTENTS

Abstract	i
Acknowledgements	v
<u>CHAPTER 1 INTRODUCTION</u>	1
1.1 LOCALITY DESCRIPTION	1
1.1.1 Geographic Location	1
1.1.2 Mine History	1
1.1.3 General Geology	3
1.2 SCOPE OF THIS STUDY	4
<u>CHAPTER 2 KIMBERLITE PETROGRAPHY</u>	6
2.1 INTRODUCTION	6
2.1.1 The Definition of Kimberlite	7
2.1.2 Textural Classification of Kimberlites	8
2.1.3 Mineralogical Classification of Kimberlites	11
2.2 QUARRY KIMBERLITE	11
2.2.1 Macroscopic Description	11
2.2.2 Microscopic Description	14
2.2.3 Modal Analyses	20
2.3 EAST-END KIMBERLITE	21
2.3.1 Macroscopic Description	21
2.3.2 Microscopic Description	22
2.4 BRECCIA KIMBERLITE	25
2.4.1 Macroscopic Description	26
2.4.2 Microscopic Description	27
2.5 MICACEOUS KIMBERLITE DYKE	27
2.5.1 Macroscopic Description	27
2.5.2 Microscopic Description	28

<u>CHAPTER 3</u>	<u>ULTRAMAFIC XENOLITHS</u>	31
3.1	INTRODUCTION AND BRIEF OVERVIEW	31
3.2	XENOLITH ABUNDANCES AT MONASTERY	36
3.3	PETROGRAPHY	39
3.3.1	Introduction	39
3.3.2	Peridotites	39
3.3.3	Wehrlites and Olivine Clinopyroxenites	44
3.3.4	Olivine Websterites	45
3.3.5	Pyroxenites	46
3.4	MINERAL CHEMISTRY	47
3.4.1	Introduction	47
3.4.2	Olivine	48
3.4.3	Orthopyroxene	49
3.4.4	Clinopyroxene	51
3.4.5	Garnet	53
3.4.6	Phlogopite	53
3.4.7	Chromites and Cr-Spinels	56
3.4.8	Ilmenite	58
3.4.9	Amphibole	58
3.5	GEO THERMOMETRY AND GEOBAROMETRY	60
3.5.1	Introduction and Brief Review	60
3.5.2	Results	66
3.6	DISCUSSION	71
<u>CHAPTER 4</u>	<u>ECLOGITE XENOLITHS</u>	79
4.1	INTRODUCTION AND BRIEF REVIEW	79
4.2	PETROGRAPHY	82
4.3	MINERAL CHEMISTRY	84
4.3.1	Introduction	84
4.3.2	Recognition of Group I and II Eclogites	85
4.3.3	Choice of a Differentiation Index	86
4.3.4	Garnet	88
4.3.5	Clinopyroxene	89
4.3.6	Estimation of Bulk Composition	92
4.4	GEO THERMOMETRY	93
4.5	DISCUSSION	94
4.5.1	Group I Eclogites	95
4.5.2	Group II Eclogites	99

<u>CHAPTER 5</u>	<u>DIAMONDS AND MINERAL INCLUSIONS IN DIAMONDS</u>	101
5.1	INTRODUCTION	101
5.2	PHYSICAL CHARACTERISTICS OF THE MONASTERY DIAMONDS	104
5.2.1	Size	105
5.2.2	Shape	106
5.2.3	Colour	108
5.2.4	Surface Features	109
5.3	THE MINERAL INCLUSIONS	110
5.3.1	Methods of Inclusion Recovery and Analysis	110
5.3.2	Minerals Observed	112
5.4	MISCELLANEOUS INCLUSIONS	114
5.4.1	Sulphides	114
5.4.2	Oxides	115
5.4.3	Plagioclase	118
5.4.4	Zircon	118
5.4.5	Phlogopite	119
5.4.6	Moissanite	120
5.5	PERIDOTITIC PARAGENESIS	122
5.5.1	Inclusion Compositions	122
	Olivine	122
	Garnet	123
	Clinopyroxene	123
5.5.2	Discussion	124
5.6	ECLOGITIC PARAGENESIS	126
5.6.1	Inclusion Compositions	126
	Garnet	126
	Clinopyroxene	129
	Coesite/Quartz	130
	Corundum	130
	Websterite association	130
	Compositional variations within inclusions from the same diamond	131
	Mixed paragenesis inclusions within a single diamond	133

5.6.2	Discussion	134
	Comparison of inclusions with minerals in eclogite nodules from Monastery	134
	The Websterite Association	137
	Group B Garnets	139
	- Review of experimental studies relating to the solid solution of pyroxene in garnet	141
	- Pyroxene solid solution in the Group B garnets	144
	- Sodium in garnet	149
	- Geothermometry	153
	- Disequilibrium inclusions	155
	- The transition-zone of the upper-mantle	157
	- Discussion	160
5.7	SUMMARY	164
<u>CHAPTER 6 MEGACRYSTS</u>		167
6.1	INTRODUCTION AND REVIEW	167
6.2	RELATIVE ABUNDANCES OF MEGACRYSTS AT MONASTERY	173
6.3	PHLOGOPITE	175
6.4	ZIRCON	178
	6.4.1 Introduction	178
	6.4.2 Discrete Zircons	180
	Physical Characteristics	180
	Zircon-kimberlite interface zones	180
	6.4.3 Zircon-Ilmenite Association	183
	Zircon-ilmenite interface zones	184
	Ilmenite mineral chemistry	185
	Comparison with other ilmenite megacryst associations at Monastery	188
	6.4.4 Zircon-Olivine Association	191
	6.4.5 Zircon-Phlogopite Association	193
6.5	COEXISTING MEGACRYST ASSEMBLAGES	194
	6.5.1 Introduction	194
	6.5.2 Petrography	195
	6.5.3 Mineral Chemistry and Geothermometry	197
6.6	DISCUSSION	199
<u>CHAPTER 7 SUMMARY</u>		209
<u>REFERENCES</u>		225

## ABSTRACT

The hypabyssal quarry kimberlite is the most abundant phase at Monastery. Four petrographically distinct varieties are recognized. Mineralogically, the Q1 and Q4 kimberlites are opaque oxide-rich serpentine-phlogopite kimberlites, the Q2, a phlogopite-monticellite kimberlite and the Q3, a monticellite-phlogopite kimberlite. The East-end kimberlite is an opaque oxide-rich serpentine-monticellite kimberlite, but is poorly exposed and highly weathered. The breccia kimberlite hosts abundant country rock fragments in a soft serpentinous matrix. It is an opaque oxide-rich phlogopite serpentine kimberlite breccia. The precursor kimberlite dyke associated with the diatreme is an opaque oxide-rich calcite kimberlite.

The ultramafic xenoliths at Monastery are predominantly coarse grained and exhibit a high incidence of modal metasomatism. Some textures intermediate between porphyroclastic and granuloblastic were noted. Significant annealing has occurred. Garnet, orthopyroxene and clinopyroxene may have been derived by exsolution from high temperature aluminous orthopyroxenes. Minerals in the peridotites and pyroxenites have similar compositions to those from other localities. Two groups of phlogopite composition have been noted. Wehrlitic rocks have phlogopite similar to that in richterite-bearing peridotites from Kimberley. The coarse xenoliths at Monastery display an exceptionally large range of calculated equilibration conditions ( $\sim 700-1050^{\circ}\text{C}$ ; 20-40 kbars) which define an array of similar configuration to

theoretical geotherms for continental shield areas. A bimodal temperature distribution which correlates with texture is also noted. Low T-P rocks (~700-850°C) correspond with those petrographically classified as intermediate and granuloblastic. A correlation was noted between low pressure and the presence of chromite in garnet lherzolites. A variety of geothermometers based on different phase equilibria yield similar results which apparently do not represent blocking temperatures.

Eclogite xenoliths are rare. Two groups of eclogite are discriminated on the basis of Na<sub>2</sub>O in garnet and K<sub>2</sub>O in clinopyroxene. Coexisting garnets and clinopyroxenes define an ordered array of tie-lines on a Ca:Mg:Fe ternary, with no crosscutting relationships. Relationships between Mg/Mg+Fe, TiO<sub>2</sub> and Cr<sub>2</sub>O<sub>3</sub> in clinopyroxenes and Mg/Mg+Fe, TiO<sub>2</sub>, CaO and Na<sub>2</sub>O in garnets are consistent with Group I eclogites having formed in a single igneous event, but geothermometric calculations show a trend of increasing temperature with increasing degree of fractionation (1075-1307°C). The Group I eclogites may possibly represent original high pressure garnetite which has undergone subsolidus re-equilibration exsolving pyroxene. Garnets from Group II eclogites define an Fe-enrichment trend with little variation in Ca and oxides such as TiO<sub>2</sub> and Na<sub>2</sub>O remain essentially constant with changing Mg/Mg+Fe. Calculated equilibration temperatures dominantly range between 1060 and 1107°C. Group II eclogites may represent crystallised partial melts from a garnet lherzolite source.

Inclusions in the Monastery diamonds are predominantly eclogitic, but peridotitic minerals and sulphides, oxides, plagioclase, phlogopite and moissanite are also reported. The peridotitic inclusions suggest a lherzolitic association. Calculated formation temperatures for the peridotitic inclusions are in the range 1000 to 1180°C. Two populations of eclogitic garnet are distinguished. One group (Group A) has similar compositions to eclogitic garnet inclusions from other localities, while the second (Group B) display the effects of pyroxene in solid solution. Eclogitic clinopyroxenes possess a wide range in compositions which trend towards lower jadeite and diopside contents compared to clinopyroxene inclusions from other localities. Some clinopyroxenes and most of the Group A garnet inclusions are similar to minerals of Group I eclogite xenoliths at Monastery and a minor proportion of the diamonds may be derived from such xenoliths. Accessory eclogitic inclusions include suspected coesite and a primary corundum. Inclusions showing disequilibrium compositions have been found. One diamond contained an olivine as well as an eclogitic garnet. Two diamonds hosted polyphase websterite inclusion assemblages which yield calculated temperatures in excess of 1400°C. Their relationship with the peridotitic and eclogitic paragenesis inclusions is unclear. Formation pressures indicated by the Group B garnet inclusions are in the range 55 to 145 kbars, suggesting a deep seated asthenospheric origin.

Phlogopite megacrysts are constituents of the Cr-poor megacryst suite. Zircon has been found in association with megacrystic ilmenite, Fe-rich olivine and phlogopite. Two populations of ilmenite are associated with zircon and neither

is associated with ilmenite coexisting with pyroxenes or garnet. The olivines and phlogopites which coexist with zircon are Fe-rich. Specific features imply the existence of more than one population of megacrysts. Coexisting megacryst phases support the proposal that at least the less evolved megacrysts formed in a single igneous event at a pressure of 51 kbars. The phase equilibria of Wyllie (1987) provide a framework for modelling the formation of megacrysts by partial melting of a rising asthenospheric diapir.

## ACKNOWLEDGEMENTS

It was indeed a privilege to study under John Gurney and I thank him for his sound advise and guidance.

The Foundation for Research and Development of the CSIR and De Beers Consolidated Mining provided financial support. GEMEX, Mr. Sydney Gasson and the mine manager of Monastery, Mr. Auret van Jaarsveld are thanked for friendly co-operation and for arranging the sampling of the diamonds investigated in this study.

My friends and fellow students in the department all played some role in this project. In particular, Marshall, Jenny and Tom provided excellent company in the evenings and over weekends. A big thanks to Roddy, Nadima, Scott, Susie, Dick, Charlie and David who all helped with technical aspects of this thesis. Andy Duncan and Dave Hill provided an excellent computer facility and plenty of friendly help. Lynn O'Neill mothered me through some tough times and always turned a blind eye when the stationary cupboard was opened. Anton le Roex is thanked for his regular doses of good common sense advise.

The De Beers team in Kimberley (Jock, Simon, Dave, Libby, Mike and Roger) taught me something of the intricacies of kimberlite petrography and I thank Jock & Jill and Simon & Trish for their hospitality during visits to Kimberley.

It is impossible to express my gratitude to Ruth Mennie (a truly remarkable woman) who put in a superhuman effort in the final stages of this thesis. Marshall and Ruth I owe you one!

Finally to my silently suffering wife, Jill who has unselfishly supported me through thick and thin. Jill never lost heart when deadline after deadline was broken. Many thanks for the superb effort put into the Appendix volume.

## CHAPTER 1: INTRODUCTION

### 1.1 LOCALITY DESCRIPTION

#### 1.1.1 Geographic Location

The Monastery kimberlite is situated in the Winburg district of the Orange Free State, South Africa, approximately 250km due east of Kimberley. This is within the bounds of the Kaapvaal Craton and close to the north-eastern border of Lesotho (Fig. 1.1). The precise location of the mine is  $28^{\circ}48'40''$  south and  $27^{\circ}25'20''$  east, at an elevation of 1600m above sea level.

#### 1.1.2 Mine History

The following account of the history of Monastery Mine is largely based on information presented by Whitelock (1973) and Gurney (1980). The mine was first recognised as a diamondiferous kimberlite pipe by a prospector in 1876, only 6 years after the first kimberlites were recognised as diamond ore bodies at Kimberley and Jagersfontein. Large-scale mining started in 1886 and was stopped at the outbreak of the Anglo-Boer War in 1899. During these operations, some 150 000 tonnes were mined from the quarry area (Fig. 1.2).

Apart from two short lived attempts to restart the mine in 1904 and 1912, the mine lay dormant until 1965. In 1965 prospecting operations were restarted by a local farmer (and

mineral rights holder) Mr Sydney Gasson and some 3 200 tonnes of kimberlite were treated between 1965 and 1967. The central and eastern portions of the pipe were explored underground at the -30m level. This development included a drive along the major axis of the pipe with a single crosscut extending to the pipe margins, access was from a winze. A vertical shaft was also sunk in the eastern part of the pipe, but did not connect with the underground development.

In 1967 Rand Mines Limited prospected the pipe and during this time, the drives on the 30m level were extended and an extensive diamond drilling programme undertaken under the direction of T.K. Whitelock.

In 1978 Namex (Pty) Limited obtained an interest in the mine. Namex was the managing company for Octha (Pty) limited. Extensive prospecting was undertaken and a development programme initiated. Namex was reorganised in 1980 and the control of the mine was obtained by Monex (Pty) Limited.

In November 1980 an Australian company, Gem Exploration and Minerals Limited (GEMEX) purchased the shares in the mine held by Monex. Gemex and Mr. Sydney Gasson are the current owners of the mine.

The most recent prospecting/mining operation (with Mr. Auret van Jaarsveld as project manager) was launched in 1980 following the installation of a sophisticated ore reduction and diamond recovery plant. These operations have been restricted to the western area of the pipe which has been mined to the -30m level. Mining operations ceased midway through 1982 due to

economic factors.

### 1.1.3 General Geology

The Monastery diatreme is roughly elliptical in shape with dimensions of 180m by 70m (surface area ~1 Ha) (Whitelock, 1973). It is a Group I kimberlite (Smith, 1983a) which has been dated at 90my by two independent methods. Allsopp and Barrett (1975) report a Rb-Sr age of  $90 \pm 4$ my for fresh phlogopite megacrysts while Davis et al. (1976) obtained a U-Pb zircon age of 90.4my.

The kimberlite is intruded into sediments of the Elliot Formation (the former "Red Beds") of the Karoo Supergroup. This sedimentary unit is Triassic in age and consists of essentially flat lying red mudstones and shales interbedded with fine grained yellowish lenticular sandstones (Truswell, 1977). Deposition is considered to have taken place on alluvial flats (Botha, 1968). Overlying this formation are the aeolian deposits of the Clarens Formation (formerly The Cave Sandstones), which form flat topped hills in the countryside surrounding the Monastery kimberlite. Dolerite dykes which acted as feeders to the Stormberg volcanic episodes are also common in the area.

The Monastery kimberlite is a multiple intrusion which has been emplaced in several phases. Whitelock (1973) recognised four distinct kimberlite types which he termed the quarry kimberlite, the east-end kimberlite, the breccia kimberlite and the fine grained kimberlite (Fig. 1.2).

Associated with the diatreme is a diamondiferous kimberlite dyke which can be followed in an ESE/WNW direction for more than 2000m (Fig. 2.1). A small pipe or blow is developed on the dyke just east of the main diatreme (Fig. 2.1). The width of this blow as revealed by trenching is at least 22m (Fielding, 1981).

A blind kimberlite vent, termed the South Vent, was discovered during the Rand Mines tenure of the property (Figs. 1.2 & 2.1). It is elliptical in shape with dimensions of 50 by 40 metres. The South Vent has recently been shown to outcrop, although the southern portion is capped by 22m of Karoo rocks. Drilling has revealed it to be composed of a core of massive, fine grained kimberlite with few foreign xenoliths (Fielding, 1981).

## 1.2 SCOPE OF THIS STUDY

Monastery Mine is widely regarded as the type locality for the occurrence of the Cr-poor megacryst suite and consequently, Monastery megacrysts have received considerable attention in the literature (e.g. Jakob, 1977; Gurney et al., 1979<sup>b</sup>; Haggerty et al., 1979; Harte and Gurney, 1981; and papers quoted by these authors). However, apart from a brief description of the general geology of the pipe (Whitelock, 1973) other aspects of this kimberlite have not been investigated in any detail. This thesis therefore examines aspects of the kimberlite, diamonds and mantle-derived xenoliths not previously described. Major aspects covered include:

- (1) A description of the petrography of the major kimberlite phases represented in the diatreme.
- (2) An examination of the petrography, mineral chemistry and equilibration conditions of mantle-derived xenoliths including peridotites, pyroxenites, wehrlites and eclogites.
- (3) A detailed investigation of Monastery diamonds including a description of their physical characteristics and the chemical characterization of a suite of mineral inclusions.
- (4) An assessment of the various mantle derived xenoliths as potential source rocks for diamond based on their compositional characteristics.
- (5) An investigation of the relationship of phlogopite and zircon to the Cr-poor megacryst suite.

2.1     INTRODUCTION

An updated geological plan of the Monastery kimberlite is presented in Fig. 2.1. The revised outline of the pipe is based on the accurately surveyed mine plan prepared by Fielding (1981)., The most significant difference between the updated map and that of Whitelock (1973) (Fig. 1.2) is the shape of the western portion of the diatreme where Fielding's survey indicated the pipe to be considerably narrower than portrayed on Whitelock's plan. The author's field observations verify the findings of Fielding (1981).

Large quantities of mine debris and partial flooding in certain areas of the pipe made it difficult to accurately locate and map both kimberlite/country rock contacts as well as contacts between the various kimberlite phases within and the pipe. Consequently, the relative distribution of the kimberlite phases in Fig. 2.1 should not be regarded as being absolutely accurate.

Additional information contained on the revised map includes:

- (a) the approximate outcrop areas of four distinct varieties of quarry kimberlite, termed Q1 to Q4, recognised in this study (see Section 2.2);
- (b) the position of a precursor kimberlite dyke which terminates in a small blow

(c) an accurate outline of the South Vent as revealed by exploratory drilling (Fielding, 1981).

The fine-grained kimberlite described by Whitelock (1973) could not be located in this study.

An indication of depth levels attained during mining operations is illustrated in Fig. 2.2. Only the quarry kimberlite in the western area of the pipe has been mined in significant quantities.

Some comments on the definition of kimberlite and an overview of the classification schemes adopted in this study follows as an introduction to a detailed description of the petrography of the Monastery kimberlites.

#### 2.1.1 The Definition of Kimberlite

Several definitions of kimberlite are firmly entrenched in the literature (e.g. Dawson, 1962, 1967a, 1971, 1980; Gary et al., 1972; Edwards and Hawkins, 1966; Kennedy and Nordlie, 1968; Mitchell, 1970, 1979a), and this has not only led to terminological confusion, but has also resulted in unwarranted implications regarding possible petrogenetic associations between kimberlites and other rock types (Mitchell, 1970, 1979<sup>a</sup>). Clement et al. (1977) presented a formal definition of kimberlite which avoided both genetic connotations as well as excessive petrologic restrictions. The revised definition presented by Clement et al. (1984) is presented below:

Kimberlite is a volatile-rich, potassic, ultrabasic igneous

rock which occurs as small volcanic pipes, dykes and sills. It has a distinctively inequigranular texture resulting from the presence of macrocrysts set in a finer grained matrix. This matrix contains, as prominent primary phenocrystal and/or groundmass constituents, olivine and several of the following minerals: phlogopite, carbonate (commonly calcite), serpentine, clinopyroxene (commonly diopside), monticellite, apatite, spinels, perovskite and ilmenite. The macrocrysts are anhedral, mantle-derived, ferromagnesian minerals which include olivine, phlogopite, picroilmenite, chromian spinel, magnesian garnet, clinopyroxene (commonly chromian diopside) and orthopyroxene (commonly enstatite). Olivine is extremely abundant relative to the other macrocrysts, all of which are not necessarily present. The macrocrysts and relatively early-formed matrix minerals are commonly altered by deuteric processes mainly serpentinization and carbonatization. Kimberlite commonly contains inclusions of upper mantle-derived ultramafic rocks. Variable quantities of crustal xenoliths and xenocrysts may also be present. Kimberlite may contain diamond but only as a very rare constituent.

#### 2.1.2 Textural Classification of Kimberlites

The textural-genetic classification scheme originally proposed by Clement and Skinner (1979) and subsequently updated by Clement and Skinner (1985) has been adopted in this study. This classification is primarily based on macroscopic textural features and reflects the view that textural variants of

kimberlite are mainly related to different near-surface emplacement and kimberlite pipe-forming processes (Clement and Skinner 1985).

The classification is shown in Table 2.1. It recognises three broad groups of kimberlite: hypabyssal-facies, diatreme-facies and crater-facies kimberlites which usually correspond to the major depth zones of kimberlite pipes, namely the root, diatreme and crater zones (Hawthorne, 1975). This initial facies subdivision provides a clear distinction between rocks which were emplaced in markedly different ways (Clement and Skinner, 1985).

Hypabyssal facies kimberlite is subdivided into "kimberlite" and "kimberlite breccia" (Table 2.1). Kimberlite is the "normal" crystallization product of kimberlite magma and at no stage has solid-vapour fluidization been involved in its development. Kimberlite and kimberlite breccia are distinguished from one another only by the abundance of relatively large (>4mm) country rock xenoliths and /or fragments of earlier crystallized kimberlite (autoliths) that are present. The dividing line has been set at 15 vol% fragments, so the breccias merely reflect an increased incorporation of rock fragments by the kimberlite. There is a complete gradation between the two rock types.

Hypabyssal facies kimberlites are further subdivided into three textural varieties, namely macrocrystic, segregatory and aphanitic kimberlite (Table 2.1).

**Macrocrystic kimberlite** is a kimberlite with an inequigranular texture imposed by the presence of abundant anhedral, upper

mantle derived crystals which may include olivine, phlogopite, picroilmenite, chromian spinel, magnesian garnet, clinopyroxene and orthopyroxene.

**Segregationary kimberlites** show textures which reflect the crystallization of certain minerals (or groups of minerals) in discrete areas of the rocks, often in well defined "pools". The most common examples involve the separation of "early-" and "late-" crystallizing groundmass phases.

**Aphanitic kimberlites** are devoid of the coarse-grained ferromagnesian macrocryst mineral assemblage which is usually a prominent feature of most kimberlites. This variety of kimberlite is relatively rare.

Kimberlite breccias may also exhibit macrocrystic, aphanitic and porphyritic textures.

The details of the classification of diatreme and crater facies kimberlites are not dealt with here, as kimberlites from these facies are not represented at Monastery. Briefly, diatreme facies kimberlites are the end product of a complex vapour-rich fluidised intrusive system. They are commonly composed of abundant and diverse xenolithic material set in a fine grained cementing medium which represents the quenched products of residual magmatic fluids (Dawson, 1971,1980; Clement, 1979,1982).

Crater facies kimberlites are only preserved at a few localities because the present day erosion level (including that of Monastery) is often considerably below the crater zone of the original diatreme.

### 2.1.3 Mineralogical Classification of Kimberlites

The mineralogical classification of kimberlites proposed by Skinner and Clement (1977, 1979) is adopted in this study. The classification, which is illustrated in Table 2.2, is based on the modal proportions of five matrix minerals, namely diopside, monticellite, phlogopite, calcite and serpentine. The macrocryst assemblage as well as the matrix olivine phenocrysts are not considered in the scheme. In the first stage of classification, five basic subdivisions of kimberlite are recognised depending upon which of the five minerals is volumetrically most abundant. Further subdivisions can be made if one or more of these five minerals, or any other mineral, is present to the extent of, or exceeding, two-thirds of the volumetric abundance of the dominant mineral. In cases where the total opaque mineral content of the matrix equals or exceeds two-thirds of the abundance of the dominant mineral, the kimberlite is qualified as "opaque-mineral-rich" (Skinner and Clement, 1979).

## 2.2 QUARRY KIMBERLITE

### 2.2.1 Macroscopic Description

The quarry kimberlite is by far the dominant kimberlite type in the diatreme, occupying most of the western area of the pipe (Fig. 1.2; 2.1). It varies considerably in appearance and in this study, four distinct varieties (termed Q1 to Q4) have been recognised. The distinguishing features of each of these kimberlites will first be outlined, followed by a discussion of

the features common to quarry kimberlite in general.

**The Q1 Quarry kimberlite** is the most common variety of quarry kimberlite. It is dark blue-green in colour, hard, brittle and resistant to weathering (Plate 2.1). The rock is a hypabyssal facies kimberlite which displays a macrocrystic texture, resulting mostly from the presence of abundant anhedral olivine macrocrysts ranging in size between 2 and 14mm, set in a uniform textured, fine grained matrix. The olivine macrocrysts constitute between 5 and 25 vol% of the rock (average 14%). Phlogopite and ilmenite macrocrysts are well represented, each constituting an average of 4 vol% of the rock. Ilmenite macrocrysts are distinguished from megacrysts by being less than 1.5cm in longest dimension. Rare occurrences of garnet macrocrysts have been recorded. Xenoliths of upper mantle origin as well as megacryst suite minerals are abundant in this kimberlite and these will be considered in more detail later.

**The Q2 Quarry kimberlite** is essentially identical to the Q1 kimberlite in virtually all macroscopic features with the major exception being colour. It is characteristically pale bluish-grey in colour (Plate 2.2) and on occasions a yellowish tint is discernible in the groundmass. The Q1 and Q2 kimberlites outcrop and grade into one another in a random fashion within the area depicted in Fig. 2.1, with the Q2 variety being considerably less abundant than the Q1 kimberlite. Kimberlites with intermediate colour characteristics do occur, but are not common. The absence of a systematic outcrop pattern between these two kimberlites indicates that they do not represent two distinct phases of kimberlite intrusion.

**The Q3 Quarry kimberlite** outcrops in a restricted area in the south-western lobe of the diatreme (Fig. 2.1). It is a hypabyssal facies macrocrystic-segregatory kimberlite which is pale brown to greenish-brown in colour, and deeply altered (Plate 2.3). Abundant anhedral pseudomorphs after olivine macrocrysts ranging in size between 2 and 15mm constitute between 11 and 20 vol.% of the rock. Olivine macrocrysts are pseudomorphed by a mixture of serpentine and carbonate. Fresh phlogopite macrocrysts and megacrysts are particularly abundant in this kimberlite, constituting on average ~6 vol% of the rock. The groundmass of the Q3 kimberlite displays a well developed globular segregational texture (Plates 2.3 & 2.21) and this is described in more detail in Section 2.2.2. A number of examples of the Q3 kimberlite transected by dykelets of fine grained aphanitic kimberlite have been observed (e.g. Plate 2.4). These dykelets are usually 4 to 6cm wide and have very sharp contacts with the host kimberlite.

**The Q4 Quarry kimberlite** occurs in the central northern area of the pipe (Fig. 2.1). It is essentially an extension of the Q1 kimberlite, but is distinguished by its high content of country rock fragments (~10vol%) (Plate 2.4), and the presence of a well developed globular segregatory texture in the groundmass. A number of xenoliths of Q3 kimberlite have been observed in the Q4 kimberlite (e.g. Plate 2.6), implying that the former predates the latter.

All phases of the quarry kimberlite hosts abundant megacrysts of olivine, ilmenite, garnet, diopside, enstatite and phlogopite. Lamellar intergrowths of ilmenite/diopside and

ilmenite/enstatite are also common. Ultramafic nodules of upper mantle origin are also well represented in the quarry kimberlite. The nodule suite is dominated by coarse textured lherzolites, garnet lherzolites, harzburgites and rare pyroxenites, a high proportion of which contain phlogopite (see Chapter 3). Peridotite nodules with deformed textures as well as eclogite nodules are extremely rare.

Xenoliths of country rock which are on average ~3cm in size are present in generally low proportions. These include a variety of sedimentary rock fragments as well as angular pieces of dolerite. Nodules of basement gneiss which are usually extensively carbonatised are also frequently encountered.

The estimated diamond grade of the quarry kimberlite reported by Jakob (1977) is 50 cts/100 tonnes. More recent estimates are much lower than this, being 15 cts/100 tonnes on average (A.P. van Jaarsveld, Pers. Comm. 1982). This dropoff in grade may be a function of recovery problems, since the new plant gave constant teething problems, especially with respect to desliming.

### 2.2.2 Microscopic Description

The two populations of olivine characteristic of kimberlites are easily recognisable in the quarry kimberlite. This is evident in the histograms presented in Fig. 2.3 which reflect a size analysis of olivines in the Q1 quarry kimberlite. Petrographic observations indicate the size analysis to be representative of all four varieties of quarry kimberlite.

Olivine phenocrysts are characteristically small, ranging in size between 0.01 and 0.9mm but most commonly between 0.1 and 0.3mm, while olivine macrocrysts range between 0.8 and 13mm in longest dimension with the dominant size range being between 1 and 4mm (Fig. 2.3).

Olivine macrocrysts are usually rounded, but may be elongate in shape and commonly display fresh cores, (particularly in the Q1 kimberlite). Even extremely fresh macrocrysts have a rim of serpentine of variable thickness and, fractures within the macrocrysts are commonly lined with serpentine. In the Q3 kimberlite, olivine macrocrysts have been extensively carbonated. Examples of polycrystalline olivine macrocrysts as well as macrocrysts displaying undulose extinction are rare in all varieties of quarry kimberlite.

Olivine phenocrysts are very seldom preserved in the quarry kimberlite and fresh remnant cores are only present in the freshest samples of Q1 kimberlite (Plate 2.7). The nature of the alteration of olivine phenocrysts, varies considerably, and has been described in some detail by Clement (1982). Examples of most of the replacement textures described by Clement (op. cit.) are present in the quarry kimberlite. Alteration is dominated by serpentinization but replacement by calcite may also be extensive in some samples. The imprint of weathering in the form of clay mineral development at the expense of serpentine is also common (Plate 2.7). The size distribution analysis (Fig. 2.3) indicates the mode of the phenocryst population to be ~0.26mm.

Phlogopite macrocrysts are well represented in the quarry kimberlite and are usually in the size range 1-5mm. They vary considerably in their state of preservation, but are generally considerably altered. Fresh macrocrysts are pale brown in colour and exhibit normal pleochroism. An example of a typical partially altered phlogopite macrocryst is illustrated in Plate 2.8 (a). A complex alteration zone separates the "fresh" core from the fine dusting of magnetite grains demarcating the original outline of the macrocryst. The alteration zone is typically composed of a mixture of serpentine, fine grained phlogopite, calcite, chlorite and magnetite (Plate 2.8b). Laths of groundmass phlogopite have on occasions been observed to extend into the alteration zone of macrocrysts. Remnant cores of phlogopite macrocrysts are commonly optically zoned to darker rims (Plate 2.8a). Stringers of calcite may be developed along cleavage traces, or as isolated segregations in the interface zones between fresh and altered phlogopite (Plate 2.8a). In some cases entire phlogopite macrocrysts have been replaced by a mixture of serpentine, groundmass phlogopite, calcite and magnetite and their original presence is often only indicated by the dusting of magnetite grains (e.g. Plate 2.9).

Phlogopite is a prominent groundmass phase in the quarry kimberlite where it occurs as randomly oriented laths with length to breadth ratios of 10:1 and an average grain size of 1.2mm by 0.1mm (Plate 2.10). Clement (1982) interprets the interlocking texture displayed by groundmass phlogopite to be indicative of in situ post-intrusion crystallization. Further evidence for phlogopite representing a late-crystallizing groundmass phase is found in the abundance of spinel,

monticellite and perovskite inclusions (Plate 2.10). In some cases, inclusions are so abundant that the phlogopites display a sieve texture (Plate 2.11 a&b). Groundmass phlogopite is usually fresh (Plates 2.10, 2.11), but may be considerably altered by serpentization and chloritization (Plate 2.12). A second generation of extremely fine grained (~30-100 um) groundmass phlogopite is also present in the quarry kimberlite. This is illustrated in Plate 2.13, where the two generations are contrasted.

Opaque minerals are abundant in the groundmass of the quarry kimberlite. Spinel dominates and are mostly equant euhedral to subhedral crystals ranging in size between 0.01 and 0.1mm. They often display complex zonations and atoll textures are common (Plate 2.14). Complex intergrowths between spinels of different composition, ilmenite and perovskite are also frequently encountered (Plate 2.15). Groundmass ilmenites are generally rounded to ovoid in outline and are larger than groundmass spinels (commonly around 0.3mm in diameter). Ilmenite commonly forms cores to zoned spinels (Plate 2.15).

Perovskite is an important accessory groundmass phase in the quarry kimberlite and on occasions may constitute several modal percent of the rock. It most commonly occurs as discrete euhedral to subhedral grains which range in size between 0.01 and 0.14mm (Plate 2.16). Anhedral grains also occur, particularly when perovskite is intergrown with other phases. Associations in which it commonly occurs include perovskite cores to spinel grains; reaction mantles around ilmenite macrocrysts; rims of perovskite enclosing spinel grains; and

complex intergrowths with ilmenite and a variety of spinels.

Monticellite is generally well represented in the quarry kimberlite but varies considerably in abundance within the four subgroups of this kimberlite (see Section 2.2.3). It occurs as closely packed colourless, low birefringent subhedral to euhedral grains within the groundmass. Monticellite is usually extremely fine grained, being on average  $\sim 0.04$ mm in diameter (Plate 2.17). Another common mode of occurrence is as inclusions in sieve textured groundmass phlogopites (Plate 2.11) which indicates it to be an earlier crystallizing phase than groundmass phlogopite. Monticellite may be fresh, but is commonly altered to serpentine or on occasions calcite. Its original presence is recognisable by ghost outlines of the altered grains. Serpentine commonly occurs in the interstitial areas between granular textured monticellite.

Calcite is a common primary constituent of the quarry kimberlite where it occurs as rounded or irregular-interstitial segregations often in often in association with serpentine and/or apatite (Plates 2.18 a&b; 2.19; 2.20). Calcite segregations show a considerable range in size, but most are between 0.1 and 0.3mm in largest dimension. Staining tests using Alizarin Red organic dye indicate that virtually all the carbonate in the quarry kimberlite is calcite, but small quantities of dolomite are present. As already mentioned, secondary calcite may be associated with the breakdown of olivine and monticellite. Localised veins of secondary calcite may also be present, but are rare.

Serpentine is an important and abundant phase in the quarry kimberlite. It occurs in two basic associations, namely as a product of deuteric alteration of pre-existing phases, and as a primary groundmass constituent. As already mentioned, the alteration of olivine phenocrysts is often complex, many having undergone two or three distinguishable (by colour and texture) serpentinization episodes. Primary groundmass serpentine may occur as extremely homogeneous, pale brown, featureless pools or segregations associated with calcite as illustrated in Plates 2.18 (a&b). However, primary serpentine also occurs in a fine grained fibrous form in the interstitial areas between monticellite and other groundmass phases (e.g. Plate 2.12).

Apatite is an accessory mineral in many kimberlites and it is generally well represented in the quarry kimberlite. It usually occurs as discrete colourless subhedral to euhedral, prismatic crystals, but other modes of occurrence are also noted. These include:

- (a) radiating clusters of acicular crystals (Plate 2.19) which Dawson et al. (1975) ascribe to quench crystallization.
- (b) subhedral to euhedral inclusions within calcite segregations (Plate 2.20).

The grain size of apatite varies considerably with discrete crystals usually measuring between 0.04 and 0.12mm, while apatite clusters and inclusions within calcite segregations are generally larger, commonly between 0.10 and 0.49 mm.

### 2.2.3 Modal Analyses

Twenty-six quantitative modal analyses of the quarry kimberlite have been performed and representative analyses from each of the four varieties are presented in Table 2.3. The remaining data is tabulated in Appendix 2.1. Column A in Table 2.3 represents the modal proportions of each phase in volume percent of the rock, while column B represents the groundmass phases recalculated to 100% on an olivine free basis for mineralogical classification purposes. Modal analyses are based on 500 point-counts per sample (usually 1 thin section). Repetitive analyses on the same thin section have indicated that 500 counts are sufficient to produce a representative analysis.

The modal data in Table 2.3 indicates the quarry kimberlite to be mineralogically variable. The Q1 and Q4 kimberlites are extremely similar, both being 'opaque-mineral-rich serpentine-phlogopite kimberlites (mineralogical classification of Skinner and Clement, 1979). However, the previously mentioned abundance of country rock fragments as well as the globular segregatory texture in the groundmass of the Q4 kimberlite serve to distinguish the two.

The Q2 kimberlite is a phlogopite-monticellite kimberlite. The essential difference between the Q1 and Q2 kimberlites is the greater abundance of monticellite (with a concomitant decrease in calcite and opaque-minerals) in the Q2 variety. A gradation between the Q1 and Q2 kimberlites exists, with intermediate varieties showing intermediate abundances in the above mentioned groundmass phases (see Appendix 1).

The Q3 kimberlite is a monticellite-phlogopite kimberlite which has considerably lower abundances of groundmass opaque phases relative to the other varieties of quarry kimberlite (Table 2.3).

Petrographic considerations indicate that the four varieties of quarry kimberlite have been derived from a single phase of kimberlite intrusion. The specific features which distinguish these kimberlites (i.e. variations in modal abundances of groundmass phases, differences in country rock xenolith content and variations in groundmass texture) are thought to reflect localised differences in physical and/or chemical conditions during kimberlite eruption and crystallization.

## 2.3 EAST-END KIMBERLITE

### 2.3.1 Macroscopic Description

The east-end kimberlite occupies the eastern portion of the pipe (Fig. 2.1) and because of the very limited mining activities in this area of the pipe (Fig. 2.2), it is generally poorly exposed. It is a hypabyssal facies macrocrystic kimberlite which is pale yellowish brown to pale bluish grey in colour and is deeply weathered (Plate 2.22). The macrocrystic texture is derived from abundant macrocrysts and megacrysts of olivine (pseudomorphs) and ilmenite being set in a fine grained groundmass which is usually uniform in texture, but which may display globular segregations. Phlogopite macrocrysts are exceedingly rare in this kimberlite.

Megacryst-suite minerals are not as abundant as in the quarry kimberlite and olivine megacrysts dominate. The olivines are almost always stained to a pale reddish brown colour in response to the oxidation of iron, possibly indicating that they most commonly belong to the high-iron group of olivine megacrysts (Gurney et al. 1979<sup>b</sup>). Sporadic ilmenite, garnet and lamellar orthopyroxene (Group II of Gurney et al. 1979<sup>b</sup>) megacrysts occur, but are usually relatively small (commonly less than 2cm in diameter). Phlogopite megacrysts as well as lamellar pyroxene/ilmenite intergrowths are rare. Whitelock (1973) reports the occurrence of gem quality zircons in this kimberlite.

Ultramafic xenoliths are rare in comparison to the quarry kimberlite, and where present, are usually extensively altered. The east-end kimberlite hosts large segregations of carbonate (up to 20cm) and it is unclear whether these represent extensively carbonated xenoliths, or primary segregations of carbonate. The former appears more likely.

The diamond grade reported by Whitelock (1973) is 4 carats/100 tonnes, but the diamonds are of superior quality to those in the quarry kimberlite (Pers. Comm., A.P. van Jaarsveld, 1982).

### 2.3.2 Microscopic Description

Both populations of olivine have been extensively altered, mainly to serpentine, but calcite may also be developed. Olivine macrocrysts range in size between 1 and 10mm but are

most commonly ~2mm in diameter. Phlogopite macrocrysts are extremely rare, and where present are extensively altered. Macrocrysts of ilmenite are relatively abundant, and range in size between 0.8 and 7mm. They characteristically display reaction rims consisting of perovskite and spinel.

Pseudomorphs after olivine phenocrysts are plentiful. They show complex alteration textures with the development of several generations of serpentine together with calcite. No remnants of fresh olivine phenocrysts are present, and only very seldom are small cores to olivine macrocrysts preserved. Small rounded grains of ilmenite are rarely observed as inclusions in pseudomorphs after olivine phenocrysts. Random measurements of olivine phenocrysts and macrocrysts indicate similar size characteristics to the quarry kimberlite (Fig. 2.3).

Groundmass phlogopite is an important matrix constituent of the east-end kimberlite where it occurs as randomly oriented laths, usually ~1mm by 0.1mm in size. It is commonly partially replaced by a mixture of serpentine and chlorite. Groundmass phlogopites often host inclusions of spinel, perovskite and monticellite.

Groundmass opaque oxides are extremely abundant and as in the case of the quarry kimberlite, complex zonations and intergrowths between spinels, ilmenite and perovskite are present. Spinels range in size between 0.01 and 0.1mm and usually display euhedral to subhedral morphology while groundmass ilmenites are usually larger (commonly ~0.3mm) and show rounded morphologies.

Perovskite is present in accessory proportions as discrete equant grains throughout the groundmass as well as in the reaction mantles around ilmenite megacrysts and macrocrysts.

Monticellite is volumetrically an extremely important groundmass constituent of the east-end kimberlite. It is largely altered, but easily recognisable due to its ghost remnant texture (Plate 2.23). Monticellite is most commonly replaced by serpentine or a fine grained intergrowth of serpentine and calcite, but in some samples calcite is the only replacement phase. Monticellite occurs either as clusters of fine grained (~0.04mm) subhedral to anhedral crystals, or as inclusions in sieve textured groundmass phlogopite.

Serpentine is a major constituent of the east-end kimberlite. Because of the altered nature of this kimberlite, it is often difficult to distinguish between groundmass serpentine and serpentine in pseudomorphs after olivine phenocrysts. Groundmass serpentine occurs as fine grained, discontinuous infillings of interstitial areas and is often associated with monticellite (Plate 2.23).

Primary calcite is not abundant in the east-end kimberlite but where present forms small interstitial segregations often in association with serpentine. Secondary calcite occurs as a replacement product of olivine phenocrysts and macrocrysts. A number of samples have been found to be dominated by secondary calcite in the form of discontinuous veinlets locally forming larger segregations in the groundmass.

Apatite is a very rare accessory component of the east-end kimberlite and where present occurs as scattered small (0.06mm) stubby prismatic grains.

The globular segregations developed in the east-end kimberlite are similar to the autoliths described by Ferguson et al. (1973). They are relatively common and when liberated from the kimberlite are observed to be near spherical in shape (Plate 2.24). The segregations range from a few millimetres in diameter up to 10 centimetres. They usually contain a nucleus (often a macrocryst or megacryst) which is surrounded by concentric layers of groundmass phases (Plate 2.24). Microscopic observations indicate the globular segregations to be composed of a dense aggregate of altered monticellite, serpentine and opaque oxides.

Modal analyses of the east-end kimberlite (Table 2.4) indicate it to be an "opaque-mineral-rich" serpentine-monticellite kimberlite. An example of east-end kimberlite which has been invaded by calcite (ROM-92) is included in Table 2.4. This sample is classified as a serpentine-calcite kimberlite.

#### 2.4 BRECCIA KIMBERLITE

The breccia kimberlite is an approximately oval shaped body situated in the central region of the diatreme (Fig. 2.1). Access to this kimberlite was severely restricted because stockpiles of quarry kimberlite obscured the limited surface

outcrop. An attempt to sample the breccia kimberlite by means of an exploratory tunnel (from previous prospecting operations, Whitelock, 1973) at the -30m level was unsuccessful because of flooding. Consequently, observations on the breccia kimberlite are based on a single outcrop of limited extent.

#### 2.4.1 Macroscopic Description

The breccia kimberlite is greenish-grey with abundant sub-angular sandstone, shale and dolerite fragments set in a soft serpentinous, micaceous matrix (Plate 2.25). It is a hypabyssal facies kimberlite breccia. Evidence for its hypabyssal character is indicated by the baked nature of abundant shale xenoliths (implying a high intrusion temperature) (Plate 2.25). The kimberlite is classified a breccia due to the abundance of country rock xenoliths (>15 vol%). Whitelock (1973) reports that in some areas sedimentary xenoliths comprise 80 vol% of the rock and the authors observations support this report.

Olivine (pseudomorphed), ilmenite and phlogopite megacrysts are abundant in the breccia kimberlite, while garnet megacrysts are less common. Pyroxene megacrysts (including pyroxene-ilmenite intergrowths) as well as ultramafic xenoliths were not observed. Whitelock (1973) reports that this kimberlite possesses a brecciated texture and soft serpentinous matrix to a depth of 200m (the deepest level drilled).

#### 2.4.2 Microscopic Description

In thin section, the breccia kimberlite is observed to be little more than a featureless mass of extensively altered turbid material cementing together a wide variety of xenolithic fragments. Phlogopite macrocrysts are reasonably well preserved in contrast with the highly altered pseudomorphs after olivine macrocrysts. Alteration in the groundmass is so advanced that pseudomorphs after olivine phenocrysts can only rarely be identified. Mineralogically, the groundmass is composed of serpentine, phlogopite, opaque minerals and calcite (in order of decreasing modal abundance). Opaque minerals are represented by both spinel and ilmenite, with the former being more abundant than the latter. Perovskite is absent as a discrete groundmass phase but may be present in the reaction rims surrounding ilmenite macrocrysts. The kimberlite is qualitatively classified (not based on point counting) as an opaque-mineral rich phlogopite-serpentine kimberlite.

#### 2.5 MICACEOUS KIMBERLITE DYKE

##### 2.5.1 Macroscopic Description

Associated with the Monastery diatreme, is a precursor kimberlite dyke which outcrops over a distance of 2 000m, striking ESE/NWN (Whitelock, 1973) (Fig. 2.1). It intersects the main diatreme in its north western lobe where it is truncated (Fig. 2.1). The dyke has also been traced from the south eastern extremity of the pipe for ~50 metres where it terminates in a small blow which is ~22 metres in diameter

(Fielding, 1981). Only one outcrop of the dyke kimberlite was located by the author (due to extensive vegetation overgrowth and mine rubble), this being exposed in the northwestern wall of the mine.

In hand specimen the dyke is dark bluish grey in colour, hard, brittle and relatively unaltered (Plate 2.26). It is a macrocrystic kimberlite which is easily distinguishable from the quarry kimberlite. Macrocrysts of olivine, phlogopite and rare ilmenite are set in a fine grained uniform textured groundmass. Small country rock xenoliths (mainly fine grained sediments) are present in trace amounts (<1 vol%). This kimberlite has not been observed to host megacryst suite minerals or mantle derived xenoliths.

#### 2.5.2 Microscopic Description

In thin section both populations of olivine are observed to be extensively altered to a mixture of serpentine and calcite. The olivine macrocrysts are clearly smaller in this kimberlite than in the other varieties of kimberlite, ranging in size between 1 and 7mm. Phlogopite macrocrysts are characteristically abundant and their length to breadth ratios are usually in the region of 10:1, ranging in size between 1 to 7mm in length and 0.1 to 1mm in width (Plate 2.27a). They are fresh, and commonly zoned, with rims being darker than cores (Plate 2.27b). Stringers of calcite may be developed along the cleavage traces of phlogopite macrocrysts. Ilmenite macrocrysts are present but are rare. They range in size between 1 and 6mm in longest dimension (average 1.5mm).

Olivine phenocrysts occur in a large range of sizes between 0.05 and 0.85mm and generally display a high degree of idiomorphism. They have been replaced by at least two generations of serpentine, and may also have magnetite and calcite as associated replacement products (e.g. Plate 2.28).

Opaque oxides are abundant in the groundmass and consist of subhedral to euhedral spinels, commonly between 0.01 and 0.1mm in size. Complex zonations between various spinels and groundmass ilmenite are again common, with atoll textures being particularly abundant. No perovskite is present in this kimberlite, which is in marked contrast to the other kimberlite varieties at Monastery. Groundmass ilmenites are again subordinate to spinel, but are well represented. They are usually larger than the groundmass spinels (average ~0.3mm) and commonly show rounded morphologies.

The bulk of the groundmass is composed of altered monticellite, serpentine, calcite and apatite in intimate association (Plate 2.29). Monticellite has been extensively replaced by calcite and is often difficult to recognise. Calcite may occur as irregular segregations in the interstitial areas of the groundmass along with serpentine, but is also present in the form of crude laths hosting inclusions of apatite and groundmass spinel. Dolomite is also well represented in this kimberlite, particularly as a replacement product of olivine macrocrysts.

Apatite is present in unusually high abundances in the dyke kimberlite. It most commonly occurs as inclusions within large calcite grains, but is also present as discrete subhedral to

euohedral grains ranging in size between 0.02 and 0.10mm. The radiating acicular clusters of apatite crystals which were found to be relatively common in the quarry kimberlite are absent in the dyke kimberlite.

Modal analyses presented in Table 2.4 indicate the dyke kimberlite to be an "opaque-mineral-rich" calcite kimberlite. The features distinguishing this kimberlite from the other kimberlite phases at Monastery include:

- (a) the high abundance and well preserved nature of phlogopite macrocrysts
- (b) the extremely low abundance of phlogopite in the groundmass
- (c) the absence of perovskite both as a discrete groundmass phase as well as in the reaction mantle around ilmenite macrocrysts
- (d) the high abundance of apatite, serpentine and calcite, indicating it to be a volatile-rich kimberlite.

3.1    INTRODUCTION AND BRIEF OVERVIEW

Important sources of information as to the nature of the upper mantle as well as mantle processes are provided by suites of xenoliths found in alkali basalts and kimberlites. A simple consideration of the variety of such xenoliths, suggests that the upper mantle must be heterogeneous (Gurney and Harte, 1980). Four major groups of mantle derived xenoliths can be recognised (Harte, 1983), namely:

- peridotites and pyroxenites
- eclogites
- megacrysts or discrete nodules
- glimmerites and marid suite xenoliths

Peridotites are by far the volumetrically most important group of xenoliths and a brief overview of their major features is relevant. More comprehensive reviews have been provided by Meyer (1977), Harte (1978), Gurney and Harte (1980) and Harte (1983). The eclogite and megacryst xenolith categories are reviewed in subsequent sections (4.1 and 6.1 respectively) while MARID suite xenoliths are not considered in this study, because they are rare at Monastery.

In spite of the relatively restricted mineralogy of peridotite xenoliths, there is an abundance of modal varieties and petrographic types. However, harzburgites (olv + opx) and clinopyroxene-poor lherzolites (olv + opx + cpx) both of which

often contain garnet, account for the majority of nodules in this group. Olivine and orthopyroxene usually make up > 90 % of the rock with olivine characteristically dominant. Variable amounts of chromian spinel and/or phlogopite may also be present.

A wide variety of textures and fabrics are developed in peridotite xenoliths in response to deformation and subsequent attempts at recovery (recrystallization and grain growth). An almost equally diverse terminology has been developed in the literature to describe these textures (e.g. Nixon and Boyd (1973 a); Harte et al. (1975); Boullier and Nicolas (1973, 1975); Dawson et al. (1975)) which led Harte (1977) to propose a classification scheme to standardize the nomenclature. Four basic textures are recognised namely coarse, porphyroclastic, mosaic porphyroclastic and granuloblastic (see Table 1 of Harte, 1977). The degree of deformation increases from the essentially undeformed coarse texture to the highly deformed mosaic porphyroclastic texture. Rocks which display a fully recrystallized, strain-free recovered texture are classified granuloblastic.

Two groups of whole rock compositions can generally be recognised in peridotite xenoliths. These were first recognised for nodules from Thaba Putsoa by Nixon and Boyd (1973 a) who labelled them 'depleted' and 'fertile'. The fertile nodules are enriched in Fe, Al, Ca, Na and Ti relative to the depleted nodules and, with the exception of  $K_2O$ , would be capable of yielding a partial melt of basaltic composition. In contrast, the depleted peridotites exhibit refractory compositions consistent with a

residue after basalt extraction. Some workers now relate bulk rock compositions to processes other than melt extraction from the "depleted" lherzolites. For example, Gurney and Harte (1980) attribute the chemical characteristics of the more "fertile" deformed lherzolites to localised diffusive metasomatic exchange near the site of an intrusive event which crystallizes minerals found in kimberlite as discrete nodules.

Studies of mantle-derived xenoliths have placed considerable emphasis on the calculation of equilibration temperatures and pressures using a wide variety of geothermometers and geobarometers. Results have demonstrated that xenoliths at most localities show a bimodal distribution of temperature estimates. This distribution is usually more marked when temperatures are based on the pyroxene solvus rather than Fe-Mg distribution coefficients (Harte, 1983). One group has clinopyroxenes with Ca/Ca+Mg ratios from 0.43 - 0.49 which translate to temperatures in the range 900 - 1100°C whilst the other has subcalcic clinopyroxenes (Ca/Ca+Mg ~ 0.28 - 0.38) which imply temperatures of ~ 1150 to 1400°C. The high temperature group of rocks is frequently deformed, but it is emphasised that deformation is not a characteristic feature of "hot peridotites". In this regard, deformed peridotites from Matsoku and the Kimberley Mines have equilibration temperatures below 1100°C (Harte et al., 1975; Dawson et al., 1975; Boyd and Nixon, 1978).

Peridotite xenoliths can thus be categorised on the basis of texture, geochemical character and calculated equilibration temperature. Harte (1983) proposed a classification in which

three sub-groups are recognised: coarse, deformed and modally metasomatised. The essential features of this classification are summarised in Fig. 3.1. The division into coarse and deformed is based on the textural classification of Harte (1977) with the deformed group including the porphyroclastic and mosaic porphyroclastic types. Rocks in the modally metasomatised group are ones showing evidence of infiltration metasomatism by virtue of the presence of introduced phases such as phlogopite, richterite, ilmenite as well as other oxide phases and sulphides. The chemical subdivisions in Harte's classification are based on mineral chemistry, with the subdivision into Mg-rich and Fe-rich being dependent on whether the  $Mg/(Mg+Fe)$  of olivine is greater or less than 0.91 (Harte, 1983).

Pyroxenites (cpx, opx  $\pm$  minor garnet, olivine) are generally a widespread but volumetrically rare fraction of the xenolith population in kimberlites. Localities hosting extensive pyroxenite suite xenoliths include Matsoku (Cox et al., 1973, Gurney et al., 1975); Koffiefontein (Cardoso, 1980) and Bellsbank (Boctor et al. 1983). Pyroxenites are usually coarse or very coarse grained and are rarely deformed. They commonly show the effects of subsolidus re-equilibration in the form of widespread exsolution textures. The mineral chemistry of the pyroxenites is generally related to that of the peridotites and transitional types with variable amounts of olivine linking the two categories (Harte, 1978).

Evidence of widespread mantle metasomatism is recorded in some peridotite nodules sampled by kimberlite. Pioneering papers on mantle metasomatism include that of Lloyd and Bailey

(1975) who described metasomatism in xenoliths from potassic volcanics of South West Uganda and the West Eifel in Germany. Harte and Gurney (1975) also documented convincing evidence in support of the metasomatic introduction of phlogopite and ore minerals to peridotites from Matsoku.

More recently, Erlank and Rickard (1977), Erlank and Shimizu (1977), Dawson (1979), Erlank et al. (1982), Jones et al. (1982) and Erlank et al. (1987) have documented a suite of metasomatic peridotites from the Bultfontein kimberlite pipe in Kimberley. Metasomatically introduced phases include phlogopite, potassic-richterite, ilmenite, rutile, and sulphides. Extremely rare occurrences of the Ba- and K-titanates lindsleyite and mathiasite have also been documented by Haggerty et al., 1983. Erlank and Rickard (1977) and Erlank et al. (1982) have postulated a possible progressive sequence of metasomatism from peridotites without primary metasomatic minerals, through phlogopite peridotites to phlogopite-richterite peridotites during which garnet is removed. Isotopic data indicates that this suite of nodules has experienced more than one metasomatic event, neither of which is related to their transport in the host kimberlite (Erlank et al., 1982, 1987; F.G. Waters, Pers. Comm.).

Dawson (1982, 1984c) distinguishes two types of metasomatism which he terms 'patent' and 'cryptic' metasomatism. The evidence for patent metasomatism is seen in petrographically recognisable hydrous phases. While cryptic metasomatism refers to a more subtle process causing incompatible element enrichment in depleted peridotites (in terms of basaltic components) in the

absence of replacement minerals. Available isotopic data appears to indicate that cryptic metasomatism is an ancient event (~ 2 by) (Menzies and Murthy, 1980; Cohen et al., 1982; Dawson, 1984<sup>c</sup>).

### 3.2 XENOLITH ABUNDANCES AT MONASTERY

The nomenclature adopted in this study follows that of Streickeisen (1976) with an exception being made for distinguishing between lherzolites and harzburgites. Lherzolites are identified on the basis of the presence of diopside in the sample, rather than in the specified proportions exceeding 5 vol.% (Dawson, 1980). The qualifiers phlogopite- and spinel- are used in the case of rocks hosting primary phlogopite or accessory spinel respectively. No modal limit is set for the use of these qualifiers and in essence they imply phlogopite bearing and spinel bearing. It should be noted that the use of the qualifier 'spinel' is intended as a general term to accommodate the entire range of spinel-group mineral compositions and is only used in cases where no compositional data is available. The more specific qualifiers 'chromite-' and 'Cr-spinel-' are adopted where appropriate and where analytical data is available.

Some additional points concerning the nature and abundance of phlogopite in peridotite xenoliths need to be made at this point. Erlank et al. (1987) have stressed the point that the great majority of peridotites from the Kimberley pipes probably contain at least some primary phlogopite. This is often only

revealed during crushing and mineral separation (Richardson et al., 1985) or when several thin sections are prepared. It has been the author's experience that a similar situation, if not worse, exists at Monastery and it is therefore stressed that the rocks classified as phlogopite-free apparently contain no primary phlogopite.

In order to obtain a quantitative estimate of the relative abundances of the various mantle-derived xenolith types at Monastery, a sample of 600 nodules have been examined and classified. One hundred nodules were identified in situ in the kimberlite and the remaining 500 were sampled from coarse tailings dumps (-32 +20 mm). Emphasis was placed on sampling technique in an effort to obtain a random and representative sample. Xenoliths were examined under a binocular microscope to obtain a more accurate classification.

The results of the survey are summarised in a series of histograms in Fig. 3.2. Dealing firstly with the xenolith population as a whole (Fig. 3.2A), it is evident that garnet lherzolite is by far the most abundant xenolith type present, accounting for 47% of the total population examined. Lherzolites and harzburgites are the next most abundant being represented in approximately equal proportions (22 % and 18 % respectively). Garnet-bearing harzburgites are less than half as abundant as garnet-free harzburgites, which contrasts with the lherzolite suite, where garnet-bearing assemblages dominate by a factor of 2 over the garnet-free assemblages. This is a direct reflection of the residual nature of the harzburgite suite (i.e. garnet and clinopyroxene are the first phases to be

consumed during partial melting). It is likely that the abundance estimate for garnet harzburgites represents an overestimate because of the possibility of diopside not being detected on the small external surfaces of the nodules.

Websterites, wehrlites and pyroxenites are present, but they only constitute a minor proportion of the xenolith population (5%). Marid-suite xenoliths are rare.

A more detailed breakdown of the constitution of the four main categories of xenoliths is provided in Fig. 3.2 B to E. The relative abundances of the various assemblages are clearly illustrated and do not require further comment, however, a number of features warrant highlighting.

- (a) Phlogopite-bearing assemblages abound, indicating a high incidence of modally metasomatised xenoliths at Monastery. It should be noted that due to the considerations discussed above, these estimates represent minimum values.
- (b) Lherzolithic rocks display a higher incidence of modal metasomatism than harzburgitic rocks.
- (c) Within the lherzolite category, garnet-free assemblages more commonly host phlogopite than do garnet-bearing lherzolites.
- (d) Spinel is an unusually common accessory phase.
- (e) Rocks composed of a five and even six mineral phase assemblage are relatively common.
- (f) A small percentage of lherzolites and harzburgites host both garnet and spinel.

### 3.3 PETROGRAPHY

#### 3.3.1 Introduction

In an attempt to characterise the entire suite of mantle-derived xenoliths at Monastery, samples representing a wide range of mineral assemblages have been selected for analysis. These include 15 garnet lherzolites, 3 lherzolites, 6 harzburgites, 5 garnet harzburgites, 8 wehrlites, 3 olivine clinopyroxenites, 2 olivine websterites and 4 pyroxenites (Table 3.1 and Fig. 3.3). Because of the diversity of the suite, petrography is described under four headings, namely:

(a) peridotites (lherzolites and harzburgites), (b) wehrlites and olivine clinopyroxenites, (c) websterites and (d) pyroxenites. The textural classification of Harte (1977) is adopted, details of which are outlined in Appendix 3.1. A full listing of the xenoliths investigated together with textural and modal information is presented in Appendix 3.2.

#### 3.3.2 Peridotites

Nineteen of the twenty-nine peridotite xenoliths have coarse textures. Olivine and orthopyroxene which usually accounts for >90 vol% of the rock (Fig. 3.3) commonly occurs as irregular grains with smoothly curving boundaries collectively forming an interlocking granular texture. Orthopyroxene grain shapes are often more elongate-tabular with consequent straight to gently curving grain boundaries. Grain size predominantly ranges between 2 and 7mm but may be over 1 cm. A small proportion of the coarse peridotites (<15%) show evidence of strain in the form of undulose extinction and kink banding

(Plate 3.1). Within these samples, rare small (generally <1mm) tabular strain-free olivine grains are found (Plate 3.2). These represent recrystallized neoblasts which have undergone grain growth subsequent to deformation.

Garnet typically occurs as large (usually between 3 and 6mm) rounded to irregular fractured crystals which are pale red to violet in colour. They are generally extremely fresh, with only thin kelyphitic margins developed.

Clinopyroxene most commonly occurs as discrete, irregular shaped grains 1 to 3mm in size. They are usually fresh, bright green in colour and show little evidence of internal strain. In some examples alteration has resulted in the development of cloudy grain margins. Similar features described by Carswell (1975) have been attributed to the combined effects of decompression and metasomatism during transport of the xenolith in the kimberlite.

Cox et al. (1987) have noted that garnet and pyroxenes in garnet lherzolites frequently display a close spatial association. This they interpret to indicate that garnet lherzolites may develop from harzburgites by exsolution of clinopyroxene and garnet from high-temperature aluminous and calcium-rich orthopyroxenes. The above mentioned association is observed in the Monastery peridotites (e.g. Plate 3.3) and it is particularly evident in the re-equilibrated rocks shortly to be discussed. Another textural association between garnet and clinopyroxene observed in a coarse garnet lherzolite (ROM-377 LH-108) is illustrated in Plates 3.4 a&b. Here the two phases appear to reflect a reaction relationship with clinopyroxene

replacing garnet.

The common occurrence of phlogopite in the Monastery peridotites has already been highlighted. Both the primary and secondary textural forms recognised by Carswell (1975) are represented. Primary phlogopite occurs as lath shaped grains which are in textural equilibrium (Plate 3.5). They are most commonly <3mm in size, but grains up to 7mm have been noted. Primary phlogopites are characteristically optically uniform although a few examples have been noted to display thin dark brown rims. A spatial association between phlogopite and clinopyroxene is commonly observed. An example of the nature of the secondary phlogopite is illustrated in Plate 3.3.

Amphibole occurs in three of the peridotites investigated (two garnet harzburgites and one phlogopite harzburgite, Table 3.1). It is pale green in colour with a subtle pleochroism to pale-brownish green. In most cases the amphibole displays an interstitial poikilitic texture, in character with its inferred metasomatic origin. The amphibole has been observed to be associated with the breakdown of olivine, orthopyroxene and garnet. This is illustrated in Plate 3.6 (a) where amphibole is observed poikilitically enclosing remnants of an originally larger garnet crystal. Plate 3.6 (b) illustrates amphibole replacing olivine and orthopyroxene. In both cases no phlogopite is present. In the garnet-free harzburgite illustrated in Plate 3.6 (c), all traces of garnet have been reacted out, but remnant textures imply its original presence. In this rock, phlogopite and amphibole are intimately associated.

A large number of the peridotite suite xenoliths contain red-brown chromite as an accessory phase. These are considered to be primary unlike the small Al-rich spinels associated with the kelyphitic rims around garnet. Chromites are usually small (~0.2 - 0.5mm) but can be up to 1.6mm in size. They occur as discrete grains or as inclusions in the four main silicate phases described above. The discrete chromite grains most commonly display anhedral 'interstitial' grain shapes, but more regular morphologies are observed in those occurring as inclusions.

Nine peridotites display textures which are intermediate between porphyroclastic and granuloblastic. They show a wide range in grain size (0.5 to 6mm) which is distinctly bimodal. Large irregular shaped olivine and orthopyroxene grains (4 to 6mm) form a porphyroclasts within an assemblage of smaller (0.5 to 2.5mm) polygonal textured grains (Plate 3.7). These rocks have undergone deformation at some point in their history. This is recorded by the presence of undulose extinction and minor kink banding in some olivine and orthopyroxene porphyroclasts as well as by the presence of elongate or disrupted spinel grains in some harzburgites (Plate 3.8). However, significant grain growth has occurred subsequent to recrystallization so that virtually no fine grained neoblasts remain. A history of subsolidus re-equilibration is evident in the extensive exsolution textures developed in these rocks.

Three varieties of exsolution are associated with the orthopyroxene porphyroclasts:

- tiny brown tablets of Mg-Cr-spinel (see Plate 3.5)

- ultra fine clinopyroxene lamellae parallel to (100)  
(Plate 3.9)
- garnet exsolution in the form of lamellae and/or coagulations  
(Plates 3.10 a&b)

Clinopyroxene exsolution lamellae are typically more concentrated in the regions immediately adjacent to kink bands (this is illustrated in Plate 3.9). Small discrete clinopyroxene grains are also present in these rocks and since these are usually spatially associated with orthopyroxene, it is likely that they have exsolved from orthopyroxene. Fine examples of garnet exsolving from orthopyroxene are observed where the exsolved garnet takes the form of elongate lamellae (Plate 3.10 a) as well as localised coagulations (necklace textures) along orthopyroxene grain boundaries (Plate 3.10 b). Exsolution textures are never observed in recrystallized (polygonal) orthopyroxene grains.

From the above description, it is evident that the textural features of this group of rocks do not strictly match any of the textural categories of the Harte (1977) classification and consequently have been termed 'intermediate peridotites'.

One garnet lherzolite (BD-2234) has a bimodal grain size distribution (average grain sizes of 0.75 and 3mm) in which both populations are dominated by polygonal textured grains (Plate 3.11). Very rare examples of orthopyroxene porphyroclasts with irregular grain shapes and Cr-spinel exsolution lamellae are present. However, the general texture represents a strain-free equilibrium assemblage in which the effects of grain growth clearly dominate and as such can be classified as

granuloblastic. Garnet is present as small ( $\emptyset$ .25 - 1.5mm) rounded grains distributed throughout the rock but always in close proximity to orthopyroxene and as such may be the products of exsolution. The polygranular aggregate of garnet grains illustrated in Plate 3.12 provides an excellent example of a large garnet grain formed by the coalescence of multiple smaller garnets derived from surrounding orthopyroxene grains.

Only one example of a mosaic porphyroclastic textured peridotite was observed (ROM-377 DP-61). It is a garnet lherzolite in which the bulk of the olivines have recrystallized to a mosaic of small strain-free neoblasts ( $<\emptyset$ .3mm) with olivine porphyroclasts being extremely rare. Orthopyroxene occurs as irregular strained porphyroclasts (~1-3mm) showing elongation along the direction of stress. They commonly exhibit recrystallization to a mosaic of neoblasts along grain margins (Plate 3.13 a). Clinopyroxene is well represented and occurs as irregular to rounded strained crystals which show no evidence of recrystallization. They do however commonly display a narrow cloudy zone around grain margins and along fractures, while the core regions are clear and fresh (Plate 3.4 b). This phenomenon has been attributed to decompression effects (Ehrenberg, 1982). Garnets are commonly 1 to 1.5mm in size, rounded in outline with well developed kelyphitic rims (Plates 3.13 a&b).

### 3.3.3 Wehrlites and Olivine Clinopyroxenites

Eight wehrlites and three olivine clinopyroxenites constitute this group of rocks. The majority are extremely

fresh, but some do show variable degrees of alteration. Textures are dominantly coarse equant (Plate 3.14), but three samples have similar textures to the intermediate peridotites previously described (i.e. intermediate between the porphyroclastic and granuloblastic textures of Harte, 1977). Phlogopite is a common constituent and occurs both as large unzoned texturally equilibrated laths (~1.5mm) in intimate association with clinopyroxene (Plate 3.15), as well as in the form of fine grained laths (~0.2mm) within clinopyroxene grains (Plate 3.14). Irregular grains of chromite are also common inclusions in clinopyroxene (Plate 3.14). The high incidence of phlogopite in these rocks may indicate that they have been modally metasomatised and further evidence of this is indicated by the presence of K-richterite in one of the wehrilites (ROM-301) (illustrated in Plate 3.16 a&b).

#### 3.3.4 Olivine Websterites

The two olivine websterites are modally dominated by orthopyroxene (Fig. 3.3). Textures are illustrated in Plates 3.17 and 3.18. Both websterites have coarse grained orthopyroxene (1-3cm) which show extensive exsolution of clinopyroxene and garnet in the form of continuous stringers both within the orthopyroxene as well as along grain boundaries (necklace textures). Exsolved garnet always dominates over clinopyroxene. Minor signs of strain are evident by undulose extinction in the large orthopyroxenes. In both samples olivine occurs as polygonal textured grains and irregular grains of accessory chromite are disseminated throughout.

### 3.3.5 Pyroxenites

Four pyroxenites have been selected for study and these include samples composed of approximately equal proportions of clinopyroxene and orthopyroxene (JJG-1965, JJG-1975 and ROM-318 PY-01) as well as one extremely coarse textured orthopyroxenite (ROM-108). The two-pyroxene rocks display a large range in grain size (0.2-10mm) with large irregular grains of both ortho- and clinopyroxene forming the dominant interlocking texture. Superimposed on this are extensive exsolution features as well as the localised development of polygonal grains (see Plates 3.19 a-c). Primary textured phlogopite is well represented in the two-pyroxene pyroxenites (Plate 3.19 c) and small laths of phlogopite are also hosted as inclusions in clinopyroxene. Anhedral grains of chromite also form common inclusions in clinopyroxene (Plate 3.19 c).

The ultra-coarse orthopyroxenite is illustrated in Plate 3.20. Orthopyroxene grains are irregular and range in size between 1 and 3cm. No sign of deformation is evident. Elongate exsolution lamellae of garnet and clinopyroxene are developed along the well defined cleavage traces of the orthopyroxene. Clinopyroxene lamellae are extremely fine compared to garnet lamellae which frequently form localised coagulations, either within orthopyroxene grains, or along grain boundaries. In the interstitial regions between the coarse orthopyroxenes, small irregular grains (0.5-1.5mm) of clinopyroxene, garnet and rare phlogopite occur. The clinopyroxene and garnet grains are thought to be the products of exsolution.

### 3.4 MINERAL CHEMISTRY

#### 3.4.1 Introduction

The major element compositions of constituent minerals in 46 peridotite and pyroxenite xenoliths have been determined by electron microprobe analysis (see Appendix 1 for analytical details). In addition, a further 95 clinopyroxene and 114 garnet chips taken from a random sample of ultramafic nodules from the coarse tailings dumps have been analysed in a pilot study aimed specifically at:

- (a) assessing the range in equilibration temperature indicated by Monastery xenoliths (from the Ca/Ca+Mg ratio of the clinopyroxenes).
- (b) attempting to locate depleted garnet harzburgites hosting 'G10' garnets.

(pilot study data is presented Appendix 3.3).

For comparative purposes, the mineral compositions of a suite of xenoliths from the nearby Lesotho kimberlite province are featured on some plots. Localities represented are Matsoku (Cox et al., 1973; Gurney et al., 1975); Thaba Putsoa and Mothae (Nixon and Boyd, 1973<sup>a</sup>) and Pipe 200 (Carswell et al., 1979). The Matsoku suite consists of coarse and porphyroclastic textured garnet lherzolites and pyroxenites (some of which are banded). Both coarse and deformed garnet lherzolite are represented in the rocks from Thaba Putsoa and Mothae, while all of the Pipe 200 xenoliths are coarse textured peridotites.

Analyses are listed in Appendix 3.3 and compositions graphically illustrated in Figures 3.4 to 3.21. Summary data for the major mineral species are provided in Table 3.2. In

presenting the mineral chemistry data, five groups of rocks are distinguished, namely:

lherzolites (18), harzburgites (11), wehrlites and olivine clinopyroxenites (11), olivine websterites (2) and pyroxenites (4). Lherzolites and harzburgites are further subdivided according to the presence or absence of garnet. The single mosaic-porphyroclastic textured garnet lherzolite (ROM-377 DP-01) is distinguished on all plots since it represents the only significantly deformed xenolith sampled.

#### 3.4.2 Olivine

A full listing of olivine compositions is listed in Appendix 3.3 A (summary data in Table 3.2). Histograms of forsterite content (Fig 3.4) show that olivines from lherzolites and harzburgites are compositionally indistinguishable, both having forsterite contents within the range 90.9 to 93.6. The presence or absence of garnet in these two groups of rocks is also not reflected in olivine compositions. Olivine from the deformed garnet lherzolite is marginally more Fe-rich ( $FO_{90.3}$ ) than that in the coarse lherzolites and harzburgites. Wehrlites and olivine clinopyroxenites show a wide range in olivine compositions ( $FO_{86.0}$  to  $FO_{91.9}$ ) which are generally more Fe-rich than those in lherzolites and harzburgites. The two olivine-websterites have widely contrasting olivine compositions ( $FO_{86.0}$  and  $FO_{91.1}$ ).

The olivines in Matsoku xenoliths extend to more Fe-rich compositions and display wider range than the full range of compositions observed at Monastery. At Thaba Putsoa and Mothae,

olivine compositions are grouped according to texture with the coarse rocks being similar to those at Monastery (i.e. lherzolites and harzburgites). The single deformed peridotite at Monastery has an olivine composition within the range defined by the deformed peridotites at Thaba Putsoa and Mothae. Olivines from Pipe 200 extend to higher forsterite contents than those at Monastery.

Nickel concentrations in the Monastery olivines dominantly range between 0.30 and 0.45 wt% NiO which is average for olivines from mantle-derived peridotite xenoliths (Meyer, 1977). Minor elements (Ti, Al, Cr, Ca) were only detectable in olivines from deformed garnet lherzolite (Appendix 3.3 A).

#### 3.4.3 Orthopyroxene

Microprobe analyses of orthopyroxenes are listed in Appendix 3.3 B (summary data in Table 3.2). Histograms of  $100(\text{Mg}/\text{Mg}+\text{Fe})$  (at%) are plotted in Fig. 3.5 and compositional distributions similar to those observed for olivines are evident (see Fig. 3.4). Coarse textured lherzolites and harzburgites show a restricted range for  $100(\text{Mg}/\text{Mg}+\text{Fe})$  between 92.1 and 94.5 at %, while the deformed garnet lherzolite is more Fe-rich ( $100(\text{Mg}/\text{Mg}+\text{Fe}) = 90.3$ ). Enstatites from websterites, wehrlites and pyroxenites show a wide range in  $100(\text{Mg}/\text{Mg}+\text{Fe})$  between 89 and 95 at.%. Two rocks in this category have uncharacteristically magnesian compositions namely an websterite (ROM-318 PY-07, M# = 93.5) and the ultra-coarse grained orthopyroxenite (ROM-108).

Titanium concentrations in orthopyroxenes are extremely low (<0.07 wt% TiO<sub>2</sub>) except for those from the deformed garnet-lherzolite (0.33 wt%) and an orthopyroxene-bearing wehrlite (0.19 wt%).

Histograms illustrating the Al<sub>2</sub>O<sub>3</sub> contents of orthopyroxene are presented in Fig. 3.6. Lherzolites, garnet lherzolites and garnet harzburgites have enstatites with restricted Al<sub>2</sub>O<sub>3</sub> (between .65 and .91 wt%). Similar trends are observed for orthopyroxenes from the Matsoku rocks as well as from coarse peridotites from Thaba Putsoa and Mothae. Orthopyroxene in the deformed garnet lherzolite is slightly enriched in Al<sub>2</sub>O<sub>3</sub> (1.02 wt%) which is in character with its higher temperature as shown to a greater extent by the deformed rocks from Thaba Putsoa. Enstatites from harzburgites show a bimodal distribution of Al<sub>2</sub>O<sub>3</sub> concentrations, a feature also observed in the Pipe 200 data. The four harzburgites with elevated Al<sub>2</sub>O<sub>3</sub> contents (2.33 to 2.59 wt%) also contain aluminous Cr-spinels rather than the more common Al-poor chromites. Wehrlites, websterites and pyroxenites have orthopyroxenes with Al<sub>2</sub>O<sub>3</sub> contents ranging between .20 and .93 wt%.

In the majority of xenoliths, orthopyroxene chrome concentrations fall within the range 0.1 to 0.5 wt% Cr<sub>2</sub>O<sub>3</sub>. However, the orthopyroxene in the four aluminous harzburgites show slight enrichments in Cr<sub>2</sub>O<sub>3</sub> (.51 to .67 wt%).

Figure 3.7 illustrates the CaO contents of the orthopyroxenes. Coarse lherzolites, garnet lherzolites and harzburgites have orthopyroxene CaO concentrations which range

between .19 and .67 wt%. Orthopyroxenes from garnet harzburgites have very restricted CaO contents between .23 and .38 wt%. The deformed garnet lherzolite has slightly elevated CaO in orthopyroxene as is the case at Thaba Putsoa and Mothae. Orthopyroxene from the pyroxenites, websterites and one wehrlite show very low and restricted CaO concentrations (.22 to .24 wt%), but the second orthopyroxene-bearing wehrlite is enriched in CaO (1.09 wt%).

Enstatites in Monastery peridotites have similar CaO contents to those in the coarse textured peridotites from Thaba Putsoa, Mothae and Pipe 200, however, enstatites from the Matsoku xenoliths tend towards marginally higher values of CaO.

Na<sub>2</sub>O concentrations range between .01 and .19 wt% in orthopyroxenes from all xenoliths excluding the deformed garnet lherzolite which has orthopyroxene with 0.24 wt% Na<sub>2</sub>O.

#### 3.4.4 Clinopyroxene

Clinopyroxene compositions (Appendix 3.3 C) indicate that they are calcic diopsides with restricted 100(Ca/Ca+Mg) ratios (Fig. 3.8). The majority of diopsides analysed in the pilot study have Ca/Ca+Mg ratios between 45 and 50. This is similar to the coarse peridotites from Thaba Putsoa, Matsoku and Pipe 200, indicating hot deformed-textured peridotites to be extremely rare at Monastery. For the entire suite of xenoliths studied, only diopside in the deformed garnet lherzolite had a 100(Ca/Ca+Mg) ratio outside the range 45 to 50 and its value of 39 correlates with the calcic (cool) extreme of the deformed

peridotites at Thaba Putsoa.

Similar trends of  $100(\text{Mg}/\text{Mg}+\text{Fe})$  to those described for olivines and orthopyroxenes are observed for diopside (not illustrated). Diopsides in the pilot study showed a range between 88 and 96 which accommodates the range observed in the xenoliths (lherzolites - 90.3 to 95.6; pyroxenites and wehrlites - 88.8 to 91.8; Table 3.2).

$\text{TiO}_2$  concentrations are dominantly below 0.3 wt% with only the diopside in the deformed lherzolite (0.62 wt%) and three wehrlites showing higher levels (0.32 - 0.45 wt%).

Clinopyroxene compositions are discriminated into two groups on plots of  $\text{FeO}$  vs  $\text{Al}_2\text{O}_3$  and  $\text{Na}_2\text{O}$  vs  $\text{Al}_2\text{O}_3$  (Figs. 3.9 and 3.10). Figure 3.9 shows that peridotitic and websteritic diopsides have lower  $\text{FeO}$  (1.39 - 2.52 wt%) and generally higher  $\text{Al}_2\text{O}_3$  contents (1.66 - 4.44 wt%) than those in wehrlites and pyroxenites ( $\text{FeO} = 2.11 - 3.71$ ;  $\text{Al}_2\text{O}_3 = .34 - 2.31$ ). On the plot of  $\text{Na}_2\text{O}$  vs  $\text{Al}_2\text{O}_3$  (Fig. 3.10), the two groups both display a positive correlation between the oxides plotted, but define separate trends. The observed correlation relates to Na and Al being major components of the jadeite molecule ( $\text{NaAlSi}_2\text{O}_6$ ). Diopsides from wehrlites and pyroxenites show a more restricted range and lower average  $\text{Na}_2\text{O}$  concentration than those for peridotitic and websteritic diopsides (1.17 - 2.24 wt% respectively). Similar features are observed for  $\text{Cr}_2\text{O}_3$  but are not illustrated (see Table 3.2).

### 3.4.5 Garnet

A listing of garnet analyses is presented in Appendix 3.3 D (summary data in Table 3.2). Figure 3.11 shows that garnets from the pilot study as well as those from lherzolites and harzburgites have  $100 \text{ (Mg/Mg+Fe)}$  ratios in the range 80 to 88 at% and as such are similar to garnets from Thaba Putsoa and Pipe 200. Garnets from the websterites and pyroxenites show some overlap, but range to the more Fe-rich compositions observed at Matsoku.

$\text{TiO}_2$  concentrations are typically below detection limits except for the garnet in the deformed garnet lherzolite which has 1.32 wt%  $\text{TiO}_2$ . Trace levels of  $\text{Na}_2\text{O}$  (0.09 wt%) were also detected in this garnet.

A plot of CaO against  $\text{Cr}_2\text{O}_3$  (Fig. 3.12) illustrates that garnets from all groups of xenoliths analysed, plot on the lherzolite trend of Gurney and Switzer (1973) and Sobolev et al (1973). CaO concentrations range between 4.39 and 6.01 wt% and  $\text{Cr}_2\text{O}_3$  between 2.38 and 6.12 wt%. The majority of garnets from the pilot study (98 of the 116 analysed) also plot on the lherzolite trend, but some garnets and from harzburgites show calcium undersaturation. One example of a harzburgite similar to the Group II harzburgites found at Premier (Danchin, 1979) was noted in the pilot study.

### 3.4.6 Phlogopite

Carswell (1975) drew attention to the textural and chemical differences between primary and secondary phlogopite in

peridotite xenoliths sampled by kimberlite. Since then, much data on the composition of phlogopites from kimberlites and associated xenoliths has become available (e.g. Dawson and Smith, 1975, 1977; Harte and Gurney, 1975; Smith and Dawson, 1975; Smith et al, 1978; Delaney et al., 1980; Jones et al., 1982; Erlank et al., 1987) indicating that some overlap between the different textural groups exists. Delaney et al. (1980) therefore points out that careful consideration should be given to both textural and chemical features when discussing the origin of phlogopites. All phlogopites analysed in this study (Appendix 3.3E; Table 3.2) are considered to be primary and phlogopites from kelyphite rims surrounding garnets, forming rims or overgrowths on other minerals, or occurring in serpentinous veins, have not been analysed.

Examination of the ranges in phlogopite compositions for individual groups of xenoliths (Table 3.2) indicates that the phlogopite in lherzolites, harzburgites and websterites are compositionally similar, while those in wehrlites and pyroxenites group together. Consequently, only two groups of phlogopites (for simplicity referred to as peridotitic and wehrlitic) are distinguished in the discussion and diagrams which follow.

Peridotitic phlogopites show a range for  $100 \text{ (Mg/Mg+Fe)}$  of between 92.0 and 95.2, while wehrlitic phlogopites display a range of between 89.7 and 94.4 for this ratio. A plot of atomic Si versus atomic Al (Fig. 3.13) shows that the peridotitic phlogopites have values for  $\text{Si} + \text{Al} > 8.0$  (for  $O=22$ ), while those from the wehrlite group generally have  $\text{Si} + \text{Al} \sim 8.0$ .

This indicates that for both groups of phlogopite  $Fe^{3+}$  is not stoichiometrically necessary to fill the tetrahedral sites.

Figure 3.14 demonstrates the primary nature of the phlogopites analysed in this study. Peridotitic phlogopites have FeO between 2.34 and 3.03 wt% and  $Cr_2O_3$  between .62 and .95 wt% and plot within or close to the primary peridotite field of Dawson and Smith (1977). Wehrlitic phlogopites have lower  $Cr_2O_3$  (.13 - .54 wt%) and higher average FeO (2.80 - 5.16 wt%) and as such fall almost exclusively in the metasomatic field demarcated by Dawson and Smith (1977). The ultra-coarse orthopyroxenite (ROM-108) contains phlogopite which is chemically similar to peridotitic phlogopite.

$Cr_2O_3$  and FeO are again plotted in Fig. 3.15 where the Monastery phlogopites are compared with primary phlogopites from two of the peridotite groups in Kimberley Pool xenoliths (Erlank et al., 1987) as well as primary phlogopites from the Matsoku xenoliths (Harte and Gurney, 1975). The Monastery peridotitic phlogopites show similarities with the field of compositions defined by phlogopite in garnet-phlogopite peridotites (GPP), while those from wehrlites fall within the low  $Cr_2O_3$  (<0.6 wt%) field of phlogopites from the metasomatised phlogopite-richterite peridotites (PKP). Matsoku phlogopites (Harte and Gurney, 1975) define a range in compositions which extends into both groups.

Plotting  $Cr_2O_3$  against  $TiO_2$  (Fig. 3.16) shows that the peridotitic phlogopites at Monastery have similar  $TiO_2$  concentrations (.01 - .83 wt%) to those in GPP phlogopites. Moreover, the Monastery wehrlitic phlogopites again correlate

with those from the PKP rocks, but extend to lower  $\text{TiO}_2$  contents (.10 - .60 wt%). Phlogopites from Matsoku are noted to be substantially enriched in  $\text{TiO}_2$ .

A plot of  $\text{Na}_2\text{O}$  against  $\text{Al}_2\text{O}_3$  (Fig. 3.16) again effectively discriminates between peridotitic and wehrlitic phlogopites. The former have high  $\text{Al}_2\text{O}_3$  (12.44 - 15.17 wt%) and  $\text{Na}_2\text{O}$  (.16 - 1.49 wt%) compared to the generally lower concentrations for these oxides ( $\text{Al}_2\text{O}_3$  10.96 - 12.40 wt%;  $\text{Na}_2\text{O}$  .18 - 0.56 wt%) in the latter. The similarities between the peridotitic phlogopites and Kimberley GPP phlogopites as well as the wehrlitic phlogopites and Kimberley PKP phlogopites is again demonstrated.

The series of plots presented has demonstrated the existence of two compositionally distinct groups of phlogopite in Monastery xenoliths. Phlogopites from lherzolites, harzburgites and websterites are compositionally similar to those in garnet-phlogopite peridotites from the Kimberley Pool (Erlank et al., 1987), while those in wehrlites and pyroxenites show the compositional characteristics of phlogopite in the metasomatised phlogopite-richterite peridotites described by Erlank and co-workers. The possible significance of this will be addressed in the forthcoming discussion section.

#### 3.4.7 Chromites and Cr-Spinels

Due to the considerable compositional range displayed by primary spinels in mantle xenoliths, Carswell (1980) proposed that three classes of spinel-bearing xenoliths be recognised,

namely: Al-spinel peridotites [spinel  $100\text{Cr}/(\text{Cr}+\text{Al}) < 25$ ], Cr-spinel peridotites [spinel  $100\text{Cr}/(\text{Cr}+\text{Al}) - 25-65$ ] and chromite peridotites [spinel  $100\text{Cr}/(\text{Cr}+\text{Al}) > 65$ ]. Carswell's terminology is adopted in this study and Fig. 3.18 indicates the spinels in Monastery xenoliths to be chromites and Cr-spinels with the latter group only being represented in harzburgites. A full listing of chromite and Cr-spinel analyses is presented in Appendix 3.3 F and compositional statistics in Table 3.3.

The low  $\text{Fe}_2\text{O}_3$  and  $\text{TiO}_2$  contents of the chromites and Cr-spinel indicate only a small component of inverse spinel (i.e. magnetite and ulvospinel) to be present. This means that compositions are confined to the base of the spinel prism of Haggerty (1976) and therefore that major compositional variations are observed in the normal spinel components Cr, Al,  $\text{Fe}^{2+}$  and Mg.

The plot of  $\text{Fe}^{2+}$  versus Mg presented in Fig. 3.19 shows the spinel compositions to closely follow the tetrahedral site control line for normal spinels. The Cr-spinels are more magnesian than the chromites and it is noted that chromites in pyroxenites, websterites and wehrlites are enriched in iron relative to those in garnet lherzolites and garnet harzburgites (see Table 3.3 and Appendix 3.3).

The clear break in compositions between the Cr-spinels and chromites is well illustrated on the Cr versus Al plot presented in Fig. 3.20. Cr-spinel closely follow the octahedral site line, while the marginal departure of the chromite compositions from this line is caused by the presence of Ti and  $\text{Fe}^{3+}$  substituting for Cr and Al in the octahedral site.

Spinel compositions are generally homogeneous both on the individual grain scale, as well as within single samples. However, some zonation and compositional variation within samples is noted (see Appendix 3.3 F analyses 11-16). Zonation trends are always Cr and Fe enrichment with complimentary Al and Mg depletion from grain cores to margins.

#### 3.4.8 Ilmenite

Ilmenite was found to be extremely rare in the Monastery xenoliths, occurring only as an accessory phase in a wehrlite (ROM-197) and a phlogopite-chromite harzburgite (BD-2279). Compositions which are listed in Appendix 3.3 G show moderately high MgO contents (8.61 - 12.86 wt%) with relatively low levels of Cr<sub>2</sub>O<sub>3</sub> (1.76 - 2.31 wt%). End-member compositions indicate the dominance of the ilmenite (FeTiO<sub>3</sub>) and geikielite (MgTiO<sub>3</sub>) molecules with only a minor presence of hematite (Fe<sub>2</sub>O<sub>3</sub>).

#### 3.4.9 Amphibole

Three garnet-harzburgites and one of each of a phlogopite-harzburgite, olivine-websterite and phlogopite-wehrlite contained amphibole which on a textural basis is considered to be metasomatic (see for example Plates 3.6 a-c). Microprobe analyses are presented in Appendix 3.3 H and compositional statistics in Table 3.4. Five of the six amphibole occurrences are edenitic and pargasitic hornblendes (terminology of Leake, 1978), with richterite being present in

the phlogopite wehrlite (ROM-301). The edenitic amphiboles have 100 (Mg/Mg+Fe) ranging between 91.4 and 93.6 and contain substantial Al<sub>2</sub>O<sub>3</sub> (Av 11.13 wt%), Cr<sub>2</sub>O<sub>3</sub> (Av 2.11 wt%), Na<sub>2</sub>O (Av 3.88 wt%) and K<sub>2</sub>O (Av 1.09 wt%) (Table 3.4). As such, they are similar to the amphiboles described by Boyd (1971 b) and Dawson and Smith (1975) to be intergrown with 'fingerprint' textured Cr-spinels. Figure 3.21 illustrates that all but one of the edenitic amphiboles appear to be in chemical equilibrium with co-existing primary silicate phases (orthopyroxene shown in Fig. 3.21).

The richterite in the phlogopite-wehrlite (ROM-301) is characteristically low in Al<sub>2</sub>O<sub>3</sub> and CaO but enriched in SiO<sub>2</sub>, TiO<sub>2</sub>, MgO and K<sub>2</sub>O relative to the edenitic amphiboles (Appendix 3.3 H).

Site occupancies in the amphiboles calculated according to the method of Leake (1978) are shown in Table 3.5. In the edenitic amphiboles, the tetrahedral sites are completely filled by Si and Al while the M<sub>1,2</sub> and 3 octahedral sites are occupied by Al<sup>VI</sup>, Cr, Ti, Mg and Fe<sup>2+</sup>, with excess Fe<sup>2+</sup> combining with Ca and small amounts of Na to fill the M<sub>4</sub> site. Occupancy of the 12 co-ordinated alkali site (A-site) approaches 1.0 in all cases. The richterite amphibole (ROM-301) has insufficient Al to fill the tetrahedral site and a small amount of Cr<sup>3+</sup> is required to fill the vacancy. Furthermore, a major proportion of the Na present is accommodated in the octahedral M<sub>4</sub> site. Details of the Leake (1978) classification are also provided in Table 3.5.

### 3.5 GEO THERMOMETRY AND GEOBAROMETRY

#### 3.5.1 Introduction and Brief Review

The concept of geothermometry and geobarometry relies on the fact that the constituent minerals of an equilibrium assemblage will respond to changes in physical conditions e.g. temperature (T) and pressure (P) with systematic and predicted compositional changes. The specific reactions which are P, T sensitive may therefore be calibrated by experimental and/or theoretical methods, enabling the equilibration conditions of nodule suites to be calculated from mineral compositions. A wide variety of problems and uncertainties are however encountered, and these require careful consideration. The more important shortcomings and problems discussed by Bell (1985) are outlined below:

- (a) Probably the most commonly encountered and serious problem is a failure to attain chemical equilibrium during the experimental calibrations of the P,T sensitive reactions.
- (b) Extrapolation of experimental data from pure systems to natural complex systems is a major source of potential error. Commonly the effects of elements such as Ti, Al, Cr, Fe, Ca and Na are not accommodated and they may be significant components of natural mantle minerals.
- (c) Extrapolations beyond the physical bounds of experimental data are often made and this represents a potential source of significant error. A good example of this is the application of the MacGregor (1974) barometer to systems in which the orthopyroxene contains less than 2 wt%  $Al_2O_3$ .

- (d) A small degree of error derived from the application of statistical techniques to experimental data (e.g. best-fit regression lines through data points) is commonly inherent in geothermometer and geobarometer equations.
- (e) A major shortcoming of many thermometers is the failure to quantify the pressure effect on the reaction.
- (f) Analytical error in the mineral compositional data applied to geothermometer and geobarometer equations will affect the accuracy of the result.
- (g) The assumption that all Fe is present as  $\text{Fe}^{2+}$  or the estimation of the amount of  $\text{Fe}^{3+}$  based on stoichiometry are potential sources of error.
- (h) Pressure often has to be estimated in order to satisfy the pressure-term in many geothermometer equations. This obviously introduces a degree of uncertainty to the calculated result.

Of the large variety of potentially useful reactions investigated, only a few have enjoyed extensive application. These include:

- (i) **the diopside-enstatite solvus** (geothermometer)  
e.g. Davis and Boyd (1966); Wood and Banno (1973); Nehru and Wyllie (1974); Mori and Green (1975); Lindsley and Dixon (1976); Lindsley and Andersen (1983); Brey and Huth (1984) and Bertrand and Mercier (1985).
- (ii) **Fe-Mg exchange between garnet and clinopyroxene**  
(geothermometer) e.g. Raheim and Green (1974); Mori and

Green (1978); Ellis and Green (1979); Ganguly (1979) and Saxena (1979).

**(iii) Fe-Mg exchange between garnet and olivine**

(geothermometer) e.g. O'Neill and Wood (1979); Kawasaki (1979); O'Neill (1981).

**(iv) Al content of orthopyroxene equilibrium with garnet**

(geobarometer) e.g. MacGregor (1974); Wood (1974); Akella (1976); Lane and Ganguly (1980); Perkins and Newton (1980); Perkins et al. (1981); Yamada and Takahashi (1984); Gasparik (1984); Nickel and Green (1985).

A comprehensive review of the merits and shortcomings of each of the above thermometers and barometers is beyond the scope of this study. Reviews have been provided by Carswell and Gibb (1980), Mitchell et al. (1980) and Finnerty and Boyd (1984). Carswell and Gibb (op cit) undertook a comprehensive comparison of a large number of thermometers and they adopted an approach whereby the temperatures obtained from each method were plotted against the mean value given by all of the ten methods tested. They then selected five thermometers that consistently gave results closest to the average and concluded that the mean result from the five 'superior' methods would yield the most accurate estimate of the true equilibration temperature. The validity of this approach has been questioned by other workers e.g. Boyd and Finnerty (1980); Finnerty and Boyd (1984) and Mitchell (1984<sup>b</sup>) who believe that such averaging would produce a less accurate result than a well chosen single calibration.

Finnerty and Boyd (op. cit.) adopted an approach whereby individual thermometer-barometer pairs were tested for accuracy by determining whether the P-T estimates derived for selected nodules complied with other petrological constraints such as the presence of diamond, graphite or phlogopite in these nodules. Precision was evaluated by measuring the scatter of P-T estimates produced when applying the thermobarometers to a number of analyses from individual nodules. These authors concluded that the combination of the uncorrected diopside enstatite miscibility gap of Lindsley and Dixon (1976) with the uncorrected Al-enstatite barometer of MacGregor, (1974) to be most satisfactory. They also found that the thermometers based on  $\text{Fe}^{2+}/\text{Mg}$  exchange reactions were imprecise compared to the pyroxene solvus thermometers because of the uncertainties related with the oxidation state of iron.

Several new thermometers and barometers have become available since the evaluations of Carswell and Gibb (1980) and Finnerty and Boyd (1984) and a brief overview of these follows.

Harley (1984a) experimentally investigated the pressure-temperature-compositional dependence of the solubility of  $\text{Al}_2\text{O}_3$  in orthopyroxene coexisting with garnet in the P-T range 5-30 kbars and 800-1200°C in the system  $\text{FeO-MgO-Al}_2\text{O}_3\text{-SiO}_2$  (FMAS). The results of these experiments were then extended to the CFMAS system to determine the effects of calcium in the system. Harley (1984b) tested the garnet-orthopyroxene geobarometer developed by Harley (1984a) on a suite of peridotite and pyroxenite xenoliths selected from the literature. Temperatures were calculated by the methods of

Ellis and Green (1979) and Wells (1977). The P-T estimates obtained were in good general agreement with previously determined geotherms at lower temperatures but pressures were underestimated for the high-temperature rocks. Harley (op cit) stressed that calculated pressures are critically dependant on the estimated temperature and hence on the thermometer used. He also emphasised the point that analytical uncertainty particularly in the determination of low levels of Al in orthopyroxene is greatly magnified in the calculating of equilibration pressures. He estimates that for the higher P-T xenoliths the total error in calculated pressures may be as great as  $\pm 10$  kbars.

Nickel and Green (1985) performed experiments in the systems CaO-MgO-Al<sub>2</sub>O<sub>3</sub>-SiO<sub>2</sub> (CMAS) and SiO<sub>2</sub>-MgO-Al<sub>2</sub>O<sub>3</sub>-CaO-Cr<sub>2</sub>O<sub>3</sub> (SMACCR) and in natural peridotite compositions in the pressure range 20-40 kbars and temperature range 1000-1400°C to evaluate the influence of Cr<sub>2</sub>O<sub>3</sub> on the orthopyroxene-garnet geobarometer. They assessed the applicability of the barometer to natural systems by two means. The first involved crystallizing two natural peridotite compositions at 35 kbars over a temperature range from 1000 to 1400°C and then analysing a set of 10 run products. The calculated pressures yielded a mean of 35.5 kbars with a 1.6 Kbar standard deviation. The second method of evaluation involved the selection of five garnet lherzolites which yielded temperature estimates using Wells (1977) in the range 930-960°C. These nodules had garnets with Cr<sub>2</sub>O<sub>3</sub> concentrations ranging from 2 to 8 wt%. The calculated pressures derived from the Wood (1974) method varied with

Cr<sub>2</sub>O<sub>3</sub> content (from 27 to 33 kbars) suggesting a systematic error. However, the Cr corrected barometer of Nickel and Green yielded a consistent estimate of 37± 2 kbars for all nodules. Nickel and Green 1985 noted that the Harley (1984a) barometer yields systematically lower pressure estimates (of the order of 3-5 kbars) than their barometer and they consider this to be mainly due to the different approaches to the calculation of  $x^{M1/Al}$  adopted in the two methods.

Bertrand and Mercier (1985) have recently published a geothermometer based on the mutual solubility of coexisting orthopyroxene and clinopyroxene. They made use of an iterative technique whereby the geothermometer was developed in a stepwise process from very simple systems (e.g. CMS, MAS) using simple solution models. After each step in the process, data was compared with experimental data from a natural system. They concluded that the CFMS system provides an excellent analogue of the natural system, with only a correction for Na being necessary. They indicate that the derived geothermometer is directly applicable to natural samples within the entire range of equilibrium conditions reasonably expected from a mantle xenolith suite.

Two further geothermometers have recently become available, namely that of Harley (1984c) based on the Fe/Mg exchange between garnet and orthopyroxene, and the two pyroxene thermometer of Nickel et al. (1985). These methods are not considered further due to the serious limitations on accuracy and precision of the former, and the inapplicability of the latter to natural rocks.

A comprehensive assessment of the results derived from a large number of geothermometer/barometer combinations is not an aim of this study. Three geothermometers (Lindsley and Dixon, 1976; Bertrand and Mercier, 1985; O'Neill and Wood, 1979) and two geobarometers (MacGregor, 1974; Nickel and Green, 1985) have been selected to calculate T,P estimates. The O'Neill and Wood (1979) thermometer is necessary for the garnet harzburgite assemblages, while the choice of the Lindsley and Dixon (1976) geothermometer in combination with the MacGregor (1974) barometer, is based on the recommendation of Finnerty and Boyd (1984). A combination of the recent Bertrand and Mercier (1985) and Nickel and Green (1985) methods has been calculated for comparison with the Lindsley and Dixon (1976) - MacGregor (1974) results.

In the discussion which follows, the following abbreviations are adopted:

- LD76 - Lindsley and Dixon (1976)
- M74 - MacGregor (1974)
- BM85 - Bertrand and Mercier (1985)
- NG85 - Nickel and Green (1985)
- OW79 - O'Neill and Wood (1979)

### 3.5.2 Results

The results of the T, P calculations are tabulated in Table 3.6 and plotted on P-T diagrams in Fig. 3.22 (a&b) where they are compared to the theoretical geotherms of Clarke and Ringwood (1964) and Pollack and Chapman (1977). Also plotted are the

diamond-graphite univariant curve of Kennedy and Kennedy (1976), the dry peridotite solidus of Ito and Kennedy (1967), the vapour saturated peridotite solidus of Boettcher et al. (1979) and the ZIVC solidus of Egglar and Wendlandt (1979).

The LD76 vs M74 combination (Fig. 3.22 a) yields a wide range in calculated P,T values (483-1268°C; 9.7-57.5 kbars) which when plotted, collectively define an array in P, T space of similar configuration but intermediate between the two theoretical geotherms shown. Garnet lherzolites are represented in the entire range of equilibration conditions, while garnet harzburgites are restricted to the range 800-900°C, 30-38 kbars. Websterites, pyroxenites and wehrlites dominate the low T, P range of the suite (620-800°C; 19-27 kbars; see also Table 3.6) and according to the combination of methods applied, all but two of the xenoliths have equilibrated in the graphite stability field. The single deformed garnet lherzolite yields a calculated T and P of 1268°C and 58 kbars and as such plots with the hot deformed peridotites from Thaba Putsoa and Mothae. The coarse textured Lesotho xenoliths from Thaba Putsoa, Mothae and Pipe 200 indicate a more restricted range of equilibration conditions which coincide with the majority of garnet lherzolites and harzburgites from Monastery. However, the Monastery pyroxenites, websterites as well as five garnet lherzolites yield significantly lower calculated T's and P's. The Matsoku suite does not define a P-T array, but indicates xenoliths to have equilibrated under essentially uniform P, T conditions (~1050°C, 48 kbars).

The data from the BM85 vs NG85 combination (Fig. 3.22b) define a significantly narrower range in calculated T and P compared to the LD76 vs M74 results. Data points are systematically displaced to slightly lower pressures, so that the defined P,T array is virtually coincident with the  $42\text{mWm}^{-2}$  convection related continental shield geotherm of Clarke and Ringwood (1964). The ZIVC solidus of Egglar and Wendlandt (1979) approximates the upper stability limit of phlogopite (Finnerty and Boyd, 1984) and all samples plot below this solidus indicating that the constraints imposed by the presence of phlogopite are not violated. This is also true for the LD76 vs M74 data (Fig. 3.22a) Moreover, it is noted that the amphibole-bearing garnet harzburgites plot within the amphibole stability field of Kushiro (1970) when the NG85 barometer is combined with the BM85 thermometer (Fig. 3.22b), but fall outside this field when M74 pressures are adopted (Fig. 3.22a). Only the deformed garnet lherzolite falls equilibrated within the diamond stability field.

A more comprehensive comparison of calculated T's and P's is presented in Figures 3.23 to 3.25. There is generally a reasonable agreement between the ranges of calculated temperatures for the three thermometers employed (Fig. 3.23). The coarse textured rocks define a bimodal temperature distribution for all methods and this is most clearly defined for the BM85 technique, which shows distinct clusterings in the temperature ranges  $750\text{--}800^\circ\text{C}$  and  $850\text{--}950^\circ\text{C}$ . The BM85 temperatures are higher than LD76 temperatures in the low-T range ( $<800^\circ\text{C}$ ) and this is more clearly illustrated in Fig. 3.24 (a) where xenoliths with LD76 temperatures between  $480$

and 800°C are shown to have BM85 temperatures in the restricted range 700-800°C. A good correlation between the two methods exists for temperatures exceeding 800°C.

A similar feature is observed when LD76 temperatures are compared with OW79 temperatures (Fig. 3.24 b), but in this case there are also considerable discrepancies for temperatures exceeding 950°C where OW79 significantly underestimates. Comparing the results of the BM85 and OW79 methods (Fig. 3.24 c), agreement is generally reasonable below 950°C with OW79 temperatures being marginally higher in the low temperature range. Again the OW79 thermometer is observed to underestimate for temperatures exceeding 950°C.

The BM85 values appear to be the most reliable, since they agree with the OW79 results in the low temperature range (where the LD76 method yields spurious results) as well as correlating extremely well with the LD76 results for temperatures exceeding 800°C (where the LD76 method has been shown to be reliable, Finnerty and Boyd, 1984). The OW79 method has previously been noted to underestimate temperatures in the range above 1000°C (Finnerty and Boyd, 1984).

A significant point to be noted is that all methods result in a bimodal temperature distribution for the coarse xenolith suite at Monastery.

Pressure estimates are compared on histograms in Fig. 3.25, where it is shown that values obtained for the M74 technique have a wider range than those for the NG85 method which are also systematically lower. It is difficult to assess these

observations, since pressure estimates are significantly affected by the temperature values adopted in the calculation. The observed trends therefore largely represent a reflection of the temperature discrepancies previously discussed.

When T, P estimates are compared with the textural features observed in the xenoliths (Fig. 3.26 a&b), it is evident that the bimodal temperature distribution for the coarse rocks correlates with texture. The low T,P group of rocks correspond with those petrographically classified intermediate and granuloblastic textures. One coarse textured garnet lherzolite (RCM-69) plots with this group, but does not show petrographic evidence of re-equilibration. As previously pointed out, the single garnet lherzolite with a mosaic porphyroclastic texture, displays significantly higher calculated temperatures and pressures of equilibration compared to the coarse suite of xenoliths.

There appears to be a correlation between equilibration pressure and the presence of chromite in the garnet lherzolite assemblage. This is illustrated in a series of histograms in Fig. 3.27 which show that rocks hosting both garnet and chromite (C & D in Fig. 3.27) generally have lower equilibration pressures than chromite-free garnet lherzolites (A & B in Fig. 3.27). This correlation is observed for both techniques of pressure calculation, but is more pronounced in the M74 data. This feature could be due to a number of effects which will be addressed in the ensuing discussion.

### 3.6 DISCUSSION

Two major features to emerge from this investigation of the ultramafic xenolith at Monastery have been firstly, the extreme rarity of deformed xenoliths and secondly, the high incidence of modally metasomatised xenoliths at this locality. This is evident in Table 3.7 which summarises the Monastery suite classified according to the scheme of Harte (1983). The overwhelming majority of coarse textured xenoliths are Mg-rich with only websterites, wehrlites and pyroxenites being represented in the Fe-rich categories.

The P-T diagrams presented in Fig. 3.22 have indicated that the calculated equilibration conditions for the Monastery xenoliths define an array of similar configuration to theoretically calculated geotherms for continental shield areas. The problems associated with the application of geothermometers and barometers to natural systems have already been outlined and various authors (e.g. Harte, 1978; Harley and Thompson, 1984) have cautioned against accepting P, T estimates at face value. The geothermometers and geobarometers adopted in this study are however considered to be reliable indicators of at least the relative differences in P,T conditions within the suite, but fine-scale interpretation of the data is not warranted.

Considerable controversy has surrounded the interpretation of P-T arrays defined by xenolith suites. Boyd and Nixon in a series of papers (Boyd, 1973; Nixon and Boyd, 1973 a&b; Boyd and Nixon, 1973, 1975) interpreted the arrays to represent fossil geotherms with inflections resulting from perturbations caused by stress heating associated with lithospheric plate movements.

The xenoliths were thus interpreted as representing a near continuous vertical sample of a section of the upper mantle. Various authors doubted the feasibility of the stress-heating hypothesis and reinterpreted the inflection using mantle diapir or plume models (Green and Gueguen, 1974; Parmentier and Turcotte, 1974). Subsequently, Boyd and Nixon (1978) discarded the stress-heating aspect of their model in favour of a diapir model to account for the perturbation in the geotherm. Other suggestions put forward to account for the inflection include that it represents an artifact of the method of calculation (Mercier and Carter, 1975) or that it is the result of faulty experimental calibration (Howells and O'Hara, 1978).

Irving (1976) and MacGregor and Basu (1976) suggested that the P-T arrays calculated for xenoliths reflect dynamic "geotherms" or equilibration paths related solely to the response of wall rock mantle to the physical and chemical state of the intruding magma which eventually accidentally incorporated the xenoliths.

Harte et al. (1975), Mitchell (1978), Harte (1978) and Gurney et al. (1979<sup>b</sup>) link the textural and P-T features of xenoliths to processes occurring in the mantle envelope surrounding a diapir during pre-eruptive uprise in the early stages of kimberlite generation. Mitchell<sup>et al.</sup> (1980) viewed the deduced kinked geotherms to include a "transient upper-limb" where the P-T conditions reflect the presence of a thermal aureole about a rising mantle diapir, and a "normal" sub-continental mantle geotherm defining the shallower limb.

It has also been suggested that the P-T arrays are not related to any geothermal gradient, but are created by different element diffusion closure temperatures (Fraser and Lawless, 1978).

The issue of inflected geotherms will not be considered in this discussion, due to the lack of data for high T-P xenoliths at Monastery. However, the P-T array defined by the coarse-cold peridotites warrants some comment. It has been noted that two groupings of equilibration conditions are evident for the coarse xenoliths at Monastery. The low T-P group consists of 5 garnet lherzolites and 3 garnet harzburgites together with the full range of websterites (2), wehrlites and olivine clinopyroxenites (11) and pyroxenites (4) (temperatures for the wehrlites and pyroxenites based on based on Ca/Ca+Mg ratios of clinopyroxene). All of these samples, are however not represented on the various P-T diagrams because the frequent absence of key phases restricts the application of the full variety of T-P equations employed.

It has also been noted that the groupings based on P-T data correspond with textural features observed in the rocks (Fig. 3.26). The question to be addressed is what is the significance of the calculated T,P conditions recorded by these rocks? Harte and Freer (1982) have suggested that coarse lherzolites may reflect the blocking temperatures of various cations and not ambient mantle conditions at the time of kimberlite eruption. This is based on diffusion rate studies which indicate that major aspects of the mineral chemistry of coarse ultramafic minerals assemblages will be unable to

equilibrate in a time period of several hundred million years unless temperatures exceed about  $900^{\circ}\text{C}$ . They thus consider that the uppermost mantle lithosphere may contain largely frozen mineral compositions which are unlikely to yield consistent T-P data appropriate to their ambient T-P conditions.

The temperatures indicated by the re-equilibrated rocks at Monastery range between  $740$  and  $830^{\circ}\text{C}$  for the BM85 method (Figs. 3.22b, 3.23) which is significantly lower than the approximate blocking temperatures inferred from diffusion data ( $\sim 900^{\circ}\text{C}$ ) (Harte and Freer, 1982).

In order to ensure that the low calculated temperatures were not merely an artifact of the pyroxene-solvus method of temperature calculation, results were tested against thermometers based on different mineral equilibria. It has already been shown that the OW79 thermometer (Fe-Mg exchange between garnet and olivine) shows broad agreement with the BM85 results (Fig. 3.24 c), but OW79 temperatures are noted to be marginally higher for the low T, P group of rocks (OW79 =  $750$ - $850^{\circ}\text{C}$ ; BM85 =  $740$ - $790^{\circ}\text{C}$ ).

Good agreement is observed between the BM85 results and those for the Mori and Green (1978) thermometer based on Fe-Mg exchange between garnet and clinopyroxene (MG78 =  $760$ - $820^{\circ}\text{C}$ ; BM85 =  $740$ - $830^{\circ}\text{C}$ ) (two samples with anomalously high temperatures for the MG78 method are not reflected in the range shown). It should also be noted that the pyroxene solvus method of Wells (1977) yields very similar temperatures to the BM85 results in the range of interest (W77 =  $780$ - $850$ , BM85 =  $740$ - $830$ ).

It is clear from the above that the low temperatures recorded by these xenoliths represent a real feature, with the generally good agreement between the methods involving different mineral equilibria indicating good chemical equilibrium. Chemical equilibrium is also indicated by the absence of detectable differences in composition between "porphyroclasts" and polygonal grains as well as between exsolved phases and discrete grains of the same phase. However, the abundant exsolution features and bimodal grain populations (both in terms of size and morphology), indicate textural disequilibrium. The exsolution textures imply that these rocks have cooled slowly from significantly higher formation temperatures, while the polygonal crystals indicate substantial grain growth in the absence of deformation. In the case of the pyroxenites, wehrlites and websterites which may represent the products of igneous processes, the subsolidus textures are easily accounted for by slow cooling below the solidus. Moreover, the residence time between crystallization and sampling by the kimberlite under the ambient subsolidus P-T conditions (apparently ~ 700-800°C; 20-30 kbars) in the upper mantle could have resulted in the metamorphic component of the textures observed (polygonization).

Systematically lower equilibration pressures have been recorded by chromite-bearing xenoliths compared to garnet-bearing assemblages (Fig. 3.27). MacGregor (1970) has shown that the stability of garnet in the mantle is dependant upon the whole rock Cr/Cr+Al ratio i.e. rocks with high Cr/Cr+Al require higher pressures to stabilize garnet than those with lower Cr/Cr+Al. This means that at a given pressure and

temperature in the mantle, the whole rock Cr/Cr+Al determines whether garnet lherzolite or chromite lherzolite is stable. A large proportion of the chromite-bearing samples at Monastery also host garnet, indicating that they are derived from a transitional garnet-spinel stability field, the width of which may increase with increasing bulk Cr/Cr+Al (Mitchell et al., 1980). In the absence of whole-rock data it cannot be assessed whether the T-P trends observed correlate with bulk composition. Lherzolites from nearby Pipe 200 which have a narrow range in bulk Cr/Cr+Al define two groups, with chromite lherzolites having generally lower equilibration temperatures than garnet lherzolites (Mitchell et al., 1980).

It has been shown that the coarse xenoliths at Monastery display an exceptionally large range of equilibration conditions (~700-1050°C; 20-40 Kbars - Figs 3.22 a&b), with the texturally intermediate rocks recording significantly lower temperatures than the coarse peridotites from Lesotho (Fig. 3.22a) and other localities (Kimberley pipes - Boyd and Nixon, 1978; Premier - Danchin, 1979 and Jagersfontein - Harte and Gurney, 1982). It is unlikely that these temperatures represent blocking temperatures since they range to 200°C below the estimated blocking temperature for peridotites suggested by Harte and Freer (1982). Moreover, one would not expect blocking temperatures for the variety of phase equilibria used to be coincident, which is what is observed. The fact that the P-T array defined by the Monastery suite coincides with the theoretical geotherm is not considered to be geologically significant since calculated pressures and temperatures are interdependent to such an extent that the pressures calculated

for a suite of nodules showing a large range in equilibration temperatures will invariably result in a calculated P-T array which coincides with the theoretical geotherms.

It has already been stated on several occasions that an outstanding feature of the coarse textured xenolith suite at Monastery is the high incidence of modal metasomatism. Mineral chemistry data for phlogopite has clearly indicated the existence of two distinct compositional groups (Fig. 3.13 to 3.17) corresponding to peridotites (lherzolites, harzburgites and websterites) and wehrlites (wehrlites and pyroxenites). It has also been noted that the wehrlitic group of phlogopite shows compositional similarities with phlogopite in the richterite-bearing peridotites (PKP) from the Kimberley group of kimberlites (Erlank et al., 1987). Moreover, one of the wehrlites (ROM-301), has been found to contain K-richterite. These features may indicate that the wehrlites and pyroxenites have experienced a similar (if not the same) metasomatic event to that recorded by the PKP rocks at Kimberley.

Low levels of  $Al_2O_3$  is a characteristic compositional feature of the constituent minerals of the PKP xenoliths (Erlank et al., 1987) and the low levels of  $Al_2O_3$  in the Monastery wehrlitic phlogopites features prominently in their discrimination from peridotitic phlogopites. It may be that the distinctive composition of these phlogopites simply reflects the signature of a garnet-free assemblage. However, this is considered unlikely, since oxides such as  $Cr_2O_3$ , FeO and  $Na_2O$  also show significant differences between the two groups.

The PKP rocks from Kimberley are thought to contain a component of metasomatic clinopyroxene (F.G. Waters, Pers Comm). This raises the possibility that the Monastery wehrlites and olivine clinopyroxenites represent original dunites which have had clinopyroxene and phlogopite metasomatically introduced. The textural relationships between these two phases in the wehrlitic rocks allows such an origin. To test this possibility, the composition the clinopyroxene in the two suites of rocks have been compared. Figure 3.28 clearly illustrates that the clinopyroxenes in PKP rocks show a considerably more restricted range in  $Al_2O_3$  concentrations with a wider range in FeO than the wehrlitic clinopyroxenes. Significant differences are also observed for  $TiO_2$  and  $Cr_2O_3$  concentrations (not shown). These compositional differences effectively preclude any genetic correlation between the clinopyroxene in the PKP metasomites and the wehrlitic rocks from Monastery.

It would appear that the wehrlitic and pyroxenitic rocks are primarily igneous rocks which have been metasomatised, with only phlogopite (and K-richterite in ROM-301) being a product of this metasomatism. However, considering the textural and chemical equilibrium displayed by the phlogopite in these rocks, it is also possible that they represent frozen igneous melts with phlogopite being a primary igneous phase.

## CHAPTER 4    ECLOGITE XENOLITHS

### 4.1    INTRODUCTION AND BRIEF REVIEW

Eclogites are essentially biminerally coarse-grained rocks consisting of garnet and clinopyroxene, with a limited number of accessory minerals. They have basaltic compositions and it has been demonstrated by many workers e.g. Yoder and Tilley (1962); Green and Ringwood (1967); O'Hara and Yoder (1967) and Green (1967) that eclogites can be synthesised from a spectrum of basaltic compositions. Eclogites occur in a variety of different geological environments (e.g. Eskola, 1921) and a number of authors have proposed classification schemes in an attempt to categorise the various types of eclogite (e.g. Coleman et al., 1965; Banno, 1970; MacGregor and Carter, 1970).

Eclogites occur as xenoliths in most kimberlites but are usually less abundant than peridotite-suite xenoliths. There are however exceptions such as Roberts Victor (Johnson, 1906; Wagner, 1914; Williams, 1932; MacGregor and Carter, 1970; Hatton, 1978), Orapa (Shee, 1978; Shee and Gurney, 1979; Robinson et al., 1984), and Bellsbank (Smyth et al., 1984; Smyth and Caporuscio, 1984) in South Africa and Zagadochnaya in the USSR (Sobolev, 1970; Sobolev et al., 1976) where eclogites dominate the mantle xenolith suite. Eclogite xenoliths in kimberlite have been shown to be chemically, mineralogically and texturally diverse (Kushiro and Aoki, 1968; MacGregor and Carter, 1970; Hatton, 1978; Walker, 1979; Shee and Gurney,

1979). In addition to garnet and clinopyroxene, they may contain one or more of the following accessory minerals: kyanite, corundum, rutile, coesite, orthopyroxene, graphite, diamond, amphibole, phlogopite, sulphide and ilmenite (Dawson, 1980).

MacGregor and Carter (1970) subdivided eclogites from Roberts Victor into two textural groups which they interpreted as cumulates (Group I) and associated liquids (Group II). Group I eclogites are characterized by generally rounded cloudy garnets set in a matrix of anhedral interstitial clinopyroxene which is commonly altered. Group II eclogites are less common and exhibit interlocking textures. They are also generally less altered than the Group I variety (MacGregor and Carter, 1970). Hatton (1978) found that the two textural groups could be readily distinguished in some cases, but noted gradations between the two types even within single samples. He therefore distinguished a large number of eclogite categories at Roberts Victor while still retaining the essential features of the MacGregor and Carter classification.

Hatton (1978) also noted chemical differences between the constituent minerals of the different eclogite groups, a feature which has since been confirmed by McCandless and Gurney (1986). McCandless and Gurney (op. cit.) adopt the terms "Group I" and "Group II" in their chemical classification of eclogites and their terminology and classification is followed in this study (Section 4.3.2) (Hatton, 1978 uses the terms "Type I" and "Type II" eclogites). Garnets in Group I eclogites have sodium concentrations in excess of 0.1 wt% Na<sub>2</sub>O while clinopyroxenes

contain detectable potassium ( $>.08$  wt%  $K_2O$ ). In contrast, Group II eclogites have potassium-poor ( $<.08$  wt%  $K_2O$ ) clinopyroxenes and garnets with sodium concentrations below  $0.09$  wt.%  $Na_2O$ .

Some eclogites exhibit a well defined layering marked by modal variations of garnet and clinopyroxene and on occasions, kyanite. In the case of kyanite layering the kyanite bearing portions of the rock have often been found to exhibit different compositions to the rest of the rock (Chinner and Cornell, 1974; Lappin and Dawson, 1975; Hatton, 1978).

Diamond-bearing eclogites have been found at several kimberlite localities in southern Africa and Yakutia, U.S.S.R. (Rickwood et al., 1969; Reid et al., 1976; Sobolev et al., 1976; Sobolev, 1977; Shee and Gurney, 1979; Hatton and Gurney, 1979; Robinson, 1979; Robinson et al., 1984). Shee (1978) proposed the disaggregation of diamond-bearing eclogites as a source for diamonds at Orapa, but the recent study of Robinson et al. (1984) demonstrated both in terms of geochemical evidence as well as by a consideration of the physical characteristics of diamonds that diamondiferous eclogites are not the predominant source for the general diamond production at Orapa.

The constituent minerals of eclogite display a wide variation in composition. Garnet compositions commonly define an Fe-Ca enrichment trend in their evolution from pyrope-rich compositions to grossular-rich compositions while clinopyroxenes range from diopside-rich to jadeite-rich compositions. The majority of eclogite nodules display homogeneous mineral compositions indicating equilibrium. However, chemical zonation

in both garnet and clinopyroxene may occur e.g. Lappin and Dawson (1975); Harte and Gurney (1975); Lappin (1978) and Hatton (1978) report zonation in some kyanite eclogites and grosspydites.

A number of ideas concerning the genesis of eclogites have been proposed in the literature. These include that they have been derived from a series of partial melts (Kushiro and Aoki, 1968); as a set of cumulates and related liquids (MacGregor and Carter, 1970; Hatton, 1978) or as a series of cumulates (O'Hara et al., 1975). Other models envisage eclogite as representing subducted crust (Helmstaedt and Doig, 1975; Smyth, 1977; Jagoutz et al., 1984), the residue after the extraction of andesite from subducted oceanic crust (Green and Ringwood, 1968), while Press (1970) considers eclogite to be a primary mantle material. The most recent model is that of Hatton and Gurney (1987) who propose that Group I eclogites at Roberts Victor represent a crystallized diapir of remelted oceanic crust trapped in the subcratonic lithosphere, while the Group II eclogites are thought to have formed in the volatile-enriched thermal aureole between the Group I eclogites and surrounding garnet lherzolite.

#### 4.2 PETROGRAPHY

Eclogite xenoliths have been found to be rare at Monastery and as a consequence, the seventeen samples considered in this study have been sampled from the heavy mineral coarse tailings dump of the diamond recovery plant. Since this material has all passed through the primary crusher, specimen sizes range between

2 and 5 cm in longest dimension and consequently, samples showing layering and gross inhomogeneities such as those exhibited by some Roberts Victor eclogites (Hatton, 1978) have not been observed. Most of the samples are blocky and subangular in shape with rough fracture surfaces bearing witness to the crushing and milling processes they have been subjected to in the diamond recovery process. Smooth surfaced rounded nodules are not found.

The rocks are coarse grained and this together with the small size of most of the specimens prohibited comprehensive textural studies and modal determinations. However, their general petrographic features are outlined below. Brief petrographic descriptions of each sample are included in Appendix 4.1.

Garnets are golden red-brown in colour and usually fresh. They range between 3 and 6mm in size, but may be up to 12mm. Grain shapes vary from completely irregular through subrounded to subhedral. Intricate networks of microfractures are commonly developed, often with associated minor alteration which rarely open into rounded pools (~Ø.15mm) of turbid secondary material.

Clinopyroxene is generally more altered than garnet but fresh portions are deep emerald green to light green in colour. Average grain sizes are in the region of 4mm in longest dimension. Clinopyroxene occurs both as irregular grains forming tightly interlocking textures with garnet, and as more regular grains with straight to gently curving grain boundaries. The effects of decompression and/or small degrees of partial

melting are evident in a number of samples as turbid regions usually confined to the margins of clear grains.

Textures are highly variable and few samples strictly conform with the MacGregor and Carter (1970) textural classification. However, samples were classified on the basis of dominant diagnostic features (subjective and often ambiguous) and of the 16 specimens investigated 9 were classed as Group I, 3 as Group II and 5 were judged to be intermediate. A large variation in modal abundance of garnet and clinopyroxene is noted within the eclogite nodules and this is illustrated in the histogram presented in Fig. 4.1 Modal estimates are also presented in Table 4.1.

The only accessory phases encountered were rutile and sulphide. Rutile occurs as small (~1mm) subhedral grains hosting fine exsolution lamellae of ilmenite. Sulphide is only present in one sample and it was optically identified as pyrrhotite with fine exsolution lamellae of pentlandite. Secondary phlogopite with associated fine grained spinel is developed in extensively altered areas of some nodules.

### 4.3 MINERAL CHEMISTRY

#### 4.3.1 Introduction

Only garnet and clinopyroxene have been analysed and compositions are reported in Tables 4.2 and 4.3 respectively. A minimum of five analyses of each phase in each sample were obtained and since statistically significant zoning was not

observed, average compositions are reported. Ferric iron has not been determined or calculated for the garnets and clinopyroxenes, so that total iron is quoted as FeO in all data tables.

#### 4.3.2 Recognition of Group I and II Eclogites

Histograms of Na<sub>2</sub>O in garnet (Na<sub>2</sub>O<sub>gt</sub>) and K<sub>2</sub>O in clinopyroxene (K<sub>2</sub>O<sub>cpX</sub>) are presented in Fig. 4.2 where they are compared with the critical cutoff values between Group I and II eclogites proposed by McCandless and Gurney (1986). Samples classified on the basis of texture were found to correlate with the chemical classification, with intermediate textures being accommodated in both chemical groups. A generally good agreement with the McCandless and Gurney classification is noted, but Group I clinopyroxenes marginally overlap into the Group II field. A clear distinction between the two groups is still evident in K<sub>2</sub>O<sub>cpX</sub>, but the Monastery data indicates a cutoff concentration of 0.06 wt% K<sub>2</sub>O to discriminate between Group I and II eclogites. It is also noted from Fig. 4.2 that a Group II eclogite (EC-11) has garnet with marginally elevated Na<sub>2</sub>O concentrations (0.10 wt%) while the clinopyroxene in a Group I eclogite (EC-20) is depleted in K<sub>2</sub>O (0.04 wt%). The elevated Na<sub>2</sub>O in the garnet of sample EC-11 may be a "secondary effect" associated with Na<sub>2</sub>O release from clinopyroxene, which in this rock displays extensive partial melting/decompression textures. It is also possible that the low K<sub>2</sub>O concentrations in the clinopyroxene from sample EC-20 may be related to alteration. Another notable feature is the

high level of Na<sub>2</sub>O observed in some of the Group I garnets (up to 0.23 wt%) compared to the maximum of 0.17 wt% for garnets from Roberts Victor eclogites (Hatton, 1978, McCandless and Gurney, 1986). Stoichiometric considerations indicate that this is not due to the presence of a component of pyroxene in solid solution as is the case for some eclogitic garnet inclusions in diamonds which show elevated Na<sub>2</sub>O concentrations (Moore and Gurney, 1985; Chapter 5 of this study).

Textural and chemical features have clearly demonstrated both Group I and II eclogites to be present in the Monastery suite. The mineral chemistry of both groups will be discussed simultaneously, with the two groups being discriminated on all plots. Compositional statistics for garnet and clinopyroxene are presented in Table 4.4

#### 4.3.3 Choice of a Differentiation Index

In order to establish the presence or absence of igneous fractionation trends and to assess their significance if present, the choice of a suitable differentiation index is necessary. Hatton (1978) used the sodium content of clinopyroxene as a differentiation index. This choice was based on the fact that in upper mantle mineralogies, Na<sub>2</sub>O is only present at high levels in clinopyroxene, and consequently exchange reactions between solid phases at various P,T conditions will have little effect on the behaviour of Na<sub>2</sub>O. Hatton argued that in an equilibrium between clinopyroxene and melt, sodium would be preferentially partitioned into the melt, so that during the evolution of a magma by fractional

crystallization, the sodium content of the melt and of the clinopyroxene in equilibrium with the melt would increase.

It is well established that the evolution of any magma by fractional crystallization will result in both melt and crystallizing phases becoming progressively enriched in iron with increasing differentiation. Following from this, a good correlation should exist between  $\text{Na}_2\text{O}_{\text{Cpx}}$  and  $\text{Mg}/\text{Mg}+\text{Fe}$  for clinopyroxene and garnet if  $\text{Na}_2\text{O}$  in clinopyroxene varies systematically with differentiation.  $\text{Na}_2\text{O}_{\text{Cpx}}$  is plotted against  $\text{Mg}/\text{Mg}+\text{Fe}$  for clinopyroxene and garnet in Figures 4.3 and 4.4 respectively and it is evident that while the expected negative correlation exists between these parameters, the relationships between the Group I eclogites is complicated by the apparent existence of two trends. It is unclear whether these trends indicate the existence of two distinct populations of Group I eclogite.

The possibility exists that  $\text{Na}_2\text{O}$  concentrations in clinopyroxene are not always reliable differentiation indicators since it has been established that clinopyroxenes exhibiting textural evidence of decompression/localised partial melting show large variations in  $\text{Na}_2\text{O}_{\text{Cpx}}$  (J.J. Gurney and C.B. Smith, unpublished data). While this effect was not specifically noted in the Monastery eclogites, a number of samples had very little clinopyroxene preserved so that systematic comparisons between the compositions of cloudy and fresh clinopyroxene could not be made.

Considering the uncertainty in the relationship between  $\text{Na}_2\text{O}$  in clinopyroxene and possible igneous fractionation

trends, Mg/Mg+Fe is preferred as a differentiation index in this study.

#### 4.3.4 Garnet

In terms of classical end members the garnets in the Monastery eclogites are mixtures of pyrope (Mg), almandine (Fe) and grossular (Ca) with very little spessartine (Mn), knorringite/uvarovite (Cr) or andradite ( $\text{Fe}^{3+}$ , Ti).

Garnet and clinopyroxene compositions are plotted on a Ca-Mg-Fe ternary in Fig. 4.5 with tie-lines joining coexisting phases. The tie-lines are a graphical representation of garnet-clinopyroxene Ca, Mg, Fe equilibration and their positions are a function of varying temperature, pressure and host rock bulk composition. Tie-lines for garnet-clinopyroxene pairs from a suite of xenoliths formed in an equilibrium process will be arranged in a rational manner with no crosscutting relationships. This is clearly the case for the Monastery suite. Garnets show a wide range in composition and it is noted that the Group II garnets define a trend of changing Fe/Mg ratio while Ca remains essentially constant. Group I garnets are generally more iron-rich than Group II garnets and show a trend of Ca-enrichment with increasing Fe. These trends are considerably less complex than those observed for garnets from eclogites at Roberts Victor (Hatton, 1978) and Orapa (Shee, 1978). Figure 4.6 illustrates that in Type I eclogites from Roberts Victor, two trends of garnet compositions are recognised, namely an iron-enrichment and a calcium-enrichment trend. Similar trends are observed for the Orapa eclogites

(Fig. 4.7). Further details of the garnet compositions at these localities are provided in the captions to Figs. 4.6 and 4.7.

Figures 4.8 and 4.9 illustrate that  $\text{TiO}_2$  and  $\text{Na}_2\text{O}$  in Group I garnets show good negative correlation with  $\text{Mg}/\text{Mg}+\text{Fe}$ . This together with the trend of increasing Ca with Fe-enrichment (Fig. 4.5) is consistent with a related suite of fractionated igneous rocks. Group II garnets show virtually constant  $\text{TiO}_2$  (Av. 0.24 wt%) which is significantly lower than the levels of  $\text{TiO}_2$  in Group I garnets (Av. 0.65 wt%, Table 4.4). High  $\text{TiO}_2$  and  $\text{Na}_2\text{O}$  are features of garnets in diamond eclogites (Gurney, 1984; McCandless and Gurney, 1986) indicating that the Group I eclogites may represent a potential source for diamonds at Monastery. This possibility is evaluated in Chapter 5.

Chrome shows the opposite trend to  $\text{TiO}_2$  in that Group II garnets have higher  $\text{Cr}_2\text{O}_3$  (Av. 0.27 wt%) than Group I garnets (Av. 0.07 wt%; Table 4.4).  $\text{Cr}_2\text{O}_3$  shows a broad positive correlation with  $\text{Mg}/\text{Mg}+\text{Fe}$  (not shown).

#### 4.3.5 Clinopyroxene

Clinopyroxene compositions plotted on a Ca-Mg-Fe ternary (Fig. 4.5) essentially illustrates their compositional variation in terms of the QUAD end members: Enstatite (Mg) - Diopside-Wollastonite (Ca) - Hedenbergite-Ferrosilite (Fe). The clinopyroxenes show considerably more restricted  $\text{Mg}/\text{Mg}+\text{Fe}$  ratios than coexisting garnets (Table 4.4), but the Fe-enrichment trend accompanied by moderate increases in Ca shown in Fig. 4.5 is compatible with changing garnet compositions. Group II

clinopyroxenes have higher average Mg/Mg+Fe (81.54) than Group I clinopyroxenes (76.30) and show very little variation in Ca content.

Clinopyroxene end-member compositions have been calculated according to the method proposed by Hatton (1978) (see Appendix 4.2) and results are listed in Table 4.5. Hatton recognised eleven end-members but incorporated minor end-members into major components so that only five are calculated. The clinopyroxenes in the Monastery eclogites are dominantly a solid solution of diopside-hedenbergite and jadeite. This is well illustrated on a plot of diopside and jadeite content presented in Fig. 4.10, where it is shown that most are composed of between 78 and 85 mol% diopside plus jadeite. A well defined negative correlation is also observed between the two end-members. Figure 4.10 shows Group I clinopyroxenes to have higher jadeite contents than Group II clinopyroxenes (17.2-34.5 mol% vs 11.9-18.2 mol%).

Besides jadeite and diopside-hedenbergite, four other end-members may be present. The enstatite-ferrosilite ( $(\text{Mg,Fe})_2\text{Si}_2\text{O}_6$ ) end-member is present at levels of 6.4 - 18.3 mol% in Group I clinopyroxenes and rather uniform levels of 13.3 - 14.8 mol% in Group II clinopyroxenes. Ferric iron is accommodated in the acmite molecule ( $\text{NaFe}^{3+}\text{Si}_2\text{O}_6$ ) and generally low levels are observed (0 - 8.5 mol% and 3.3 - 6.6 mol% for Group I and II clinopyroxenes respectively).

The amount of calcium tschermak's molecule ( $\text{CaAlAlSiO}_6$ ) in solid solution in a clinopyroxene decreases with increasing pressure, but high temperatures favour increased levels of this molecule in solid-solution (Hatton, 1978). The amount of

calcium tschermak's molecule is equivalent to the amount of garnet in solid solution in clinopyroxene so that a clinopyroxene crystallized at high temperature may on cooling exsolve considerable amounts of garnet (Hatton, 1978). Clinopyroxenes in both Group I and II eclogites at Monastery contain less than 5 mol% of the calcium tschermak's molecule (Table 4.5).

Clinopyroxene with cation deficiencies (i.e. cation sums <4.000 for 6 oxygens) are invoked to contain the "pseudojadeite" or "Ca-Eskola" molecule ( $\text{Ca}_{0.5}\text{AlSi}_2\text{O}_6$ ) (Cawthorn and Collerson, 1974; Smyth, 1980). Pseudojadeite is stable only at high pressures and is very readily altered to calcium tschermak's molecule and quartz in near surface environments (Smyth, 1977, 1980). Only four of the Group I clinopyroxenes contain pseudojadeite, and levels do not exceed 5 mol%. Group II clinopyroxenes do not contain a pseudojadeite component. Hatton (1978) reports pseudojadeite contents up to 17 mol% in Roberts Victor eclogites containing grossular rich garnets and in kyanite-bearing eclogites.

The good positive correlation between  $\text{Al}_2\text{O}_3$  and  $\text{Na}_2\text{O}$  (Fig. 4.11) and the well defined negative correlations between  $\text{CaO}$  and  $\text{Na}_2\text{O}$  as well as  $\text{MgO}$  and  $\text{Na}_2\text{O}$  (Figs. 4.12 and 4.13 respectively) reflect the coupled substitution  $\text{NaAl-CaMg}$  in the M-sites of the clinopyroxenes as jadeite increases at the expense of diopside (illustrated in Fig. 4.10). The two groups of clinopyroxene are clearly discriminated on all three plots with Group I clinopyroxenes having higher  $\text{Al}_2\text{O}_3$  and  $\text{Na}_2\text{O}$  and lower  $\text{CaO}$  and  $\text{MgO}$  than Group II clinopyroxenes (see also

Table 4.4).

Group I clinopyroxenes show a broad negative correlation between  $\text{TiO}_2$  and  $\text{Mg}/\text{Mg}+\text{Fe}$  (Fig. 4.14) and a trend of decreasing  $\text{Cr}_2\text{O}_3$  with decreasing  $\text{Mg}/\text{Mg}+\text{Fe}$  (Fig. 4.15). Again this is consistent with an origin by igneous fractionation. Group II clinopyroxenes have lower levels of  $\text{TiO}_2$  than those in Group I eclogites and show very little variation (.29 - .31 wt%).  $\text{Cr}_2\text{O}_3$  shows no correlation with  $\text{Mg}/\text{Mg}+\text{Fe}$  in the Group II clinopyroxenes (Fig. 4.15), but their significantly higher levels of  $\text{Cr}_2\text{O}_3$  (.11 - .21 wt%) are clearly illustrated.

#### 4.3.6 Estimation of Bulk Composition

Numerous workers, have estimated bulk-rock compositions by calculation from modal abundance and mineral chemistry data (e.g. Hatton, 1978; Shee, 1978; Smyth and Caporuscio, 1984; Ater et al., 1984). However, such a calculation was not justified in this study because of the extremely dubious nature of the modal estimates. Errors in modal estimates are caused by:

- (a) the combination of small samples and coarse grain-size
- (b) clinopyroxene is preferentially eroded by the kimberlite
- (c) sample fragments may not be representative of the larger eclogite body because of layering

#### 4.4. GEO THERMOMETRY

The only geothermometer applicable to eclogitic assemblages is that based on Fe-Mg exchange between garnet and clinopyroxene. The most recent experimental calibration of this thermometer (Ellis and Green, 1979) is applied in this study. Calculations assume all iron to be divalent and temperatures are calculated for pressures of 30 and 50 Kbars. All iron was assumed to be in the ferrous state because ferric-iron calculations based on stoichiometric considerations are significantly affected by analytical error and since clinopyroxene in eclogites has generally low iron concentrations, relatively small analytical errors could result in large variations in calculated Kd ratios ( $Kd = Fe/Mg_{gt} / Fe/Mg_{cpx}$ ). Hatton (1978) reports that wet chemical determinations of ferric iron in garnet and clinopyroxene from Roberts Victor eclogites carried out by O'Hara et al. (1975) indicate between 25 and 33% of iron in clinopyroxenes and less than 5% iron in garnet to be in the ferric state. The effects of these levels of  $Fe^{3+}$  on calculated temperatures have been determined and are tabulated in Table 4.6. The presence of ferric iron in garnet causes an increase in calculated temperature, while its presence in clinopyroxene results in a decrease. The combination is compensating, but the higher levels of  $Fe^{3+}$  in clinopyroxene will mean that the assumption of all iron being present in the ferrous state will result in temperatures being overestimated. However, trends may still be meaningful.

Distribution coefficients, compositional parameters and calculated equilibration temperatures are tabulated in Table

4.7. The plot of  $\text{Fe/Mg}_{\text{cpx}}$  versus  $\text{Fe/Mg}_{\text{garnet}}$  presented in Fig. 4.16, shows the majority of Monastery eclogites to have Kd ratios in the range 2.3 - 3.0. More specifically Kd's range between 2.37 and 3.01 in Group I eclogites and 1.59 and 2.87 in Group II eclogites. Kd's of mantle eclogites from kimberlites range between 2.5 and 6 (e.g. Kushiro and Aoki, 1968; MacGregor and Carter, 1970; Sobolev, 1977; Carswell et al., 1981; Ater et al., 1984), with kyanite eclogites at the upper end of the range. Since Kd is inversely proportional to temperature, the low Kd's of the Monastery eclogites represent the high temperature extreme of this range. Group I eclogites have calculated equilibration temperatures in the range 1060-1307°C (Ellis and Green, 1979; 50 kbars), while four of the Group II eclogites have temperatures in the restricted range 1060-1107°C, the fifth being substantially hotter at 1359°C.

#### 4.5 DISCUSSION

Monastery eclogites are successfully discriminated into two groups using the McCandless and Gurney (1986) classification based on the levels of  $\text{Na}_2\text{O}$  in garnet and  $\text{K}_2\text{O}$  in clinopyroxene. This grouping is confirmed by other elements and the trends defined on a number of the variation diagrams presented indicate that the Group I and II eclogites were formed in separate processes.

The eclogites display metamorphic textures but no evidence of subsolidus re-equilibration in the form of exsolution features were observed. There is little doubt that subsolidus

cooling and re-equilibration has occurred, but the relatively high calculated temperatures indicate that this may not have been as extensive as the 200°C subsolidus cooling suggested for the Roberts Victor eclogites by Gurney et al., 1984b. The absence of accessory phases such as diamond and graphite prevent any estimation of formation pressure.

The ordered array of tie-lines linking coexisting garnet and clinopyroxene compositions (Fig. 4.5) is consistent with, but in no way proves that the eclogites were formed in a single fractionation process. In this regard, it is noted that the Group II eclogites form a continuous trend with the Group I eclogites, where other considerations have demonstrated that these two groups must have been formed in separate processes.

#### 4.5.1 Group I Eclogites

The variation of Na<sub>2</sub>O in clinopyroxenes was not used as a differentiation index in this study because of the confusing relationship observed between Na<sub>2</sub>O<sub>Cpx</sub> and Mg/Mg+Fe in Group I garnets and clinopyroxenes (Figs. 4.3 and 4.4). A consequence of this was that the Hatton and Gurney (1987) approach to interpreting the petrogenesis of eclogites could not be applied to the Group I eclogites.

Relationships between Mg/Mg+Fe and TiO<sub>2</sub> and Cr<sub>2</sub>O<sub>3</sub> in clinopyroxenes and Mg/Mg+Fe and TiO<sub>2</sub>, CaO and Na<sub>2</sub>O in garnets (Figs 4.14, 4.15, 4.8, 4.5, 4.9) are consistent with the Group I eclogites being formed in a **single** igneous event. However, the calculated paleotemperature data represents a

potential stumbling block for this interpretation. This is evident from a plot of  $\ln K_d$  versus  $X_{Ca}^{gt}$  (Fig. 4.17;  $K_d = Fe/Mg_{gt}/Fe/Mg_{cpx}$ ) which shows a clear trend of increasing  $X_{Ca}^{gt}$  (Fig. 4.17) which shows a clear trend of increasing Ca in garnet with increasing temperature for Group I eclogites. Calcium in garnet has been demonstrated to increase with fractionation (i.e. decreasing  $Mg/Mg+Fe$ ) (Fig. 4.5) and consequently a trend of declining temperature with increasing  $X_{Ca}^{gt}$  would be expected. Eclogites from Roberts Victor as well as eclogitic diamond inclusion suites from Orapa and Roberts Victor which have been interpreted to reflect igneous fractionation trends show a decrease in  $X_{Ca}^{gt}$  with declining temperature (Hatton, 1978; Gurney et al., 1984 a,b). The range in values for both  $X_{Ca}^{gt}$  and calculated temperature are sufficiently large and the relationship between them sufficiently well defined on Fig. 4.17, that one cannot call on thermometer error over a particular temperature or compositional range to account for the observed trends. It is possible that the systematic chemical trends displayed by garnet and clinopyroxene do in fact represent igneous fractionation trends but calculated temperatures indicate that individual mineral grains have not attained complete chemical equilibrium during subsolidus annealing and re-equilibration processes. In this regard it is instructive to recall that fractional crystallization is not an equilibrium process since only the outer surface of crystals are in equilibrium with each other and the melt at any one time so that in a vertical column of magma it is feasible for crystals to sink from the local environment in which they crystallized into an area where they are not in equilibrium with surrounding

crystals or melt (compensated crystal settling; Cox and Bell, 1972). Chemical disequilibrium resulting from such a process could conceivably account for the observed discrepancies between fractionation trends and calculated equilibration temperature. However, the degree of disequilibrium which would be required to produce the large temperature range observed should be evident in form of chemical inhomogeneities between individual grains as well as by zoning. Neither of these features are observed in the Monastery eclogites. Moreover, if the calculated temperatures were related to disequilibrium processes, one would expect a more random relationship between  $\ln K_d$  and calcium in garnet than the systematic trend observed in Fig. 4.17. The above considerations indicate chemical disequilibrium to be an unlikely explanation for the observed increase in calculated equilibration temperature with increasing degree of fractionation.

Another feature of the Group I eclogites needs to be considered in order to further assess their petrogenesis. Hatton (1978) and Hatton and Gurney (1987) made extensive use of the relationship between CaO in garnet and Na<sub>2</sub>O in clinopyroxene in their interpretation of the genesis of the Roberts Victor eclogites. They plotted the compositional field for South African garnet lherzolites on a CaO<sub>gt</sub> versus Na<sub>2</sub>O<sub>cpx</sub> plot and emphasised the point that partial melting trends should issue from the composition of the source rock. A plot of corrected CaO in garnet versus corrected Na<sub>2</sub>O in clinopyroxene (see figure caption for explanation) is presented in Figure 4.18. This diagram clearly illustrates that Group I eclogites do not represent crystallized partial melts of garnet

lherzolite. However, this does not rule out garnet lherzolite as an ultimate source rock for the Group I eclogites, since they may represent second generation derivatives from garnet lherzolite.

Hatton and Gurney (1987) proposed a model for the Roberts Victor eclogites in which the Group I eclogites represent a crystallized diapir of remobilised oceanic crust (based on the Ringwood, 1982 subduction model) while the Group II eclogites formed in a volatile-enriched thermal aureole between the Group I eclogites and surrounding garnet lherzolite. Considering the fact that Monastery diamonds have been found to host eclogitic garnet inclusions which are believed to have formed at depths of up to 400 km (Moore and Gurney, 1985; Chapter 5 of this study), it is possible that the at least some of the eclogite xenoliths at Monastery represent original high pressure garnetites (see Section 5.6.2) which have undergone subsolidus reequilibration. This could imply that they have crystallized from a diapir of recycled oceanic crust, but in the absence of isotopic and bulk rock geochemical data, this possibility cannot be quantitatively assessed.

In summary, available chemical data is consistent with the Group I eclogites having been formed in a single igneous event. However, no suitable explanation has been found to account for the calculated paleotemperature data. The small number of available samples together with the lack of isotopic data and reliable bulk-rock compositions prevents the formulation of a conclusive model for the petrogenesis of Group I eclogites. However, the objective of chemically characterizing the Group I

eclogites for comparison with the compositions of eclogitic mineral inclusions in diamonds has been achieved.

#### 4.5.2 Group II Eclogites

The Ca-Mg-Fe ternary diagram presented in Fig. 4.5 shows that garnets in Group II eclogites define an Fe-enrichment trend with little variation in Ca. Moreover, oxides such as  $\text{TiO}_2$  and  $\text{Na}_2\text{O}$  remain essentially constant with changing Mg/Mg+Fe for both clinopyroxenes and garnets (Figs 4.3, 4.8, 4.9, 4.14). Calculated equilibration temperatures (assuming 50 kbars) dominantly range between 1060 and 1107°C with one exception being the most magnesian Group II eclogite (EC-03) which is substantially hotter at 1359°C. There is no obvious reason for this large temperature discrepancy other than that this single eclogite was formed in a separate event. However, this is not considered likely due to its compatibility with other chemical features of the Group II eclogites.

Group II eclogites define an apparent trend of positive slope on the  $\text{CaO}_{\text{gt}}$  vs  $\text{Na}_2\text{O}_{\text{cpx}}$  plot in Fig. 4.18 which issues from the field of garnet lherzolite compositions. Hatton and Gurney (1987) assessed the relations between  $\text{CaO}_{\text{gt}}$  and  $\text{Na}_2\text{O}_{\text{cpx}}$  during partial melting and fractional crystallization both in the presence and absence of orthopyroxene, and in so doing distinguished three potential mechanisms for producing a positive correlation between these two compositional parameters, namely:

- (1) Fractional crystallization with orthopyroxene absent from

the cumulate.

- (2) Partial melting with no orthopyroxene in the source and no reaction relation.
- (3) Partial melting with orthopyroxene reaction relation.

The fact that the Group II eclogites show a positive correlation between  $\text{CaO}_{\text{gt}}$  and  $\text{Na}_2\text{O}_{\text{cpx}}$  (Fig. 4.18) together with the fact that this trend issues from the field of South African garnet lherzolite compositions, may indicate that they represent crystallized partial melts from a garnet lherzolite source. Their low  $\text{TiO}_2$  and  $\text{Na}_2\text{O}$  and elevated  $\text{Cr}_2\text{O}_3$  contents are also consistent with this possibility. However, the formulation of a model for their petrogenesis cannot be justified on the basis of five samples.

5.1    INTRODUCTION

The physical and chemical properties of diamond are such (inert, impermeable and hard) that syngenetic inclusions occasionally trapped within them have been effectively shielded from chemical reaction with surrounding material since the formation of the diamond. It is generally believed that diamonds have formed under stable equilibrium conditions at depths in excess of 100km (Kennedy and Nordlie, 1968) and the minerals included in them thus not only provide information on the formation of diamonds, but also represent a window into certain unmodified mantle mineral compositions (Meyer and Boyd, 1972).

A considerable literature on mineral inclusions in diamond exists, and comprehensive reviews have been provided by Sobolev (1977), Meyer and Tsai (1976), Robinson (1978), Harris and Gurney (1979), Meyer (1987) and Gurney (1987). In all, twenty-two different mineral species have been identified as inclusions in diamonds, but a large number of these are considered to be epigenetic (secondary). Sulphide, olivine, orthopyroxene, garnet, chromite, clinopyroxene and kyanite constitute more than 99% of all primary mineral inclusions found in diamond (Gurney, 1984). Studies on mineral inclusions in diamond have shown that diamonds worldwide have two dominant parageneses - peridotitic and eclogitic (Table 5.1) (Sobolev et al., 1971<sup>a+b</sup>; Meyer and Boyd, 1972; Prinz et al., 1975). Minerals

from both suites have been present at every locality studied (Harris and Gurney, submitted), but have rarely been found together in one host diamond, probably indicating that they formed in separate processes (Gurney, 1984). Sulphide minerals, however, coexist with both eclogitic and peridotitic mineral inclusions and have therefore been assigned to both parageneses (Meyer and Tsai, 1976; Harris and Gurney, 1979). Recently Yefimova et al. (1983) have shown that sulphides from the two parageneses can be characterised on the basis of their Ni concentrations (Sobolev, 1984).

The diamonds from a given kimberlite commonly show a marked predominance of inclusions of one suite, and this does not necessarily correlate with the predominant xenolith type at that locality e.g. Roberts Victor (Gurney et al., 1984b).

Recent abundance data on mineral inclusions in diamonds worldwide suggests that peridotitic diamonds outnumber eclogitic diamonds (Yefimova and Sobolev, 1977; Harris and Gurney, submitted). However, Harris and Gurney (op. cit.) have indicated that eclogitic inclusions may be more significant in the larger diamond sizes.

Peridotitic inclusions show restricted compositions which are broadly similar to the constituent phases of common peridotite nodules. However, olivine and orthopyroxene inclusions are typically more magnesian than the corresponding phases in peridotite xenoliths, while garnet inclusions characteristically show lower levels of Ca coupled with higher Cr/Al and Mg/Mg+Fe ratios. The low CaO contents of peridotitic suite inclusions suggests that the included minerals and host

diamond equilibrated in the absence of clinopyroxene and this corresponds with the scarcity of clinopyroxene amongst peridotitic suite silicate inclusions (Harte et al., 1980).

Eclogitic garnets and clinopyroxenes are characterised by a wide range in major element compositions which generally match those for the corresponding minerals in eclogite xenoliths found in kimberlites. Garnets are characteristically solid solutions of pyrope and almandine while clinopyroxenes are essentially mixtures of diopside and jadeite. Sodium enrichment in the garnets and potassium in the clinopyroxenes at trace element levels are nearly always noted in the eclogitic inclusions (Gurney, 1984).

Temperatures and pressures of equilibration based on the compositions of coexisting inclusions in diamond have been calculated by numerous authors (Meyer and Tsai, 1976; Gurney et al., 1979<sup>a</sup>; 1984a,b; Hervig et al., 1980; Boyd and Finnerty, 1980) using experimentally derived geothermometers and barometers (e.g. MacGregor, 1974; Lindsley and Dixon, 1976; O'Neill and Wood, 1979; Ellis and Green, 1979). In general, the results indicate that the peridotitic suite equilibrated at temperatures of 1000 to 1200°C and pressures between 45 and 60 kbars. In the case of eclogitic suite inclusions, pressures cannot be calculated, but if pressures of 50 to 60 kbars are assumed, the equilibration temperatures range between 1000 and 1300°C.

The recent discovery of the ancient origins of some diamonds has served to stimulate research in this field. This was first brought to notice by Kramers (1979) in a study of

composited sulphide inclusions from the Finsch, Kimberley and Premier Mines. Other studies using a variety of techniques have also indicated very old ages for diamond (Takoaka and Ozima, 1978; Melton and Giardini, 1980; Evans and Qi, 1982; Ozima et al., 1983, 1984; and Kurz and Gurney, 1986). Model ages in excess of 3.2 by were demonstrated for peridotitic garnet inclusions from Finsch and Bultfontein by Richardson et al. (1984). However, it appears as though eclogitic paragenesis diamonds may be younger, based on the recently reported Sm-Nd isochron ages of 1150 and 1580 my for eclogitic garnet and clinopyroxene inclusions from Premier and Argyle respectively (Richardson, 1986). These ages correlate quite well with the pipe emplacement ages of 1100-1200 my (Kramers, 1979; Skinner et al., 1985) which suggests that eclogitic diamonds may be related in time and space to kimberlite or lamproite magmatism. However, Smith et al. (1986) have recently reported a model age of 1670 my for eclogitic garnet inclusions from a single diamond from the Cretaceous Finsch kimberlite pipe, which effectively preclude the possibility of a direct relationship between eclogitic diamonds and the host kimberlite. More work is required to clarify this important discrepancy.

## 5.2 PHYSICAL CHARACTERISTICS OF THE MONASTERY DIAMONDS

A temporary phase of trial mining in 1982 provided a brief opportunity to sample diamonds hosting mineral inclusions from the mine's production. Monastery was considered an inviting target for a study of mineral inclusions in diamonds because it

is geographically well separated from the established kimberlite diamond mines in southern Africa. It is also a kimberlite with an abundance of fresh xenoliths and xenocrysts of mantle rocks and minerals to which the inclusions and hence the diamonds might be related.

A total of 4600 carats of diamond was examined. The sample was slightly unrepresentative of the mine's total production in that all cuttable stones had been removed. However, cuttable stones only constitute 5% of the mines production on average, the remaining 95% being composed of industrial quality diamonds (5%), and bort (95%) (A.P. van Jaarsveld, pers. comm.).

#### 5.2.1 Size

The entire sample was sieved, using Scott's diamond sieves (Table 5.2), into 16 size groups between +23 and -1 sieve size. A histogram of the size distribution is presented in Fig. 5.1 and it is evident that the general diamond production at Monastery Mine displays an essentially gaussian size distribution which is the case for most kimberlites (Hall and Smith, 1984). The most abundant diamonds are in the size range +3 to -12 (1 to 3 mm) with the population mode being in the range -11 +9 (~2.8mm). However, diamonds smaller than 1mm are screened out during the mining process so that the size distribution shown is not strictly representative of the natural diamond population.

The shaded area in Fig. 5.1 represents the size fractions examined for mineral inclusions i.e. all diamonds in the size

range -9 +5 together with 530 carats and 100 carats in the size ranges -11 +9 and -12 +11 respectively, amounting to 2 300 carats in total.

### 5.2.2 Shape

Monastery diamonds are in general almost completely devoid of primary crystal forms. An extremely high proportion exhibit some form of breakage surface, in fact, large numbers have more breakage surfaces than crystal faces. In spite of this, an attempt has been made to classify the diamonds selected for inclusion study into five categories adapted from Harris et al. (1975) and Robinson (1978). The categories are as follows:

1. Octahedral
2. Tetrahedral
3. Macles
4. Crystal Aggregates
5. Irregulars

The first three categories are illustrated in Fig. 5.2. whilst examples of each category are illustrated in Plates 5.1 to 5.5.

In order to classify diamonds exhibiting both octahedral and tetrahedral crystal forms, an arbitrary point had to be established in the resorption progression. Transitional crystals which have (111) faces dominating over the developing (110) faces, e.g. Fig. 5.2(d) have been classified as octahedra, while crystals with (110) faces of equal or greater surface area than (111) faces have been designated

tetrahexahedra e.g. Fig. 5.2(e).

Macles include contact twins only and broken forms were included in this category where they were recognisable macles. Both octahedral and tetrahexahedral macles (Fig. 5.2 i&j) are represented at Monastery and an example of a tetrahexahedral macle is illustrated in Plate 5.3.

Crystal aggregates include two or more diamonds in some form of conjunction. A diamond may be imbedded in the surface of another, or many stones may be aggregated together (Harris et al. 1975). Interpenetrant twins (e.g. Plate 5.4) have been included in the crystal aggregate category.

Only diamonds where greater than 50% of the surface area is fractured or irregular are designated "irregular". The irregular category is composed of:

- (a) formless masses of diamond (40%)
- (b) dominantly broken fragments but with remnant tetrahexahedroid crystal faces (40%)
- (c) broken fragments with remnant octahedral crystal faces (20%).

Almost all of the breakage surfaces examined display the effects of etching and are thus natural features. An example of a typical irregular category diamond is illustrated in Plate 5.5.

The proportions of diamonds assigned to each morphological category are presented in a histogram in Fig. 5.3(a). The salient features of this diagram include:

- (a) Irregulars are by far the most abundant crystal form in the sample studied.

- (b) The octahedral and tetrahexahedral forms are present in approximately equal proportions both in the single crystal categories and the contact twinned categories (macles).
- (c) The crystal aggregate category is composed of approximately equal proportions of irregular aggregates and interpenetrant twins.

If the subdivisions in the irregular class are considered, then the tetrahexahedral form of diamond dominates at Monastery, which indicates that the diamonds have experienced considerable resorption (Robinson, 1979). Another characteristic feature of Monastery diamonds is that very few are free of inclusions and impurities which mostly take the form of black specks (sulphides and/or graphite?). The high incidence of inclusions correlates with the equally high number of broken diamonds in the sample, since most natural diamond breakage is probably a consequence of internal strain about inclusions (Sutton, 1928).

### 5.2.3 Colour

Only two basic colours were represented in the diamonds examined, namely colourless and brown. Two shades of brown are however distinguishable - pale brown and dark brown. A histogram showing the frequency of occurrence of these diamond colours is presented in Fig. 5.3(b), where it is noted that the sample is composed of approximately equal proportions of colourless and brown diamonds. Yellow diamonds are conspicuously absent and no green staining due to radiation damage was noted.

It has been suggested that brown colouration in diamond may be due to the presence of high levels of elements such as iron, aluminium and magnesium occurring in the form of submicroscopic inclusions (Bibby et al., 1975). Brown colouration has also been attributed to submicroscopic regions of amorphous carbon or graphite localised at lattice dislocations (Urosovskaya and Orlov, 1964). Robinson (1979) demonstrated a strong correlation between brown colour in diamond and the presence of lamination lines (see Appendix 5.1). He concluded that the process responsible for the formation of lamination lines (i.e. shear stress) is also responsible for the colouration of a large proportion of brown diamonds implying that brown diamonds have usually undergone a high degree of plastic deformation.

#### 5.2.4 Surface Features

A wide variety of surface features are well represented on Monastery diamonds (see Table 5.3). Initial observations of these features were made by means of a binocular microscope, after which a subset of representative samples were closely examined by means of a scanning electron microscope (SEM). A brief review of diamond surface features is presented in Appendix 5.1. Only the features represented on Monastery diamonds are discussed, and each is illustrated by means of SEM photomicrographs.

The most common surface features on Monastery diamonds are trigons, hexagonal etch pits, corrosion sculptures and shallow depressions. These are all textures formed in response to high temperature etching. It has already been noted that the

resorbed tetrahedral form of diamond is common at Monastery and resorption related surface textures such as shield-shaped laminae, elongate hillocks and pyramidal hillocks are also well represented. The high incidence of resorption and etch related features in the diamonds suggests that they have experienced temperatures in excess of  $1000^{\circ}\text{C}$  within a hostile environment (Robinson, 1978). Furthermore, lamination lines are present on some diamonds and these are thought to form in response to plastic deformation (Williams, 1932; Urosovskaya and Orlov, 1964). Evans (1976) suggests that temperatures of at least  $1300^{\circ}\text{C}$  and pressures of approximately 50 kbars would be required for natural plastic deformation. However, this may be an overestimate (Harris, 1987).

Since most of the tetrahedral diamonds display etch features (e.g. corrosion sculptures), it would appear that etching either post-dates resorption or that the processes occur simultaneously. The temperatures necessary for the formation of negatively-oriented etch features ( $> 1000^{\circ}\text{C}$ ) are unlikely to be attained in the near surface environment during kimberlite emplacement which would imply that etching, and by implication resorption, probably occurred at mantle depths.

### 5.3 THE MINERAL INCLUSIONS

#### 5.3.1 Methods of Inclusion Recovery and Analysis

In this study, 131 inclusion bearing diamonds in the size range -9 +5 (Table 5.2) have been selected from 4 600 carats of general production. The diamonds are less than 3mm in largest

dimension and average approximately 0.12 carats/stone. Inclusion bearing diamonds were selected after careful examination under a binocular microscope equipped with fine beam fibre optics and up to 80 times magnification.

After recording the features specific to each diamond (e.g. the presence of fractures, size and morphology of inclusions, presence of coexisting mineral pairs etc), the diamonds were immersed in hydrofluoric acid for 24 hours. Following this, they were soaked in aqua regia for an hour and then repeatedly rinsed with deionised water. Inclusions were liberated from their host by breaking the diamond in an enclosed steel cracker. They were then recovered either intact or occasionally in a few pieces by picking through the diamond fragments under a binocular microscope equipped with polarizers. The individual inclusions, usually between 75 and 250 $\mu$ m were mounted in epoxy resin on glass slides and polished. Mineral compositions were then determined by means of microprobe analysis (see Appendix 1 for analytical details).

The chemical analyses presented in plots and tables in this study each represent an average of at least 3 individual spots, either from the same inclusion, or several inclusions from the same diamond. Rare examples of two or more inclusions of a single diamond have been found to possess significantly different compositions. In these cases, more than one analysis for that mineral species is presented for the diamond and each example is individually discussed. A total of 413 electron microprobe analyses are represented in the 108 average analyses presented.

### 5.3.2 Minerals Observed

Abundance estimates of the mineral inclusions in the Monastery diamonds based on visual identification are tabulated in Table 5.4. No attempt has been made to distinguish between olivine, omphacitic clinopyroxene and orthopyroxene optically, as misidentification is easily achieved, leading to confusion in abundance estimates (see Harris and Gurney, 1979). Notable features include:

- (a) Sulphide minerals are by far the most frequently encountered mineral species, occurring in ~60% of the inclusion bearing diamonds.
- (b) Colourless inclusions are well represented and based on the rarity of purple garnets, they are more likely to be omphacitic clinopyroxene than olivine.
- (c) Coexisting mineral pairs are exceedingly rare.

A summary of relative abundances determined subsequent to inclusion recovery and analysis is presented in Table 5.5. Inclusions have been classified into four categories, namely, eclogitic, peridotitic, websteritic and miscellaneous, with the latter category accommodating inclusions of uncertain paragenesis. The salient features recorded in this table are:

- (a) Eclogitic inclusions overwhelmingly dominate over peridotitic inclusions, with garnet being considerably more abundant than clinopyroxene. Accessory eclogitic phases represented include coesite and corundum.
- (b) Peridotitic inclusions are largely represented by olivine. Considering the low number of inclusions of this paragenesis, the presence of Cr-diopside is surprising.

- (c) Two examples of multiphase inclusions of websteritic affinity are present.
- (d) Sulphides represent a major inclusion phase in Monastery diamonds.
- (e) Miscellaneous inclusions recovered include a variety of oxide phases, plagioclase, zircon, phlogopite and moissanite.

An interesting discrepancy between the two sets of abundance data is the large number of eclogitic garnets recovered (47) compared with the moderate numbers actually observed in the diamonds prior to breakage (26). One of the reasons for this was that a large number of garnet inclusions were present in the form of eyes to sulphide rosettes, and consequently their presence was only revealed subsequent to diamond breakage. Errors (particularly underestimates) in the observational data also resulted from the general lack of good windows into the diamonds through which inclusions could be observed.

Another feature which warrants mentioning is the dramatically lower recovery figure for sulphide inclusions compared to the observed abundances. This was due to two reasons. Firstly, a significant number of visually identified sulphides turned out to be magnetite, and secondly, a number of sulphide rosettes consisted of thin films along stress fractures only and did not contain sulphide "eyes". The films were not recoverable. These features do not alter the fact that sulphides represent the most abundant inclusion species in Monastery diamonds.

In summary, the inclusion abundance data indicates that the majority of Monastery diamonds were formed in an eclogitic paragenesis. Furthermore, Monastery represents yet another locality at which sulphides are the dominant mineral inclusion phase found in diamond. It is also interesting to note that not a single chromite inclusion was recovered. In the ensuing text, a detailed account of the mineral inclusion suite is presented under the categories featured in Table 5.5.

#### 5.4 MISCELLANEOUS INCLUSIONS

##### 5.4.1 Sulphides

A detailed investigation of the sulphide inclusions was not an objective of this study. A total of 55 sulphide inclusions representing 30 individual diamonds were successfully recovered. Inclusion sizes range between 20 and 200 $\mu\text{m}$ , but are on average rather small (~60 $\mu\text{m}$ ). Only 9 contained optically discernible exsolutions which appear to be pentlandite [(Fe,Ni)<sub>9</sub>S<sub>8</sub>] and on rare occasions small amounts of chalcopyrite (CuFeS) in a host of pyrrhotite (Fe<sub>1-x</sub>S). The majority of sulphide inclusions appear to be homogeneous pyrrhotite although some may represent monosulphide solid solutions (see Kullerud et al., 1969).

Considering the findings of Yefimova et al. (1983) that sulphides associated with peridotitic diamonds are Ni rich, it would appear that the rare sulphide inclusions hosting pentlandite lamellae are of peridotitic affinity while the majority of pyrrhotite and monosulphide solid solution

inclusions could represent eclogitic paragenesis inclusions.

#### 5.4.2 Oxides

Twenty three oxide inclusions were recovered from 16 diamonds originally classified as hosting sulphide inclusions. Minerals represented include:

magnetite (9); spinel (6); hematite (6); ilmenite (1);  
and magnesio-wustite (1)

In a number of cases, more than one oxide phase is present within a single diamond. Diamond Al-21 hosted 5 oxide inclusions, which included 1 magnetite, 3 spinels of varying composition and 1 hematite. Single inclusions of magnetite and spinel were recovered from diamond Al-14, whilst diamonds Al-11 and B13-01 both contained single inclusions of magnetite and hematite within the same diamond.

Microprobe analyses of the oxide inclusions are presented in Appendix 5.2A and representative analyses in Table 5.6. Magnetite inclusions display virtually pure end-member compositions, but a few have minor amounts of  $Al_2O_3$  (up to 1.54 wt%) and MgO (up to 0.33 wt%) as trace constituents. Apart from a single aluminous spinel (M1A), the spinel inclusions are iron-rich with subordinate concentrations of  $TiO_2$ ,  $Al_2O_3$  and MgO (up to 3.59, 3.36 and 10.55 wt% respectively). The majority of hematite inclusions are pure  $Fe_2O_3$ , but two contain minor  $Al_2O_3$  (up to 0.5 wt%) and MgO (up to 0.82 wt%). The single ilmenite inclusion is iron-rich (51.82 wt%  $FeO^*$ ) with minor MgO (3.15 wt%) and  $Al_2O_3$  (2.25 wt%). An

Fe-Mg oxide mineral which has been termed magnesian-wustite ( $\text{FeO} = 93.01 \text{ wt\%}$ ,  $\text{MgO} = 7.29 \text{ wt\%}$ ) has also been recovered (Moore et al., 1986).

The high incidence of black spots and impurities made correlation between the inclusions observed within the diamond with oxide inclusions liberated upon diamond destruction extremely difficult. In many cases it was not possible to claim with confidence that a particular inclusion was derived from a primary setting within the diamond. The primary nature of a small number of magnetite inclusions was beyond dispute and this includes some which were observed to be associated with primary sulphide inclusions.

A number of reports of magnetite occurring as inclusions are to be found in the literature. Harris (1968) provided X-ray identification for the presence of syngenetic magnetite in diamond while Prinz et al. (1975) reports the occurrence of octahedral shaped magnetite inclusions within diamonds with no external fractures leading to them. They provide chemical data illustrating the magnetites to be essentially pure which is in agreement with the data from this study (Table 5.6 and Appendix 5.2A). Prinz et al. (op. cit.) made use of the diamond burning technique to liberate inclusions from their host and the magnetites recovered contained variable amounts of Ni, Co and Cu inhomogeneously distributed as small spots. These they interpreted to represent remnants of sulphide minerals (e.g. pentlandite, chalcopyrite) which were intergrown with the magnetite before the diamond was burned. Magnetite has also been recorded with native iron and sulphides in a diamond from

the Mir kimberlite, Yakutia (Sobolev et al., 1981).

The six spinel inclusions recovered in this study bear no compositional resemblance to primary spinel inclusions from diamonds worldwide. Primary spinels (chromites) are always extremely rich in chromium ( $\text{Cr}_2\text{O}_3$  ~65 wt%) (Meyer, 1987) and are associated with the peridotitic paragenesis. Compositional considerations therefore indicate that the spinel inclusions recovered in this study most likely represent epigenetic inclusions derived from cracks and fractures in the diamonds.

Hematite inclusions are also considered to be epigenetic since they are generally altered and associated with serpentinous material.

Ilmenite is exceedingly rare as an inclusion in diamond. Meyer and Svisero (1975) reported a stoichiometric ilmenite ( $\text{FeTiO}_3$ ) as a primary inclusion in a diamond from Brazil. Subsequent reports of ilmenite inclusions (Sobolev et al., 1976; Tsai, 1978; Mvuemba Ntanda et al., 1982) indicate them to be Mg-ilmenites which are compositionally similar to other kimberlite associated ilmenites. The ilmenite inclusion recovered in this study is extremely iron-rich and magnesium deficient (51.82 wt%  $\text{FeO}^*$ ; 3.15 wt%  $\text{MgO}$ ) (Table 5.6). It is also enriched in ferric iron ( $\text{Fe}^{2+}/\text{Fe}^{3+} = 1.35$ ) and intuitively one would not expect ilmenite of this composition to be syngenetic with the diamond. Its composition also does not correspond with ilmenites from other associations at Monastery, e.g. megacrysts and groundmass ilmenites and therefore contamination from these sources can also be ruled out. No firm

conclusion can be reached as to the paragenesis of this ilmenite inclusion, but the most likely explanation is that it represents a secondary inclusion from a source unrelated to the kimberlite.

#### 5.4.3 Plagioclase

A plagioclase inclusion was recovered from a diamond hosting an eclogitic garnet (diamond A4-02) but was not observed within the diamond prior to its destruction. It is compositionally different to other feldspar inclusions reported in the literature in that it is a labradorite with 14.03 wt% CaO; 3.52 wt% Na<sub>2</sub>O and 0.12 wt% K<sub>2</sub>O (An<sub>68.30</sub>Ab<sub>31.01</sub>Or<sub>0.70</sub>) (Table 5.6). Prinz et al. (1975), Meyer and McCallum (1986) and Otter and Gurney (1986) report inclusions of almost pure sanidine (virtually no Na<sub>2</sub>O or CaO) while Gurney et al., (1984a) report almost pure albite as an inclusion in a diamond from the Roberts Victor kimberlite.

#### 5.4.4 Zircon

A single inclusion of zircon which was observed to be primary within a diamond has been recovered. The inclusion was identified by means of qualitative microprobe techniques. Only three other cases of zircon occurring as an inclusion in diamond have been reported (Meyer and Svisero, 1975; Mvuemba Ntanda et al., 1982 and Otter and Gurney, 1986).

#### 5.4.5 Phlogopite

A single phlogopite inclusion has been recovered from a diamond (A5-13) hosting two inclusions of eclogitic clinopyroxene of different compositions (see Table 5.13 for clinopyroxene compositions). The phlogopite was not observed within the diamond and the possibility therefore exists that it may be epigenetic. An analysis of its composition is presented in Table 5.6.

Several reports of phlogopite occurring as inclusions in diamond have been recorded in the literature. Prinz et al. (1975) identified phlogopite intergrown with rutile and omphacitic pyroxene in a diamond of unknown origin. The composition of this phlogopite is unusual in that it has low MgO (12.6 wt%) and relatively high TiO<sub>2</sub> and FeO (10.8 and 12.1 wt% respectively). Phlogopite has also been reported in association with an omphacitic clinopyroxene in a diamond from the Finsch kimberlite (Gurney et al., 1979<sup>a</sup>), a synopsis of its composition being: TiO<sub>2</sub> (1.71 wt%), Al<sub>2</sub>O<sub>3</sub> (13.2 wt%); FeO (5.38 wt%) and MgO (25.9 wt%). Meyer and McCallum (1986) reported phlogopite inclusions in diamonds from the Sloan kimberlite which display compositional similarities to MARID micas, and suggested that they were epigenetic. The Monastery phlogopite is similar to that reported by Meyer and McCallum (1986) in that it shows close chemical similarities to MARID micas (Dawson and Smith, 1977). It has an Mg/(Mg+Fe) ratio of 0.82, (Si + Al) < 8, moderate TiO<sub>2</sub> (2.18 wt%) and rather low Al<sub>2</sub>O<sub>3</sub> (7.19 wt%) (Table 5.6).

It can be claimed with confidence that the phlogopite inclusion does not represent contamination by kimberlite groundmass phlogopite which may have penetrated a crack in the diamond, since its composition is significantly different to that of groundmass phlogopite in the Monastery kimberlite (groundmass phlogopite is depleted in  $TiO_2$  and  $FeO$  and enriched in  $Al_2O_3$  and  $MgO$  relative to the inclusion). Furthermore, it is compositionally distinct from phlogopites of other kimberlitic associations, namely, primary and secondary phlogopites in peridotite xenoliths and megacryst phlogopites (see Chapters 3 and 6).

In the absence of optical observations of the phlogopite inclusion within the diamond, no firm conclusion can be reached as to its paragenesis and significance. The options appear to be that the inclusion either represents a syngenetic inclusion of eclogitic paragenesis or an epigenetic inclusion with a possible affinity to the MARID suite, derived by contamination in a crack in the diamond.

#### 5.4.6 Moissanite

Three inclusions of moissanite ( $SiC$ ) have been recovered from Monastery diamonds. These, together with three moissanite inclusions in diamonds from the Sloan diatremes in the U.S.A., represent the first report of the occurrence of this mineral as an inclusion in diamond (Moore et al., 1986). All inclusions were observed to be primary within the diamonds before cracking.

Moissanite has been reported from a wide variety of geological environments, including a number of Soviet kimberlites (e.g. Marshintsev et al., 198 ). However, the validity of the numerous documentations of "natural" SiC have been seriously questioned by a number of authors. Milton and Vitaliano (1984) believe that not a single report convincingly proves its existence in nature and that industrial contamination is the real source.

The moissanite inclusions range in size between 40 and 125  $\mu\text{m}$  and are pale green (translucent) with high birefringence. The morphological characteristics of two of the inclusions in the diamonds were not well noted, but the third (Cl6-01) was described as having a distinctive flattened disc shape (Plate 5.6). This inclusion was analysed by X-ray diffraction (XRD) techniques using a 57.4mm Gandolfi camera and the results are tabulated in Table 5.7. The remaining inclusions were identified by semi-quantitative microprobe techniques which together with careful qualitative scans over the full spectrum of elements detectable on the microprobe indicated them to be pure SiC (~67%Si; 33% C). The procedure adopted in the microprobe analysis of moissanite is outlined in Appendix 5.3.

Although the general structure of silicon carbide is relatively simple (essentially long chains of SiC tetrahedra), detailed structures may be extremely complex due to one dimensional disorder or polytypism ( Shaffer, 1969). Over 75 polymorphs have been identified in the literature. The XRD analysis of the inclusion (Table 5.7) does not perfectly match any of the nine polymorphs for which detailed XRD data was

available ( Shaffer, 1969). However, specific peaks from the 2H and 6H polymorphs correspond with a large number of the inclusion reflections. It is possible that the moissanite inclusion represents a mixture of more than one SiC polymorph, or more likely, that it represents a polymorph for which XRD data was not available to this author.

Two of the moissanite inclusions were liberated from diamonds hosting eclogitic garnets, whilst the third occurred as a discrete monomineralic inclusion. The implications of these mineral associations will be discussed in a subsequent section.

## 5.5 PERIDOTITIC PARAGENESIS

### 5.5.1 Inclusion Compositions

#### **Olivine**

Six olivine inclusions have been recovered and analysed (Table 5.8, Appendix 5.2C) and a histogram of their forsterite contents is presented in Fig. 5.4. Also featured in this figure for comparative purposes are the compositions of olivine inclusions from worldwide localities (Meyer, 1987) as well as the forsterite contents of olivine in lherzolite and harzburgite xenoliths from Monastery (this study). An interesting feature is that only one olivine has a composition in the range typically observed for olivines included in diamond (Fo<sub>93-95</sub>); the rest have compositions in the range Fo<sub>90-92</sub>. The olivines in the xenoliths are also generally more magnesian (Fo<sub>91-96</sub>) than the inclusions. This is unusual in that peridotitic

inclusions in diamonds are mostly more magnesian than olivines in peridotite xenoliths.

Olivine inclusions in diamond often exhibit enrichments in  $\text{Cr}_2\text{O}_3$  above the values observed in olivines of similar forsterite content from other associations. The olivines reported here are no exception, with  $\text{Cr}_2\text{O}_3$  concentrations ranging between 0.04 and 0.11 wt% (Table 5.8). Nickel concentrations are also high (0.34 to 0.38 wt% NiO).

### **Garnet**

The one peridotitic garnet recovered is compositionally somewhat different to the majority of peridotitic garnets included in diamonds from other localities (Meyer, 1987) and coexists with an olivine ( $\text{Fo}_{91.6}$ ). Distinguishing features include high levels of  $\text{SiO}_2$  and  $\text{TiO}_2$  (43.77 and 0.51 wt% respectively) as well as slight enrichments in FeO (7.23 wt%) and CaO (3.66 wt%) compared to the characteristic "G10" garnets (Gurney, 1984) of the harzburgitic paragenesis.

### **Clinopyroxene**

The single peridotitic clinopyroxene recovered is a chrome diopside with 2.00 wt%  $\text{Cr}_2\text{O}_3$ ; 1.69 wt%  $\text{Al}_2\text{O}_3$  and 20.34 wt% CaO (Table 5.8). It is compositionally very similar to the rare peridotitic clinopyroxenes included in diamonds from other localities (Fig. 5.5).

### 5.5.2 Discussion

Two interesting features emerge from the compositions of the olivine inclusions. Firstly, their generally lower than average forsterite content is similar to compositions at other localities where eclogitic diamonds overwhelmingly dominate over peridotitic diamonds e.g. Orapa (Gurney et al., 1984a) and Sloan (Otter and Gurney, 1986). Secondly, the very limited olivine compositional data defines a bimodal distribution of forsterite contents (Fig. 5.4). There is a high probability that this simply reflects the lack of sufficient data, but it is also possible that it indicates that the bimodal olivine distribution described for diamonds from the Premier Mine (Gurney et al., 1985) is also present at Monastery.

Despite the fact that the single peridotitic garnet recovered displays only moderate concentrations of  $\text{Cr}_2\text{O}_3$  (5.34 wt%) together with rather high levels of CaO (3.66 wt%), it can still be classified as a "G10" garnet (classification of Dawson and Stevens (1975) as applied by Gurney (1984)). In a number of respects the garnet inclusion displays compositional similarities to garnets from deformed peridotite nodules, particularly with respect to  $\text{TiO}_2$ , FeO and CaO concentrations. However, its higher  $\text{Cr}_2\text{O}_3$  and MgO contents effectively rule out any direct link between the two associations.

The single coexisting garnet-olivine pair available to estimate the equilibration temperature of the peridotitic paragenesis diamonds, yields a calculated (O'Neill and Wood, 1979, 50Kb) equilibration temperature of  $1173^\circ\text{C}$ . An independent temperature estimate of  $1002^\circ\text{C}$  was made from the

Ca/Ca+Mg of the clinopyroxene inclusion (Lindsley and Dixon, 1976; 20 Kb) based on the assumption that it equilibrated in the presence of orthopyroxene.

The very limited data available therefore suggests that the peridotitic diamonds at Monastery have formed in the temperature range 1000° to 1200°C. This is in agreement with equilibration temperatures estimates for peridotitic diamonds from other localities (see Meyer, 1987 for a compilation of geothermometry and barometry data). The absence of orthopyroxene inclusions of peridotitic affinity precludes the possibility of calculating pressure estimates.

Data on the peridotitic inclusion suite at Monastery is insufficient to adequately characterize this paragenesis of diamonds. However, two features may indicate that they have been derived from a garnet lherzolite paragenesis rather than the refractory harzburgitic paragenesis characteristic of peridotitic diamonds worldwide (e.g. Gurney, 1984). These are:

- (a) The presence of Cr-diopside which is characteristically absent or extremely rare in peridotitic diamonds.
- (b) The Fe-rich nature of the olivine which is more similar to olivines in common peridotite xenoliths than olivines included in diamonds worldwide.

The elevated TiO<sub>2</sub> and FeO concentrations could indicate that the source region of the peridotitic diamonds has been subjected to a metasomatism involving the introduction of Fe and Ti by a diffusive process similar in nature to that described by Harte (1983).

## 5.6 ECLOGITIC PARAGENESIS

### 5.6.1 Inclusion Compositions

#### **Garnet**

Fifty six eclogitic garnets representing fifty individual diamonds have been analysed and representative analyses are presented in Table 5.9. A full listing of garnet analyses is presented in Appendix 5.2D. Their wide range in compositions are illustrated on a Ca:Mg:Fe ternary plot in Fig. 5.5, where they define a calcium enrichment trend with moderate iron enrichment. Included in Fig 5.5 for comparison are compositional fields for garnet and clinopyroxene inclusions from worldwide localities (Meyer, 1987).

Two populations of eclogitic garnets are present in the diamonds and their compositional statistics are tabulated in Table 5.10. The two groups are most easily distinguished on a plot of Si versus Na (Fig. 5.6). One group of 8 (termed Group A) have compositions similar to those described from diamonds worldwide (Meyer and Tsai, 1976; Harris and Gurney, 1979; Gurney et al., 1984 a,b; Prinz et al., 1975; Tsai et al., 1979; Sobolev et al., 1972). They have Na<sub>2</sub>O concentrations which range from 0.10 to 0.25 wt%, variable quantities of FeO, MgO and CaO typical of eclogitic garnets included in diamond, and SiO<sub>2</sub> and Al<sub>2</sub>O<sub>3</sub> present in normal stoichiometric proportions, namely from 39.0 to 42.0wt% and 20.2 to 23.1 wt% respectively (Table 5.10). A series of histograms illustrating the compositional variations displayed by the eclogitic garnets are presented in Fig. 5.7.

Two of the Group A inclusions display slightly aberrant compositions. Inclusion Al-18 has high  $\text{TiO}_2$  concentrations (2.36 wt%) when compared with the average  $\text{TiO}_2$  concentration of 0.60 wt% for the remaining Group A garnets. Eclogitic garnets included in diamonds worldwide typically have  $\text{TiO}_2$  concentrations in the range 0.1 to 1.2 wt%. Inclusion Al-03 displays an extreme depletion in CaO (1.52 wt%) together with high MnO (1.17 wt%). However, this inclusion showed signs of alteration around its margins which may account for these compositional irregularities.

The second group (termed Group B) consists of 46 garnets that form a related suite of unusual compositions which have recently been reported by Moore and Gurney (1985). Particularly extreme concentrations of  $\text{SiO}_2$  and  $\text{Al}_2\text{O}_3$  range to as high as 47.43 wt% and as low as 11.29 wt% respectively (Fig. 5.7, Table 5.10). It should be noted that the low  $\text{Al}_2\text{O}_3$  values are not supported by high  $\text{Cr}_2\text{O}_3$  concentrations as is the case for peridotitic garnets since their average  $\text{Cr}_2\text{O}_3$  concentration is 0.11 wt%. Sodium can be present in extremely high concentrations, ranging from 0.14 to 1.08 wt%  $\text{Na}_2\text{O}$ . The Group B garnets contain variable amounts of FeO and MgO typical of eclogitic garnets included in diamond and the observed range of  $\text{TiO}_2$  concentrations (0.13 to 2.09 wt%) is also typical for garnets of this paragenesis. They are however dominantly enriched in Ca relative to worldwide compositions (Meyer, 1987) and this is illustrated in Fig. 5.5 where they dominantly plot in the region between the clinopyroxene and garnet compositional fields.

A feature of the Group B garnets is that they display an excess of cations (+0.013 to +0.042) above the ideal value of 8.000, based on a formula unit of 12 oxygens. Careful checks performed under identical analytical conditions on eclogitic garnet inclusions from both Premier and Sloan diamonds, as well as on garnets in eclogite nodules from Monastery, yielded significantly lower cation sums (typically 8.000 to 8.025), indicating that the high cation sums are not a result of analytical error. The most likely explanation for this is a significant portion of trivalent iron. Ferric iron calculations have been based on the assumption of perfect stoichiometry (Finger, 1972) in preference to a site allocation method since these garnets have perfect garnet structures (see subsequent section). Both methods were carefully investigated and details thereof are provided in Appendix 5.4 together with a worked example illustrating each method. Also provided in this Appendix are tabulations of FeO and Fe<sub>2</sub>O<sub>3</sub> values for all garnet inclusions calculated according to both methods.

Results indicate that the majority of garnets possess between 15 and 30% of their iron in the ferric state (Fig. 5.8). This is abnormally high for upper mantle derived garnets, particularly in the light of wet chemical determinations of garnets in Roberts Victor eclogites which reveal low concentrations of Fe<sub>2</sub>O<sub>3</sub> (<5 % of Fe present) (Hatton, 1978). If these ferric iron calculations are correct, then the Group B garnets formed in a relatively oxidising environment.

## Clinopyroxene

Thirteen eclogitic clinopyroxenes from eleven diamonds have been analysed. Representative analyses are presented in Table 5.9 and compositional statistics in Table 5.11. A full listing of analyses is provided in Appendix 5.2E. They exhibit a wide range in compositions, which is manifested in the major variations in calculated end-member compositions (for method see Appendix 4.2). End-member compositions are listed in Table 5.12 where it is noted that diopside contents range between 5 and 78 mol%, jadeite between 5 and 25 mol% and enstatite between 9 and 60 mol%. Clinopyroxene compositions expressed as ternary percentages of Ca, Mg and Fe are plotted in Fig. 5.5, where it is noted that half plot within the field of compositions displayed by eclogitic clinopyroxenes from other localities (Meyer, 1987) while the other half range to more magnesian and less calcic compositions. A series of histograms presented in Fig. 5.9 illustrates the range in individual major element concentrations.

Two clinopyroxenes liberated from the same diamond (A5-12) (Appendix 5.2E) have high  $\text{Al}_2\text{O}_3$  concentrations (11.83 and 12.33 wt%) in combination low  $\text{SiO}_2$  (47.15 and 48.60 wt%) and  $\text{Na}_2\text{O}$  (0.78 and 2.49 wt%). This indicates low jadeite contents with a complementary high component of the Ca-Tschermak's molecule ( $\text{CaAlSiAlO}_6$ ). This may imply that a component of garnet is present in solid solution in these clinopyroxenes.

## **Coesite/Quartz**

Two inclusions of pure  $\text{SiO}_2$  have been recovered (see Appendix 5.2F) but it could not be determined whether they represent coesite or quartz, because once liberated from the diamond, they were too small for X-ray diffraction analysis ( $<80 \mu\text{m}$ ). However, their primary setting within their host diamonds argues in favour of them being coesite rather than quartz.

## **Corundum**

A single primary corundum inclusion has only  $\text{TiO}_2$  (3.05 wt%) (Appendix 5.2F) as a minor component which contrasts with the corundum with 1.3 wt%  $\text{Cr}_2\text{O}_3$  reported by Meyer and Gubelin (1981). It is pale translucent green with moderate birefringence.

## **Websterite Association**

Two orthopyroxene inclusions were found to coexist with phases of eclogitic affinity and as such are similar to those reported from Orapa by Gurney et al. (1984<sup>a</sup>). One forms part of a three phase polymineralic inclusion together with garnet (B11-01-01) and clinopyroxene, while the other (A5-17) was intergrown with clinopyroxene (Appendix 5.2G). Both orthopyroxenes are enriched in  $\text{Al}_2\text{O}_3$  (4.10; 11.77 wt%),  $\text{CaO}$  (1.47; 1.14 wt%) and  $\text{Na}_2\text{O}$  (0.26; 0.42 wt%) and have low  $\text{Mg}/\text{Mg}+\text{Fe}$  (0.83 and 0.85) ratios. The intergrown orthopyroxene A5-17 is more aluminous than the other one. The coexisting clinopyroxenes are also aluminous (4.83 and 12.46 wt%  $\text{Al}_2\text{O}_3$ ) and are depleted in calcium (Appendix 5.2G, Fig. 5.5). The two garnets from diamond B11-01 are compositionally distinct from

the Group A eclogitic garnet inclusions. Their magnesium-rich compositions (accompanied by severe calcium depletion in one) are illustrated in Fig. 5.5, while their low levels of  $\text{Na}_2\text{O}$  and slightly elevated  $\text{Cr}_2\text{O}_3$  concentrations are illustrated in Fig. 5.7. The two garnets display substantial differences in composition, with extreme depletion of Ca in the garnet of the polyphase inclusion (B11-01-01) being particularly noteworthy. This garnet is also somewhat unusual in that it is pale green in colour. The most likely explanation for the differences in composition between the two garnet inclusions is that one has undergone diffusive exchange with the coexisting pyroxenes, whilst the discrete garnet has been isolated by the host diamond. However, one would then expect the more Ca-rich garnet to coexist with the pyroxenes, which is not the case.

#### **Compositional variations within inclusions from the same diamond**

Seven examples of multiple inclusions of the same phase in a single diamond, show distinct differences in composition between inclusions. This is an extremely unusual feature in that previous studies (e.g. Meyer, 1987) specifically note that multiple inclusions of a single phase within a diamond usually have the same composition. Five cases of garnet and two of clinopyroxene are presented in Table 5.13.

Diamond A4-11 hosted two Group B garnets which show major differences in concentration for almost all of the analysed elements (Table 5.13). Some of the more substantial differences are in their concentrations of  $\text{SiO}_2$ ,  $\text{Al}_2\text{O}_3$ , FeO, MgO and  $\text{Na}_2\text{O}$  which vary by 3.73 wt%, 6.00 wt%, 5.03 wt%, 7.50 wt% and

0.64 wt% respectively. The host diamond was a single octahedron. Both inclusions were observed within the diamond prior to its destruction, but no record is available of their relative location within the diamond.

Diamonds A2-04 and A4-12 each hosted two Group B garnets which show large differences in composition. Particularly noteworthy are the large variations in their  $\text{TiO}_2$ ,  $\text{Al}_2\text{O}_3$ , FeO and MgO concentrations (Table 5.13). Diamond A2-04 was of tetrahedral morphology. No good windows into the interior of the stone were available, and consequently, only one large orange garnet was observed in situ. Diamond A4-12 was an octahedron with some good crystal faces. A large garnet was observed to be associated with a sulphide rosette while a smaller garnet was noted in the vicinity of an internal fracture which intersected the exterior of the diamond. This could indicate the disequilibrium to be a secondary feature.

Diamond A6-01 hosted three separate garnet inclusions of different compositions. Two are Group B garnets (A6-01-12 and A6-01-13) and the third (A6-01-15) a Group A garnet (Table 5.13). The host diamond was a resorbed octahedron which was free of internal cracks. All three inclusions were observed within the diamond prior to its destruction.

The disequilibrium between the inclusions in the websteritic diamond B11-01 has already been mentioned.

Two clinopyroxene inclusions from diamond A5-12 display significant differences in composition (Table 5.13). Both inclusions are pristine fresh crystals and the host diamond was

a resorbed octahedron devoid of cracks and fractures.

Diamond A5-13 hosted two clinopyroxene inclusions, a Group B garnet (Table 5.9) and a phlogopite (Table 5.6). The major differences in composition between the two clinopyroxenes are in their concentrations of  $\text{TiO}_2$ ,  $\text{Al}_2\text{O}_3$ ,  $\text{CaO}$  and  $\text{Na}_2\text{O}$ . The host diamond was a resorbed octahedron which was free of internal fractures.

#### **Mixed paragenesis inclusions within a single diamond**

A single diamond (A4-09) was found to host an eclogitic garnet in addition to an olivine inclusion. The garnet is a Group B eclogitic garnet with no compositional affinities to the peridotitic paragenesis (e.g.  $\text{Cr}_2\text{O}_3 = 0.04$  wt%, Appendix 5.2D analysis 16). The olivine has a forsterite content of 94.9 which is considerably more magnesian than the other olivine inclusions recovered (Table 5.8; Fig. 5.4).

A small degree of uncertainty exists concerning the reliability of this report. There is no doubt about the presence and primary nature of the garnet which was well documented prior to inclusion recovery. However, the same cannot be claimed for the olivine. Observations made prior to diamond destruction, established the possible presence of two small colourless inclusions which could not be adequately documented due to the lack of a clear window into the diamond. In the recovery process, only two inclusions were found, one garnet and one very small colourless inclusion (the second possible colourless inclusion was not recovered). Despite the fact that it cannot be unequivocally claimed that both

inclusions were observed to be of a primary nature within the same diamond, the author is cautiously confident that this represents a genuine case of both eclogitic and peridotitic paragenesis inclusions occurring within a single diamond.

Three other occurrences of olivine being present within the same diamond as eclogitic paragenesis mineral inclusions have been reported. Prinz et al. (1975) reports a diamond hosting an olivine (Fo<sub>92.6</sub>) with 0.11 wt% Cr<sub>2</sub>O<sub>3</sub> together with rutile, silica (quartz or coesite) and omphacitic clinopyroxene inclusions. Hall and Smith (1984) report an olivine (Fo<sub>91</sub>) to be present in an Argyle diamond hosting a sodium-rich clinopyroxene as well as a grossular-pyrope-almandine garnet with 0.24 wt% Na<sub>2</sub>O. Otter and Gurney (1986) report an olivine (Fo<sub>92</sub>) and an eclogitic garnet occurring as separate inclusions within an interpenetrant twin from one of the Sloan Diatremes in the U.S.A. All of these reports are however recorded as uncertain cases.

#### 5.6.2 Discussion

#### **Comparison of Inclusions with Minerals in Eclogite Nodules from Monastery.**

The compositions of the Group A eclogitic garnet inclusions, the eclogitic clinopyroxene inclusions and websteritic garnet and clinopyroxene inclusions have been compared with those from the eclogite nodule at Monastery in order to evaluate any possible relationships. As already discussed in Chapter 4, the eclogite nodules have been

chemically discriminated into two groups on the basis of  $\text{Na}_2\text{O}$  in garnet and  $\text{K}_2\text{O}$  in clinopyroxene.

Compositions for the inclusions and nodules are plotted on a Ca:Mg:Fe ternary diagram in Fig. 5.10 and salient features include:

- (1) In terms of the three components considered, Group A garnet inclusions span virtually the entire range of compositions recorded by Group I and II eclogite nodules.
- (2) The two websteritic garnet inclusions are more magnesian (and one substantially less calcic) than even the garnet in Group II eclogite nodules.
- (3) Clinopyroxenes in both groups of eclogite nodules show considerably more restricted compositions than the eclogite inclusions which range to substantially less calcic compositions.
- (4) The websteritic clinopyroxenes show extreme depletions in calcium and have no compositional similarities with the xenolith minerals.

Consideration of the  $\text{Na}_2\text{O}$  contents of garnets (Fig. 5.11) shows that Group A inclusions and Group I eclogites have similar ranges in composition (Gp A inclusions = 0.10 - 0.25 wt%; Gp I nodules = 0.11 - 0.23) whilst the low concentrations of  $\text{Na}_2\text{O}$  in garnets from Group II eclogites (< 0.08 wt%) effectively precludes a direct relationship between them and the Group A garnet inclusions. The websteritic garnet inclusions have low  $\text{Na}_2\text{O}$  concentrations (< 0.10 wt%).

A plot of  $\text{TiO}_2$  against  $\text{Na}_2\text{O}$  for the garnets (Fig. 5.12) shows that with the exception of two

of the Group A garnet inclusions, garnets from Group I eclogites and Group A inclusions show coincident trends of moderate  $\text{TiO}_2$  enrichment with increasing  $\text{Na}_2\text{O}$ .

$\text{Cr}_2\text{O}_3$  is plotted against  $100(\text{Mg}/\text{Mg}+\text{Fe})$  in Fig. 5.13 and again it is noted that (with the exception of two inclusions) the Group A inclusions show similar low  $\text{Cr}_2\text{O}_3$  concentrations to those observed in garnets from Group I nodules. The two websteritic garnets show elevated  $\text{Cr}_2\text{O}_3$  along with a garnets from a Group II nodule.

It has been noted from Fig. 5.10 that a significant number of the clinopyroxene inclusions show substantial differences in composition to the clinopyroxenes in the nodules. This feature is well highlighted by a comparison of end-member compositions. A plot of jadeite content against diopside content for the clinopyroxenes (Fig. 5.14) shows that only three of the inclusions plot within the field defined by the xenolith clinopyroxenes. Moreover, the inclusion clinopyroxenes show uncharacteristically low jadeite contents (as well as jadeite plus diopside contents). The relatively low jadeite content of the clinopyroxene inclusions is also manifested on a plot of  $\text{Al}_2\text{O}_3$  against  $\text{Na}_2\text{O}$  (Fig. 5.15) where the clinopyroxenes from Group I nodules clearly show higher concentrations of these oxides. With the exception of the two aluminous eclogitic clinopyroxene inclusions and the websteritic clinopyroxene inclusions, the clinopyroxenes from all associations define a continuous trend of positive slope for these two oxides.

The plot of  $\text{TiO}_2$  versus  $100(\text{Mg}/\text{Mg}+\text{Fe})$  presented in Fig. 5.16 shows the clinopyroxenes in the Group I nodules to be

generally enriched in  $\text{TiO}_2$  relative to the eclogitic clinopyroxene inclusions. The overall more magnesian character of the clinopyroxene inclusions is also evident. Clinopyroxenes from all associations define a trend of increased  $\text{TiO}_2$  with decreasing  $\text{Mg}/\text{Mg}+\text{Fe}$ . Three inclusions do not however follow this trend.

The compositional data presented above has shown that whilst the majority of Group A garnet inclusions are compositionally very similar to garnets from Group I eclogite nodules at Monastery, a major proportion of the clinopyroxene inclusions show substantial compositional differences to the clinopyroxenes in the Group I nodules. This may imply that most of the clinopyroxene inclusions are associated with the Group B eclogitic paragenesis which clearly has no direct simple link with the Group I xenoliths. However, it is still possible that the diamonds hosting Group A garnet inclusions and at least some of those with clinopyroxene inclusions, have been derived from disaggregated diamondiferous Group I eclogites.

#### **The Websterite Association**

The compositional characteristics of the websteritic inclusions are intermediate between eclogitic and peridotitic. The atomic  $\text{Mg}/\text{Mg}+\text{Fe}$  ratios of the garnets are similar to those of peridotitic garnets but an association with this paragenesis is ruled out by their low  $\text{Cr}_2\text{O}_3$  contents. The Fe-rich nature of the pyroxenes also precludes an association with the peridotitic paragenesis. Calculated equilibration temperatures for both mineral pairs in the diamonds are in the range 1400 to 1428°C

(Lindsley and Dixon, 1976; Bertrand and Mercier, 1985) and a pressure of 38 kbars was calculated (Nickel and Green, 1985) for diamond B11-01 (see Table 5.17). The apparent disequilibrium between the garnet and pyroxenes in the polymineralic inclusion (B11-01) is manifested in the extremely high garnet-clinopyroxene (Ellis and Green, 1979) temperature of 1680°C which is 280° hotter than the cpx-opx temperature. There are no real grounds to dispute the validity of the two-pyroxene temperatures, but the pressure estimate must be rejected on the grounds of the disequilibrium between the garnet and the pyroxene inclusions, which has resulted in apparent equilibration conditions (1400°C and 38 kbars) which are not within the diamond stability field.

An examination of the  $P-X_{\text{Opx}}$  diagram of MacGregor (1974) indicates that the maximum T,P conditions at which an orthopyroxene with 11 wt%  $\text{Al}_2\text{O}_3$  can coexist with garnet is 1450°C and 27 kbars. This clearly is not within the diamond stability field. In order to accommodate these levels of  $\text{Al}_2\text{O}_3$  in orthopyroxene in the presence of garnet within the diamond stability field, unrealistically high temperatures would be required. This is implied by the steep nature of the isopleths for  $\text{Al}_2\text{O}_3$  rich compositions (MacGregor, 1974). While it is possible for an orthopyroxene in equilibrium with garnet to accommodate such high levels of  $\text{Al}_2\text{O}_3$ , this cannot be achieved at reasonable temperatures within the diamond stability field. It is therefore concluded that the assemblage represented in diamond A5-17 crystallized in the absence of garnet and as such, cannot be directly related to the eclogitic inclusions at Monastery.

Although the websteritic inclusions display a number of similarities to megacryst compositions and have their high equilibration temperatures, they differ in a number of key aspects, namely the low levels of  $\text{TiO}_2$  in the garnets and the high levels of  $\text{Al}_2\text{O}_3$  in the pyroxenes. These differences preclude a genetic link between these diamonds and the megacryst suite at Monastery.

### **The Group B Garnets**

As already mentioned, the Group B garnets have an eclogitic affinity but display anomalous major element compositions. In fact, at first glance, the more extreme cases resemble amphibole compositions (Table 5.9; Fig. 5.7). Particular compositional features which require explanation include the high  $\text{SiO}_2$  concentrations, low  $\text{Al}_2\text{O}_3$  and high levels of  $\text{Na}_2\text{O}$ . The first objective was to confirm their optical identification as garnets. This was achieved by analysing a subset of samples spanning the compositional range by means of X-ray diffraction (XRD) techniques using a 57.4mm Gandolfi camera and  $\text{Co K}\alpha$  radiation. Analysis by single crystal XRD techniques was an extremely difficult task. Only inclusions larger than  $100\ \mu\text{m}$  in longest dimension could be considered for analysis.

High quality diffraction photographs were obtained and the results indicate that all samples analysed (2 Group A and 4 Group B) possess garnet structures, unequivocally confirming that both Group A and B inclusions represent true garnets (see Table 5.14).

Cell parameters ( $a_0$ ) calculated according to the equation :

$$a^2 = (h^2 + k^2 + l^2) d^2$$

where:

- $a_0$  = the unit cell parameter
- hkl = Miller index for a crystal plane
- d = d-spacing of the crystal

and using the (10 4 0) reflection, range between 11.564 and 11.629 Å, which correlate well with cell parameters for pyrope, almandine and grossular which are 11.455, 11.53 and 11.85 respectively.

The pyroxene and garnet mineral families have closely related basic chemical formulae in that both possess cation to oxygen anion ratios of 2:3. It is well known that under appropriate P,T conditions, small quantities of garnet may be taken into solid solution in pyroxenes (Boyd and England, 1964; MacGregor, 1974). As pressure is increased, however, this solid solution breaks down into low-alumina pyroxene plus exolved garnet (Ringwood, 1967). Experimental evidence has demonstrated that the opposite of this reaction is also possible, namely the solution of pyroxene in garnet (Ringwood, 1967; Ringwood and Major, 1971; Akimoto and Akaogi, 1977; Akaogi and Akimoto, 1977,1979), and because of the large density difference involved, this reaction would also be expected to be strongly pressure dependent. The Group B garnets are interpreted to represent the first natural occurrence of the solid solution of pyroxene in garnet, and consequently, the experimental work relating to the relevant pyroxene-garnet equilibria will be discussed in some detail.

**(i) Review of experimental studies relating to the solid solution of pyroxene in garnet**

The pioneering experimental work on these equilibria was undertaken by Ringwood and Major (1966) and Ringwood (1967). Using a homogeneous glass of composition (wt%)  $90\text{MgSiO}_3 \cdot 10\%\text{Al}_2\text{O}_3$  as a starting composition and subjecting it to a series of desired pressures at  $900^\circ\text{C}$ , Ringwood (1967) reported a number of interesting results. At pressures up to 90 kbars, the  $\text{MgSiO}_3 \cdot 10\% \text{Al}_2\text{O}_3$  glass crystallized to a mixture of about 40% pyrope, 60% clinoenstatite which is the correct proportion for this glass composition assuming the phases to be pure  $\text{MgSiO}_3$  and pure  $\text{Mg}_3\text{Al}_2\text{Si}_3\text{O}_{12}$ . However, as the pressure was increased from 90 to 110 kbars, the proportion of garnet increased from 40% to 80%, and in the pressure range from 110 to 150 kbars, the proportion of garnet increased more slowly from 80 to >95%. These results demonstrated the synthesis of a series of  $\text{Mg}_3\text{Al}_2\text{Si}_3\text{O}_{12}$ - $\text{MgSiO}_3$  garnet solid solutions, extending, at a pressure of about 150 kbars, to a homogeneous garnet of composition  $\text{MgSiO}_3 \cdot 10\%\text{Al}_2\text{O}_3$ . Glasses of composition  $\text{CaMgSi}_2\text{O}_6 \cdot 10\%\text{Al}_2\text{O}_3$  and  $\text{CaSiO}_3 \cdot 10\%\text{Al}_2\text{O}_3$  were found to behave in an analogous manner at high pressure (Ringwood and Major, 1971). The structure of the homogeneous garnet synthesised at 150 kbars implied that one quarter of the silicon and one quarter of the magnesium atoms occupied the octahedral sites in the garnet structure.

Ringwood (1967) extended his experiments to a series of runs on two glasses of eclogitic composition. He found that at

pressures from 16 to 18 kbars, a typical eclogitic assemblage of pyrope-rich garnet and omphacitic clinopyroxene was stable. However, at a pressure of about 100 kbars the solid solution of pyroxene in garnet commenced and this was manifested by an abrupt and major increase in the lattice parameter of the garnet, together with an increase in the relative proportion of garnet to clinopyroxene and an increase in the density of the assemblage. At pressures of 108 kbars, the eclogite had been converted into a "garnetite" (>95% garnet). The behaviour of the eclogites at high pressures was thus demonstrated to be essentially similar to the simple systems previously discussed.

The original experimental work on the pyroxene-garnet transformation has been refined and extended (Akimoto and Akaogi, 1977; Akaogi and Akimoto, 1977, 1979). These studies were carried out on high-pressure apparatus capable of generating pressures up to 250 kbars at high temperatures (1000 to 1500°C) for extended periods of time, thereby enabling the transformation to be accurately documented in a number of chemical systems. Phase relations in the systems  $Mg_4Si_4O_{12}$ - $Mg_3Al_2Si_3O_{12}$  and  $Fe_4Si_4O_{12}$ - $Fe_3Al_2Si_3O_{12}$  at 1000 °C (Akaogi and Akimoto, 1977) and in the system  $Ca_2Mg_2Si_4O_{12}$ - $Ca_{1.5}Mg_{1.5}Al_2Si_3O_{12}$  at 1200°C (Akaogi, 1978) at pressures up to 200 kbars are shown in Fig. 5.17. The experimental results illustrated in this figure indicate the existence of a single-phase field of garnet compositions, a broad two phase region where garnet solid solutions coexist with pyroxene solid solutions and a three-phase field of modified spinel ( $\beta$ ) + stishovite + garnet

solid solutions. Considering for a moment only the system  $Mg_4Si_4O_{12} - Mg_3Al_2Si_3O_{12}$  as an example, it was found that the maximum solubility of enstatite ( $Mg_4Si_4O_{12}$ ) in pyrope ( $Mg_3Al_2Si_3O_{12}$ ) to form a homogeneous garnet solid solution is 60 mol% at 175 kbars and 1000°C. Figure 5.17 shows that at this composition, the relative concentration of garnet solid solution to pyroxene solid solution increases gradually from about 40 to 140 kbars, and then increases rapidly up to 175 kbars. Above 175 kbars the garnet solid solution decomposes into a mixture of modified spinel, stishovite and garnet solid solution containing less than 60 mol%  $Mg_4Si_4O_{12}$ . Similar trends of high pressure transformations are observed in the Fe- and Ca- systems, however, the garnet solvi in these systems occur at respectively lower and higher pressures than the garnet solvus in the system  $Mg_4Si_4O_{12}-Mg_3Al_2Si_3O_{12}$  (Fig. 5.17).

Akaogi and Akimoto (op. cit.) expanded their experimental studies from simple systems to a natural garnet lherzolite assemblage from a Lesotho kimberlite (PHN 1611) and successfully demonstrated a continuous increase in the solubility of pyroxene in garnet in the pressure range 45-205 kbars at temperatures of 1050 to 1200°C (Akaogi and Akimoto, 1979).

Very recently, Sekine et al. (1986) and Irifune et al. (1986)<sup>a+b</sup> investigated the subsolidus phase equilibria of two basaltic (eclogitic) compositions in the pressure range 5 to 180 kbars at 1200°C. This study is of particular relevance to the interpretation of the Group B garnets, due to similarities in bulk composition of the experimental starting materials and the

Group B garnets. In particular, the experimental systems contained significant quantities of sodium (1.9 and 0.65 wt% Na<sub>2</sub>O). Similar results to those discussed previously were obtained, namely that at pressures above 100 kbars, the proportion of garnet in the run products increased quite rapidly with the amount of clinopyroxene diminishing in a complementary fashion. Complete transformation to a pyroxene-free garnetite assemblage occurred at 140 to 150 kbars.

### (ii) Pyroxene solid solution in the Group B garnets

The above review of the experimental studies confirms that considerable amounts of clinopyroxene enter into solid solution in garnet at high pressures. In the process, Al<sup>3+</sup> ions in the octahedral sites of the garnet are replaced by M<sup>2+</sup> and Si<sup>4+</sup> ions (M<sup>2+</sup> = Mg<sup>2+</sup>, Fe<sup>2+</sup> and Ca<sup>2+</sup>). The garnet solid solution can be expressed by the general formula:



where: M = Mg, Fe<sup>2+</sup>, Ca and superscripts denote the coordination number of that cation (Irifune et al., 1986<sup>b</sup>).

This substitution results in an excess of Si atoms over the ideal value of 3 for 12 oxygens with a concomitant fall off in the number of Al atoms below the ideal value of 2 for the same number of oxygens. This phenomenon was well demonstrated by Akaogi and Akimoto (1979) who plotted the number of Si and Al+Cr atoms (based on 12 oxygen atoms) in their synthesised garnets against pressure (reproduced in Fig. 5.18). The salient

features of this diagram include:

- (a) at a pressure of 45 kbars, the number of Si atoms is almost exactly 3 which is expected from the ideal stoichiometry of the garnet formula.
- (b) at 75 kbars, the value increases slightly from 3 to about 3.05.
- (c) at 144-146 kbars a remarkable increase to about 3.3 is observed.
- (d) at the same time as the number of Si atoms increases, the number of Al + Cr atoms decreases from about 1.95 to 1.40.

The Group B garnet inclusions display similar characteristics to the garnets experimentally synthesised by Akaogi and Akimoto (1979) and Irifune et al. (1986<sup>b</sup>). They possess an excess of Si once the tetrahedral site has been filled. The number of Si ions (for 12 oxygens) ranges from 3.046 to 3.429 (see Fig. 5.6). The sympathetic decrease in Al concentrations with increasing Si is also observed in these garnets (cation proportions of Al range from 1.812 down to 0.962). It is therefore proposed that the Group B garnets represent the first natural examples of garnet hosting a component of pyroxene in solid solution.

A more detailed comparison of the compositions of the garnets experimentally synthesised by Akaogi and Akimoto (1979) and Irifune et al. (1986<sup>b</sup>) lends strong support to this interpretation (see Table 5.15). Features of the garnet compositions presented in this table which warrant highlighting include:

- (1) Systematic increases in  $\text{SiO}_2$  concentrations with a decrease in  $\text{Al}_2\text{O}_3$  are observed with increasing pressure in both experimental systems. Identical trends are observed in the inclusion garnets where the range in values for these elements is matched and even extended.
- (2) The garnets synthesised by Akaogi and Akimoto (1979) show an increase in MgO and CaO with increasing pressure while only CaO increases with pressure in the garnets synthesised by Irifune et al., 1986<sup>b</sup>. Since these elements are major components of pyroxene (along with  $\text{SiO}_2$ ), these trends are expected with progressive dissolution of pyroxene in garnet.
- (3) Analyses 8 and 12 represent homogeneous garnet solid solutions in which all of the pyroxene in the system is accommodated (i.e. the eclogite to garnetite transition is complete).
- (4) The garnets synthesised in the Na bearing basaltic (eclogitic) system (analyses 9 to 12) also contain the extremely high levels of  $\text{Na}_2\text{O}$  measured in the Group B garnets, demonstrating that at ultra high pressures, Na becomes incorporated in the garnet structure.

Pursuing the point raised above concerning the correlation between increasing concentrations of CaO and MgO in garnet (i.e. major constituents of pyroxene) and pressure, it is noted that the value of the factor M (where  $M = (\text{Mg} + \text{Fe} + \text{Ca} + \text{Na})$ ) in the Group B garnets increases in sympathy with the increase of Si in the garnet formula above the ideal value of 3.0 (Fig. 5.19). Although M is not a good indicator of the presence of pyroxene

in solid solution in garnet compared with Si, an increase of both M and Si is required to form garnet solid solution with pyroxene components (since pyroxene is essentially composed of Si + M).

The values for Si and Al in the Group B garnets have been plotted on the experimentally produced curves of Akaogi and Akimoto (1979) in Fig. 5.20. The diamond inclusion data spans the entire range of compositions produced in the experimental runs and a few samples extend this range to more extreme compositions invoking even higher pressures of formation.

The pressures of formation indicated by direct comparison of Group B garnet compositions with the experimental data (Fig. 5.20) suggests that they have formed at pressures ranging between 70 and 170 kbars. However, a number of factors need to be taken into consideration. Firstly, the experimental runs were performed isothermally at a temperature of 1200°C which could be an oversimplification in a natural system. Secondly, the pressure at which pyroxene begins to dissolve into the garnet structure and the rate at which this reaction proceeds, is significantly affected by the bulk composition of the system (see Fig. 5.17). It is envisaged that the bulk composition featured in the experimental system (natural peridotite PHN-1611) would provide a reasonable approximation to the reaction rate at high pressure of the eclogitic system in question, since the effects of the additional Fe and Ca in the eclogitic system would be essentially self cancelling (see Fig. 5.17). Irifune et al. (1986<sup>b</sup>) indicate that the pressure calibrations of Akaogi and Akimoto (1979) were overestimated by

approximately 40 kbars in the maximum pressure region of the experiments. Taking this error into consideration, the estimate of the range of formation pressures indicated by the Group B garnets is 60 to 150 kbars.

A notable feature is the tendency for the Ca-rich Group B garnets to have lower Si contents than the magnesian garnets, indicating that they have less pyroxene in solid solution. This is illustrated in Fig. 5.21 where a crude negative correlation between Si and Ca is observed (in this diagram, the Ca-poor compositions represent the Mg-rich garnets (refer to Fig. 5.5)). This is consistent with the data of Akaogi and Akimoto (1979) who found that systematically higher pressures are required for the solution of pyroxene in garnet in Ca-rich systems (Fig. 5.17). In addition, the Fe-Ca rich Group B garnets show more extreme enrichments in Na and lesser depletions of Al than the magnesian Group B garnets. This might be due to a similar effect as that described for inclusions in diamonds from the Orapa Mine (Gurney et al., 1984<sup>a</sup>), where the composition of the pyroxene in equilibrium with garnet changes sympathetically with garnet composition. It is envisaged that the pyroxene being absorbed by the garnet will become progressively enriched in the jadeite molecule as the composition of the host garnets migrate along an Fe-Ca enrichment path. This concept is schematically illustrated in Fig. 5.22 to avoid confusion. The magnesian garnets will host a clinopyroxene which is diopside rich and this will result in enrichments in Si, Mg and Ca at the expense of Al. The levels of Na in the host garnet would be expected to increase, but not dramatically, due to the relatively low proportion of the jadeite molecule in the pyroxene being taken

into solution. The changes in Ca and Mg in the garnets (from the diopside component of the pyroxene) are not so evident since these elements represent major components of the garnets under discussion. However, the Group B garnets are systematically enriched in Ca and extend to more magnesian compositions than eclogitic garnet inclusions from other localities (see Fig. 5.5).

The more evolved Fe-Ca rich garnets will be expected to host in solid solution a jadeite-rich ( $\text{NaAlSi}_2\text{O}_6$ ) clinopyroxene, resulting in large enrichments in Na and lesser depletions of Al in the host garnet relative to the magnesian garnets.

### **(iii) Sodium in garnet**

Sodium is a highly incompatible element in the garnet structure. Despite this fact, a number of reports of low levels of Na being present in both natural and experimentally synthesised garnets are to be found in the literature. A variety of possible substitutional schemes enabling Na to enter the garnet structure have been suggested. Sobolev and Lavrent'ev (1971) found that garnets from diamond bearing eclogites and garnets occurring as inclusions in diamonds commonly contain significant amounts of sodium (up to 0.26 wt%  $\text{Na}_2\text{O}$ ) whereas garnets from ordinary eclogites contained only very small amounts of sodium, suggesting that the elevated concentrations of Na may be correlated with high pressure. They proposed that Na enters the garnet structure according to the equation:



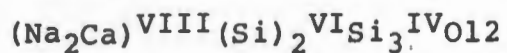
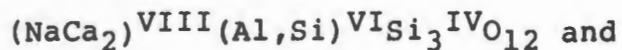
(roman numerals indicate the coordination of the cations)

thereby invoking some Si to be present in octahedral coordination.

Ringwood and Lovering (1970) described the high pressure transformation of a pyroxene-ilmenite lamellar intergrowth into a homogeneous garnet solid solution at pressures in excess of 100kbars. They suggested that the 1.2 wt% Na<sub>2</sub>O present in the starting material might be accommodated in the garnet as (CaNa<sub>2</sub>)Ti<sub>2</sub>Si<sub>3</sub>O<sub>12</sub> and (Ca<sub>2</sub>Na)(AlTi)Si<sub>3</sub>O<sub>12</sub> components, implying the coupled substitution of (Na+Ti) for (Ca+Al) in the grossular structure. However, they never analysed the run products and only accommodated 85% of starting material products in the garnet. Therefore, the Na<sub>2</sub>O could all have been left in the remaining 50% of melt. Ringwood and Major (1971) found that a glass of composition (CaNa<sub>2</sub>)Ti<sub>2</sub>Si<sub>3</sub>O<sub>12</sub> crystallized completely to garnet in runs at pressures between 50 and 120 kbars, indicating that in the presence of Ti, a substantial amount of Na may enter the garnet structure at rather modest pressures.

Ringwood and Major (1971) were also successful in synthesising majorite (Mg,FeSiO<sub>3</sub>; i.e. pyroxene with a garnet structure) at pressures between 250 and 300 kbars and temperatures of 1000°C. The majorite contained 0.63 wt% Na<sub>2</sub>O, but insufficient Ti was present to account for the presence of sodium via the Na-Ti substitution. They therefore opted for the Na-Si substitution independently proposed by Sobolev and Lavrent'ev (1971), thereby implying the existence of

garnets of the type:

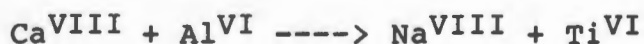


In this scheme, the entry of each Na atom is accompanied by the substitution of a silicon atom in the octahedrally coordinated site.

On the basis of these experiments, Ringwood and Major (1971) suggested that in the depth interval between 350 and 650Km of the mantle, sodium may be accommodated in Na bearing complex garnet solid solutions rather than in a jadeitic pyroxene which they suggest would not be present.

Thompson (1975) reported 0.06 to 0.57 wt%  $\text{P}_2\text{O}_5$  in garnets synthesised from anhydrous basaltic melts at 18-45 kbars and 1200-1450°C and proposed a coupled substitution between Na-P and Ca-Si. He points out that since the sum of atomic radii of Na and P is less than that of Ca and Si, the substitution of an Na-P couple into the garnet structure would be enhanced by high pressure.

Bishop et al. (1976) favour the idea that Na in garnets from peridotites and eclogites can be explained by substitutions of the type:



without the need to invoke octahedral Si. Bishop et al. (1976) also point out the existence of a weak tendency for Na, Ti and P in garnets from eclogites to increase as  $K_D$  ( $K_D = \frac{\text{FeO}/\text{MgO}}{\text{gt}} / \frac{\text{FeO}/\text{MgO}}{\text{cpx}}$ ) decreases. Since  $K_D$  has

been shown from laboratory synthesis (Raheim and Green, 1974) to decrease with increasing temperature and decreasing pressure, Bishop et al. (op. cit.) suggests that this may imply that the substitution of these minor elements in garnet increases with the depth of formation.

The Group B garnets have been carefully analysed for P (refer to Appendix 5.5 for analytical details) and found to have  $<0.01$  wt%  $P_2O_5$ . The coupled substitution between Na-P and Ca-Si is thus not feasible in this case. The coupled substitution between Ca-Al and Na-Si proposed by Sobolev and Lavrent'ev (1971) and Ringwood and Major (1971) is also not possible, due to the existence of a negative correlation between Si and Na in these garnets (Fig. 5.6). The excellent negative correlation observed between Si and Al (Fig. 5.23) however, probably indicates that the substitutional scheme proposed by Akaogi and Akimoto (1979) to account for the compositions of their experimentally synthesised garnets, is also applicable to these garnets. The scheme involves the substitution of  $Al^{3+}$  ions in the octahedral site of the garnet structure by  $M^{2+}$  and  $Si^{4+}$  ions from the pyroxene structure ( $M^{2+} = Mg^{2+}, Fe^{2+}$  and  $Ca^{2+}$ ). Na may be accommodated in the 8-coordinated dodecahedral site, as suggested by Sobolev and Lavrent'ev (1971).

The highest reported sodium value in an eclogitic garnet included in diamond was until recently 0.26 wt%  $Na_2O$  (Sobolev and Lavrent'ev (1971), but Hall and Smith (1984) have reported Na rich eclogitic garnets from Argyle, the highest concentration being 0.52 wt%  $Na_2O$ . Although they also failed to find a

correlation between Na, Ti and P, appreciable  $P_2O_5$  was detected and there is no evidence in the published analyses for excess silica or a deficiency of aluminium. Their garnets do not therefore appear to be similar to those described here.

#### **(iv) Geothermometry**

The majority of studies undertaken on mineral inclusions in diamond to date have placed considerable emphasis on attempting to estimate the temperatures and pressures under which diamonds form (e.g. Gurney et al., 1979 a; 1984a,b; Hervig et al., 1980; Boyd and Finnerty, 1980). These attempts are based on the application of compositional data from coexisting mineral pairs to various experimental and theoretical geothermometers and barometers (e.g. MacGregor, 1974; Lindsley and Dixon, 1976; Ellis and Green, 1979). A major problem with the application of the above equations to minerals in diamonds is that two important assumptions often have to be made. Firstly, in the majority of cases the inclusions are separated by host diamond so that chemical exchange between them is impossible. This means that one has to assume that the inclusions were in equilibrium prior to being included in the diamond, and that they were incorporated almost simultaneously. A second assumption has to be made when all of the phases necessary to apply a geothermometer or barometer are not present, e.g. garnet may have to be assumed to have coexisted with orthopyroxene and clinopyroxene.

Only two diamonds hosting Group B garnet inclusions contained complementary inclusion phases required for

geothermometry. Microprobe analyses of the coexisting phases are presented in Table 5.16, and calculated equilibration temperatures are tabulated together with those from the websteritic assemblages in Table 5.17.

Diamond A5-13 hosts a Group B garnet together with two omphacitic clinopyroxenes. All inclusions were entirely isolated from each other by the host diamond. The two clinopyroxenes possess differences in composition, particularly with respect to their  $\text{Al}_2\text{O}_3$ , FeO, MgO, CaO and  $\text{Na}_2\text{O}$  concentrations (Table 5.13). This is an example of chemical disequilibrium between inclusions within a single diamond. Equilibration temperatures calculated for the two combinations of garnet and clinopyroxene (Ellis and Green, 1979; 50 kbars) are  $1486^\circ\text{C}$  (Cpx 1) and  $1208^\circ\text{C}$  (Cpx 2) (Table 5.17). Diamond B10-01 hosted a Group B garnet and an omphacitic clinopyroxene as discrete inclusions. This pair yields an Ellis and Green (1979) temperature of  $1548^\circ\text{C}$  (50 kbars assumed) (Table 5.17).

Despite the fact that the calculated equilibration temperatures appear reasonable (particularly considering their high pressure origins), they are considered to be geologically meaningless. This is because the application of a geothermometer based on an Fe-Mg exchange reaction to a system in which the garnet hosts a component of pyroxene in solid solution, violates the basic assumptions of the geothermometer concerning substitutional schemes and site occupancies.

## **(v) Disequilibrium Inclusions**

A detailed investigation of the disequilibrium of inclusions within large diamonds is currently in progress in the Soviet Union (Gurney, pers. comm. 1985). Workers are reported to have observed significant variations in the compositions of eclogitic garnet and clinopyroxene inclusions within single stones. These chemical differences appear to be systematic in that inclusions situated in the central regions of a diamond appear to be more magnesian than inclusions located in the outer zones of the crystal. Unfortunately, no relative location data is available for the inclusions in this study, so no direct comparison of these trends can be made. However, it appears that variations in inclusion composition within single diamonds may not be as rare as originally thought. The Soviet work may well turn out to be of extreme importance to future ideas concerning diamond genesis.

Several possible explanations are available to account for the lack of equilibrium between some of the inclusions observed in this study and it is unlikely that a single explanation will suffice.

One possibility is that the diamonds hosting these inclusions represent diamond aggregates composed of two or more individual crystals which have grown at different times. This explanation is unsuitable for all of the diamonds described in this study because careful observations revealed them to be single crystals.

Interaction between inclusions and a fluid phase (which has gained entry to the diamond via micro-fractures could also be a cause of chemical disequilibrium. The features observed in diamond A4-12 may have been the result of such a process. Support for this is found in the fact that one inclusion was located near to an internal fracture which intersected the surface of the diamond. Furthermore, the garnet with an elevated  $\text{TiO}_2$  concentration (A4-12-02; Table 5.13), shows signs of minor alteration around its edges. Interaction with a kimberlitic fluid would most likely result in an enrichment in  $\text{TiO}_2$ .

Another possible method of producing chemical disequilibrium between inclusions is by inclusions in contact with other phases undergoing chemical exchange while monomineralic inclusions in the same diamond are isolated from chemical reaction. As already mentioned, this mechanism may be applicable to the websteritic assemblage in diamond B11-01-01.

The favoured explanation to account for the majority of cases of compositional heterogeneities amongst inclusions is that they simply reflect the complex and episodic growth history of the diamond. Meyer (1985) suggested that the presence of an alternating stratigraphy of Type I and II diamond within a single stone, indicates a discontinuous growth with minor chemical variation occurring in the environment in which growth occurred. Further evidence of this is provided by the presence of diamond as an inclusion in diamond. However, there is still no real concensus on the process involved in diamond genesis. It has been suggested that diamonds form under subsolidus

conditions in the solid state (Meyer and Boyd, 1969; Boyd and Finnerty, 1980), or as a product of a form of metasomatism (Shee et al., 1982) or by igneous crystallization from a magma (Meyer and Boyd, 1972; Gurney et al., 1979 a; Harte et al., 1980; Meyer, 1982 ). Whatever the process, it is possible to envisage diamond growth taking place over a long enough period of time to enable the chemical nature of the earlier formed inclusions to be significantly different to the more evolved compositions of those included at a later stage. The work of Sunagawa (1984) is consistent with this, since he suggests that diamond grew at a slow rate by spiral growth under conditions of low carbon super-saturation.

An important implication of the multiple inclusions of the same phase within a single diamond displaying different compositions is that assumptions of chemical equilibrium between phases useful for geothermometry may not necessarily be valid in all cases.

#### **(vi) The transition-zone of the upper-mantle**

The discovery of garnets from the upper mantle hosting pyroxene in solid solution and having Si in octahedral coordination is important to current petrologic modeling of the mantle. A controversial issue currently under debate amongst geophysicists and experimentalists is the composition of the transition zone of the mantle. The transition zone refers to the region between 220 and 670km depth (Anderson, 1979). There is general consensus and abundant evidence that peridotite dominates in the uppermost portion of the mantle, but the debate

focuses on whether this situation can be generalised to the whole upper mantle. Two opposing models have been put forward.

Anderson (1979), Anderson and Bass (1984) and Bass and Anderson (1984) have proposed that the upper mantle between depths of 200km (or 400)km and 670km is composed predominantly of basaltic material in the eclogite or garnetite facies. Their model is largely based on the seismic properties of the transition zone which they interpret to be more consistent with eclogite than peridotite. Bass and Anderson (1984) introduced a hypothetical olivine-bearing eclogite rock termed 'piclogite' which provided a better match with the densities and velocities throughout the transition region. The low-pressure mineralogy of piclogite is 23% diopside, 21% jadeite, 37% garnet, 16% olivine and 3% orthopyroxene. Anderson and his coworkers envisage a mantle stratigraphy consisting of basalt, peridotite, eclogite, (piclogite) garnetite overlying a depleted peridotitic lower mantle.

Models for the constitution of the transition zone have to adequately account for the seismic discontinuities which occur at depths of 220, 400 and 670km. Anderson (1979) suggests that the 220km seismic discontinuity represents the compositional boundary between depleted peridotite and the underlying eclogite (piclogite). However, Bass and Anderson (1984) concede that both a peridotitic (pyrolitic) and eclogitic assemblage satisfy the seismic properties between 200 and 400km and suggest that the 400km seismic discontinuity may either represent a chemical boundary between pyrolite and piclogite, or phase transformations in the olivine and orthopyroxene components of

the piclogite. The eclogite-garnetite transition, which takes place by the progressive solution of pyroxene in garnet with increasing pressure, has also been proposed as a possible model for the 400km seismic discontinuity (Anderson, 1982; 1984). However, Liu (1980a,b), Bina and Wood (1984) and Irifune et al. (1986<sup>b</sup>) demonstrated that the density increase in the pyroxene-garnet transition cannot account for the 400km seismic discontinuity.

The more widely accepted model for the transition zone of the mantle is that it is dominated by a peridotitic or 'pyrolitic' composition (Ringwood, 1975). The model composition of pyrolite has been reviewed by Green et al. (1979). Phase relationships among pyrolite mineral assemblages in the uppermost 100km of the mantle have been discussed by Green and Ringwood (1970). Below 100km, pyrolite crystallizes to an assemblage of olivine (~57 wt%), orthopyroxene (~17 wt%), garnet (~14 wt%) and diopside (~12 wt%) Ringwood (1975). The sequence of mineral assemblages occurring in pyrolite with increasing depth is depicted in Fig. 5.24 (Fig. 2 of Ringwood, 1982). Mantle structure to a depth of 600km is primarily based on the results of Ringwood (1975) and Akaogi and Akimoto (1977, 1979). Liu (1980a) suggests that the 200km seismic discontinuity can be successfully correlated with the lower boundary of the two phase region of the pyroxene-garnet transition. The 400km seismic discontinuity is attributed to the transformation of olivine to  $\beta(\text{Mg,Fe})_2\text{SiO}_4$ . Further transformation of the  $\beta$  phase to  $(\text{Mg,Fe})_2\text{SiO}_4$  (spinel) occurs at 550km. It should be noted that the progressive solid solution of pyroxene in garnet features strongly in this model

in the depth range 200 to 400km (see Fig. 5.24). Furthermore, between depths of 400 and 600km, the second major phase to  $(\text{Mg,Fe})_2\text{SiO}_4$  is a complex garnet solid solution characterised by partial octahedral coordination of silicon (Ringwood, 1975). The phase transformations occurring below 600km are not of specific relevance to this discussion. Suffice to say that they are based on the results of Liu (1977; 1979); Ringwood and Major (1971); Liu and Ringwood (1975) and Yagi et al. (1979).

The Group B garnets represent the first natural sample of garnet hosting a component of pyroxene in solid solution and this may be taken as direct evidence for the occurrence of the eclogite to garnetite transition in the upper mantle. The progressive solid solution of pyroxene in garnet with increasing depth is a feature of both mantle models outlined above. This reaction occurs in the region between 200 and 400 km depth. Neither model can be unequivocally favoured on the basis of findings of this study. The fact that the Group B garnets have eclogitic affinities does not imply that the entire transition zone of the mantle is composed of eclogite.

#### **(vii) Discussion**

It is pertinent at this point to discuss the moissanite inclusions reported in Section 5.4.6, since two of the three were found in diamonds hosting Group B garnets (A4-03, A1-15). This association implies that the moissanite-bearing diamonds were derived from a high pressure environment. More specifically, estimates of the formation pressures of these two

diamonds based on the composition of their garnet inclusions are 70 and 100 kbars. At Sloan, one moissanite inclusion was associated with a diopside of peridotitic affinity, while another formed the crystalline eye to a sulphide rosette (Otter and Gurney., 1986; Moore et al., 1986). High temperatures and pressures of formation ( $\sim 1370^{\circ}\text{C}$ ; 60 kbars) are also implied for the peridotitic inclusions, but data is very limited (Otter and Gurney, 1986). The common factor between the two occurrences is thus the apparently high T,P conditions under which moissanite-bearing diamonds were formed. Furthermore, it is evident that moissanite is not restricted to either peridotitic or eclogitic paragenesis diamonds (the same is observed for sulphide inclusions). Data on the physical (P,T) and chemical conditions ( $f\text{O}_2$ ) favoured by moissanite is insufficient to justify speculation as to its significance to diamond formation and mantle petrology but its occurrence as a primary inclusion in diamond implies an extremely reducing environment for diamond growth. This is consistent with the common occurrence of sulphide inclusions as well as the rare reports of metallic iron in diamonds (Meyer, 1987).

The high formation pressures indicated by the group B garnets imply that a substantial proportion of the diamonds at Monastery have formed in the depth interval from 160km to in excess of 450km. This extends into the transition zone of the mantle (Anderson and Bass, 1986). Diamonds of peridotitic paragenesis from the Kimberley and Finsch kimberlites in South Africa, have been shown to be extremely old (>3by) (Richardson et al., 1984) and indications are that they formed at depths of 150 to 200 km in the lithospheric root zones of the Kaapvaal

Craton (e.g. Boyd et al., 1985). If the high pressure diamonds at Monastery were formed in a lithospheric environment, then ultra-deep subcontinental root zones are implied (e.g. Jordan, 1981). It is however more likely that they had their origin in the asthenosphere.

Irrespective of the actual process responsible for diamond formation, the diamonds must have formed at the ultra-high pressures indicated by the inclusions (70-150 kbars). However, it should be noted that the diamonds would have been capable of residing in a lower pressure environment for a significant period of time without the inclusions undergoing re-equilibration due to the restraining pressure of the host diamond on the inclusion (Takahashi, pers. comm. 1986).

A possible model for the derivation of these diamonds from the depths indicated can be formulated from the basic concepts of the model of recycling oceanic crust as proposed by Hoffman and White (1982) and Ringwood (1982). In brief, Ringwood's model envisages a relatively cold slab of oceanic lithosphere (basalt underlain by harzburgite) being subducted to depths of 650km in the mantle. The physical characteristics of the slab at this depth are such that further subduction is impaired and the slab buckles to form a large relatively cool "megalith" of mixed former harzburgite and basaltic crust (now eclogite). In the process of thermal re-equilibration (time scale of 1-2 my) the bulk density of the megalith is decreased so that diapirs of harzburgite with entrained eclogite separate and begin an upward ascent. Diapirs of this nature could provide an environment for the formation of the high pressure diamonds observed at Monastery.

It is possible that diamonds may have crystallized from partial melts within a rising diapir, with the source of carbon being former oceanic sediment. Episodic diamond crystallization could occur over the depth interval from 450 km until the base of the lithosphere was encountered. During the period of diamond crystallization, previously formed diamonds could act as nucleation sites for further diamond crystallization, thereby providing a mechanism for producing the disequilibrium observed between the inclusions in some diamonds. The impermeable nature of the rigid lithosphere would cause the diapir to be underplated onto the keel of the subcontinental lithosphere. A significant time lapse would be required between underplating and kimberlite eruption, to enable the constituent material of the diapir to re-equilibrate to the T,P conditions at the base of the lithosphere. This would be necessary since no evidence of ultra-high pressure xenolithic material (particularly eclogite) has been recovered at Monastery. In this model, the diamonds would necessarily be xenocrysts which are significantly older than the kimberlite. Furthermore, an ultra-deep source for kimberlites is not required.

Another possibility is that the high pressure diamonds have been derived from an asthenospheric source and have been sampled by hotspot-related kimberlite. Recent plate tectonics reconstruction models have indicated a possible correlation between South Atlantic hotspots and the Cretaceous kimberlites within southern Africa (e.g. Crough et al., 1980; Duncan, 1981). Furthermore, le Roex (1986) has demonstrated chemical

correlations between Group I and II kimberlites and the South Atlantic hotspots. The diamonds could have formed by crystallisation from a melt which ultimately gave rise to the kimberlite (i.e. the diamonds are phenocrysts from a hotspot-related kimberlite). Alternatively, they may have been sampled from pre-existing pockets of diamondiferous eclogite over the depth interval 450-150 km by a hotspot related kimberlite.

#### 5.7 SUMMARY

1. A large proportion of Monastery diamonds are almost completely devoid of primary crystal form and the majority exhibit some form of breakage surface often accompanied by the effects of severe resorption. The high percentage of broken diamonds correlates with the high incidence of inclusions. The diamonds display a gaussian size distribution, are predominantly colourless or shades of brown and display a wide variety of surface textures.
2. Inclusions in Monastery diamonds are predominantly eclogitic, but peridotitic and miscellaneous paragenesis inclusions are also present (the latter category comprising inclusions of uncertain paragenesis).
3. Primary inclusions within the miscellaneous category include sulphides, magnetite, magnesio-wustite, zircon and moissanite while plagioclase, phlogopite, hematite and spinel are considered to be epigenetic.

4. The moissanite inclusions described in this study together with those from Sloan (Otter and Gurney, 1986; Moore et al., 1986) represent the first report of this mineral as an inclusion in diamond.
5. Inclusions of peridotitic paragenesis are poorly represented. The very limited compositional data available suggests that these diamonds formed in the temperature range 1100° to 1200°C. The absence of orthopyroxene inclusions prevented pressure calculations. It appears likely that the peridotitic diamonds were derived from a garnet lherzolite association rather than the refractory harzburgitic paragenesis characteristic of peridotitic diamonds worldwide. This interpretation is supported by the compositional characteristics of the olivine and garnet inclusions as well as by the presence of Cr-diopside.
5. Two populations of eclogitic garnet are distinguished. One (Group A) has similar compositions to eclogitic garnet inclusions from other localities, while the second (Group B) display the effects of pyroxene in solid solution. These garnets represent the first natural example of this experimentally predicted reaction. Eclogitic clinopyroxenes possess a wide range in compositions which trend towards lower jadeite and diopside contents compared to eclogitic clinopyroxenes from other localities. Accessory eclogitic phases include two suspected coesites and a primary corundum.
7. Some clinopyroxenes and most of the Group A garnet inclusions are similar to minerals of Group I eclogite xenoliths at Monastery so that a minor proportion of the diamonds may be

derived from such xenoliths.

8. Two diamonds hosted polyphase websterite inclusion assemblages which yield calculated temperatures in excess of  $1400^{\circ}\text{C}$ . Their relationship with the peridotitic and eclogitic paragenesis inclusions is unclear.
9. Seven diamonds contained multiple inclusions of the same phase which are not in equilibrium. Episodic diamond growth within an environment of changing chemical composition is favoured as the most likely mechanism to account for the compositional variations.
10. One diamond was found to host an olivine ( $\text{Fo}_{94.9}$ ) as well as an eclogitic Group B garnet. This phenomenon has now been observed by three other authors, and it is considered that genuine cases of mixed paragenesis diamonds do occur.
11. Moissanite-bearing diamonds at Monastery appear to belong to the eclogitic paragenesis and associated Group B garnets imply formation pressures of 70-100 kbars. The presence of moissanite inclusions may indicate extremely reducing conditions for diamond growth.
12. The high formation pressures indicated by the garnet inclusions hosting pyroxene in solid solution (60 to 150 kbars), imply that a substantial proportion of the diamonds at Monastery were formed in the depth interval from 160km to in excess of 450km.

## CHAPTER 6    MEGACRYSTS

### 6.1    INTRODUCTION AND REVIEW

Megacrysts (also termed discrete nodules) are single anhedral crystals of large size (by definition >1cm) which form widespread and sometimes abundant inclusions in kimberlite, in particular Group I varieties. Three distinct suites of megacrysts have been recognised on the basis of major element compositions and physical characteristics, namely Cr-poor megacrysts, Cr-rich megacrysts and the Granny Smith diopside association.

Cr-rich megacrysts are less common than the Cr-poor suite and have been documented at fewer localities (Eggler et al., 1979; Shee and Gurney, 1979). As well as being more Cr-rich, these megacrysts (of olivine, orthopyroxene, clinopyroxene and garnet) are more magnesian and lower in  $TiO_2$  than the Cr-poor suite (Harte, 1983). Diopsides display higher Ca/Ca+Mg ratios indicating generally lower equilibration temperatures compared to the Cr-poor suite. Cr-rich megacrysts are not generally considered to be cognate to kimberlite. Nevertheless, rare earth element (REE) contents of diopsides from this suite require crystallization from a light REE enriched melt more similar to kimberlite than to basalt (Smith et al., 1982). Eggler et al. (1979) suggest that the Cr-rich megacrysts may be derived from hybrid liquids formed by interaction of lithospheric and asthenospheric material in the

immediate vicinity of the rising diapir responsible for the Cr-poor suite.

Granny Smith diopsides are a relatively minor variety of megacryst which are locally common in the Kimberley area (Boyd et al., 1984). These diopsides are easily distinguished from Cr-rich and Cr-poor varieties by their distinct apple green colour. They commonly exhibit deformation textures and are frequently intergrown with ilmenite and phlogopite. Granny Smith diopsides have  $\text{Ca}/\text{Ca}+\text{Mg} > 0.45$ ,  $\text{Mg}/\text{Mg}+\text{Fe} > 0.90$ ,  $0.2 - 0.4$  wt%  $\text{TiO}_2$  and  $0.5 - 3$  wt%  $\text{Cr}_2\text{O}_3$ . They also have  $\text{Na} > (\text{Al}+\text{Cr})$  which is similar to the diopside in MARID nodules, but contrasts with diopsides in peridotites and the Cr-poor megacryst suite (Boyd et al., 1984). Kramers (1979) demonstrated on the basis of Pb-isotopic data that Granny Smith diopsides did not form in equilibrium with their host kimberlite.

Monastery Mine is widely recognised as the type locality for Cr-poor megacrysts (Gurney et al., 1979<sup>b</sup>). They are however widespread in southern African kimberlites and have been described at a number of localities:

Northern Lesotho (Nixon and Boyd, 1973<sup>b</sup>), Frank Smith (Boyd, 1974; Pasteris et al., 1979), Karoo Province (Robey and Gurney, 1979), Kimberley Pool (Boyd and Nixon, 1978), East Griqualand (Boyd and Nixon, 1979), Orapa (Shee and Gurney, 1979), Angola (Boyd and Danchin, 1974), Jagersfontein (Hops et al., 1986). Important features stemming from these studies are summarised below.

The Cr-poor megacryst suite includes the minerals olivine, orthopyroxene, clinopyroxene, garnet, ilmenite, phlogopite and rarely zircon. Megacrysts most commonly occur as discrete monomineralic fragments but lamellar (regular) and granular (irregular) ilmenite-silicate intergrowths can be found. Inclusions of one silicate phase within a different host megacryst also occur but are rare.

The Cr-poor megacrysts show a wide range in chemical compositions and are characteristically chemically homogeneous. Individual mineral species show tightly controlled trends of changing Mg/Mg+Fe with the more Fe-rich silicates coexisting with ilmenite. The relationship between  $TiO_2$ ,  $Cr_2O_3$  and Mg/Mg+Fe in enstatites, diopsides and garnets are consistent with their crystallization from fractionating liquids in a single igneous process (Gurney et al., 1979<sup>b</sup>; Ehrenberg, 1982). Evidence that megacrysts may be related to a liquid of a kimberlitic composition is provided by the occurrence of kimberlitic melt inclusions in some olivine and ilmenite megacrysts (Haggerty and Boyd, 1975; Gurney et al., 1979<sup>b</sup>; Schulze, 1982).

Temperature estimates calculated by a variety of methods are commonly in the range 1400-1050°C, with the lower temperatures being associated with the silicates intergrown with ilmenite. Pressures estimated from the  $Al_2O_3$  content of orthopyroxene are commonly in the region of 45 kbars and show very little range within individual suites (Gurney et al., 1979<sup>b</sup>).

McCallister and Nord (1981) found no evidence for slow, post crystallization cooling and annealing in an electron microscope study of megacryst pyroxenes. The only subsolidus features observed were submicroscopic pigeonite exsolution lamellae, indicating rapid quenching. Megacrysts can therefore not have been formed long before the kimberlite which transported them to the surface.

Nixon and Boyd (1973<sup>b</sup>) and Boyd and Nixon (1973) postulated that the wide temperature and chemical variations displayed by megacrysts reflect their formation in crystal mush magmas dispersed over a vertical range of ~50 km in the upper mantle. They envisage the magma to show a decrease in temperature and the associated megacrysts to become increasingly more Fe-rich with decreasing depth. However, the apparent isobaric crystallization conditions of megacrysts (Gurney et al., 1979<sup>b</sup>; Ehrenberg, 1982) led Harte and Gurney (1981) to propose a model whereby megacrysts of widely differing compositions and crystallization temperatures form simultaneously in an essentially isobaric magma body of wide lateral extent.

Isotopic studies have shown that Cr-poor megacrysts are not in isotopic equilibrium with kimberlite (Barrett, 1975; Kramers, 1979; Kramers et al., 1981; Smith, 1983 a&b; Jones, 1984). Diopside megacrysts from widely separated southern African kimberlites have a restricted range in  $^{87}\text{Sr}/^{86}\text{Sr}$  ratios of 0.7028 to 0.7030, which are significantly lower than those of their Group I kimberlite hosts (commonly in the range 0.7035 to 0.7045) (Smith, 1983a; Jones, 1984). Nd isotopes also show restricted ranges for megacrysts ( $\epsilon\text{Nd} +3 - +5$ ) which overlap

with kimberlite. Jones (1984) reports a Nd-isochron age of  $101 \pm 15$  Ma for Monastery diopside and garnet megacrysts and the initial  $^{143}\text{Nd}/^{144}\text{Nd}$  of  $0.51268 \pm 3$  derived from this isochron overlaps with the initial ratio of  $0.51272 \pm 2$  for Monastery kimberlite given by Smith (1983b), indicating that the megacryst magma and the host kimberlite might be related. Considering the combined Sr and Nd compositions, Cr-poor megacrysts define a restricted field on a Sr-Nd correlation diagram which is close to but separate from the compositions of the Cretaceous Group I kimberlites (i.e. slightly offset below the mantle array in the depleted mantle quadrant).

Limited Pb-isotopic data indicates megacrysts to show rather variable radiogenic compositions with  $^{206}\text{Pb}/^{204}\text{Pb}$  ranging between 19.3 and 20.6 (Smith, 1983 b). However, Smith points out that megacryst diopsides only contain between 0.1 and 0.2 ppm Pb so that contamination from the kimberlite is possible.

Rare earth elements (REE) analyses of Monastery diopside, garnet and ilmenite megacrysts show small but significant variations in the patterns for the individual minerals, and some of this variation can be ascribed to simple crystal fractionation processes (Jones, 1984). Jones investigated the nature of potential melts in equilibrium with megacrysts by the application of experimentally determined crystal-liquid distribution coefficients and concluded that the megacryst magma was more similar to primitive alkali-basalt than the host kimberlite. However, this data should be treated with caution since REE Kds calibrated in basaltic systems were used in the

absence of data applicable to kimberlitic systems. In this regard it should be noted that crystal-liquid distribution coefficient patterns for diopside-liquid vary by a factor of four (Irving<sup>and Frey</sup>, 1978). Kramers et al. (1981) adopted a different approach and argued that megacrysts could have crystallized directly from kimberlite if the kimberlite had lower crystal-liquid distribution coefficient values than for basaltic systems.

Differences in Sr and Pb isotopic composition between megacrysts and kimberlite argue against a direct relationship between the two. However, features such as their similar Nd isotopic compositions, agreement in formation ages, the presence of kimberlitic melt inclusions in olivines and ilmenites as well as the widespread correlation between megacrysts and Group I kimberlites are factors in favour of megacryst-kimberlite consanguinity. Models proposing this alternative therefore argue that the primary kimberlite is isotopically contaminated after megacryst crystallization by interaction with enriched subcontinental lithosphere either by melt contamination or xenolith entrainment and disaggregation (Nixon et al., 1981; Smith, 1983 b).

The restricted isotopic compositions of megacrysts indicates that they were derived from a widespread isotopically homogeneous source. Sr-isotopic compositions are consistent with an asthenospheric source, but their relatively low  $^{143}\text{Nd}/^{144}\text{Nd}$  ratios together with their radiogenic Pb isotopic compositions preclude a MORB type source. Megacrysts are however isotopically similar to many ocean island basalts

(OIB) (White and Hofmann, 1982), indicating that they may have been derived from similar asthenospheric source regions from which OIB are derived. Smith (1983 b) showed that the isotopic compositions of Group I kimberlites are also consistent with such a source.

## 6.2 RELATIVE ABUNDANCES OF MEGACRYSTS AT MONASTERY

Observations made during five visits to Monastery Mine over the period 1982 to 1986 have indicated that both Nixon and Boyd (1973 b) and Gurney et al. (1979<sup>b</sup>) underestimated the abundance of olivine megacrysts. Gurney et al. (op.cit.) observed the following abundances of megacrysts (in decreasing order).

- (1) ilmenite
- (2) diopside/ilmenite
- (3) garnet
- (4) diopside
- (5) olivine
- (6) phlogopite
- (7) orthopyroxene
- (8) garnet/ilmenite
- (9) orthopyroxene/diopside
- (10) rare finds of garnet/diopside and olivine/ilmenite

It is the authors opinion that olivine is only marginally subordinate to ilmenite in abundance. In some areas within the quarry kimberlite, olivine megacrysts are so abundant that only a few centimetres separate individual megacrysts within the kimberlite. This is also true of the east-end kimberlite, but because of severe alteration, recognition of the olivine is more difficult. Olivine and ilmenite megacrysts also dominate the mantle-derived xenolith component of the coarse tailings dumps but olivine megacrysts are not easily recognised in these dumps due to their dull dark brown colour. This could be a reason for

previous underestimates of their abundance.

The relative abundance of diopside and phlogopite megacrysts warrant some comment. In contrast to earlier findings recent observations indicate diopside to be a rare phase in the suite. Furthermore, previous studies have made little mention of phlogopite megacrysts, but new exposure gained from mining operations have revealed fresh phlogopite megacrysts to be plentiful. The apparent decrease in the abundance of diopside megacrysts is difficult to account for. It is possible that localised areas within the kimberlite may be enriched in one phase relative to another. Some evidence of this has been observed at Koffiefontein where the xenolith population was comprehensively sampled in 1977 and found to be almost exclusively composed of pyroxenites (Cardoso, 1980), while a second sampling in 1980 recovered only peridotites and no pyroxenites (Bell, 1981).

In view of the above comments, a slightly revised estimate of the relative abundance of the various megacryst phases from that given by Gurney et al. (1979) is as follows (decreasing order of abundance):

1. ilmenite
2. olivine
3. diopside/ilmenite
4. garnet
5. phlogopite
6. diopside
7. orthopyroxene
8. orthopyroxene/ilmenite
9. ilmenite/garnet
10. orthopyroxene/diopside
11. rare finds of garnet/diopside; olivine/garnet;  
olivine/orthopyroxene; olivine/diopside;  
phlogopite/ilmenite; zircon; zircon/ilmenite;  
zircon/olivine and zircon/phlogopite.

### 6.3 PHLOGOPITE

Previous studies of the megacryst suite at Monastery Mine (Jakob, 1977; Gurney et al., 1979<sup>b</sup>) did not include a chemical characterization of phlogopite megacrysts because of the highly altered (vermiculitized) nature of material available to them at the time of sampling. However, subsequent mining operations have provided access to less weathered kimberlite hosting an abundance of fresh phlogopite megacrysts. Compositional data on phlogopite megacrysts in the literature is limited to the small number of analyses presented by Dawson and Smith (1975). The "megacrysts" described by Boettcher and O'Neill (1980) and Farmer and Boettcher (1981) are thought to represent macrocrysts rather than true megacrysts.

Phlogopite megacrysts are medium to dark brown in colour and range in size between 1 and 6cm (Plate 6.1). They are usually fresh, but may display a narrow marginal alteration zone (Plate 6.1) composed of a fine grained assemblage of spinel, groundmass phlogopite laths and calcite. A small proportion display kink banding along (001) planes (Plate 6.1). Phlogopite megacrysts have been observed to be intergrown with megacrystic ilmenite, Fe-rich olivine and zircon and these associations will be discussed later.

Sixty phlogopite megacrysts have been analysed and compositions are listed in Appendix 6.1. Compositional statistics are summarised in Table 6.1. Core-rim analyses on a number of test samples revealed no chemical zoning and consequently analyses were undertaken on grain mounts of chips taken from phlogopite megacrysts. In the plots which follow,

phlogopites intergrown with ilmenite and/or zircon are indicated by different symbols and their specific compositional features will be discussed in subsequent sections.

Phlogopite compositions are plotted on a  $\text{Cr}_2\text{O}_3$  vs FeO plot in Fig. 6.1 where they are compared with compositional fields for phlogopites from various associations compiled by (Dawson and Smith, 1975). A large proportion are noted to plot outside the megacryst field of Dawson and Smith (1975). They range to higher FeO concentrations (4.53 - 7.64 wt%), overlapping into the MARID field and show considerably lower and more restricted levels of  $\text{Cr}_2\text{O}_3$  (0.01 - 0.27 wt%). This plot also demonstrates the megacryst phlogopites to be compositionally distinct from primary and secondary peridotitic phlogopites as well as metasomatic phlogopite. The higher  $\text{Cr}_2\text{O}_3$  and lower FeO concentrations indicated by the Dawson and Smith (1975) megacryst field may imply that they mistook phlogopite macrocrysts for Cr-poor megacrysts. A break in FeO concentrations is noted in the region of 6 wt% and it is not clear whether this represents a significant compositional feature, or merely reflects a sampling problem.

Assuming all iron to be ferrous, megacryst phlogopites show a sum of  $\text{Si}^{4+}$  and  $\text{Al}^{3+}$  cations which is close to 8.0 (for O=22) (Fig. 6.2). More specifically, they define a broad trend which runs from less than 8 atoms for the high-Si phlogopites to greater than 8 for the low-Si phlogopites. Phlogopites with  $(\text{Si}+\text{Al}) < 8$  may require  $\text{Fe}^{3+}$  to fill the tetrahedral sites, but this cannot necessarily be assumed since Farmer and Boettcher (1981) have suggested a tetrahedral site preference of

Si > Al > Ti > Fe<sup>3+</sup> for phlogopites showing normal pleochroism. Limited observations indicate phlogopite megacrysts to show normal pleochroism (based on observations made on 5 thin sections) so that tetrahedral Ti is possible. Whatever the case, indications are that Fe<sup>3+</sup> is not present at significant levels in megacryst phlogopites.

TiO<sub>2</sub> is plotted against Mg/Mg+Fe in Fig. 6.3 where they are noted to range between 0.64 and 1.52 wt% and 84.1 to 90.5 at% respectively. This plot illustrates that phlogopites with Mg/Mg+Fe > 85 show a trend of decreasing TiO<sub>2</sub> with Fe-enrichment, while the small number of phlogopites with Mg/Mg+Fe < 85 show increasing TiO<sub>2</sub> with increasing Fe. This latter trend is consistent with normal igneous fractionation trends and the positive correlation between TiO<sub>2</sub> and Mg/Mg+Fe displayed by the majority of phlogopites is interpreted to reflect their crystallization in the presence of ilmenite. The intersection of these two trends therefore reflects the point at which ilmenite ceases to crystallize. The compositional break previously noted is evident between Mg/Mg+Fe values of 87 and 88.

Figure 6.4 illustrates a broad correlation between Cr<sub>2</sub>O<sub>3</sub> and Mg/Mg+Fe with Cr<sub>2</sub>O<sub>3</sub> tending to decrease with iron enrichment. The limited range and low levels of Cr<sub>2</sub>O<sub>3</sub> contribute to the diffuse trend observed.

Megacryst phlogopites contain between 11.35 and 12.75 wt% Al<sub>2</sub>O<sub>3</sub> which is similar to Al<sub>2</sub>O<sub>3</sub> concentrations in primary peridotitic phlogopite (Carswell, 1975), but significantly higher than those in MARID phlogopites (Dawson and

Smith, 1977).  $\text{Al}_2\text{O}_3$  shows a good positive correlation with  $\text{TiO}_2$  (Fig. 6.5). Arai (1984) points out that Al in phlogopites may vary according to three kinds of coupled substitutions;  $\text{Mg.Si} = 2\text{Al}$  (Tschermak's substitution),  $2\text{Si} = \text{Mg}.2\text{Al}$  (Seifert and Schreyer, 1971) and  $\text{Mg}.2\text{Si} = \text{Ti}.2\text{Al}$  (Robert, 1976). The good positive correlation between  $\text{Al}_2\text{O}_3$  and  $\text{TiO}_2$  in the megacryst phlogopites (Fig. 6.5) may therefore be a reflection of the coupled substitution  $\text{Mg}.2\text{Si} = \text{Ti}.2\text{Al}$ .

$\text{Na}_2\text{O}$  (0.12 - 0.42) and  $\text{K}_2\text{O}$  (9.74 - 10.54 wt%) collectively fill the alkali sites and show no systematic correlation with other elements.

#### 6.4 ZIRCON

##### 6.4.1 Introduction

Zircon ( $\text{ZrSiO}_4$ ) is an extremely rare accessory mineral found in Group I kimberlites. Previous studies on kimberlitic zircons e.g. Kresten (1973 a), Kresten et al. (1975) have found that they typically display a rounded to subrounded morphology with euhedral examples being almost entirely absent. They also commonly show perfect parting along (100) and (111) as well as a high incidence of fluid inclusions occupying healed fractures.

Zircon is particularly important because of its suitability for U-Pb radiometric dating of kimberlites. However, kimberlitic zircons do not contain high concentrations of uranium (typically 7 to 28 ppm, Ahrens et al., 1967) which complicates the dating procedure.

Kresten et al. (1975) suggested that the parting found in kimberlitic zircons could be the result of shear stress in the low velocity zone and following the Nixon and Boyd (1973 a) model for megacryst and sheared peridotite formation, proposed a possible relationship between zircons and the megacryst suite. Further evidence for this association is the common occurrence of ilmenite-zircon intergrowths at Monastery (Whitelock, 1973). Zircons have also been reported to host mineral inclusions which include chrome diopside (Holmes and Paneth, 1936); diamond, magnesian ilmenite and phlogopite (Kresten, 1973b); pyrrhotite, pentlandite, native copper, rutile, ilmenite, pyroxene and phlogopite (Raber, 1978).

Zircon is present in above average concentrations at Monastery and a large sample of zircon-bearing kimberlite fragments have been recovered due to it being concentrated in the sortex diamond recovery process. Zircon has been found in four different associations, namely:

- (a) discrete rounded crystals within kimberlite
- (b) intergrown with megacryst ilmenite
- (c) intergrown with megacryst olivine
- (d) intergrown with megacryst phlogopite

A breakdown of the number of specimens comprising each association is tabulated in Table 6.2.

#### 6.4.2 Discrete Zircons

##### **Physical Characteristics**

A random sample of 480 discrete zircons have been measured to determine the size characteristics of the zircon suite and results are displayed on a histogram in Fig. 6.6. The sample defines a slightly positively-skewed normal distribution with zircons ranging in size between 2 and 30mm in the longest dimension. The population mode is between 8 and 10mm. The overall nature of the zircon suite is thus characteristically coarse grained.

Colour variations within zircons have also been noted. Dominant colours are a pale brownish honey colour and clear-colourless. The honey-coloured variety dominate the colourless zircons in the proportion 85% to 15%. It is interesting to note that when the honey coloured zircons are heated to 900°C for approximately one minute, they lose their colour. This could indicate that the brownish tint may be due to a high incidence of fluid inclusions which volatilise upon heating.

##### **Zircon-Kimberlite Interface Zones**

Kimberlitic zircons are generally covered with a fine white coating which was found by Kresten (1973 a&b) to be composed of variable mixtures of monoclinic and tetragonal  $ZrO_2$ . Raber and Haggerty (1979) described the occurrence of Ti-rich baddeleyite ( $(Zr,Ti)O_2$ ) in the interface zones between zircon and kimberlite and zircon and ilmenite. Reflected light microscopy undertaken in this study confirms the presence of

baddeleyite in these interface zones (Plates 6.2 & 6.3). Plate 6.2 illustrates an example of baddeleyite developed within a zircon crystal surrounding a calcite inclusion, while Plate 6.3 illustrates the vastly different optical properties of baddeleyite when observed in reflected light under glycerine immersion. Euhedral baddeleyite has been found to be abundant in these reaction zones (Plates 6.2 & 6.3) which is in contrast to the findings of Raber and Haggerty (1979).

A distinctive feature of baddeleyite layers surrounding zircon, is that they usually display well defined zones with sharp boundaries separating each zone. This zonation is illustrated in Plate 6.4 and Fig. 6.7 which is a schematic representation of an average baddeleyite layer surrounding zircon. In some cases not all of the zones illustrated above are developed, and the relative width of each zone also varies considerably. A brief description of each zone follows (refer to Fig. 6.7):

Zone 1 is the layer immediately adjacent to the zircon and is not always developed, but in some cases may be up to 2mm in width. This layer is composed of extremely fine grained irregular baddeleyite crystals which combine to produce an overall texture of large irregular pseudo-grain outlines. This texture is illustrated in Plate 6.5.

Zone 2 is composed of coarser grain size ( $0.02\text{mm}$ ) anhedral baddeleyite crystals which are intergrown in a random fashion within a turbid amorphous matrix.

Zone 3 is characterized by larger ( $0.08\text{mm}$ ) euhedral to subhedral baddeleyite laths which usually display two preferred directions of orientation as illustrated in Plate 6.6. This zone is

usually substantially narrower than the other zones, commonly approximately 0.2mm in width.

Zone 4 is very similar to zone 2 in overall texture, but is noticeably finer grained, the average grain size being approximately 0.01mm.

Zone 5 is composed of relatively large (0.2mm) euhedral to subhedral baddeleyite crystals. This zone is in contact with the kimberlite groundmass and it is well illustrated in Plate 6.4. Zone 5 commonly consists of a central layer of lath shaped grains enclosed on either side by large anhedral baddeleyite grains.

Rare examples of ilmenite, spinels and sulphide minerals are also present within the baddeleyite layers surrounding zircon. Ilmenites may be completely anhedral and resorbed in appearance (Plate 6.7) or they may be subhedral to euhedral (Plate 6.8). Sulphides represented include pyrrhotite, pyrite, covellite and chalcopyrite (Plate 6.9). Extremely rare traces of native copper have also been observed within the baddeleyite layers.

Baddeleyite is thought to form in a desilicification reaction (Raber and Haggerty, 1979).



The problem with the above reaction is that no silica phase has been identified in the baddeleyite zones. The nature of the presumed silica phase could be important in that it could place constraints on the timing of the reaction e.g. the presence of

coesite would indicate that baddeleyite formed in a high pressure environment i.e. pre-kimberlite eruption. The turbid material interstitial to baddeleyite crystals could possibly represent a silica phase, but only monoclinic baddeleyite has been detected in powder X-ray diffraction analyses.

Butterman and Foster (1967) have shown that zircon breaks down to tetragonal baddeleyite plus cristobalite at 1676°C. They also show that monoclinic baddeleyite plus zircon are stable below 1170°C and between this temperature and 1676°C tetragonal baddeleyite plus zircon are stable. The apparent absence of tetragonal baddeleyite in the zircon-kimberlite interface zones indicates that the reaction occurred at least below 1170°C.

Indications are that the desilicification reaction occurred during and immediately after kimberlite emplacement. The silica liberated during the breakdown of zircon to form baddeleyite is either partitioned into the final crystallizing groundmass phases, or dissolved into a late stage fluid phase and removed from the reaction site in solution. The rare oxide and sulphide phases in the baddeleyite zones represent accidentally enclosed groundmass phases rather than phases related to the breakdown reaction.

#### 6.4.3 Zircon-Ilmenite Association

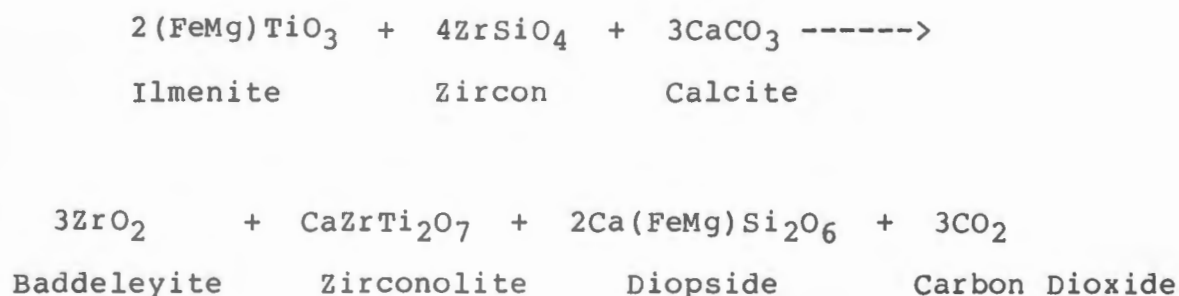
As previously stated, zircon intergrown with ilmenite has been found to be a common association at Monastery. A total of 248 zircon/ilmenite intergrowths have been recovered which

represents 11% of the total zircon population sampled (Table 6.2). Characteristically, ilmenite forms the host mineral, and both minerals are usually anhedral in form. This association has also been reported from other localities including the Kimberley pipes and Mothae in Lesotho (Raber and Haggerty, 1979) as well as Lekkerfontein (Robey and Gurney, 1979). An example of a zircon/ilmenite intergrowth is illustrated in Plate 6.10.

### Zircon-Ilmenite Interface Zones

The interface zones between zircon and ilmenite can contain an unusual mineral assemblage consisting of zirconolite ( $\text{CaZrTi}_2\text{O}_7$ ) (see Plate 6.11), Ti-rich baddeleyite ( $(\text{TiZr})\text{O}_2$ ), diopside ( $\text{CaMgSi}_2\text{O}_6$ ) and calcite ( $\text{CaCO}_3$ ).

Raber and Haggerty (1979) suggested that these assemblages are formed in an intercrystalline reaction triggered by a carbonatitic fluid. A Ca-rich fluid phase was suggested because the reaction assemblages only occur in samples with calcite in the mineral interface zones and CaO is the only component necessary for the formation of the observed minerals because Zr, Si, Fe, Mg and Ti are already present in the zircon and ilmenite. The reaction proposed is as follows:



Raber and Haggerty (1979) could not establish the precise timing of the reaction, nor the stage of kimberlite formation which accompanied the reaction but they consider it to be a secondary reaction which may have developed during fluidization or emplacement. These reaction assemblages are therefore of no assistance in constraining the origin of the zircon-ilmenite intergrowths.

### **Ilmenite Mineral Chemistry**

Ninety-three ilmenites associated with zircon have been analysed by electron microprobe techniques. Analyses were performed on grain mounts of chips taken from the nodules. A full listing of analyses is provided in Appendix 6.2 and compositional statistics are summarised in Table 6.3.

A striking compositional feature of these ilmenites is that two distinct groups are discriminated on the basis of  $\text{Al}_2\text{O}_3$  concentrations. This is well illustrated on a plot of  $\text{Al}_2\text{O}_3$  versus  $\text{Cr}_2\text{O}_3$  (Fig. 6.8) where a clear compositional break is noted between 0.19 and 0.27 wt%  $\text{Al}_2\text{O}_3$ .  $\text{Cr}_2\text{O}_3$  concentrations span a narrow range (0.65 - 1.16 wt%) and show no correlation with  $\text{Al}_2\text{O}_3$ . The two groups have mean  $\text{Al}_2\text{O}_3$  concentrations of 0.14 and 0.32 wt%.

In order to further investigate the possible existence of two populations of ilmenite associated with zircon, ilmenites have been divided into two groups on the basis of their  $\text{Al}_2\text{O}_3$  contents. Compositional statistics of the two groups are tabulated in Table 6.4.

Ilmenites associated with zircon are iron-rich in comparison to kimberlitic ilmenites. Total iron expressed as FeO\* range between 37.6 and 44.5 wt% and upon recasting into FeO and Fe<sub>2</sub>O<sub>3</sub> (Finger, 1972), it is found that the high Al<sub>2</sub>O<sub>3</sub> ilmenites contain a generally higher ferric-iron component than the low Al<sub>2</sub>O<sub>3</sub> ilmenites (Fig. 6.9). However, the two groups show similar FeO concentrations (Fig. 6.10).

Both MgO and TiO<sub>2</sub> show reasonable correlation with the groupings based on Al<sub>2</sub>O<sub>3</sub> (Figs 6.11 and 6.12 respectively). Overlap between the two groups is evident in both plots, but it is clear that the low Al<sub>2</sub>O<sub>3</sub> ilmenites have generally higher concentrations of TiO<sub>2</sub> and MgO compared to the high Al<sub>2</sub>O<sub>3</sub> ilmenites (see also Table 6.4).

When atomic Mg is plotted against atomic Fe<sup>2+</sup> (Fig. 6.13), the two groups define separate trends both of negative slope within the same range of Fe<sup>2+</sup> concentrations. However, a small number of samples in both groups do not adhere to this correlation.

The plots presented above demonstrate that oxides such as Fe<sub>2</sub>O<sub>3</sub>, MgO and TiO<sub>2</sub> show a general correlation with the grouping based on Al<sub>2</sub>O<sub>3</sub> concentrations. However, this grouping is not completely rigid since a number of samples show inconsistent chemical characteristics. Two possible explanations for the observed groupings have been considered.

Ilmenites often host subsolidus-reduction "exsolution" lamellae of spinel (commonly titanomagnetite) (e.g. Haggerty,

1975<sup>a</sup>). It is possible that available  $\text{Fe}^{3+}$  and Al will be preferentially partitioned into the spinel lamellae during the "exsolution" process causing the host ilmenite in lamellae-bearing samples to be depleted in spinel-forming elements relative to lamellae-free ilmenites. The distribution of spinel lamellae is characteristically sporadic i.e. some areas within a polygranular ilmenite nodule may contain lamellae, while an immediately adjacent grain or area may be completely devoid of lamellae. It therefore follows that the random sampling of chips from the ilmenite/zircon assemblages (for microprobe analysis) yielded both lamellae-bearing and lamellae-free ilmenite grains. If the above described process were responsible for the observed compositional grouping, all low  $\text{Al}_2\text{O}_3$  ilmenites would be spinel-bearing and the high  $\text{Al}_2\text{O}_3$  ilmenites homogeneous. A schematic representation of this model is presented in Fig. 6.14.

A second possible mechanism for producing the compositional groupings could be that the high  $\text{Al}_2\text{O}_3$  ilmenites represent analyses where the electron beam of the microprobe has overlapped onto spinel lamellae. Since the lamellae are titanomagnetites, contaminated ilmenite analyses would be expected to be enriched in  $\text{Fe}_2\text{O}_3$  and  $\text{Al}_2\text{O}_3$  with a sympathetic drop-off in  $\text{TiO}_2$ ,  $\text{MgO}$ ,  $\text{MnO}$  and  $\text{FeO}$  concentrations, all of which are features of the high  $\text{Al}_2\text{O}_3$  ilmenites.

In order to test the feasibility of the above two explanations, individual ilmenite grains on which analyses were performed have been examined under reflected light using a high power glycerine immersion objective. Neither of the

explanations are possible when the petrographic data is considered.

The first explanation is not feasible because 60% of the low  $\text{Al}_2\text{O}_3$  ilmenites do not have a trace of spinel lamellae present. The second alternative is equally implausible since 40% of the high  $\text{Al}_2\text{O}_3$  ilmenite grains analysed have no spinel lamellae. It is therefore evident that no direct simple relationship exists between the occurrence of titanomagnetite lamellae in the ilmenites associated with zircon and the observed compositional groupings and in the absence of any other suitable explanation, it is concluded that two distinct populations of ilmenite are associated with zircon.

#### **Comparison with other ilmenite megacryst associations at Monastery**

A large data set of analyses of monomineralic ilmenite megacrysts as well as megacrystic ilmenites coexisting with silicate phases has been compiled for comparison with the compositions of the ilmenites associated with zircon. This data includes analyses undertaken in this study, as well as data from Jakob (1977) and Mitchell (1977). A full listing of mineral analyses is provided in Appendix 6.3. In order to avoid lengthy repetitions, the phrases "ilmenites coexisting with zircon" and "ilmenites coexisting with silicates" are abbreviated to "Z-ilmenites" and "S-ilmenites" respectively. Ilmenites intergrown with silicates include the regular lamellar intergrowths of ilmenite with enstatite and diopside, as well as irregular granular intergrowths of ilmenite with enstatite, diopside and garnet. Ilmenites associated with phlogopite are

not included in this group since they are discussed separately.

Compositional statistics for the three associations are summarised in Table 6.5. Examination of this data reveals that a considerable overlap in composition exists between the ilmenites of the three associations. Both Z- and S-ilmenites show restricted compositions within the range of monomineralic ilmenite compositions. Z-ilmenites are characterized by lower average  $\text{Al}_2\text{O}_3$  and  $\text{MgO}$ , and considerably higher  $\text{Cr}_2\text{O}_3$ . They also show more restricted and generally higher concentrations of  $\text{Fe}_2\text{O}_3$ ,  $\text{FeO}$  and  $\text{MnO}$  compared to the monomineralic ilmenites and S-ilmenites.

The compositional range of the analysed ilmenites expressed as the ternary percentages of ilmenite ( $\text{FeTiO}_3$ ), geikielite ( $\text{MgTiO}_3$ ) and hematite ( $\text{Fe}_2\text{O}_3$ ) are illustrated in Fig. 6.15. The salient features illustrated in this ternary are:

- (1) Z-ilmenites show restricted compositions within the range of monomineralic ilmenite megacryst compositions, occupying the iron-rich extreme of this field
- (2) the two groups of Z-ilmenite compositions can be distinguished in terms of end-member components: the high  $\text{Al}_2\text{O}_3$  ilmenites are more enriched in hematite than the low  $\text{Al}_2\text{O}_3$  ilmenites
- (4) S-ilmenites also show restricted compositions within the range of monomineralic megacryst compositions but are generally more magnesian than Z-ilmenites.

Plotting  $\text{Al}_2\text{O}_3$  against  $\text{Cr}_2\text{O}_3$  (Fig. 6.16) shows that while the majority of monomineralic ilmenites and all of the S-ilmenites have substantially lower  $\text{Cr}_2\text{O}_3$  and higher  $\text{Al}_2\text{O}_3$  than Z-ilmenites, a significant number of monomineralic ilmenites match their compositions in terms of these two oxides. Furthermore, all of the ilmenites intergrown with phlogopite plot with the Z-ilmenites. A break in  $\text{Cr}_2\text{O}_3$  concentrations is evident between .55 and .64 wt%.

$\text{Fe}_2\text{O}_3$  is plotted against  $\text{Cr}_2\text{O}_3$  in Fig. 6.17. Here the limited (i.e. relative to the other ilmenite associations) range of  $\text{Fe}_2\text{O}_3$  concentrations displayed by the Z-ilmenites is illustrated. It is also noted that while a large number of monomineralic ilmenites have similar compositions to those of the low  $\text{Al}_2\text{O}_3$  group of Z-ilmenites, very few show the combination of elevated  $\text{Cr}_2\text{O}_3$  and  $\text{Fe}_2\text{O}_3$  displayed by the high  $\text{Al}_2\text{O}_3$  Z-ilmenites.

A plot of MgO versus FeO (Fig. 6.18) shows the negative correlation expected for these two oxides. The S-ilmenites have higher MgO and define a trend of shallower slope compared to the Z-ilmenites. Monomineralic ilmenites however, show a wide range in MgO and FeO contents which includes that shown by the low  $\text{Al}_2\text{O}_3$  Z-ilmenites which occupy the Fe-rich, Mg-poor region of this trend. The high  $\text{Al}_2\text{O}_3$  Z-ilmenites form a unique trend with only a small number of monomineralic ilmenites matching their compositions. One of the ilmenites associated with phlogopite plots with the low  $\text{Al}_2\text{O}_3$  Z-ilmenites but the remaining three are amongst the most magnesian ilmenites analysed. These are enclosed in a field labelled P2 and will be

discussed in more detail later.

MgO shows a good positive correlation with  $TiO_2$  (Fig. 6.19). In this plot, ilmenites from all associations define a single trend. The Z-ilmenites occupy the MgO-poor,  $TiO_2$ -poor region of the trend and again it is noted that very few monomineralic ilmenites are similar to the high  $Al_2O_3$  Z-ilmenites. The compositional distinctions between the S-ilmenites and Z-ilmenites are again evident.

The plots presented above show the relationships between the various megacrystic ilmenite associations at Monastery to be rather complex. Notable features include:

- (1) the two groupings of compositions associated with Z-ilmenites.
- (2) the distinctive trend defined by the high  $Al_2O_3$  Z-ilmenites on the MgO versus FeO plot (Fig. 6.18).
- (3) the higher  $Cr_2O_3$  signature accompanying the Z-ilmenites, ilmenites associated with phlogopite as well as a significant number of monomineralic ilmenite megacrysts.
- (4) the highly magnesian character of three of the ilmenites coexisting with phlogopite.

These features will be addressed in the subsequent discussion section.

#### 6.4.4 Zircon-Olivine Association

Sixteen zircon/olivine intergrowth assemblages have been recovered from the zircon-bearing coarse concentrate. Ten of

these are two-phase assemblages of zircon-olivine; five consist of the assemblage zircon-olivine-ilmenite and one is a four phase assemblage zircon-olivine-ilmenite-phlogopite (see Table 6.9). Since these nodules have all passed through the primary crusher during mining operations, the original size of the olivine crystals cannot be established. However, they are all single crystals >2cm in size, and as such represent megacrysts by definition. The coexisting zircons are also coarse grained (average ~ 10mm) and in a number of cases, whole crystals are preserved. An example of a zircon-ilmenite-olivine assemblage is illustrated in Plate 6.12. Analyses of olivines associated with zircon are presented in Table 6.6.

Gurney et al. (1979 b) found on the basis of a small data set (34 olivines) that the olivine megacrysts at Monastery defined two compositionally distinct populations. One hundred and fifty-five new analyses undertaken in this study confirm this finding and this is illustrated in Fig. 6.20a. "High-Fe" olivine megacrysts have forsterite contents of between 77.9 and 82.3 while the "low-Fe" olivines have forsterite values of 83.1 to 88.1. A full listing of the compositions of olivine megacrysts analysed in this study together with the data of Jakob (1977) is provided in Appendix 6.4.

Forsterite contents of the olivines intergrown with zircon are plotted in Fig. 6.20b, where it is evident that they correlate with the Fe-rich group of olivine megacrysts. Olivines associated with zircon have forsterite contents of between 78.6 and 82.7. Compositional statistics for the three olivine associations are presented in Table 6.7.

Plotting forsterite content against NiO (Fig. 6.21) confirms that the olivines associated with zircon belong to the Fe-rich, NiO-poor group of megacryst compositions. High-Fe megacryst olivines have between .05 and .14 wt% NiO, while the more magnesian olivines have between .29 and .41 wt% NiO. Figure 6.21 shows that olivines coexisting with zircon are represented over the full range of Fe-rich olivine megacryst compositions.

All of the ilmenites found in association with zircon and olivine (5 nodules) belong to the low Al<sub>2</sub>O<sub>3</sub> group of Z-ilmenites (Figs. 6.8 to 6.13).

#### 6.4.5 Zircon-Phlogopite Association

Three zircon-bearing nodules have been found to host megacrystic phlogopite. Two of these are zircon-ilmenite-phlogopite assemblages, whilst the third is the four-phase (zircon-ilmenite-olivine-phlogopite) assemblage previously mentioned (e.g. Table 6.9). In all three samples, constituent minerals are coarse-grained (i.e. >2cm; zircon ~1cm) and anhedral.

The compositions of phlogopites coexisting with zircon are listed together with the megacryst phlogopites in Appendix 6.1. Compositional statistics for these two phlogopite associations are tabulated in Table 6.8. Data points for the phlogopites associated with zircon are highlighted on Figs. 6.1 to 6.5 where it is clearly illustrated that they are chemically indistinguishable from megacrystic phlogopite. They are

however, amongst the most Si-rich, Al-poor of the megacrystic phlogopites (Fig. 6.2), and although they do not represent the most iron-rich of the phlogopite megacrysts, they are more iron-rich than average (Fig.6.1 and Table 6.8).

Phlogopites coexisting with zircon and ilmenite are noted to be amongst the most  $TiO_2$ -poor of the phlogopite compositions. They plot in the transition region of the two trends defined on the plot of  $TiO_2$  versus  $Mg/Mg+Fe$  (Fig. 6.3). The ilmenites in these samples may therefore be representative of the last ilmenite to crystallize from the megacryst magma, since the more Fe-rich phlogopites appear to have crystallized in the absence of ilmenite (because  $TiO_2$  in these phlogopites increases with Fe-enrichment, Fig. 6.3). The ilmenites in the zircon-phlogopite assemblages all belong to the low  $Al_2O_3$  group of ilmenites associated with zircon.

The relationship between zircon (including the phases associated with zircon ) and the Cr-poor megacrysts at Monastery is addressed in the general discussion concluding this chapter (Section 6.6).

## 6.5 COEXISTING MEGACRYST ASSEMBLAGES

### 6.5.1 Introduction

It was noted in the brief overview at the beginning of this chapter, that while intergrowths of ilmenite with diopside, enstatite and garnet are relatively common, inclusions of one megacryst silicate within another are rare. These rare

assemblages are important however, since they provide evidence for the co-precipitation of the constituent phases of the megacryst suite. One direct application of information so derived, is the justification of assumptions made for the application of geothermometry and geobarometry to pyroxene megacrysts. Furthermore, the various combinations of coexisting phases provide a means for the calculation of equilibration temperatures based on a number of different mineral equilibria.

A variety of coexisting megacryst phases have been recovered in this study with a large proportion being associated with zircon (as described in Section 6.4). Table 6.9 provides a summary of the assemblages recovered.

Previous studies have found intergrowths with olivine to be rare (Gurney et al., 1979<sup>b</sup>). This together with other considerations led Boyd et al. (1984) to suggest that olivine may not belong to the Cr-poor megacryst suite. This study has found olivine to coexist with all phases of the Cr-poor megacryst suite (Table 6.9) and this is taken as unequivocal evidence in favour of olivine being a true Cr-poor megacryst phase.

#### 6.5.2 Petrography

Two unique four-phase megacryst assemblages consisting of olivine-opx-cpx-garnet have been recovered. Both nodules were set in Q2 quarry kimberlite and hand specimens measure approximately 10 by 5 cm. A photomicrograph of a thin section of sample ROM-199 is presented in Plate 6.13. Features of note

include:

- (1) The fine-grained nature of these assemblages relative to discrete megacrysts. Grain sizes range between 0.5 and 5 mm in both samples.
- (2) Olivine is modally dominant, accounting for between 65 and 75 vol% of the rock. Modal estimates of other phases are: opx - 15-25 vol%, cpx - 5-10 vol% and garnet - 10-15 vol%.
- (3) Opx and cpx are preferentially altered.
- (4) The general texture is coarse equant (Harte, 1977).

Plates 6.14 a&b are higher magnification photomicrographs illustrating the preferential alteration of orthopyroxene which is broken down to a turbid assemblage of secondary phlogopite, serpentine and fine grained opaque oxides. This alteration could be decompression induced, or it may be the result of deuteric or metasomatic processes. One of the latter two possibilities are more likely since pyroxenes included in garnet and olivine (and thus shielded from hostile fluids and/or vapours) are unaltered (Plates 6.15 a&b). Another feature illustrated in these plates is that included phases show euhedral morphology, thereby recording remnant igneous textures.

The other coexisting silicate assemblages listed in Table 6.9 are present as single inclusion-bearing megacrysts. Inclusions are usually small in comparison with their host (~5-15mm), and usually show irregular form. Host phases for these assemblages are indicated in Table 6.9. The general petrography of the assemblages coexisting with zircon has been described in Section 6.4.

### 6.5.3 Mineral Chemistry and Geothermometry

The compositions of the phases associated with zircon have already been discussed and analyses are listed in Appendix 6.2 (ilmenite), Table 6.6 (olivine) and Appendix 6.1 (phlogopite). Analyses of coexisting phlogopite and ilmenite are presented in Table 6.10a and discussed in Section 6.6.

The compositions of the coexisting silicate phases are presented in Table 6.10b and plotted on a Ca-Mg-Fe ternary diagram in Figure 6.22. Compositional fields illustrated are from Gurney et al. (1979 b). The salient features of this diagram include:

- (1) Tie-lines linking coexisting phases define an ordered array indicating equilibrium within the suite.
- (2) Coexisting silicate phases are represented over the entire range of compositions preceding the onset of ilmenite crystallization.
- (3) Fe-rich olivines and Group II enstatites do not coexist with Group I enstatites, garnets or diopsides (see figure caption for definition of Group I and II enstatites)

Samples ROM-188 and ROM-199 (four phase assemblages) define the magnesium-rich extreme of the megacryst compositions (Fig. 6.22) and a more detailed examination of their compositions in Table 6.10 leaves no doubt that these samples represent megacryst assemblages. Characteristic compositional features not reflected in Fig. 6.22 include the moderate levels of  $\text{TiO}_2$  in the pyroxenes and garnet; the relatively high  $\text{Al}_2\text{O}_3$  contents of the enstatites and the generally low  $\text{Cr}_2\text{O}_3$  signature for all phases.

Equilibration temperatures and pressures calculated from the coexisting megacryst phases are tabulated in Table 6.11. The problems associated with geothermobarometry as well as an overview of the geothermometers applied here have been outlined in Chapter 3 (Section 3.5.1).

Systematic differences between thermometers makes temperature comparisons more difficult, but calculated temperatures are observed to decrease with Fe-enrichment. The coexisting assemblages indicate that the first stage of megacryst crystallization (i.e. prior to the onset of ilmenite crystallization) occurred over the temperature range 1387°C to 1201°C. These values confirm the temperature range of 1385°C - 1220°C reported by Gurney et al. (1979 b) for ilmenite-free diopsides based on their Ca/Ca+Mg ratios and the diopside solvus calibration of Davis and Boyd (1966) (diopside had to be assumed to be in equilibrium with enstatite in order to make these calculations). The above authors report a temperature range of 1270°C - 1130°C for the lamellar diopside/ilmenite intergrowths.

Only the four-phase assemblages facilitated the calculation of equilibration pressures. Both samples yield identical pressures which are 61 Kbars for the MacGregor (1974) calibration and 53 Kbars for the Nickel and Green (1985) method. These pressures are considerably higher than the value of 45.3 ±1 kbars calculated from the full range of Group I enstatites by Gurney et al. (1979 b). However, these authors recognise that a considerable amount of uncertainty accompany their calculations since they are based on a number of assumptions and

uncertainties. Although the absolute value of calculated pressure derived in this study is preferred, there are no grounds to dispute Gurney et al's calculations demonstrating that the megacrysts crystallized under essentially isobaric conditions.

## 6.6 DISCUSSION

This study has placed specific emphasis on investigating the relationship of phlogopite and zircon to the Cr-poor megacryst suite. Zircon has been found to be associated with megacrystic ilmenite, Fe-rich olivine and phlogopite. The Fe-rich group of olivine megacrysts at Monastery were described by Gurney et al. (1979 b), but were not accommodated in their model. Of the minerals associated with zircon, only ilmenite has been found to coexist with the less evolved phases in the megacryst suite, namely, diopside, enstatite and garnet, however, no association between ilmenite and the Fe-poor group of olivine megacrysts has been found to date.

Gurney et al. (1979 b) demonstrated that the Fe-rich olivines could not have formed during the same process which gave rise to the remaining megacrysts. Application of the Roeder and Emslie (1970) Fe-Mg distribution coefficient also revealed that these olivines were too Fe-rich to have crystallized from the quarry kimberlite. The two olivine populations must therefore have formed in separate events, with ilmenite, phlogopite and zircon forming in conjunction with the Fe-rich olivines. This implies that two populations of ilmenite

(at least) are represented in the megacryst suite.

Ilmenites from the two megacryst populations are clearly distinguished on the plot of  $\text{Al}_2\text{O}_3$  versus  $\text{Cr}_2\text{O}_3$  presented in Fig. 6.16. Z-ilmenites and ilmenites coexisting with phlogopite are characterized by a high  $\text{Cr}_2\text{O}_3$ , low  $\text{Al}_2\text{O}_3$  signature. This plot also shows that a number of monomineralic ilmenites belong to the more evolved megacryst population. However, it is most significant that no S-ilmenites show these compositions.

Further consideration of the compositions of ilmenites in the evolved megacryst association indicate that three subpopulations are present, namely:

- (1) Low  $\text{Al}_2\text{O}_3$  Z-ilmenites
- (2) High  $\text{Al}_2\text{O}_3$  Z-ilmenites
- (3) A small group (N=13) of highly magnesian ilmenites, three of which coexist with phlogopite

These groups are particularly evident in the plot of MgO versus FeO presented in Fig. 6.18 (labelled Lz, Hz and P2 respectively). The compositional differences between the low and high  $\text{Al}_2\text{O}_3$  Z-ilmenites has been dealt with in some detail and it was concluded that they represent two distinct ilmenite populations. This is supported by the fact that Fe-rich olivines and phlogopite have only been found in association with the low  $\text{Al}_2\text{O}_3$  Z-ilmenites (Appendix 6.2 and Table 6.10a). It has also been noted that very few monomineralic ilmenites match the high  $\text{Al}_2\text{O}_3$  Z-ilmenite compositions (e.g. Fig. 6.18).

The magnesian character of three of the ilmenites associated with phlogopite (within field P2 in Fig. 6.18) is most puzzling since one would expect ilmenites of this association to be at least more Fe-rich than S-ilmenites (as is the case for the other four ilmenites associated with phlogopite). This group of ilmenites represent the most magnesian megacryst ilmenite compositions analysed at Monastery. The fact that phlogopite is found in association with ilmenites spanning the entire range of Fe/Mg shown by megacryst ilmenites at Monastery, appears at first to indicate that phlogopite was crystallizing throughout the megacryst formation event. This is not however the case for a number of reasons:

- (1) the megacryst magma would require unrealistic amounts of  $K_2O$  to facilitate an extensive period of phlogopite crystallization.
- (2) Phlogopite is not stable over the pressure and temperature range (~53 kbars; 1400-1150°C) at which the less evolved megacrysts formed (Eggler and Wendlandt, 1979).
- (3) All ilmenites associated with phlogopite show a distinctive high  $Cr_2O_3$ , low  $Al_2O_3$  signature (Fig. 6.16) which effectively rules out the possibility that some may have formed in equilibrium with the ilmenites associated with the less evolved megacrysts.
- (4) Not a single example of phlogopite coexisting with Fe-poor olivine, diopside, enstatite or garnet has ever been recorded.

It is therefore concluded that phlogopite is only represented in the more evolved population of megacrysts. However, the break

in Mg/Mg+Fe observed in the phlogopites (e.g. Fig. 6.3) together with the fact that four are associated with Fe-rich ilmenites, while three contain inclusions of highly magnesian ilmenite may indicate that two populations of phlogopite are present.

It is difficult to quantitatively assess whether the evolved suite of megacrysts crystallized from a derivative of the original megacryst magma or not. Allsopp and Barrett (1975) reported a Rb/Sr isochron age of  $90 \pm 4$  my (initial ratio =  $0.7046 \pm .0016$ ) for phlogopite megacrysts from Monastery. This age is in agreement with the Sm-Nd age of  $101 \pm 15$  Ma determined for Monastery diopside and garnet megacrysts by Jones (1984), but the initial Sr isotope ratio is enriched in comparison with the range displayed by diopside megacrysts ( $0.7028 - 0.7030$ ; Smith, 1983b) and as such is more similar to that of the host kimberlite ( $0.7033$ ; Smith, 1983a). However, the large errors associated with the phlogopite initial ratio precludes a meaningful comparison. Constraints placed by the stability limits of phlogopite (Eggler and Wendlandt, 1979) imply that phlogopite megacrysts must have crystallized within the lithosphere. It is possible that the original megacryst magma (or derivative thereof) was also parental to the more evolved megacrysts but the phlogopite isotopic data (if significant) indicates substantial contamination had already occurred prior to the crystallization of phlogopite. Assimilation of Cr-rich lithospheric material could also potentially account for the elevated levels  $Cr_2O_3$  in the ilmenites of the more evolved group of megacrysts.

It is reasonable to assume that if any diamonds were formed in association with megacrysts, Monastery would be a good locality to find such diamonds. The study of the mineral inclusion suite in Monastery diamonds (Chapter 5) has demonstrated beyond doubt that no such association exists. However, it has been shown that at least the main group of megacrysts crystallized within the diamond stability field and consequently the absence of diamonds should be considered when discussing the genesis of megacrysts.

If it is accepted that Cr-poor megacryst assemblages are high pressure cognate inclusions in kimberlite, then the isotopic differences between megacrysts and host kimberlite are due to the modification of kimberlite in the mantle subsequent to megacryst crystallization (crustal contamination and alteration are not considered likely mechanisms for producing the observed isotopic discrepancies Smith (1983b), Jones (1984). Models of this nature imply that more accurate source characteristics of the kimberlite are reflected by the megacrysts (i.e. OIB). Ocean island basalts are widely accepted as being derived from plume or hot-spot sources (Morgan, 1971) and a number of authors have used isotopic, geochemical and plate tectonic evidence to suggest that at least some kimberlites may also be related to hot-spot activity (Crough et al., 1980; Duncan, 1981; le Roex, 1986). As previously discussed, the high pressure eclogitic garnet inclusions in diamonds could provide another line of evidence in support of a hot-spot origin for the Monastery kimberlite if it is accepted that the diamonds were sampled by the kimberlite from the extreme depths indicated.

The model for megacryst genesis proposed here follows the general principles of previous models put forward by Gurney et al. (1979 b); Egglar et al. (1979); Harte and Gurney (1981); Nixon et al. (1981) and Ehrenberg (1982). However, new data on the evolved megacrysts has been accommodated. Furthermore, an attempt has been made to more rigorously explain the genesis of megacrysts by adapting major aspects of the Wyllie (1987) model of kimberlite genesis.

It is proposed that the Cr-poor megacrysts formed from melts derived from a diapir which had its origins in the deep asthenosphere or even mesosphere (i.e. OIB source; Morgan, 1971). Following Wyllie's equilibria, partial melting of the rising diapir would commence at the intersection of the ambient geotherm with the peridotite-CO<sub>2</sub>-H<sub>2</sub>O solidus. This occurs at a depth of approximately 250km and a temperature of 1350°C (position 1 on Fig. 6.23). The upward movement of the diapir would be impeded by the rigid lithosphere resulting in lateral divergence (Wyllie, 1987). Melt would consequently become concentrated over a wide lateral extent in the area between the diapir and the rigid base of the lithosphere (Fig. 6.24) i.e. a magma body of similar geometry to that envisaged by Harte and Gurney (1981) would be formed. Fig. 6.23 shows that the geotherm and the solidus intersect again at a depth of approximately 180km and temperature of 1150°C (position 3) which approximately coincides with the lithosphere/asthenosphere boundary (position 2). The temperature range between these two intersections corresponds almost exactly with the range in calculated temperatures displayed by the main group of megacrysts (~1400 - 1150°C). Moreover, the equilibration

pressure of 53 kbars for megacrysts calculated in this study is also consistent with these constraints. Wyllie's model places the intersection of the geotherm and the solidus 10 to 15km within the lithosphere so that melts assimilate lithospheric material. This is not consistent with megacryst formation because of the uncontaminated isotopic signature of megacrysts. However, the depth at which the geotherm and solidus intersect will vary according to the geotherm adopted, so that it is possible that the intersection occurs at the lithosphere-asthenosphere boundary. Assuming this to be the case, the early formed megacrysts (Fe-poor olivine, enstatite, diopside, garnet and ilmenite) could crystallize under isobaric conditions immediately below the lithosphere without significant assimilation of diamond-bearing lithospheric material. Megacryst crystallization does not proceed far enough at this level in the mantle to enable residual liquids to become saturated in carbon, so that diamond cannot crystallize. However, the residual melt does become progressively enriched in volatiles which promotes crack propagation in the overlying lithosphere. In localised areas, limited volumes of fractionated melt may penetrate these cracks or zones of weakness and rise to higher levels in the lithosphere where the evolved suite of megacrysts crystallize. The previously demonstrated absence of correlation between megacrysts and diamonds together with the general rarity of phlogopite, ilmenite and zircon inclusions in diamonds is taken to indicate that the second generation of megacrysts did not crystallize within the diamond stability field. Examination of Fig. 6.23 shows that the peridotite-CO<sub>2</sub>-H<sub>2</sub>O solidus shows a

significant change in slope at depths of approximately 75km. It is suggested that the evolved suite of megacrysts crystallized when the rising pockets of melt encountered this plateau in the solidus (Fig. 6.24).

In an attempt to justify a model of kimberlite-megacryst consanguinity, Nixon et al. (1981) suggested that a proto-kimberlitic melt mixed with and was contaminated by a pre-existing lithospheric melt enriched in incompatible elements. Smith (1983b) indicates that such a process would also satisfy isotopic constraints. It is possible that partial melting in the lithosphere was induced by the thermal perturbation caused by the diapir. Diamonds hosted in the depleted root zones of the lithosphere would be released into these melts. Residual melts from the first phase of megacryst crystallization could then rise into the lithosphere by way of cracks and mix with the diamond-bearing lithospheric melts. This process could culminate in conduit formation and kimberlite eruption so that Cr-poor megacrysts are genetically related to kimberlite but the erupted kimberlite has been modified subsequent to megacryst formation by the assimilation of a lithospheric component. Such a model implies that Group I kimberlites represent hybrid magmas.

The above model implies that the two megacryst populations were derived from the same parental melt. The substantial differences in composition of the olivine represented in the two suites is accounted for by the fact that olivine ceased to crystallize prior to the onset of ilmenite crystallization in the first megacryst formation event (evident by the total

absence of an ilmenite/Fe-poor olivine association). However, the melt continued to evolve by pyroxene and ilmenite fractionation so that the second generation of olivine megacrysts crystallized from a significantly more Fe-rich, Ni-depleted melt.

The high degree of chemical similarity between the two populations of ilmenite associated with zircon rules out the possibility that they were formed in completely unrelated events. It is therefore suggested that they crystallized from separate pockets of the evolved megacryst melt. Coexisting assemblages show that Fe-rich olivine, phlogopite and zircon accompanied the crystallization of the low  $\text{Al}_2\text{O}_3$  ilmenites, but the high  $\text{Al}_2\text{O}_3$  ilmenites have only been found to coexist with zircon. This may simply reflect a sampling problem, or it may indicate that only zircon and ilmenite crystallized from the second melt segregation. More data would be required to elucidate this problem.

The group of phlogopite megacrysts associated with magnesian ilmenite is difficult to account for. The fact that they define coherent and often continuous trends with the more Fe-rich phlogopites from the zircon/ilmenite/Fe-rich olivine association (Figs. 6.2, 6.3, 6.5) is interpreted to indicate that the entire suite of phlogopites are genetically related. Moreover, the magnesian ilmenites show the high  $\text{Cr}_2\text{O}_3$ , low  $\text{Al}_2\text{O}_3$  signature of the zircon-related ilmenites (Fig. 6.16) suggesting some form of relationship.

Previous workers have found evidence of MgO enrichment in the final stages of megacryst crystallization and since these

trends are not easily rationalised in terms of a normal sequence of igneous crystallization, a variety of potential explanations have been put forward. These include:

- (1) assimilation of local wall rock (Eggler et al., 1979)
- (2)  $fO_2$  controlled  $Mg^{2+}/Fe^{2+}$  ratios (Gurney et al., 1979<sup>b</sup>)
- (3) the buffering of  $Mg^{2+}/Fe^{2+}$  with a small melt/crystal ratio (Boyd and Nixon, 1973).

None of these adequately accounts for the magnesian ilmenite/phlogopite association for the following reasons:

- (1) assimilation of the quantities of refractory lithospheric material required to affect such a significant change in  $Mg/Mg+Fe$  in ilmenite would be reflected in the concentrations of oxides such as  $Cr_2O_3$ , which is clearly not observed.
- (2) the magnesian ilmenites contain significantly lower levels of  $Fe_2O_3$  in comparison to the Z-ilmenites so that an increase in  $fO_2$  cannot be responsible for increasing the  $Mg^{2+}/Fe^{2+}$  ratio.
- (3) the entire megacryst suite is believed to have crystallized under conditions of low melt/crystal ratio.

No satisfactory explanation has been found to account for the highly magnesian ilmenites associated with phlogopite. Although the break in  $Mg/Mg+Fe$  displayed by the phlogopite megacrysts provides some grounds for the existence of two populations of phlogopite megacrysts, other compositional factors outweigh this possibility and it is therefore concluded that the entire suite of phlogopite megacrysts are genetically related.

## CHAPTER 7    SUMMARY

In this final chapter the main features and conclusions reached in each of the preceding chapters are summarised.

## CHAPTER 1    INTRODUCTION

The Monastery kimberlite is situated 250km east of Kimberley, near to the north-eastern border of Lesotho and on the Kaapvaal Craton. It is a Group I kimberlite (Smith, 1983a) which has been dated at 90my by two independent methods (Allsopp and Barrett, 1975; Davis et al., 1976). The diatreme is a multiple intrusion with dimensions of 180 by 70m and is intruded into sediments of the Elliot Formation of the Karoo Supergroup.

## CHAPTER 2    KIMBERLITE PETROGRAPHY

A revised geological plan of the kimberlite is presented based on a quantitative survey undertaken by Fielding (1981) (Fig. 2.1). The four major varieties of kimberlite have been described and these include the quarry kimberlite, the east-end kimberlite, the breccia kimberlite and a precursor kimberlite dyke. All of these phases have been found to be hypabyssal facies kimberlites. Crater and diatreme facies kimberlites are not represented at Monastery.

The quarry kimberlite is the most abundant kimberlite phase in the pipe and four distinct varieties (termed Q1-Q4) have been recognised. All phases of the quarry kimberlite contain macrocrysts of olivine, ilmenite and phlogopite as well as

smaller euhedral olivine phenocrysts, set in a fine grained matrix of groundmass phlogopite, spinel, ilmenite, calcite, serpentine, perovskite, monticellite and apatite. In terms of the mineralogical classification of Skinner and Clement (1979) the Q1 and Q4 quarry kimberlites are opaque oxide-rich serpentine phlogopite kimberlites, the Q2 kimberlite a phlogopite-monticellite kimberlite and the Q3 kimberlite a monticellite-phlogopite kimberlite. Cr-poor megacrysts are common inclusions in the quarry kimberlite and coarse textured peridotite xenoliths are also well represented. A recent estimate of the diamond grade of this kimberlite is 15 cts/100 tonnes, but earlier prospecting suggested values as high as 50 cts/100 tonnes in places.

The east-end kimberlite occupies the eastern portion of the pipe where it is generally poorly exposed. It is a macrocrystic kimberlite which is highly weathered. Mantle-derived xenoliths and megacrysts are not as abundant as in the quarry kimberlite. Similar macrocryst and groundmass phases to those in the quarry kimberlite are present, and the kimberlite is classified as an opaque-oxide rich serpentine-monticellite kimberlite.

The breccia kimberlite forms a central plug to the diatreme. It is a kimberlite breccia with abundant sub-angular sandstone, shale and dolerite fragments set in a soft serpentinous, micaceous matrix. Phlogopite and ilmenite megacrysts are common. The highly altered nature of this kimberlite prevented a detailed microscopic investigation, but it was qualitatively classified as an opaque-oxide rich phlogopite serpentine kimberlite.

A precursor kimberlite dyke is associated with the Monastery diatreme. It outcrops over a distance of 2000m striking ESE/NWN and intersects the main diatreme in the north-western lobe of the pipe where it is truncated. It is a macrocrystic kimberlite with an abundance of fresh phlogopite macrocrysts. The volatile-rich nature of this kimberlite is indicated by an abundance of apatite, serpentine and calcite in the groundmass. Mineralogically the dyke kimberlite is an opaque-oxide rich calcite kimberlite.

### CHAPTER 3 ULTRAMAFIC XENOLITHS

Garnet lherzolite is by far the most abundant xenolith type. Other mantle xenoliths represented include (in order of decreasing abundance): lherzolites, harzburgites, garnet harzburgites, wehrlites, websterites, pyroxenites and marid-suite xenoliths (Fig. 3.2). A high incidence of modal metasomatism is indicated by the abundance of phlogopite-bearing xenoliths. Accessory spinel (mostly chromite) is also unusually common.

Peridotites (lherzolites and harzburgites) are dominantly coarse (undeformed) common peridotites. A spatial association between garnet, clinopyroxene and orthopyroxene was noted which may indicate that some garnet lherzolites have formed from harzburgites by exsolution of garnet and clinopyroxene from high-temperature aluminous and calcium-rich orthopyroxenes. Edenitic amphibole was present in three harzburgites, where it is associated with the breakdown of olivine, orthopyroxene and garnet. Nine peridotites display textures which are

intermediate between porphyroclastic and granuloblastic. These rocks show textural evidence of previous deformation but significant annealing has occurred subsequent to recrystallization. A history of subsolidus re-equilibration is also evident in the extensive exsolution textures developed in these rocks. Deformed textured peridotites have been found to be extremely rare at Monastery. Only one mosaic porphyroclastic-textured garnet lherzolite was recovered despite directed searches through large volumes of xenolithic material. Wehrlites and olivine clinopyroxenites are usually fresh and show coarse and intermediate textures similar to those described for peridotites. Primary textured phlogopite is an important constituent of these rocks and K-richterite is present in one wehrlite. Websterites and pyroxenites are characterised by extensive exsolution textures. Phlogopite and spinel are common accessory phases in pyroxenites.

Olivines in peridotites show the characteristic range of forsterite contents observed for common peridotites in kimberlites (90.9 - 93.6), while wehrlitic olivines are more Fe-rich (86.0 - 91.9). Similar relative trends for Mg/Mg+Fe are observed for orthopyroxene, clinopyroxene and garnet.

Orthopyroxenes generally have Al<sub>2</sub>O<sub>3</sub> below 0.9 wt%, but those in harzburgites with aluminous Cr-spinel show elevated concentrations for this oxide (~2.5 wt%). TiO<sub>2</sub> and Cr<sub>2</sub>O<sub>3</sub> contents are usually low (<0.07 and between 0.51 and 0.67 wt% respectively) and CaO dominantly ranges between 0.1 and 0.7 wt%.

Clinopyroxenes are calcic diopsides with restricted 100(Ca/Ca+Mg) ratios of 45 to 50. Only the deformed garnet lherzolite had a 100(Ca/Ca+Mg) ratio outside this range and its value of 39 correlates with the calcic (cool) extreme of the deformed peridotites at Thaba Putsoa and Mothae. Clinopyroxene compositions are discriminated into two groups on the basis of FeO, Al<sub>2</sub>O and Na<sub>2</sub>O. Peridotitic and websteritic diopside have lower FeO (1.39 - 2.52 wt%) and generally higher Al<sub>2</sub>O<sub>3</sub> contents (1.66 - 4.44 wt%) than those in wehrlites and pyroxenites (FeO = 2.11 - 3.71; Al<sub>2</sub>O<sub>3</sub> = 0.34 - 2.31). Diopsides from wehrlites and pyroxenites show a more restricted range and lower average Na<sub>2</sub>O content than those for peridotitic and websteritic diopsides (1.17 and 2.24 wt%, respectively).

All of the garnets analysed in this study plot on the lherzolite trend when plotted on a CaO vs Cr<sub>2</sub>O<sub>3</sub> diagram. However, a small proportion of the garnets from harzburgite analysed in the pilot study are undersaturated with respect to calcium. TiO<sub>2</sub> concentrations are typically below detection limits except for the garnet in the deformed garnet lherzolite which has 1.32 wt% TiO<sub>2</sub>. Trace levels of Na<sub>2</sub>O (0.09 wt%) were also detected in this garnet.

Only primary textured phlogopites were analysed in this study and two groups of compositions recognised. Phlogopites in lherzolites, harzburgites and websterite are compositionally similar to those in garnet-phlogopite peridotites (GPP) from the Kimberley Pool (Erlank et al., 1987), while those in wehrlites and pyroxenites show the compositional characteristics of

phlogopite in the metasomatised phlogopite-richterite peridotites (PKP)

The majority of spinels represented in the Monastery xenoliths are chromites ( $100(\text{Cr}/\text{Cr}+\text{Al}) > 65$ ) but four harzburgites host more aluminous Cr-spinels ( $100(\text{Cr}/\text{Cr}+\text{Al}) = 25 - 65$ ). Ilmenite is present as a rare accessory phase and shows moderately high MgO contents (8.61 - 12.86 wt%) with significant  $\text{Cr}_2\text{O}_3$  contents (1.76 - 2.31 wt%). Edenitic/pargasitic amphibole occurs in three harzburgites and K-richterite in a phlogopite wehrlite. The edenite amphiboles show similar compositions to the amphibole intergrown with fingerprint spinels (Boyd, 1971<sup>b</sup>).

Three geothermometers (Lindsley and Dixon, 1976; Bertrand and Mercier, 1985; O'Neill and Wood, 1979) and two geobarometers (MacGregor, 1974; Nickel and Green, 1985) were selected to calculate T,P estimates, and a reasonable agreement in results was observed. The coarse xenoliths display an exceptionally large range of equilibration conditions (~700-1050°C; 20-40 kbars-Fig. 3.22a&b) compared to coarse xenolith suites from other localities. On a P-T diagram they define an array of similar configuration to theoretically calculated geotherms for continental shield areas. An important feature of the Monastery coarse xenoliths is that they define a bimodal temperature distribution which correlates with texture. The low T-P group of rocks (~700-850°C) correspond with those petrographically classified as intermediate and granuloblastic. A correlation was also noted between low pressure and the presence of chromite in garnet lherzolites.

Coarse textured xenoliths at Monastery show a high incidence of modal metasomatism. It has been noted that the phlogopite in the wehrlitic rocks shows compositional similarities with phlogopite in the richterite-bearing peridotites (PKP) from the Kimberley group of pipes and the presence of K-richterite in one wehrlite raises the possibility that the wehrlites and pyroxenites have experienced a similar metasomatism to that recorded in the Kimberley xenoliths.

#### CHAPTER 4 ECLOGITES

Eclogite xenoliths are rare at Monastery and as a consequence the sixteen nodules examined were sampled from the coarse tailings dumps. Sample sizes ranged between 2 and 5cm which meant that layering and gross inhomogeneities were not encountered. Moreover, representative textural observations and reliable modal determinations could not be achieved. The eclogites display metamorphic textures but no evidence of subsolidus reequilibration in the form of exsolution features were noted. Only a few samples strictly conform with the MacGregor and Carter (1970) textural classification but on the basis of dominant diagnostic features, nine were classed as Group I, three as Group II while five were judged to be intermediate. Modal garnet ranges between 10 and 90 vol%, Fig. 4.1. The only accessory phases encountered were rutile and sulphide.

Two groups of eclogite were defined on the basis  $\text{Na}_2\text{O}$  in garnet and  $\text{K}_2\text{O}$  in clinopyroxene (Fig. 4.2). Reasonable agreement was observed between the textural and chemical

classifications. The Monastery suite was discriminated into ten Group I eclogites and five Group II eclogites. Garnets in some Group I eclogites showed substantial enrichments in  $\text{Na}_2\text{O}$  (up to 0.24 wt%).

The constituent minerals of the Monastery eclogites show a wide variation in compositions. These are largely reflected in the pyrope, almandine and grossular contents of garnet (Fig. 4.5), and the diopside and jadeite contents of the clinopyroxenes (Fig. 4.10). Coexisting garnets and clinopyroxenes define an ordered array of tie-lines on a Ca-Mg-Fe ternary with no crosscutting relationships. Group I eclogites show a confusing relationship between  $\text{Na}_2\text{O}_{\text{Cpx}}$  and  $\text{Mg}/\text{Mg}+\text{Fe}$  for both garnet and clinopyroxene in that two apparent trends are defined on both plots (Figs. 4.3 and 4.4). Relationships between  $\text{Mg}/\text{Mg}+\text{Fe}$ ,  $\text{TiO}_2$  and  $\text{Cr}_2\text{O}_3$  in clinopyroxenes and  $\text{Mg}/\text{Mg}+\text{Fe}$ ,  $\text{TiO}_2$ ,  $\text{CaO}$  and  $\text{Na}_2\text{O}$  in garnets (Figs. 4.5, 4.8, 4.9, 4.14, 4.15) are consistent with the Group I eclogites having been formed in a single igneous event. However, geothermometry data (Ellis and Green, 1979; 50 kbars) shows a well defined trend of increasing temperature with increasing degree of fractionation (1075-1307°C; Table 4.7; Fig. 4.17). The large range in calculated temperature together with the systematic relationship between temperature and the calcium content of garnet (Fig. 4.17) imply that neither thermometer error nor incomplete equilibrium is responsible for the observed trends.

Considering the fact that Monastery diamonds have been found to host eclogitic garnet inclusions which have formed at

depths of up to 400km (Moore and Gurney, 1985; Chapter 5 of this study) an alternative explanation for the Group I eclogites could be that they represent original high pressure garnetite which has undergone subsolidus re-equilibration. This could imply that they have crystallised from a rising diapir of recycled oceanic crust, but in the absence of trace element and isotopic data, this possibility could not be quantitatively assessed.

Garnets from Group II eclogites define an Fe-enrichment trend with little variation in Ca. Moreover, oxides such as  $\text{TiO}_2$  and  $\text{Na}_2\text{O}$  remain essentially constant with changing  $\text{Mg}/\text{Mg}+\text{Fe}$  for both clinopyroxenes and garnets (Figs. 4.3, 4.8, 4.9, 4.14). Calculated equilibration temperatures (assuming 50 kbars) dominantly range between 1060 and 1107°C. Group II eclogites show a positive correlation between  $\text{CaO}_{\text{gt}}$  and  $\text{Na}_2\text{O}_{\text{cpx}}$  (Fig. 4.18) and the trend they define issues from the field of garnet lherzolite compositions. This may indicate that they represent crystallised partial melts from a garnet lherzolite source. Their low  $\text{TiO}_2$  and  $\text{Na}_2\text{O}$  and elevated  $\text{Cr}_2\text{O}_3$  contents are also consistent with this possibility.

Factors such as the small sample population available to this study as well as the absence of isotopic and bulk rock geochemical data has meant that the formulation of petrogenetic models for both Group I and II eclogites could not be justified. However, the eclogite xenoliths have been chemically characterised for comparison with eclogitic mineral inclusions in Monastery diamonds.

## CHAPTER 5 DIAMONDS AND MINERAL INCLUSIONS IN DIAMONDS

A large proportion of Monastery diamonds are almost completely devoid of primary crystal form and the majority exhibit some form of breakage surface often accompanied by the effects of severe resorption. The high percentage of broken diamonds correlates with the high incidence of inclusions. The diamonds display a gaussian size distribution, are predominantly colourless and shades of brown, and display a wide variety of surface textures.

Inclusions in Monastery diamonds are predominantly eclogitic, but peridotitic and miscellaneous paragenesis inclusions are also present (the latter category comprising inclusions of uncertain paragenesis). Primary inclusions within the miscellaneous category include sulphides, magnetite, magnésio-wustite, zircon and moissanite while plagioclase, phlogopite, hematite and spinel are considered epigenetic. The moissanite inclusions described in this study together with those from Sloan (Otter and Gurney, 1986; Moore et al., 1986) represent the first report of this mineral as an inclusion in diamond.

Inclusions of peridotitic paragenesis are poorly represented. The very limited compositional data available suggests that these diamonds formed in the temperature range 1100 to 1200°C. The absence of orthopyroxene inclusions prevented pressure calculations. It appears likely that the peridotitic diamonds were derived from a garnet lherzolite association rather than the refractory harzburgitic paragenesis characteristic of peridotitic diamonds worldwide. This

interpretation is supported by the compositional characteristics of the olivine and garnet inclusions as well as by the presence of Cr-diopside.

Two populations of eclogitic garnet are present in Monastery diamonds. One group of 8 (Group A) has similar compositions to eclogitic garnet inclusions from other localities, while the second group of 46 (Group B) display the effects of pyroxene in solid solution. These garnets represent the first natural example of this experimentally predicted reaction. Eclogitic clinopyroxenes (N=13) possess a wide range in compositions which trend towards lower jadeite and diopside contents compared to eclogitic clinopyroxenes from other localities. Accessory eclogitic inclusions recovered include two suspected coesites and a primary corundum.

Some clinopyroxenes and most of the Group A garnet inclusions are similar to minerals of Group I eclogite xenoliths at Monastery so that a minor proportion of the diamonds may be derived from such xenoliths. Two diamonds hosted polyphase websterite inclusion assemblages which yield calculated temperatures in excess of 1400°C. Their relationship with the peridotitic and eclogitic paragenesis inclusions is unclear. Seven diamonds hosted multiple inclusions of the same phase which are not in equilibrium. Episodic diamond growth within an environment of changing chemical composition is favoured as the most likely mechanism to account for the compositional variations. One diamond was found to host an olivine (Fo<sub>94.9</sub>) as well as an eclogitic Group B garnet. This phenomenon has now been observed by three other authors, and it is considered that

genuine cases of mixed paragenesis diamonds do occur.

Moissanite-bearing diamonds at Monastery appear to belong to the eclogitic paragenesis and associated Group B garnets imply formation pressures of 70-100 kbars. The presence of moissanite inclusions may indicate extremely reducing conditions for diamond growth. The high formation pressures indicated by the garnet inclusions hosting pyroxene in solid solution (60 to 150 kbars), imply that a substantial proportion of the diamonds at Monastery were formed in the depth interval from 160km to in excess of 450km.

## CHAPTER 6 MEGACRYSTS

Field observations indicate that previous estimates of the relative abundances of megacrysts at Monastery significantly underestimated the abundance of olivine. A revised abundance estimate indicates olivine to be only subordinate to ilmenite.

This study has placed specific emphasis on investigating the relationship of phlogopite and zircon to the megacryst suite. Phlogopite megacrysts are large (1 to 6 cm), generally fresh, and a small proportion show kink banding along (001) crystal planes. They show the low  $\text{Cr}_2\text{O}_3$  signature ( $\text{Cr}_2\text{O}_3 = 0.01-0.27 \text{ wt}\%$ ) characteristic of megacrysts at Monastery. Phlogopite megacrysts are also significantly more iron-rich ( $\text{FeO} = 4.53-7.64 \text{ wt}\%$ ) than primary peridotitic phlogopites and stoichiometric considerations imply low levels of ferric iron.  $\text{TiO}_2$  concentrations range between 0.64 and 1.52 wt% and the relationship between  $\text{TiO}_2$  and  $\text{Mg}/\text{Mg}+\text{Fe}$

indicates that a major portion of the phlogopite crystallization occurred in the presence of ilmenite. However, phlogopite megacrysts continued to crystallize after the cessation of ilmenite crystallization. A break in Mg/Mg+Fe is noted between 0.87 and 0.88.

Zircon is present in above average concentrations at Monastery and it has been found to be associated with megacrystic ilmenite, Fe-rich olivine and phlogopite. They are characteristically coarse-grained (average 10 mm) and are either colourless or pale brown. Zircons are usually encircled by a layer of baddeleyite ( $ZrO_2$ ) which has formed by a desilicification reaction. The interface zones between zircon and ilmenite can contain an unusual mineral assemblage consisting of zirconolite ( $CaZrTi_2O_7$ ), diopside and calcite. Raber and Haggerty (1979) suggested that these assemblages formed in an intercrystalline reaction triggered by a carbonatitic fluid. These reactions are considered to be secondary features which probably occurred during kimberlite emplacement and as such provide no assistance in constraining the origin of zircon.

Ninety-three ilmenites associated with zircon were analysed and found to be Fe-rich (Av. FeO = 29.05 wt%; Av.  $Fe_2O_3$  wt% = 13.30) with moderate  $Cr_2O_3$  (Av. 0.85 wt%) and MgO (Av. 7.91 wt%) concentrations. A striking feature of their compositions is that two distinct groups are discriminated on the basis of  $Al_2O_3$ . Other oxides such as  $TiO_2$ ,  $Fe_2O_3$  and MgO also support this grouping. No relationship could be found between ilmenite  $Al_2O_3$  contents and the occurrence of spinel exsolution lamellae in the ilmenites and in the absence

of any other explanation, it was concluded that two distinct populations of ilmenite are associated with zircon. A comparison of the ilmenites associated with zircon with megacrystic ilmenites from other associations at Monastery shows that some monomineralic ilmenites show the higher  $\text{Cr}_2\text{O}_3$  and low  $\text{Al}_2\text{O}_3$  signature of the ilmenites associated with zircon. However, it is most significant that none of the ilmenites coexisting with megacrystic silicates show these specific compositional features. Three ilmenites coexisting with phlogopite show the high  $\text{Cr}_2\text{O}_3$ , low  $\text{Al}_2\text{O}_3$  signature of the evolved ilmenites, but are highly magnesian. These ilmenites imply that phlogopite is found in association with ilmenites spanning the entire range of Fe/Mg ratio shown by megacryst ilmenites at Monastery which appears at first to indicate that phlogopite was crystallizing throughout the megacryst formation event. However, this possibility is rejected for a number of reasons. It is concluded that phlogopite is only represented in the evolved population of megacrysts. However, the break in  $\text{Mg}/\text{Mg}+\text{Fe}$  observed in the phlogopites (Fig. 6.3) together with the fact that four are associated with Fe-rich ilmenites, while three contain inclusions of highly magnesian ilmenite may indicate that two populations of phlogopite are present.

Sixteen zircon/olivine intergrowths were recovered. Ten of these are two-phase assemblages of zircon-olivine, five consist of the assemblage zircon-olivine-ilmenite and one is a four-phase assemblage zircon-olivine-ilmenite-phlogopite. The olivines in these assemblages are chemically indistinguishable from the Fe-rich olivine megacryst population recognised by

Gurney et al. (1979<sup>b</sup>). All of the ilmenites found in association with zircon and olivine (5 nodules) belong to the low Al<sub>2</sub>O<sub>3</sub> group of Z-ilmenites (ilmenites associated with zircon).

Three zircon-bearing assemblages were found to host megacrystic phlogopite. Two of these are zircon-ilmenite-phlogopite assemblages, whilst the third is a four-phase assemblage previously mentioned. Phlogopites associated with zircon are chemically indistinguishable from phlogopite megacrysts.

Two unique four-phase megacryst assemblages consisting of olivine-opx-cpx-garnet have been recovered and these together with a variety of other coexisting megacryst phases support the proposal that the less evolved megacrysts formed in a single igneous event. Equilibration temperatures and pressures calculated from the coexisting megacryst phases indicate that the first stage of megacryst crystallization (ie. prior to the onset of ilmenite crystallization) occurred over the temperature range 1387 to 1201°C. The data of Gurney et al. (1979b) shows that ilmenite crystallized over the temperature range 1270-1130°C. An equilibration pressure of 53 kbars (Nickel and Green, 1985) was calculated for the four-phase megacryst assemblage which is considerably higher than the value of 45 kbars calculated by Gurney et al. (1979b). Although the absolute value of calculated pressure derived in this study is preferred, there are no grounds to dispute Gurney et al.'s calculations demonstrating that the megacrysts crystallized under essentially isobaric conditions.

A model for megacryst formation is proposed based on previous models and the phase equilibria of Wyllie (1987). It is proposed that the Cr-poor megacrysts formed from melts derived from a diapir which had its origins deep in the asthenosphere or even mesosphere (ie. OIB source; Morgan, 1971). Partial melting of the rising diapir commences at the intersection of the ambient geotherm with the peridotite-CO<sub>2</sub>-H<sub>2</sub>O solidus. The upward movement of the diapir would be impeded by the rigid lithosphere resulting in lateral divergence. Melt would consequently become concentrated over a wide lateral extent in the area between the diapir and the base of the lithosphere ie. a magma body of similar geometry to that envisaged by Harte and Gurney (1981) would be formed. As the "less evolved group of megacrysts" crystallize, the residual liquid becomes progressively enriched in volatiles which promotes crack propagation in the overlying lithosphere. In localised areas, limited volumes of fractionated melt may penetrate these cracks or zones of weakness and rise to higher levels in the lithosphere where "the evolved suite" of megacrysts (zircon, ilmenite, Fe-rich olivine, phlogopite) crystallize. The crystallization of these megacrysts may coincide with the change of slope observed in the peridotite solidus at depths of 75 km. It is convenient to link the two groups of megacrysts to a single parental melt, but there is no evidence to prove this.

## REFERENCES

- Ahrens, L.H.; Cherry, R.D. and Erlank, A.J. (1967). Observations on the Th-U relationship in zircons from granitic rocks and from kimberlites. *Geochim. Cosmochim. Acta*, 31, 2379-2387.
- Ahrens, L.H.; Dawson, J.B.; Duncan, A.R. and Erlank, A.J. (Eds.) (1975). *Physics and Chemistry of the Earth*, Vol. 9, Pergamon Press, Oxford, 940p.
- Ahrens, T.J. (1973). Petrologic properties of the upper 670 km of the Earth's mantle: Geophysical implications. *Phys. Earth Planet. Inter.*, 7, 167-186.
- Akaogi, M. (1978). High-pressure phase equilibria of the mantle minerals and mineralogical constitution of the mantle transition zone. PhD thesis, Univ. of Tokyo.
- Akaogi, M. and Akimoto, S. (1977). Pyroxene-garnet solid solution equilibria in the systems  $Mg_4Si_4O_{12}$ - $Mg_3Al_2Si_3O_{12}$  and  $Fe_4Si_4O_{12}$ - $Fe_3Al_2Si_3O_{12}$  at high pressures and temperatures. *Phys. Earth Planet. Inter.*, 15, 90-106.
- Akaogi, M. and Akimoto, S. (1979). High pressure phase equilibria in a garnet lherzolite, with special reference to  $Mg^{2+}$ - $Fe^{2+}$  partitioning among constituent minerals. *Phys. Earth Planet. Inter.*, 19, 31-51.
- Akella, J. (1976). Garnet pyroxene equilibria in the system  $CaSiO_3$ - $MgSiO_3$ - $Al_2O_3$  and in a natural mineral mixture. *Amer. Mineral.*, 61, 589-598.
- Akimoto, S. and Akaogi, M. (1977). Pyroxene-garnet solid solution equilibria in the Earth's mantle. Ext. Abstr. 2nd Int. Kimb. Conf., Santa Fe, A.G.U., Washington. (Unpaginated).
- Akimoto, S. and Manghnani, M. (Eds.) (1982). *High Pressure Research in Geophysics. Advances in Earth and Planet. Sci. Series*, Vol. 12, Reidel Publ. Co., Holland, 632p.
- Albee, A.L. and Ray, L. (1970). Correction factors for the electron microanalysis of silicates, oxides, carbonates, phosphates and sulphates. *Analytical Chem.*, 42, 1408-1414.
- Allegre, C.J. and Turcotte, D.L. (1985). Geodynamic mixing in the mesosphere boundary layer and the origin of oceanic islands. *Geophys. Res. Lett.*, 12, 207-210.
- Allsopp, H.L. and Barrett, D.R. (1975). Rb-Sr age determinations on South African kimberlite pipes. In: Ahrens, L.H.; Dawson, J.B.; Duncan, A.R. and Erlank, A.J. (Eds.), *Phys. Chem. Earth*, Vol. 9, 605-617, Pergamon Press, Oxford.
- Anderson, D.L. (1982). Chemical compositions and evolution of the mantle. In: Akimoto, S. and Manghnani, M. (Eds.), *High Pressure Research in Geophysics*, 301-308. *Advances in Earth and Planet. Sci. Series*, Vol. 12, Reidel Publ. Co., Holland.

- Anderson, D.L. (1984). The earth as a planet: paradigms and paradoxes. *Science*, 223, 347-355.
- Anderson, D.L. and Bass, J.D. (1984). Mineralogy and composition of the upper mantle. *Geophys. Res. Lett.*, 11, 637-640.
- Anderson, D.L. and Bass, J.D. (1986). Transition region of the Earth's upper mantle. *Nature*, 320, 321-328.
- Anderson, O.L. (1979). The role of fracture dynamics in kimberlite pipe formation. In: Boyd, F.R. and Meyer, H.O.A. (Eds.), *Kimberlites, Diatremes and Diamonds: Their Geology, Petrology and Geochemistry*, 344-353, A.G.U., Washington.
- Arai, S. (1984). Pressure-temperature dependent compositional variation of phlogopitic micas in upper mantle peridotites. *Contrib. Mineral. Petrol.*, 87, 260-264.
- Ater, P.C.; Egger, D.H. and McCallum, M.E. (1984). Petrology and geochemistry of mantle eclogite xenoliths from Colorado-Wyoming kimberlites: recycled ocean crust? In: Kornprobst, J. (Ed.), *Kimberlites II: The Mantle and Crust-Mantle Relationships*, 309-318, *Developments in Petrology 11B*, Elsevier, Amsterdam.
- Banno, S. (1970). Classification of eclogites in terms of physical conditions of their origin. *Phys. Earth Planet. Inter.*, 3, 405-421.
- Barrett, D.R. (1975). The genesis of kimberlites and associated rocks: strontium isotopic evidence. In: Ahrens, L.H.; Dawson, J.B.; Duncan, A.R. and Erlank, A.J. (Eds.), *Phys. Chem. Earth*, Vol. 9, 637-653, Pergamon Press, Oxford.
- Bass, J.D. and Anderson, D.L. (1984). Composition of the upper mantle: Geophysical tests of two petrological models. *Geophys. Res. Lett.*, 11, 229-232.
- Bell, D.R. (1981). Ultramafic xenoliths from the Koffiefontein kimberlite pipe, R.S.A. Unpublished BSc(Hons) Project, Univ. Cape Town, South Africa, 88p.
- Bell, D.R. (1985). Evaluation of geothermometry and geobarometry on mantle-derived xenoliths from kimberlites. Internal report of De Beers Consolidated Mines Ltd., Kimberlite Petrology Unit, 15p.
- Bence, A.E. and Albee, A.L. (1968). Empirical correction factors for the electron microanalysis of silicates and oxides. *J. Geol.*, 76, 382-403.
- Bertrand, P. and Mercier, J-C.C. (1985). The mutual solubility of coexisting ortho- and clinopyroxene: toward an absolute geothermometer for the natural system? *Earth Planet. Sci. Lett.*, 76, 109-122.
- Bibby, D.M.; Erasmus, C.S.; Fesq, H.W. and Kable, E.J.D. (1975). The determination of trace elements in natural diamonds by instrument neutron-activation analysis. In: Report No. 1638, National Institute for Metallurgy, Johannesburg, South Africa.

- Bina, C.R. and Wood, B.J. (1984). The eclogite to garnetite transition - experimental and thermodynamic constraints. *Geophys. Res. Lett.*, 11, 955-958.
- Bishop, F.C.; Smith, J.V. and Dawson, J.B. (1976). Na, P, Ti and coordination of Si in garnet from peridotite and eclogite xenoliths. *Nature*, 260, 696-697.
- Bishop, F.C.; Smith, J.V. and Dawson, J.B. (1978). Na, K, P and Ti in garnet, pyroxene and olivine from peridotite and eclogite xenoliths from African kimberlites. *Lithos*, 11, 155-173.
- Boctor, N.Z.; Boyd, F.R. and Nixon, P.H. (1983). Pyroxenites, eclogites and megacrysts in kimberlite from the De Bruyn and Martin mine, Bellsbank, South Africa. *Carnegie Inst. Washington, Yb.* 82, 346-349.
- Boettcher, A.L. and O'Neil, J.R. (1980). Stable isotope, chemical and petrographic studies of high-pressure amphiboles and micas: Evidence for metasomatism in the mantle source regions of alkali basalts and kimberlites. *Am. J. Sci.*, 280A, 594-621.
- Boettcher, A.L.; O'Neil, J.R.; Windom, K.E.; Stewart, D.C. and Wilshire, H.G. (1979). Metasomatism of the upper mantle and the genesis of kimberlites and alkali basalts. In: Boyd, F.R. and Meyer, H.O.A. (Eds.), *The Mantle Sample: Inclusions in Kimberlites and Other Volcanics*, 173-182, A.G.U., Washington.
- Botha, B.J.V. (1968). The stratigraphy of the Red Beds Stage, Karroo System, at Elliot, Cape Province. *Trans. Geol. Soc. S. Africa*, 71, 101-117.
- Boullier, A.M. and Nicolas, A. (1973). Texture and fabric of peridotite nodules from kimberlite. In: Nixon, P.H. (Ed.), *Lesotho Kimberlites*, 57-66, Lesotho National Develop. Corp., Maseru.
- Boullier, A.M. and Nicolas, A. (1975). Classification of textures and fabrics of peridotite xenoliths from South African kimberlites. In: Ahrens, L.H.; Dawson, J.B.; Duncan, A.R. and Erlank, A.J. (Eds.), *Phys. Chem. Earth*, Vol. 9, 467-475, Pergamon Press, Oxford.
- Boyd, F.R. (1971a). Enstatite-ilmenite and diopside-ilmenite intergrowths from the Monastery mine. *Carnegie Inst. Washington, Yb.* 70, 134-138.
- Boyd, F.R. (1971b). Pargasite-spinel peridotite xenolith from the Wesselton mine. *Carnegie Inst. Washington, Yb.* 70, 138-142.
- Boyd, F.R. (1973). A pyroxene geotherm. *Geochim. Cosmochim. Acta*, 37, 2533-2546.
- Boyd, F.R. (1974). Olivine megacrysts from the kimberlites of the Monastery and Frank Smith mines, South Africa. *Carnegie Inst. Washington, Yb.* 73, 282-285.
- Boyd, F.R. and Danchin, R.V. (1974). Discrete nodules from the Artur de Paiva kimberlite, Angola. *Carnegie Inst. Washington, Yb.* 73, 278-282.

- Boyd, F.R.; Dawson, J.B. and Smith, J.V. (1984). Granny Smith diopside megacrysts from the kimberlites of the Kimberley area and Jagersfontein, South Africa. *Geochim. Cosmochim. Acta*, 48, 381-384.
- Boyd, F.R. and England, J.L. (1964). The system enstatite-pyrope. *Carnegie Inst. Washington, Yb.* 63, 157-161.
- Boyd, F.R. and Finnerty, A.A. (1980). Conditions of origin of natural diamonds of peridotite affinity. *J. Geophys. Res.*, 85, 6911-6918.
- Boyd, F.R. and Gurney, J.J. (1982). Low calcium garnets: Keys to craton structure and diamond crystallisation. *Carnegie Inst. Washington, Yb.* 81, 261-267.
- Boyd, F.R.; Gurney, J.J. and Richardson, S.H. (1985). Evidence for a 150-200-km thick Archaean lithosphere from diamond inclusion thermobarometry. *Nature*, 315, 387-389.
- Boyd, F.R. and Meyer, H.O.A. (Eds.) (1979). *The Mantle Sample: Inclusions in Kimberlites and Other Volcanics*, A.G.U., Washington, 424p.
- Boyd, F.R. and Nixon, P.H. (1973). Origin of the ilmenite-silicate nodules in kimberlites from Lesotho and South Africa. In: Nixon, P.H. (Ed.), *Lesotho Kimberlites*, 254-268, Lesotho National Develop. Corp., Maseru.
- Boyd, F.R. and Nixon, P.H. (1975). Origins of the ultramafic nodules from some kimberlites of northern Lesotho and the Monastery mine, South Africa. In: Ahrens, L.H.; Dawson, J.B.; Duncan, A.R. and Erlank, A.J. (Eds.), *Phys. Chem. Earth*, Vol. 9, 431-454, Pergamon Press, Oxford.
- Boyd, F.R. and Nixon, P.H. (1978). Ultramafic nodules from the Kimberley pipes, South Africa. *Geochim. Cosmochim. Acta*, 42, 1367-1382.
- Boyd, F.R. and Nixon, P.H. (1979). Garnet lherzolite xenoliths from the kimberlites of East Griqualand, South Africa. *Carnegie Inst. Washington, Yb.* 78, 488-492.
- Brey, G. and Huth, J. (1984). The enstatite-diopside solvus to 60 kbar. In: Kornprobst, J. (Ed.), *Kimberlites II: The Mantle and Crust-Mantle Relationships*, 257-264, *Developments in Petrology* 11B, Elsevier, Amsterdam.
- Butterman, W.C. and Foster, W.R. (1967). Zircon stability and the  $ZrO_2-SiO_2$  phase diagram. *Amer. Mineral.*, 52, 880-885.
- Cardoso, P. (1980). A study of mantle inclusions in the Koffiefontein kimberlite pipe, South Africa. Unpublished M.Sc. thesis, Univ. Cape Town, South Africa, 133p.
- Carswell, D.A.O (1975). Primary and secondary phlogopites and clinopyroxenes in garnet lherzolite xenoliths. In: Ahrens, L.H.;

- Dawson, J.B.; Duncan, A.R. and Erlank, A.J. (Eds.),  
Phys. Chem. Earth, Vol. 9, 417-429, Pergamon Press, Oxford.
- Carswell, D.A. (1980). Mantle derived lherzolite nodules associated with kimberlite, carbonatite and basalt magmatism: A review. *Lithos*, 13, 121-138.
- Carswell, D.A.; Clarke, D.B. and Mitchell, R.H. (1979). The petrology and geochemistry of ultramafic nodules from pipe 200, northern Lesotho. In: Boyd, F.R. and Meyer, H.O.A. (Eds.), *The Mantle Sample: Inclusions in Kimberlites and Other Volcanics*, 127-144, A.G.U., Washington.
- Carswell, D.A.; Dawson, J.B. and Gibb, F.G.F. (1981). Equilibration conditions of upper-mantle eclogites: implications for kyanite-bearing and diamondiferous varieties. *Mineral. Mag.*, 44, 79-89.
- Carswell, D.A. and Gibb, F.G.F. (1980). Geothermometry of garnet lherzolite nodules with special reference to those from the kimberlites of northern Lesotho. *Contrib. Mineral. Petrol.*, 74, 403-416.
- Cawthorne, R.G. and Collerson, K.D. (1974). The recalculation of pyroxene end-member parameters and the estimation of ferrous and ferric iron content from electron microprobe analysis. *Amer. Mineral.*, 59, 1203-1208.
- Chinner, G.A. and Cornell, D.H. (1974). Evidence of kimberlite-grospydite reaction. *Contrib. Mineral. Petrol.*, 45, 153-160.
- Clark, S.P. and Ringwood, A.E. (1964). Density distribution and constitution of the mantle. *Rev. Geophys.*, 2, 35-88.
- Clement, C.R. (1979). The origin and infilling of kimberlite pipes. Ext. Abstr. Kimberlite Symposium II, Cambridge, U.K. (Unpaginated).
- Clement, C.R. (1982). A comparative geological study of some major kimberlite pipes in the Northern Cape and Orange Free State. Unpublished Ph.D. thesis, Univ. Cape Town, South Africa, 432p.
- Clement, C.R. and Skinner, E.M.W. (1979). A textural-genetic classification of kimberlite rocks. Chairmans Summaries and Poster Session Abstr., Kimberlite Symposium II, Cambridge, U.K., 18-21.
- Clement, C.R. and Skinner, E.M.W. (1985). A textural-genetic classification of kimberlites. *Trans. Geol. Soc. S. Africa*, 88, 403-410.
- Clement, C.R.; Skinner, E.M.W.; Hawthorne, J.B.; Kleinjan, L. and Allsopp, H.L. (1979). Precambrian ultramafic dykes with kimberlite affinities in the Kimberley area. In: Boyd, F.R. and Meyer, H.O.A. (Eds.), *Kimberlites, Diatremes and Diamonds: Their Geology, Petrology and Geochemistry*, 101-110, A.G.U., Washington.

- Clement, C.R.; Skinner, E.M.W. and Scott-Smith, B.H. (1977). Kimberlite redefined. Ext. Abstr. 2nd Int. Kimb. Conf., Santa Fe, A.G.U., Washington. (Unpaginated).
- Clement, C.R.; Skinner, E.M.W. and Scott-Smith, B.H. (1984). Kimberlite redefined. *J. Geol.*, 92, 223-228.
- Cohen, R.S.; O'Nions, R.K. and Dawson, J.B. (1982). Pb, Nd and Sr isotopes in ultramafic xenoliths: Evidence for ancient sub-continental mantle? *EOS, Trans. A.G.U.*, 63, 460.
- Coleman, R.G.; Lee, D.E.; Beatty, L.B. and Brannock, W.W. (1965). Eclogites and eclogites: Their differences and similarities. *Geol. Soc. Am. Bull.*, 76, 483-508.
- Cox, K.G. and Bell, J.D. (1972). A crystal fractionation model for the basaltic rocks of the New Georgia Group, British Solomon Islands. *Contrib. Mineral. Petrol.*, 37, 1-13.
- Cox, K.G.; Gurney, J.J. and Harte, B. (1973). Xenoliths from the Matsoku pipe. In: Nixon, P.H. (Ed.), *Lesotho Kimberlites*, 76-91, Lesotho National Develop. Corp., Maseru.
- Cox, K.G.; Smith, M.R. and Beswetherick, S. (1987). Textural studies of garnet lherzolites: evidence of exsolution origin from high-temperature harzburgite. In: Nixon, P.H. (Ed.), *Mantle Xenoliths*, John Wiley and Sons, Chichester, England. In press.
- Crough, S.T.; Morgan, W.J. and Hargraves, R.B. (1980). Kimberlites: Their relation to mantle hot spots. *Earth Planet. Sci. Lett.*, 50, 260-274.
- Danchin, R.V. (1979). Mineral and bulk chemistry of garnet lherzolite and garnet harzburgite xenoliths from the Premier mine, South Africa. In: Boyd, F.R. and Meyer, H.O.A. (Eds.), *The Mantle Sample: Inclusions in Kimberlites and Other Volcanics*, 104-126, A.G.U., Washington.
- Danchin, R.V. and Boyd, F.R. (1976). Ultramafic nodules from the Premier kimberlite pipe, South Africa. *Carnegie Inst. Washington, Yb.* 75, 531-538.
- Danchin, R.V. and Wyatt, B.A. (1979). Statistical cluster analysis of garnets from kimberlites and their xenoliths. In: *Chairmans Summaries and Poster Session Abstr.*, Kimberlite Symposium II, Cambridge, U.K., 22-27.
- Davis, B.T.C. and Boyd, F.R. (1966). The join  $Mg_2Si_2O_6$ - $CaMgSi_2O_6$  at 30 kilobars pressure and its application to pyroxenes from kimberlites. *J. Geophys. Res.*, 71, 3567-3576.
- Davis, G.L.; Krogh, T.E. and Erlank, A.J. (1976). The ages of zircons from kimberlites from South Africa. *Carnegie Inst. Washington, Yb.* 75, 821-824.
- Dawson, J.B. (1962). Basutoland kimberlites. *Geol. Soc. Am. Bull.*, 73, 545-560.

- Dawson, J.B. (1967a). A review of the geology of kimberlite. In: Wyllie, P.J. (Ed.), *Ultramafic and Related Rocks*, 241-251, John Wiley and Sons, New York.
- Dawson, J.B. (1967b). Geochemistry and origin of kimberlite. In: Wyllie, P.J. (Ed.), *Ultramafic and Related Rocks*, 269-278, John Wiley and Sons, New York.
- Dawson, J.B. (1971). Advances in kimberlite geology. *Earth-Sci. Rev.*, 7, 187-214.
- Dawson, J.B. (1979). Veined peridotites from the Bultfontein mine, South Africa. Ext. Abstr., *Kimberlite Symposium II*, Cambridge, U.K. (Unpaginated).
- Dawson, J.B. (1980). *Kimberlites and Their Xenoliths*. Springer-Verlag, Berlin, 252p.
- Dawson, J.B. (1982). Contrasting types of mantle metasomatism. *Terra Cognita*, 2, 232-233.
- Dawson, J.B. (1984a). Petrogenesis of kimberlite. In: Glover, J.E. and Harris, P.G. (Eds.), *Kimberlite Occurrence and Origin: A basis for conceptual models in exploration*, 103-112, Univ. Western Australia, Publication No. 8.
- Dawson, J.B. (1984b). Ascent and emplacement of kimberlite magma. In: Glover, J.E. and Harris, P.G. (Eds.), *Kimberlite Occurrence and Origin: A basis for conceptual models in exploration*, 113-124, Univ. Western Australia, Publication No. 8.
- Dawson, J.B. (1984c). Contrasting types of upper-mantle metasomatism? In: Kornprobst, J. (Ed.), *Kimberlites II: The Mantle and Crust-Mantle Relationships*, 289-294, *Developments in Petrology 11B*, Elsevier, Amsterdam.
- Dawson, J.B.; Gurney, J.J. and Lawless, P.J. (1975). Palaeogeothermal gradients derived from xenoliths in kimberlite. *Nature*, 257, 299-300.
- Dawson, J.B. and Smith, J.V. (1975). Occurrence of diamond in a mica-garnet lherzolite xenolith from kimberlite. *Nature*, 254, 580-581.
- Dawson, J.B. and Smith, J.V. (1977). The MARID (mica-amphibole-rutile-ilmenite-diopside) suite of xenoliths in kimberlite. *Geochim. Cosmochim. Acta*, 41, 309-323.
- Dawson, J.B. and Stephens, W.E. (1975). Statistical classification of garnets from kimberlite and associated xenoliths. *J. Geol.*, 83, 589-607.
- Deines, P.; Gurney, J.J. and Harris, J.W. (1984). Associated chemical and carbon isotopic composition variations in diamonds from Finsch and Premier kimberlite, South Africa. *Geochim. Cosmochim. Acta*, 48, 325-342.

- Delaney, J.S.; Smith, J.V.; Carswell, D.A. and Dawson, J.B. (1980). Chemistry of micas from kimberlites and xenoliths - II. Primary- and secondary-textured micas from peridotite xenoliths. *Geochim. Cosmochim. Acta*, 44, 857-872.
- Duncan, R.A. (1981). Hotspots in the southern oceans - an absolute frame of reference for motion of the Gondwana continents. *Tectonophysics*, 74, 29-42.
- Edwards, C.B. and Howkins, J.B. (1966). Kimberlites in Tanganyika with special reference to the Mwadui occurrence. *Econ. Geol.*, 61, 537-554.
- Eggler, D.H.; McCallum, M.E. and Smith, C.B. (1979). Megacryst assemblages in kimberlites from northern Colorado and southern Wyoming: petrology, geothermometry-barometry and areal distribution. In: Boyd, F.R. and Meyer, H.O.A. (Eds.), *The Mantle Sample: Inclusions in Kimberlites and Other Volcanics*, 213-226, A.G.U., Washington.
- Eggler, D.H. and Wendlandt, R.F. (1979). Experimental studies on the relationship between kimberlite magmas and partial melting of peridotite. In: Boyd, F.R. and Meyer, H.O.A. (Eds.), *Kimberlites, Diatremes and Diamonds: Their Geology, Petrology and Geochemistry*, 330-338, A.G.U., Washington.
- Ehrenberg, S.N. (1979). Garnetiferous ultramafic inclusions in minette from the Navajo volcanic field. In: Boyd, F.R. and Meyer, H.O.A. (Eds.), *The Mantle Sample: Inclusions in Kimberlites and Other Volcanics*, 330-344, A.G.U., Washington.
- Ehrenberg, S.N. (1982). Petrogenesis of garnet lherzolite and megacrystalline nodules from the Thumb, Navajo Volcanic Field. *J. Petrol.*, 23, 507-547.
- Ellis, D.J. and Green, D.H. (1979). An experimental study of the effect of Ca upon garnet-clinopyroxene Fe-Mg exchange equilibria. *Contrib. Mineral. Petrol.*, 71, 13-22.
- Erlank, A.J.; Allsopp, H.L.; Hawkesworth, C.J. and Menzies, M.A. (1982). Chemical and isotopic characterization of upper mantle metasomatism in peridotite nodules from the Bultfontein kimberlite. *Terra Cognita*, 2, 261-263.
- Erlank, A.J. and Rickard, R.S. (1977). Potassic richterite-bearing peridotites from kimberlite and the evidence they provide for upper-mantle metasomatism. *Ext. Abstr. 2nd Int. Kimb. Conf.*, Santa Fe, A.G.U., Washington. (Unpaginated).
- Erlank, A.J. and Shimizu, N. (1977). Strontium and strontium isotope distributions in some kimberlite nodules and minerals. *Ext. Abstr. 2nd Int. Kimb. Conf.*, Santa Fe, A.G.U., Washington. (Unpaginated).
- Erlank, A.J.; Waters, F.G.; Hawkesworth, C.J.; Haggerty, S.E.; Allsopp, H.L.; Rickard, R.S. and Menzies, M.A. (1987). Evidence for mantle metasomatism in peridotite nodules from the Kimberley pipes, South Africa. In: Menzies, M.A. and Hawkesworth, C.J. (Eds.), *Mantle Metasomatism*, Acad. Press, London. In press.

- Eskola, P. (1921). On the eclogites of Norway. Vidensk. Selskapets Skr., Kristiania I. Matematisk-Natur videnskapelig KI., 8, 1-118.
- Evans, T. (1976). Diamonds. Contemporary Physics, 17, 45-70.
- Evans, T. and Qi, Z. (1982). The kinetics of the aggregation of nitrogen atoms in diamond. Proc. R. Soc. London, A381, 159-178.
- Farmer, G.L. and Boettcher, A.L. (1981). Petrologic and crystal-chemical significance of some deep-seated phlogopites. Amer. Mineral., 66, 1154-1163.
- Ferguson, J.; Danchin, R.V. and Nixon, P.H. (1973). Petrochemistry of kimberlite autoliths. In: Nixon, P.H. (Ed.), Lesotho Kimberlites, 285-293, Lesotho National Develop. Corp., Maseru.
- Field, J.E. (Ed.) (1979). The Properties of Diamond. Acad. Press, London, 674p.
- Fielding, D.C. (1981). Exploration of Mine Area at Monastery Mine, Marquard District (OFS) South Africa. Internal Company Report. Gem Exploration and Minerals Ltd., South Africa.
- Finger, L.W. (1972). The uncertainty in the calculated ferric iron content of a microprobe analysis. Carnegie Inst. Washington, Yb. 71, 600-603.
- Finnerty, A.A. and Boyd, F.R. (1984). Evaluation of thermobarometers for garnet peridotites. Geochim. Cosmochim. Acta, 48, 15-27.
- Fraser, D.G. and Lawless, P.J. (1978). Palaeogeotherms: implications of disequilibrium in garnet lherzolite xenoliths. Nature, 273, 220-221.
- Ganguly, J. (1979). Garnet and clinopyroxene solid solutions, and geothermometry based on Fe-Mg distribution coefficient. Geochim. Cosmochim. Acta, 43, 1021-1029.
- Gary, M.; McAfee, R. and Wolf, C.L. (Eds.) (1972). Glossary of Geology. Am. Geol. Inst., Washington. 857p.
- Gasparik, T. (1984). Two-pyroxene thermobarometry with new experimental data in the system CaO-MgO-Al<sub>2</sub>O<sub>3</sub>-SiO<sub>2</sub>. Contrib. Mineral. Petrol., 87, 87-97.
- Glover, J.E. and Harris, P.G. (Eds.) (1984). Kimberlite Occurrence and Origin: A basis for conceptual models in exploration. Univ. Western Australia, Publication No. 8, 298p.
- Green, D.H.; Hibberson, W.O. and Jaques, A.L. (1979). Petrogenesis of Mid-Ocean Ridge Basalts. In: McElhinny, M.W. (Ed.), The Earth: Its Origin, Structure and Evolution, 265-299, Acad. Press, London.
- Green, D.H. and Ringwood, A.E. (1967). An experimental investigation of the gabbro to eclogite transformation and its petrological applications. Geochim. Cosmochim. Acta, 31, 767-833.

- Green, D.H. and Ringwood, A.E. (1970). Mineralogy of peridotitic compositions under upper mantle conditions. *Phys. Earth Planet. Inter.*, 3, 359-371.
- Green, H.W. and Gueguen, Y. (1974). Origin of kimberlite pipes by diapiric upwelling in the upper mantle. *Nature*, 249, 617-620.
- Green, T.H. (1967). An experimental investigation of sub-solidus assemblages formed at high pressure in high-alumina basalt, kyanite eclogite and grosspydrite compositions. *Contrib. Mineral. Petrol.*, 16, 84-114.
- Green, T.H. and Ringwood, A.E. (1968). Genesis of the calc-alkaline igneous rock suite. *Contrib. Mineral. Petrol.*, 18, 105-162.
- Gurney, J.J. (1980). Report on the Monastery Mine Kimberlite Pipe. Company Report: Minerale Dienste Beleggings Edm. Bpk., 11p.
- Gurney, J.J. (1984). A correlation between garnets and diamonds in kimberlites. In: Glover, J.E. and Harris, P.G. (Eds.), *Kimberlite Occurrence and Origin: A basis for conceptual models in exploration*, 143-166, Univ. Western Australia, Publication No. 8.
- Gurney, J.J. (1987). Diamonds. In: *Proc. 4th Int. Kimb. Conf.*, Perth, Australia. In Press.
- Gurney, J.J. and Haggerty, S.E. (1975). An ilmenite-pyroxene intergrowth from the Premier mine. *Abstr. Kimberlite Symposium I*, Cambridge, U.K., 52-53.
- Gurney, J.J.; Harris, J.W. and Rickard, R.S. (1979a). Silicate and oxide inclusions in diamonds from the Finsch kimberlite pipe. In: Boyd, F.R. and Meyer H.O.A. (Eds.), *Kimberlites, Diatremes and Diamonds: Their Geology, Petrology and Geochemistry*, 1-15, A.G.U., Washington.
- Gurney, J.J.; Jakob, W.R.O. and Dawson, J.B. (1979b). Megacrysts from the Monastery kimberlite pipe, South Africa. In: Boyd, F.R. and Meyer, H.O.A. (Eds.), *The Mantle Sample: Inclusions in Kimberlites and Other Volcanics*, 227-243, A.G.U., Washington.
- Gurney, J.J.; Harris, J.W. and Rickard, R.S. (1984a). Silicate and oxide inclusions in diamonds from the Orapa mine, Botswana. In: Kornprobst, J. (Ed.), *Kimberlites II: The Mantle and Crust-Mantle Relationships*, 3-9, *Developments in Petrology 11B*, Elsevier, Amsterdam.
- Gurney, J.J.; Harris, J.W. and Rickard, R.S. (1984b). Minerals associated with diamonds from the Roberts Victor mine. In: Kornprobst, J. (Ed.), *Kimberlites II: The Mantle and Crust-Mantle Relationships*, 25-32, *Developments in Petrology 11B*, Elsevier, Amsterdam.
- Gurney, J.J.; Harris, J.W.; Rickard, R.S. and Moore, R.O. (1985). Inclusions in Premier mine diamonds. *Trans. Geol. Soc. South Africa*, 88, 301-310.

- Gurney, J.J. and Harte, B. (1980). Chemical variations in upper mantle nodules from southern African kimberlites. *Phil. Trans. R. Soc. London*, A297, 273-293.
- Gurney, J.J.; Harte, B. and Cox, K.G. (1975). Mantle xenoliths in the Matsoku kimberlite pipe. In: Ahrens, L.H.; Dawson, J.B.; Duncan, A.R. and Erlank, A.J. (Eds.), *Phys. Chem. Earth*, Vol. 9, 507-524, Pergamon Press, Oxford.
- Gurney, J.J. and Switzer, G.S. (1973). The discovery of garnets closely related to diamonds in the Finsch Pipe, South Africa. *Contrib. Mineral. Petrol.*, 39, 103-116.
- Haggerty, S.E. (1975a). The chemistry and genesis of opaque minerals in kimberlites. In: Ahrens, L.H.; Dawson, J.B.; Duncan, A.R. and Erlank, A.J. (Eds.), *Phys. Chem. Earth*, Vol. 9, 295-307, Pergamon Press, Oxford.
- Haggerty, S.E. (1975b). An analysis of correlative and non-correlative oxide parameters for spinels and ilmenites in groundmass kimberlite. *Abstr. Kimberlite Symposium I*, Cambridge, U.K., 43-45.
- Haggerty, S.E. (1976). Opaque mineral oxides in terrestrial igneous rocks. In: Rumble, D. (Ed.), *Oxide Minerals*, Chapter 8, Hg101-Hg300, Min. Soc. America, Washington, D.C.
- Haggerty, S.E. and Boyd, F.R. (1975). Kimberlite inclusions in an olivine megacryst from Monastery. *Abstr. Kimberlite Symposium I*, Cambridge, U.K.; 50-51.
- Haggerty, S.E.; Hardie, R.B. and McMahon, B.M. (1979). The mineral chemistry of ilmenite nodule associations from the Monastery diatreme. In: Boyd, F.R. and Meyer, H.O.A. (Eds.), *The Mantle Sample: Inclusions in Kimberlites and Other Volcanics*, 249-256, A.G.U., Washington.
- Haggerty, S.E.; Smyth, J.R.; Erlank, A.J.; Rickard, R.S. and Danchin, R.V. (1983). Lindsleyite (Ba) and mathiasite (K): two new chromium-titanates in the crichtonite series from the upper mantle. *Amer. Mineral.*, 68, 494-505.
- Hall, A.E. and Smith, C.B. (1984). Lamproite diamonds - are they different? In: Glover, J.E. and Harris, P.G. (Eds.), *Kimberlite Occurrence and Origin: A basis for conceptual models in exploration*, 167-212, Univ. Western Australia, Publication No. 8.
- Harley, S.L. (1984a). The solubility of alumina in orthopyroxene coexisting with garnet in FeO-MgO-Al<sub>2</sub>O<sub>3</sub>-SiO<sub>2</sub> and CaO-FeO-MgO-Al<sub>2</sub>O<sub>3</sub>-SiO<sub>2</sub>. *J. Petrol.*, 25, 665-696.
- Harley, S.L. (1984b). Comparison of the garnet-orthopyroxene geobarometer with recent experimental studies, and applications to natural assemblages. *J. Petrol.*, 25, 697-712.
- Harley, S.L. (1984c). An experimental study of the partitioning of Fe and Mg between garnet and orthopyroxene. *Contrib. Mineral. Petrol.*, 86, 359-373.

- Harley, S.L. and Thompson A.B. (1984). Xenolithic mineral assemblages in kimberlites, paleogeotherms, and the thermal structure of the mantle. In: Kornprobst, J. (Ed.), *Kimberlites II: The Mantle and Crust-Mantle Relationships*, 277-287, *Developments in Petrology 11B*, Elsevier, Amsterdam.
- Harris, J.W. (1968). The recognition of diamond inclusions. Part 1: Syngenetic mineral inclusions. Part 2: Epigenetic mineral inclusions. *Ind. Diamond Rev.*, 28, 402-410, 458-461.
- Harris, J.W. (1987). Recent physical, chemical, and isotopic research of diamond. In: Nixon, P.H. (Ed.), *Mantle Xenoliths*, John Wiley and Sons, Chichester, England. In press.
- Harris, J.W. and Gurney, J.J. (1979). Inclusions in diamond. In: Field, J.E. (Ed.), *The Properties of Diamond*, 555-591, Acad. Press, London.
- Harris, J.W. and Gurney, J.J. (1987). Inclusion abundances in diamonds from southern Africa. *Mineral. Mag.* Submitted.
- Harris, J.W.; Hawthorne, J.B. and Oosterveld, M.M. (1979). Regional and local variations in the characteristics of diamonds from some southern African kimberlites. In: Boyd, F.R. and Meyer, H.O.A. (Eds.), *Kimberlites, Diatremes and Diamonds: Their Geology, Petrology and Geochemistry*, 27-41, A.G.U., Washington.
- Harris, J.W.; Hawthorne, J.B.; Oosterveld, M.M. and Wehmeyer, E. (1975). A classification scheme for diamond and a comparative study of South African diamond characteristics. In: Ahrens, L.H.; Dawson, J.B.; Duncan, A.R. and Erlank, A.J., *Phys. Chem. Earth*, Vol. 9, 765-783, Pergamon Press, Oxford.
- Harte, B. (1977). Rock nomenclature with particular relation to deformation and recrystallisation textures in olivine-bearing xenoliths. *J. Geol.*, 85, 279-288.
- Harte, B. (1978). Kimberlite nodules, upper mantle petrology, and geotherms. *Phil. Trans. R. Soc. London*, A288, 487-500.
- Harte, B. (1983). Mantle peridotites and processes - the kimberlite sample. In: Hawkesworth, C.J. and Norry, M.J. (Eds.), *Continental Basalts and Mantle Xenoliths*, 46-91, Shiva Publ. Ltd., Cheshire, England.
- Harte, B.; Cox, K.G. and Gurney, J.J. (1975). Petrography and geological history of the upper mantle xenoliths from the Matsoku kimberlite pipe. In: Ahrens, L.H.; Dawson, J.B.; Duncan, A.R. and Erlank, A.J. (Eds.), *Phys. Chem. Earth*, Vol. 9, 477-506, Pergamon Press, Oxford.
- Harte, B. and Freer, R. (1982). Diffusion data and their bearing on the interpretation of mantle nodules and the evolution of the mantle lithosphere. *Terra Cognita*, 2, 273-275.
- Harte, B. and Gurney, J.J. (1975). Veining and banding phenomena within the upper mantle nodules from the Matsoku kimberlite pipe, Lesotho. *Abstr. Kimberlite Symposium I*, Cambridge, U.K., 57-58.

- Harte, B. and Gurney, J.J. (1981). The mode of formation of chromium-poor megacryst suites from kimberlites. *J. Geol.*, 89, 749-753.
- Harte, B. and Gurney, J.J. (1982). Compositional and textural features of peridotite nodules from the Jagersfontein kimberlite pipe, South Africa. *Terra Cognita* 2, 256-257.
- Harte, B.; Gurney, J.J. and Harris, J.W. (1980). The formation of peridotitic suite inclusions in diamonds. *Contrib. Mineral. Petrol.*, 72, 181-190.
- Hatton, C.J. (1978). The geochemistry and origin of xenoliths from the Roberts Victor mine. Unpublished Ph.D. thesis, Univ. Cape Town, South Africa, 179p.
- Hatton, C.J. and Gurney, J.J. (1979). A diamond-graphite eclogite from the Roberts Victor mine. In: Boyd, F.R. and Meyer, H.O.A. (Eds.), *The Mantle Sample: Inclusions in Kimberlites and Other Volcanics*, 29-36, A.G.U., Washington.
- Hatton, C.J. and Gurney, J.J. (1987). Roberts Victor eclogites and their relation to the mantle. In: Nixon P.H. (Ed.), *Mantle Xenoliths*, John Wiley & Sons, Chichester, England. In press.
- Hawkesworth, C.J. and Norry, M.J. (Eds.) (1983). *Continental Basalts and Mantle Xenoliths*. Shiva Publ. Ltd., Cheshire, England, 272p.
- Hawthorne, J.B. (1975). Model of a kimberlite pipe. In: Ahrens, L.H.; Dawson, J.B.; Duncan, A.R. and Erlank, A.J. (Eds.), *Phys. Chem. Earth*, Vol. 9, 1-15, Pergamon Press, Oxford.
- Hawthorne, J.B.; Gurney, J.J., and Harris, J.W. (1978). Inclusions in diamonds from South Africa. Ext. Abstr. XIIth Int. Mineral. Assoc. Meeting, Novosibirsk, USSR. (Unpaginated)
- Helmstaedt, H. and Doig, R. (1975). Eclogite nodules from kimberlite pipes of the Colorado Plateau - samples of subducted Franciscan-type oceanic lithosphere. In: Ahrens, L.H.; Dawson, J.B.; Duncan, A.R. and Erlank, A.J. (Eds.), *Phys. Chem. Earth*, Vol. 9, 95-111, Pergamon Press, Oxford.
- Hervig, R.L.; Smith, J.V.; Steele I.M.; Gurney, J.J.; Meyer, H.O.A. and Harris, J.W. (1980). Diamonds: Minor elements in silicate inclusions: Pressure-temperature implications. *J. Geophys. Res.*, 85, 6919-6929.
- Hofmann, A.W. and White, W.M. (1982). Mantle plumes from ancient oceanic crust. *Earth and Planet. Sci. Lett.*, 57, 421-436.
- Holmes, A. and Paneth F.A. (1936). Helium ratios of rocks and minerals from the diamond pipes of South Africa. *Proc. Roy. Soc. London*, A154, 385-413.
- Hops, J.J.; Gurney, J.J. and Harte, B. (1986). Megacrysts and deformed nodules from the Jagersfontein kimberlite pipe. Abstr. Series 16, 4th Int. Kimb. Conf., Perth, Geol. Soc. Australia, 256-258.

- Howells, S. and O'Hara, M.J. (1978). Low solubility of alumina in enstatite and uncertainties in estimated palaeogeotherms. *Phil. Trans. R. Soc. London*, A288, 471-486.
- Irifune, T.; Hibberson, W.O. and Ringwood, A.E. (1986a). Eclogite-garnetite transformations in basaltic and pyrolitic compositions at high pressure and high temperature. Abstr. Series 16, 4th Int. Kimb. Conf., Perth, Geol. Soc. Australia, 259-261.
- Irifune, T.; Sekine, T.; Ringwood, A.E. and Hibberson, W.O. (1986b). The eclogite-garnetite transformation at high pressure and some geophysical implications. *Earth Planet. Sci. Lett.*, 77, 245-256.
- Irving, A.J. (1976). On the validity of palaeogeotherms determined from xenolith suites in basalts and kimberlites. *Amer. Mineral.*, 61, 638-642.
- Irving, A.J. and Frey, F.A. (1978). Distribution of trace elements between garnet megacrysts and host volcanic liquids of kimberlitic to rhyolitic composition. *Geochim. Cosmochim. Acta*, 42, 771-787.
- Ito, K. and Kennedy, G.C. (1967). Melting and phase relations in a natural peridotite to 40 kbars. *Amer. J. Sci.*, 265, 519-538.
- Jagoutz, E.; Dawson J.B.; Hoernes, S.; Spettel, B. and Wanke, H. (1984). Anorthositic oceanic crust in the Archaean Earth. Abstract, 15th Lunar and Planetary Sc. Conf., Houston.
- Jakob, W.R.O. (1977). Geochemical aspects of the megacryst suite from the Monastery kimberlite pipe. Unpublished M.Sc. thesis, Univ. Cape Town, South Africa, 81p.
- Johnson, J.P. (1906). The geology of the neighbourhood of the Roberts Victor mine. *Trans. Geol. Soc. S. Africa*, 9, 117-124.
- Jones, A.P.; Smith, J.V. and Dawson, J.D. (1982). Mantle metasomatism in 14 veined peridotites from Bultfontein mine, South Africa. *J. Geol.*, 90, 435-453.
- Jones, R.A. (1984). Geochemical and isotopic studies of some kimberlites and included ultrabasic xenoliths from southern Africa. Unpublished Ph.D. thesis, Univ. Leeds, U.K., 269p.
- Jordan, T.H. (1981). Continents as a chemical boundary layer. *Phil. Trans. R. Soc. London*, A301, 359-373.
- Kawasaki, T. (1979). Thermodynamic analyses on the Fe-Mg exchange equilibrium between olivine and garnet: an application to the estimation of pressure-temperature relations of ultramafic rocks. *J. Jpn. Assoc. Mineral. Petrol. Econ. Geol.*, 74, 395-405.
- Kennedy, C.S. and Kennedy, G.C. (1976). The equilibrium boundary between graphite and diamond. *J. Geophys. Res.*, 81, 2467-2470.
- Kennedy, G.C. and Nordlie, B.E. (1968). The genesis of diamond deposits. *Econ. Geol.*, 63, 495-503.

- Kornprobst, J. (Ed.) (1984). Kimberlites II: The Mantle and Crust-Mantle Relationships. Developments in Petrology 11B, Elsevier, Amsterdam, 393 p.
- Kramers, J.D. (1977). Lead and strontium isotopes in Cretaceous kimberlites and mantle-derived xenoliths from southern Africa. *Earth Planet. Sci. Lett.*, 34, 419-431.
- Kramers, J.D. (1979). Lead, uranium, strontium, potassium and rubidium in inclusion-bearing diamonds and mantle-derived xenoliths from southern Africa. *Earth Planet. Sci. Lett.*, 42, 58-70.
- Kramers, J.D.; Smith, C.B.; Lock, N.P.; Harmon, R.S. and Boyd, F.R. (1981). Can kimberlites be generated from an ordinary mantle? *Nature*, 291, 53-56.
- Kresten, P. (1973a). Kimberlitic zircons. Ext. Abstr. Int. Kimb. Conf., Cape Town, South Africa, 191-194.
- Kresten, P. (1973b). The coating of kimberlitic zircons: A preliminary study. In: Nixon, P.H. (Ed.), *Lesotho Kimberlites*, 220-223, Lesotho National Develop. Corp., Maseru.
- Kresten, P.; Fels, P. and Berggren, G. (1975). Kimberlitic zircons - a possible aid in prospecting for kimberlites. *Mineral. Deposita*, 10, 47-56.
- Kullerud, G.; Yund, R.A. and Moh, G.H. (1969). Phase relations in the Cu-Fe-S, Cu-Ni-S and Fe-Ni-S systems. *Econ. Geol. Monograph* 4, 323-343.
- Kurz, M.D. and Gurney, J.J. (1986). Helium isotopic heterogeneity within single diamonds from the Orapa kimberlite pipe. *Abstr. Series 16, 4th Int. Kimb. Conf.*, Perth, Geol. Soc. Australia, 401-402.
- Kushiro, I. (1970). Stability of amphibole and phlogopite in the upper mantle. *Carnegie Inst. Washington, Yb.* 68, 245-247.
- Kushiro, I. and Aoki, K. (1968). Origin of some eclogite inclusions in kimberlite. *Amer. Mineral.*, 53, 1347-1367.
- Kushiro, I.; Syono, Y. and Akimoto, S. (1968). Melting of a peridotite nodule and at high pressures and high water pressures. *J. Geophys. Res.*, 73, 6023-6029.
- Lane, D.L. and Ganguly, J. (1980). Al<sub>2</sub>O<sub>3</sub> solubility in orthopyroxene in the system MgO-Al<sub>2</sub>O<sub>3</sub>-SiO<sub>2</sub>: A reevaluation, and mantle geotherm. *J. Geophys. Res.*, 85, 6963-6972.
- Lappin, M.A. (1978). The evolution of a grospydite from the Roberts Victor mine, South Africa. *Contrib. Mineral. Petrol.*, 66, 229-241.
- Lappin, M.A. and Dawson, J.B. (1975). Two Roberts Victor cumulate eclogites and their re-equilibration. In: Ahrens, L.H.; Dawson, J.B.; Duncan, A.R. and Erlank, A.J. (Eds.), *Phys. Chem. Earth*,

Vol. 9, 351-366, Pergamon Press, Oxford.

- Leake, B.E. (1978). Nomenclature of amphiboles. *Canadian Mineral.*, 16, 501-520.
- le Roex, A.P. (1986). Geochemical correlation between southern African kimberlites and South Atlantic hot-spots. *Nature*, 324, 243-245.
- Lindsley, D.H. and Andersen, D.J. (1983). A two-pyroxene thermometer. *J. Geophys. Res.*, 88 (Supplement), A887-A906.
- Lindsley, D.H. and Dixon, S.A. (1976). Diopside-enstatite equilibria at 850°C to 1400°C, 5 to 35 kb. *Am. J. Sci.*, 276, 1285-1301.
- Liu, L. (1977). The system enstatite-pyrope at high pressures and temperatures and the mineralogy of the Earth's mantle. *Earth Planet. Sci. Lett.*, 36, 237-245.
- Liu, L. (1979). The high pressure phase transformations of monticellite and implications for upper mantle mineralogy., *Phys. Earth Planet. Inter.*, 20, 25 only.
- Liu, L. (1980a). Phase relations in the system diopside-jadeite at high pressures and high temperatures. *Earth Planet. Sci. Lett.*, 47, 398-402.
- Liu, L. (1980b). The mineralogy of an eclogitic earth mantle. *Phys. Earth Planet. Inter.*, 23, 262-267.
- Liu, L. (1980c). The pyroxene-garnet transformation and its implication for the 200-km seismic discontinuity. *Phys. Earth Planet. Inter.*, 23, 286-291.
- Liu, L. and Ringwood, A.E. (1975). Synthesis of a perovskite-type polymorph of  $\text{CaSiO}_3$ . *Earth Planet. Sci. Lett.*, 28, 209-211.
- Lloyd, F.E. and Bailey, D.K. (1975). Light element metasomatism of the Continental Mantle: The evidence and the consequences. *Phys. Chem. Earth*, 9, 389-416, Pergamon Press, Oxford.
- MacGregor, I.D. (1970). The effect of  $\text{CaO}$ ,  $\text{Cr}_2\text{O}_3$ ,  $\text{Fe}_2\text{O}_3$  and  $\text{Al}_2\text{O}_3$  on the stability of spinel and garnet peridotites. *Phys. Earth Planet. Inter.*, 3, 372-377.
- MacGregor, I.D. (1974). The system  $\text{MgO-Al}_2\text{O}_3\text{-SiO}_2$ : Solubility of  $\text{Al}_2\text{O}_3$  in enstatite for spinel and garnet peridotite compositions. *Amer. Mineral.*, 59, 110-119.
- MacGregor, I.D. (1979). Mafic and ultramafic xenoliths from the Kao kimberlite pipe. In: Boyd, F.R. and Meyer, H.O.A. (Eds.), *The Mantle Sample: Inclusions in Kimberlites and Other Volcanics*, 156-172, A.G.U., Washington.
- MacGregor, I.D. and Basu, A.R. (1976). Geological problems in estimating mantle geothermal gradients. *Amer. Mineral.*, 61, 715-724.

- MacGregor, I.D. and Carter, J.L. (1970). The chemistry of clinopyroxenes and garnets of eclogite and peridotite xenoliths from the Roberts Victor mine, South Africa. *Phys. Earth Planet. Inter.*, 3, 391-397.
- Marshintsev, V.K.; Zayakina, N.V. and Leskova, N.V. (1982). Inclusions of cubic silicon carbide in moissanite from kimberlite pipes - a new occurrence in nature. *Doklady Akad. Nauk. SSSR*, 262, 204-206. (Russian)
- McCallister, R.H. and Nord, G.L.(Jr.) (1981). Subcalcic diopsides from kimberlites: Chemistry, exsolution microstructures and thermal history. *Contrib. Mineral. Petrol.*, 78, 118-125.
- McCandless, T.E. and Gurney, J.J. (1986). Sodium in garnet and potassium in clinopyroxene: Criteria for classifying mantle eclogites. *Abstr. Series 16, 4th Int. Kimb. Conf., Perth, Geol. Soc. Australia*, 282-284.
- McElhinny, M.W. (Ed.) (1979). *The Earth: Its Origin, Structure and Evolution*. Acad. Press, London, 597p.
- McKenzie, D. and O'Nions, R.K. (1983). Mantle reservoirs and ocean island basalts. *Nature*, 301, 229-231.
- Melton, C.E. and Giardini, A.A. (1980). The isotopic composition of argon included in an Arkansas diamond and its significance. *Geophys. Res. Lett.*, 7, 461-464.
- Menzies, M.A. and Hawkesworth, C.J. (1987). *Mantle Metasomatism*. Acad. Press, London. In press.
- Menzies, M. and Murthy, V.R. (1980). Enriched mantle: Nd and Sr isotopes in diopsides from kimberlite nodules. *Nature*, 283, 634-636.
- Mercier, J.-C. and Carter, N.L. (1975). Pyroxene geotherms. *J. Geophys. Res.*, 80, 3349-3362.
- Meyer, H.O.A. (1977). Mineralogy of the upper mantle: A review of the minerals in mantle xenoliths from kimberlite. *Earth-Sci. Rev.*, 13, 251-281.
- Meyer, H.O.A. (1982). Mineral inclusions in natural diamond. In: Eash, D.M. (Ed.), *Proc. Int. Gemological Symposium, Gemological Inst. of America, Santa Monica, U.S.A.*, pp. 445-465.
- Meyer, H.O.A. (1985). Genesis of diamond: a mantle saga. *Amer. Mineral.*, 70, 344-355.
- Meyer, H.O.A. (1987). Inclusions in diamond. In: Nixon, P.H. (Ed.), *Mantle Xenoliths*, John Wiley and Sons, Chichester, England. In press.
- Meyer, H.O.A. and Boyd F.R. (1969). Mineral inclusions in diamonds. *Carnegie Inst. Wash., Yb.* 67, 130-135.
- Meyer, H.O.A. and Boyd, F.R. (1972). Composition and origin of crystalline inclusions in natural diamonds. *Geochim.*

- Cosmochim. Acta, 36, 1255-1273.
- Meyer, H.O.A. and Gubelin, E. (1981). Ruby in diamond. *Gems and Gemology*, 17, 153-156.
- Meyer, H.O.A. and McCallum, M.E. (1986). Mineral inclusions in diamonds from the Sloan kimberlites, Colorado. *J. Geol.*, 94, 600-612.
- Meyer, H.O.A. and Svisero, D.P. (1975). Mineral inclusions in Brazilian diamonds. In: Ahrens, L.H.; Dawson, J.B.; Duncan, A.R. and Erlank, A.J. (Eds.), *Phys. Chem. Earth*, Vol. 9, 785-795, Pergamon Press, Oxford.
- Meyer, H.O.A. and Tsai, H.-M. (1976). The nature and significance of mineral inclusions in natural diamond: A review. *Min. Sci. Engng.*, 8, 242-261.
- Milton, C. and Vitaliano, D. (1984). Moissanite, SiC, a non-existent mineral. XXVII Int. Geol. Congress, Moscow.
- Mitchell, R.H. (1970). Kimberlite and related rocks - a critical reappraisal. *J. Geol.*, 78, 686-704.
- Mitchell, R.H. (1977). Geochemistry of magnesian ilmenites from kimberlites in South Africa and Lesotho. *Lithos*, 10, 29-37.
- Mitchell, R.H. (1978). Mineralogy of the Elwin Bay kimberlite, Somerset Island, N.W.T., Canada. *Am. Mineral.*, 63, 47-57.
- Mitchell, R.H. (1979a). The alleged kimberlite-carbonatite relationship: Additional contrary mineralogical evidence. *Am. J. Sci.*, 279, 570-589.
- Mitchell, R.H. (1979b). Mineralogy of the Tunraq kimberlite, Somerset Island, N.W.T., Canada. In: Boyd, F.R. and Meyer, H.O.A. (Eds.), *Kimberlites, Diatremes and Diamonds: Their Geology, Petrology and Geochemistry*, 161-171, A.G.U., Washington.
- Mitchell, R.H. (1984a). Mineralogy and origin of carbonate-rich segregations in a composite kimberlite sill. *N. Jb. Mineral. Abh.*, 150, 185-197.
- Mitchell, R.H. (1984b). Garnet lherzolites from the Hanaus-I and Louwrensia kimberlites of Namibia. *Contrib. Mineral. Petrol.*, 86, 178-188.
- Mitchell, R.H.; Carswell, D.A. and Clarke, D.B. (1980). Geological implications and validity of calculated equilibration conditions for ultramafic xenoliths from the Pipe 200 kimberlite, northern Lesotho. *Contrib. Mineral. Petrol.*, 72, 205-217.
- Mitchell, R.H. and Meyer, H.O.A. (1980). Mineralogy of micaceous kimberlite from the Jos Dyke, Somerset Island, N.W.T.. *Canadian Mineral.*, 18, 241-250.
- Moore, R.O. and Gurney, J.J. (1985). Pyroxene solid solution in garnets included in diamond. *Nature*, 318, 553-555.

- Moore, R.O. and Gurney, J.J. (1986). Mineral inclusions in diamonds from the Monastery kimberlite, South Africa. Abstr. Series 16, 4th Int. Kimb. Conf., Perth, Geol. Soc. Australia, 406-408.
- Moore, R.O.; Otter, M.L.; Rickard, R.S.; Harris, J.W. and Gurney, J.J. (1986). The occurrence of moissanite and ferro-periclase as inclusions in diamond. Abstr. Series 16, 4th Int. Kimb. Conf., Perth, Geol. Soc. Australia, 409-411.
- Morgan, W.J. (1971). Convection plumes in the lower mantle. *Nature*, 230, 42-43.
- Mori, T. and Green, D.H. (1975). Pyroxenes in the system  $Mg_2Si_2O_6$ - $CaMgSi_2O_6$  at high pressure. *Earth Planet. Sci. Lett.*, 26, 277-286.
- Mori, T. and Green, D.H. (1978). Laboratory duplication of phase equilibria observed in natural garnet lherzolites. *J. Geol.*, 86, 83-97.
- Mvuemba Ntanda, F.; Moreau, J. and Meyer, H.O.A. (1982). Particularites des inclusions cristallines primaires des diamants du Kasai, Zaire. *Canadian Mineral.*, 20, 217-230.
- Nehru, C.E. and Wyllie, P.J. (1974). Electron microprobe measurements of pyroxenes coexisting with  $H_2O$ -undersaturated liquid in the join  $CaMgSi_2O_6$ - $Mg_2Si_2O_6$ - $H_2O$  at 30 kbars, with applications to geothermometry. *Contrib. Mineral. Petrol.*, 48, 221-228.
- Nickel, K.G.; Brey, G.P. and Kogarko, L. (1985). Orthopyroxene-clinopyroxene equilibria in the system  $CaO$ - $MgO$ - $Al_2O_3$ - $SiO_2$  (CMAS): new experimental results and implications for two-pyroxene thermometry. *Contrib. Mineral. Petrol.*, 91, 44-53.
- Nickel, K.G. and Green, D.H. (1985). Empirical geothermobarometry for garnet peridotites and implications for the nature of the lithosphere, kimberlites and diamonds. *Earth Planet. Sci. Lett.*, 73, 158-170.
- Nixon, P.H. (Ed.) (1973). Lesotho Kimberlites. Lesotho National Develop. Corp., Maseru, 350p.
- Nixon, P.H. (Ed.) (1987). Mantle Xenoliths. John Wiley and Sons, Chichester, England. In press.
- Nixon, P.H. and Boyd, F.R. (1973a). Petrogenesis of the granular and sheared ultrabasic nodule suite in kimberlite. In: Nixon, P.H. (Ed.), Lesotho Kimberlites, 48-56, Lesotho National Develop. Corp., Maseru.
- Nixon, P.H. and Boyd, F.R. (1973b). The discrete nodule (megacryst) association in kimberlites from Northern Lesotho. In: Nixon, P.H. (Ed.), Lesotho Kimberlites, 67-75, Lesotho National Develop. Corp., Maseru.
- Nixon, P.H. and Boyd, F.R. (1973c). Discrete nodules (megacrysts) and lamellar intergrowths in the Frank Smith kimberlite pipe.

Ext. Abstr., Int. Kimb. Conf., Univ. Cape Town, South Africa, 243-246.

- Nixon, P.H.; Rogers, N.W.; Gibson, I.L. and Grey, A. (1981). Depleted and fertile mantle xenoliths from southern African kimberlites. *Ann. Rev. Earth. Planet. Sci.*, 9, 285-309.
- O'Hara, M.J.; Saunders, M.J. and Mercy, E.L.P. (1975). Garnet peridotite, primary ultrabasic magma and eclogite; Interpretation of upper mantle processes in kimberlite. In: Ahrens, L.H.; Dawson, J.B.; Duncan, A.R. and Erlank, A.J. (Eds.), *Phys. Chem. Earth*, Vol. 9, 571-604, Pergamon Press, Oxford.
- O'Hara, M.J. and Yoder, H.S. (1967). Formation and fractionation of basic magmas at high pressures. *Scott. J. Geol.*, 3, 67-117.
- O'Neill, H.St.C. (1981). The transition between spinel lherzolite and garnet lherzolite, and its use as a geobarometer. *Contrib. Mineral. Petrol.*, 77, 185-194.
- O'Neill, H.St.C. and Wood, B.J. (1979). An experimental study of Fe-Mg partitioning between garnet and olivine and its calibration as a geothermometer. *Contrib. Mineral. Petrol.*, 70, 59-70.
- Orlov, Yu.L. (1977). *The Mineralogy of the Diamond*. John Wiley and Sons, New York, 235p.
- Otter, M.L. and Gurney, J.J. (1986). Mineral inclusions in diamonds from the Sloan diatremes, Colorado-Wyoming State Line Kimberlite district, North America. *Abstr. Series 16, 4th Int. Kimb. Conf.*, Perth, Geol. Soc. Australia, 415-417.
- Ozima, M.; Takaoka, N.; Nito, O. and Zashu, S. (1984). Ar isotopic ratios and K, Na and other trace element contents in Premier and Finsch mine diamonds. In: Sunagawa, I. (Ed.), *Materials Science of the Earth's Interior*, 375-386, Terra Scientific, Tokyo.
- Ozima, M.; Zashu, S. and Nito, O. (1983).  $^3\text{He}/^4\text{He}$  ratio, noble gas abundance and K-Ar dating of diamonds - An attempt to search for the records of early terrestrial history. *Geochim. Cosmochim. Acta*, 47, 2217-2224.
- Parmentier, E.M. and Turcotte, D.L. (1974). An explanation of the pyroxene geotherm based on plume convection in the upper mantle. *Earth Planet. Sci. Lett.*, 24, 209-212.
- Pasteris, J.D.; Boyd, F.R. and Nixon, P.H. (1979). The ilmenite association at the Frank Smith mine, R.S.A.. In: Boyd, F.R. and Meyer, H.O.A. (Eds.), *The Mantle Sample: Inclusions in Kimberlites and Other Volcanics*, 265-278, A.G.U., Washington.
- Perkins, D.; Holland, T.J.B. and Newton, R.C. (1981). The  $\text{Al}_2\text{O}_3$  contents of enstatite in equilibrium with garnet in the system  $\text{MgO-Al}_2\text{O}_3\text{-SiO}_2$  at 15-40 kbar and 900-1600°C. *Contrib. Mineral. Petrol.*, 78, 99-109.

- Perkins, D. and Newton, R.C. (1980). The compositions of coexisting pyroxenes and garnet in the system  $\text{CaO-MgO-Al}_2\text{O}_3\text{-SiO}_2$  at 900-1100°C and high pressures. *Contrib. Mineral. Petrol.*, 75, 291-300.
- Phaal, C. (1965). Surface studies of diamond. *Ind. Diamond Rev.*, 25, 486-489, 591-595.
- Pokhilenko, N.P.; Sobolev N.V. and Lavrent'ev Yu. G. (1977). Xenoliths of diamondiferous ultramafic rocks from Yakutian kimberlites. Ext. Abstr. 2nd Int. Kimb. Conf., Santa Fe, A.G.U., Washington. (Unpaginated).
- Pollack, N.H. and Chapman, D.S. (1977). On the regional variation of heat flow, geotherms, and lithospheric thickness. *Tectonophysics*, 38, 279-296.
- Press, F. (1970). Earth models consistent with geophysical data. *Phys. Earth Planet. Inter.*, 3, 3-22.
- Prinz, M.; Manson, D.V.; Hlava, P.F. and Keil, K. (1975). Inclusions in diamonds: garnet lherzolite and eclogite assemblages. In: Ahrens, L.H.; Dawson, J.B.; Duncan, A.R. and Erlank, A.J. (Eds.), *Phys. Chem. Earth*, Vol. 9, 797-815, Pergamon Press, Oxford.
- Raber, E. (1978). Zircons from diamond-bearing kimberlites: Oxide reactions, fission track dating and a mineral inclusion study. Unpublished M.Sc. thesis, Univ. Massachusetts, 90p.
- Raber, E. and Haggerty, S.E. (1979). Zircon-oxide reactions in diamond-bearing kimberlites. In: Boyd, F.R. and Meyer, H.O.A. (Eds.), *Kimberlites, Diatremes and Diamonds: Their Geology, Petrology and Geochemistry*, 229-240, A.G.U., Washington.
- Raheim, A. and Green, D.H. (1974). Experimental determination of the temperature and pressure dependence of the Fe-Mg partition coefficient for coexisting garnet and clinopyroxene. *Contrib. Mineral. Petrol.*, 48, 179-203.
- Reid, A.M.; Brown, R.W.; Dawson, J.B.; Whitfield, G.G. and Siebert, J.C. (1976). Garnet and pyroxene compositions in some diamondiferous eclogites. *Contrib. Mineral. Petrol.*, 58, 203-220.
- Richardson, S.H. (1986). Latter-day origin of diamonds of eclogitic paragenesis. *Nature*, 322, 623-626.
- Richardson, S.H.; Erlank, A.J. and Hart, S.R. (1985). Kimberlite-borne garnet peridotite xenoliths from old enriched subcontinental lithosphere. *Earth Planet. Sci. Lett.*, 75, 116-128.
- Richardson, S.H.; Gurney, J.J.; Erlank, A.J. and Harris, J.W. (1984). Origin of diamonds in old enriched mantle. *Nature*, 310, 198-202.

- Rickwood, P.C.; Gurney, J.J. and White-Cooper, D.W. (1969). The nature and occurrences of eclogite xenoliths in the kimberlites of southern Africa. *Geol. Soc. S. Africa, Spec. Publ.* 2, 371-393.
- Ringwood, A.E. (1967). The pyroxene-garnet transformation in the Earth's mantle. *Earth Planet. Sci. Lett.*, 2, 255-263.
- Ringwood, A.E. (1970). Phase transformations and the constitution of the mantle. *Phys. Earth Planet. Inter.*, 3, 109-155.
- Ringwood, A.E. (1975). *Composition and Petrology of the Earth's Mantle*. McGraw-Hill, New York, 618p.
- Ringwood, A.E. (1982). Phase transformations and differentiation in subducted lithosphere: Implications for mantle dynamics, basalt petrogenesis, and crustal evolution. *J. Geol.*, 90, 611-643.
- Ringwood, A.E. and Green, D.H. (1966). An experimental investigation of the gabbro-eclogite transformation and some geophysical implications. *Tectonophysics*, 3, 383-427.
- Ringwood, A.E. and Lovering, J.F. (1970). Significance of pyroxene-ilmenite intergrowths among kimberlite xenoliths. *Earth Planet. Sci. Lett.*, 7, 371-375.
- Ringwood, A.E. and Major, A. (1966). High-pressure transformations in pyroxenes. *Earth Planet. Sci. Lett.*, 1, 351-357.
- Ringwood, A.E. and Major, A. (1970). The system  $Mg_2SiO_4-Fe_2SiO_4$  at high pressures and temperatures. *Phys. Earth Planet. Inter.*, 3, 89-108.
- Ringwood, A.E. and Major, A. (1971). Synthesis of Majorite and other high pressure garnets and perovskites. *Earth Planet. Sci. Lett.*, 12, 411-418.
- Ringwood, T. (1986). Dynamics of subducted lithosphere and implications for basalt petrogenesis. *Terra Cognita*, 5, 67-77.
- Robert, J.-L. (1976). Titanium solubility in synthetic phlogopite solid solutions. *Chem. Geol.*, 17, 213-227.
- Robey, J.vA. (1981). Kimberlites of the Central Cape Province, R.S.A. Unpublished Ph.D. thesis, Univ. Cape Town, South Africa, 261p.
- Robey, J.vA. and Gurney, J.J. (1979). Megacrysts from the Lekkerfontein kimberlite, North Central Cape, R.S.A. Ext. Abstr. Kimberlite Symposium II, Cambridge, U.K. (Unpaginated).
- Robinson, D.N. (1978). The characteristics of natural diamond and their interpretation. *Min. Sci. Engng.*, 10, 55-72.
- Robinson, D.N. (1979). Surface textures and other features of diamonds. Unpublished Ph.D. thesis, Univ. Cape Town, South Africa, 221p.

- Robinson, D.N.; Gurney, J.J. and Shee, S.R. (1984). Diamond eclogite and graphite eclogite xenoliths from Orapa, Botswana. In: Kornprobst J. (Ed.), *Kimberlites II: the Mantle and Crust-Mantle Relationships*, 11-24. *Developments in Petrology 11B*, Elsevier, Amsterdam.
- Roeder, P.L. and Emslie, R.F. (1970). Olivine-liquid equilibrium. *Contrib. Mineral. Petrol.*, 29, 275-289.
- Saxena, S.K. (1979). Garnet-clinopyroxene geothermometer. *Contrib. Mineral. Petrol.*, 70, 229-235.
- Schulze, D.J. (1982). Megacrysts from the Hamilton Branch kimberlite pipe, Kentucky: Discrete nodules and cumulate rocks. *Terra Cognita*, 2, 254-256.
- Seifert, F. and Schreyer, W. (1971). Synthesis and stability of micas in the system  $K_2O-MgO-SiO_2-H_2O$  and their relations to phlogopite. *Contrib. Mineral. Petrol.*, 30, 196-215.
- Sekine, T.; Irifune, T.; Ringwood, A.E. and Hibberson, W.O. (1986). High-pressure transformation of eclogite to garnetite in subducted oceanic crust. *Nature*, 319, 584-586.
- Shaffer, P.T.B. (1969). A review of the structure of silicon carbide. *Acta. Cryst.*, B25, 477-488.
- Shee, S.R. (1978). The mineral chemistry of xenoliths from the Orapa kimberlite pipe, Botswana. Unpublished M.Sc. thesis, Univ. Cape Town, 148p.
- Shee, S.R. and Gurney, J.J. (1979). The mineralogy of xenoliths from Orapa, Botswana. In: Boyd, F.R. and Meyer, H.O.A. (Eds.), *The Mantle Sample: Inclusions in Kimberlites and Other Volcanics*, 37-49, A.G.U., Washington.
- Shee, S.R.; Gurney, J.J. and Robinson, D.N. (1982). Two diamond-bearing peridotite xenoliths from the Finsch kimberlite, South Africa. *Contrib. Mineral. Petrol.*, 81, 79-87.
- Skinner, E.M.W. and Clement, C.R. (1977). Mineralogical classification of southern African kimberlites. *Ext. Abstr. 2nd. Int. Kimb. Conf.*, Sante Fe, A.G.U., Washington. (Unpaginated).
- Skinner, E.M.W. and Clement, C.R. (1979). Mineralogical classification of southern African kimberlites. In: Boyd, F.R. and Meyer, H.O.A. (Eds.), *Kimberlites, Diatremes and Diamonds: Their Geology, Petrology and Geochemistry*, 129-139, A.G.U., Washington.
- Skinner, E.M.W.; Smith, C.B.; Bristow, J.W.; Scott-Smith, B.H. and Dawson, J.B. (1985). Proterozoic kimberlites and lamproites and a preliminary age for the Argyle lamproite pipe, Western Australia. *Trans. Geol. Soc. S. Africa*, 88, 335-340.
- Smith, C.B. (1983a). Pb, Sr and Nd isotopic evidence for sources of southern African Cretaceous kimberlites. *Nature*, 304, 51-54.

- Smith, C.B. (1983b). Rubidium-strontium, uranium-lead and samarium-neodymium isotopic studies of kimberlite and selected mantle-derived xenoliths. Unpublished Ph.D. thesis, Univ. Witwatersrand, South Africa, 436p.
- Smith, C.B.; Allsopp, H.L.; Kramers, J.D.; Hutchinson, G. and Roddick, J.C. (1985a). Emplacement ages of Jurassic-Cretaceous South African kimberlites by the Rb-Sr method on phlogopite and whole-rock samples. *Trans. Geol. Soc. S. Africa*, 88, 249-266.
- Smith, C.B.; Gurney, J.J.; Skinner, E.M.W.; Clement, C.R. and Ebrahim, N. (1985b). Geochemical character of southern African kimberlites: A new approach based on isotopic constraints. *Trans. Geol. Soc. S. Africa*, 88, 267-280.
- Smith, C.B.; Gurney, J.J.; Harris, J.W.; Robinson, D.N.; Shee, S.R. and Jagoutz, E. (1986). Sr and Nd isotopic systematics of diamond-bearing eclogite xenoliths and eclogitic inclusions in diamond from southern Africa. *Abstr. Series 16, 4th Int. Kimb. Conf., Perth, Geol. Soc. Australia*, 332-334.
- Smith, D.; Wilson, C. and Ehrenberg, S.N. (1982). Interpretation of zoned minerals in garnet lherzolite nodules from minette, Four corners region. *EOS, Trans. A.G.U.*, 63, 463.
- Smith, J.V.; Brennesholtz, R. and Dawson, J.B. (1978). Chemistry of micas from kimberlites and xenoliths - I. Micaceous kimberlites. *Geochim. Cosmochim. Acta*, 42, 959-971.
- Smith, J.V. and Dawson, J.B. (1975). Chemistry of Mg-rich micas from kimberlites and xenoliths, with implications for volatiles in the upper mantle. *Abstr. Geol. Soc. Amer.*, 7, 1275-1276.
- Smyth, J.R. (1977). Quartz pseudomorphs after coesite. *Amer. Mineral.*, 62, 828-830.
- Smyth, J.R. (1980). Cation vacancies and the crystal chemistry of breakdown reactions in kimberlitic omphacites. *Amer. Mineral.*, 65, 1185-1191.
- Smyth, J.R. and Caporuscio, F.A. (1984). Petrology of a suite of eclogite inclusions from the Bobbejaan kimberlite. II. Primary phase compositions and origin. In: Kornprobst, J. (Ed.), *Kimberlites II: The Mantle and Crust-Mantle Relationships*, 121-132, *Developments in Petrology 11B*, Elsevier, Amsterdam.
- Smyth, J.R.; McCormick, T.C. and Caporuscio, F.A. (1984). Petrology of a suite of eclogitic inclusions from the Bobbejaan kimberlite. I. Two unusual corundum-bearing kyanite eclogites. In: Kornprobst, J. (Ed.), *Kimberlites II: The Mantle and Crust-Mantle Relationships*, 109-120, *Developments in Petrology 11B*, Elsevier, Amsterdam.
- Sobolev, N.V. (1970). Eclogites and pyrope peridotites from the kimberlites of Yakutia. *Phys. Earth Planet. Inter.*, 3, 398-404.
- Sobolev, N.V. (1977). Deep seated inclusions in kimberlites and the problem of the composition of the upper mantle. (Translation by Brown, D.A.), *A.G.U.*, Washington, 279p.

- Sobolev, N.V. (1984). Kimberlites of the Siberian Platform: Their geological and mineralogical features. In: Glover, J.E. and Harris, P.G. (Eds.), Kimberlite Occurrence and Origin: A basis for conceptual models in exploration, 275-287, Univ. Western Australia, Publication No. 8.
- Sobolev, N.V. (1985). Ultramafic and eclogitic types of paragenesis of diamonds. Ext. Abstr. In: Native elements formation in endogenic processes. Acad. Sciences USSR, Siberian division, Yakutsk. (Unpaginated).
- Sobolev, N.V.; Botkunov, A.I.; Lavrent'yev, Yu.G. and Pospelova, L.N. (1971a). Compositional characteristics of minerals associated with diamonds in the Mir pipe, Yakutia. Zap. Vses. Mineral. Obshchest., 100, 558-564. (Russian)
- Sobolev, N.V.; Gnevushev, M.A.; Mikhaylovskaya, L.N.; Futergendler, S.I.; Shemanina, Ye.I.; Lavrent'yev, Yu.G. and Pospelova, L.N. (1971b). The composition of garnet and pyroxene inclusions from the diamonds of the Urals. Doklady Akad. Nauk SSSR, 198, 190-193. (Russian)
- Sobolev, N.V. and Lavrent'yev, Yu.G. (1971). Isomorphic sodium admixture in garnets formed at high pressures. Contrib. Mineral. Petrol., 31, 1-12.
- Sobolev, N.V.; Lavrent'yev, Yu.G.; Pokhilenko, N.P. and Usova, L.N. (1973). Chrome-rich garnets from the kimberlites of Yakutia and their parageneses. Contrib. Mineral. Petrol., 40, 39-52.
- Sobolev, N.V.; Yefimova, E.S.; Koptil, V.I.; Lavrent'yev, Yu.G. and Sobolev, V.S. (1976). Inclusions of coesite, garnet and omphacite in Yakutian diamonds; the first discovery of coesite paragenesis. Doklady Akad. Nauk. SSSR, 230, 1442-1444. (Russian)
- Sobolev, N.V.; Yefimova, E.S. and Pospelova, L.N. (1981). Native iron in Yakutian diamonds and its paragenesis. (Inst. Geol. Geofiz., Novosibirsk), Geol. Geofiz., 12, 25-29. (Russian)
- Sobolev, V.S.; Sobolev, N.V. and Lavrent'yev, Yu.G. (1972). Inclusions in diamond from a diamondiferous eclogite. Doklady Akad. Nauk. SSSR, 207, 164-167. (Russian)
- Streckeisen, A. (1976). To each plutonic rock its proper name. Earth-Sci. Rev., 12, 1-33.
- Sunagawa, I. (1977). Natural Crystallisation. J. Crystal Growth, 42, 214-223.
- Sunagawa, I. (1984). Growth of crystals in nature. In: Sunagawa, I. (Ed.), Materials Science of the Earth's Interior, 63-105, Terra Scientific, Tokyo.
- Sutton, J.R. (1928). Diamond: A descriptive treatise. Murby, London, 118p.

- Takoaka T. and Ozima M. (1978). Rare gas isotopic compositions in diamond. *Nature*, 271, 45-46.
- Thompson, R.N. (1975). Is upper mantle phosphorus contained in sodic garnet? *Earth Planet. Sci. Lett.*, 26, 417-424.
- Truswell, J.F. (1977). *The Geological Evolution of South Africa*. Purnell, Cape Town, South Africa, 218p.
- Tsai, H.M. (1978). Mineralogical and geochemical investigations of mineral inclusions in diamond, kimberlite and associated rocks. Ph.D. thesis, Purdue Univ., Indiana, U.S.A., 202p.
- Tsai, H.M.; Meyer, H.O.A., Moreau, J. and Milledge, H.J. (1979). Mineral inclusions in Diamonds: Premier, Jagersfontein and Finsch kimberlites, South Africa, and Williamson mine, Tanzania. In: Boyd, F.R. and Meyer, H.O.A. (Eds.), *Kimberlites, Diatremes and Diamonds: Their Geology, Petrology and Geochemistry*, 16-26, A.G.U., Washington.
- Urosovskaya, A.A. and Orlov, Yu.L. (1964). Nature of the plastic deformation of diamond crystals. *Doklady Akad. Nauk. SSSR*, 154(5), 1099-1102. (Russian).
- Wagner, P.A. (1914). *The Diamond Fields of Southern Africa*. Transvaal Leader, Johannesburg, South Africa, 347p. Reprinted 1971 by Struik (Pty) Ltd., Cape Town, South Africa, 355p.
- Walker, D.A. (1979). Textural and compositional studies of eclogites from the Roberts Victor kimberlite, South Africa. Unpublished M.Sc. thesis, Oxford Univ., 285p.
- Welke, H.J.; Allsopp, H.L. and Harris, J.W. (1974). Measurements of K, Rb, U, Sr and Pb in diamonds containing inclusions. *Nature*, 252, 35-37.
- Wells, P.R.A. (1977). Pyroxene thermometry in simple and complex systems. *Contrib. Mineral. Petrol.*, 62, 129-139.
- White, W.M. and Hofmann, A.W. (1981). Sr and Nd isotope geochemistry of oceanic basalts and mantle evolution. *Nature*, 296, 821-825.
- Whitelock, T.K. (1973). The Monastery mine kimberlite pipe. In: Nixon, P.H. (Ed.), *Lesotho Kimberlites*, 214-218, Lesotho National Develop. Corp., Maseru.
- Williams, A.F. (1932). *The Genesis of the Diamond*. (2 vols.), E. Benn Ltd., London, 636p.
- Wood, B.J. (1974). The solubility of alumina in orthopyroxene coexisting with garnet. *Contrib. Mineral. Petrol.*, 46, 1-15.
- Wood, B.J. and Banno, S. (1973). Garnet-orthopyroxene and orthopyroxene-clinopyroxene relationships in simple and complex systems. *Contrib. Mineral. Petrol.*, 42, 109-124.
- Wyllie, P.J. (Ed.) (1967). *Ultramafic and Related Rocks*. John Wiley and Sons, New York, 464p.

- Wyllie, P.J. (1987). The genesis of kimberlites and some low-SiO<sub>2</sub>, high alkali magmas. Proc. 4th Int. Kimb. Conf., Perth, Australia. In press.
- Yagi, T.; Bell, P.M. and Mao, H.K. (1979). Phase relations in the system MgO-FeO-SiO<sub>2</sub> between 150 and 700 kbar at 1000°C. Carnegie Inst. Washington, Yb. 78, 614-618.
- Yamada, H. and Takahashi, E. (1984). Subsolidus phase relations between coexisting garnet and two pyroxenes at 50 to 100 kbar in the system CaO-MgO-Al<sub>2</sub>O<sub>3</sub>-SiO<sub>2</sub>. In: Kornprobst, J. (Ed.), Kimberlites II: The Mantle and Crust-Mantle Relationships, 247-256, Developments in Petrology 11B, Elsevier, Amsterdam.
- Yefimova, E.S. and Sobolev, N.V. (1977). Abundance of crystalline inclusions in diamonds of Yakutia. Doklady Akad. Nauk SSSR, 237(6), 1475-1478. (Russian)
- Yefimova E.S.; Sobolev N.V. and Pospelova L.N. (1983). Sulphide inclusions in diamond and specific features of their parageneses. Zap. Vses. Miner. Obsch., 112(3), 300-310. (Russian)
- Yoder, H.S. and Tilley, C.E. (1962). Origin of basalt magmas: An experimental study of natural and synthetic rock systems. J. Petrol., 3, 342-532.